



Routing Slip

This routing slip is to be included with your signature pages and is for CIHR's administrative use only.

Funding Opportunity

Operating Grant 2012-03-01

Application Number 273784**ResearchNet ID** 158528

Suggested Peer Review Committees

1st: Cell Physiology

2nd: Cell Biology & Mechanisms of Disease

Nominated Principal Applicant

Surname

Given Names

PIN

GINGRAS

Anne-Claude

157721

Project Title

Molecular mechanisms of cerebral cavernous malformations

Relevant Research Area:**Title of Priority Announcement/Funding Pools:**

Linked Programs:



Canadian Institutes
of Health Research

Instituts de recherche
en santé du Canada

PROTECTED B WHEN COMPLETED

273784

GINGRAS, Anne-Claude

Mount Sinai Hospital (Toronto)

\$260796

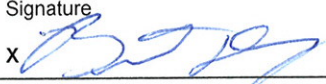
Applicant Signatures

The applicants are in the following order: Principal Applicant(s) and Co-Applicants. It is agreed that the general conditions governing grants, as well as the statement "Meaning of Signatures on Application Forms" as outlined in the CIHR Grants and Awards Guide, apply to any grant made pursuant to this application and hereby accepted by the applicant(s).

Consent to Disclosure of Personal Information

I understand that maintaining public trust in the integrity of researchers is fundamental to building a knowledge-based society. By submitting this application or by accepting funding from CIHR, NSERC and/or SSHRC, I affirm that I have read and I agree to respect all the policies of these Agencies that are relevant to my research, including the *Tri-Agency Framework: Responsible Conduct of Research* (<http://www.rcr.ethics.gc.ca/eng/policy-politique/framework-cadre/>). In cases of a serious breach of Agency policy, the Agency may publicly disclose my name, the nature of the breach, the institution where I was employed at the time of the breach and the institution where I am currently employed.

I accept this as a condition of applying for or receiving Agency funding and I consent to such disclosure.

Surname	Given Names	Role	Signature
DERRY	Brent	Co-Applicant	
Institution	Faculty	Department	Date
Hospital for Sick Children (Toronto)	Medicine	Dev. & Stem Cell Bio.	Feb. 29, 2012
Surname	Given Names	Role	Signature
			x
Institution	Faculty	Department	Date
Surname	Given Names	Role	Signature
			x
Institution	Faculty	Department	Date
Surname	Given Names	Role	Signature
			x
Institution	Faculty	Department	Date
Surname	Given Names	Role	Signature
			x
Institution	Faculty	Department	Date
<hr/>			



Canadian Institutes
of Health Research

Instituts de recherche
en santé du Canada

PROTECTED B WHEN COMPLETED

273784

GINGRAS, Anne-Claude
Mount Sinai Hospital (Toronto)

\$260796

Institution Signatures

It is agreed that the general conditions governing grants, as well as the statement "Meaning of Signatures on Application Forms" as outlined in the CIHR Grants and Awards Guide, apply to any grant made pursuant to this application and are hereby accepted by the applicant's and the applicant(s) employing Institution(s).

A signature is not required at institutions outside of Canada.

For institutions using the Electronic Approval Tool on ResearchNet, a signature is not required for block 1 if the Authorized Official can bind the institution to all obligations outlined in the "Meaning of Signatures on Application Forms". If the Authorized Official cannot bind the institution to all obligations in the "Meaning of Signatures on Application Forms", complete block 2.

1. Signature of Authorized Official: Mount Sinai Hospital (Toronto)

Print Name:

Date:

Joan Sprout, Senior VP, Finance

28/2/2012

Signature:

X

Anne Sprout

2. If the Authorized Official above cannot bind the institution to all obligations outlined in the "Meaning of Signatures on Application Forms", please provide additional signatures below as required.

Print Name:

Date:

DR. James Woodgett, Director, OISTOREY

28/2/2012

Signature:

X

James Woodgett

Print Name:

Date:

Signature:

X



Canadian Institutes
of Health Research

Instituts de recherche
en santé du Canada

**PROTECTED WHEN
COMPLETED**

Appl. # 273784

Application Details

Funding Opportunity:

Operating Grant: 2011-2012 (2012-03-01)

Proposed Start Date:

Proposed End Date:

Nominated Principal Applicant/Candidate:

Surname GINGRAS

Given Names Anne-Claude

Institution

Faculty

Department

Samuel Lunenfeld Research Institute (Toronto)

Telephone

416-585-5027

Fax

E-mail

gingras@mshri.on.ca

Project Title:

Molecular mechanisms of cerebral cavernous malformations

Primary location where research to be conducted: Samuel Lunenfeld Research Institute (Toronto)

Faculty:

Department:

Institution which will administer project funds (Institution Paid):

Mount Sinai Hospital (Toronto)

Location of proposed Activity:

Period of support requested: 5 Year(s) Month(s)

THE FOLLOWING SECTIONS ARE NOT APPLICABLE TO ALL PROGRAMS

Budget section - Amounts Requested from CIHR in the First Full Year:

Operating: 260796

Equipment: 0

Total Amount Requested: 260796

New

Renewal

Funding Reference Number (FRN):

Is this application a resubmission of a previously unsuccessful new application?

Yes No

Is this application a resubmission of a previously unsuccessful renewal application?

Yes No FRN #:

Have you applied to this program in the last two years?

Yes No

Is this a multi-center study?

Yes No



Canadian Institutes
of Health Research

Instituts de recherche
en santé du Canada

**PROTECTED WHEN
COMPLETED**

Appl. # 273784

Certification Requirements:

- Human subjects Human stem cells Animals Biohazards
- Environmental Impact Containment Level _____
- Clinical Trial
- Contains a randomized trial
- In order to carry out the proposed research in this application, an exemption from Health Canada under Section 56 of the Controlled Drugs and Substances Act is required. Should my application be approved, I understand that I will need to seek an exemption from Health Canada and provide this exemption to CIHR before any funding will be released for this application.

Other Project Information:

- For statistical purposes, does this application propose research involving Aboriginal people?
- Are sex (biological) considerations taken into account in this study?
- Are gender (socio-cultural) considerations taken into account in this study?

Please describe how sex and/or gender considerations will be considered in your research proposal:
This is a biomedical research project involving genes (proteins) mutated equally in either sex.

**Other Applicants**

Surname	Given Names	Role
DERRY	Brent	Co-Applicant
Hospital for Sick Children (Toronto)	Department	Faculty

Surname	Given Names	Role

Surname	Given Names	Role

Surname	Given Names	Role

Surname	Given Names	Role

Surname	Given Names	Role

Surname	Given Names	Role

Surname	Given Names	Role

**Lay title of the research****Abstract suitable for preparation of a press release**

Cerebral Cavernous Malformations (CCMs) are defects of the brain capillaries that can arise by inheritance of mutations in one of three 'familial' genes (CCM1, CCM2 or CCM3) or sporadically by unknown mechanisms/genes. In many ways this disease is like a ticking time bomb. Patients can live a normal life without knowing they have CCMs but, without notice, experience a range of symptoms as mild as headaches or as severe as seizures and even stroke. There are currently no therapeutic options for patients except removal of these raspberry-like lesions by invasive neurosurgery. While surgery is generally a final option it can lead to long lasting effects on balance, behaviour and memory. Because there is very little known about the molecular events that lead up to CCM disease we propose to study the basic function of these proteins using two very powerful but complementary approaches. Drs. Gingras and Derry are experts in the study of proteins and genes, respectively, and have integrated their research expertise to understand the most fundamental aspects of CCM biology. In this grant application, they propose to study how the CCM proteins communicate signals within and between cells to prevent the vascular defects that cause this disease in patients. The Gingras laboratory has discovered new components of the CCM signalling network using biochemical approaches while the Derry lab has developed a model of this disease in the tiny roundworm *C. elegans*. Together, their combined efforts will provide a much clearer picture of how the CCM1, CCM2 and CCM3 proteins work, which should uncover new non-surgical methods for the clinical management of this devastating disease in humans.

Project Descriptors *

Cerebral Cavernous Malformations, Intracellular signalling, Functional Proteomics, *C. elegans* genetics, Cytoskeletal rearrangements, Golgi polarization, Tubule formation, Mass spectrometry

Areas of Research *	Classification Codes *
Primary GENOMICS, PROTEOMICS, AND BIOINFORMATICS	Primary STROKE, HEART FAILURE
Secondary GENETICS	Secondary MULTIPLE DISEASE RELEVANCE
Themes *	Categories *
1 st Biomedical	1 st Genetics
2 nd	2 nd Circulatory and Respiratory Health
3 rd	3 rd
4 th	4 th

**Suggested Peer Review Committees:****1st Cell Physiology****2nd Cell Biology & Mechanisms of Disease****Suggested External Referee(s)***

Name Washburn, Michael

E-mail mpw@stowers.org

Area of Expertise mass spectrometry, protein interactions

Name

E-mail

Area of Expertise

Summary of Research Proposal/Résumé de la proposition de recherche

Cerebral cavernous malformations (CCMs) are common lesions of the brain that arise from a weakening of the microvasculature and result in a variety of pathophysiological conditions, including headaches, seizures and stroke. There is currently no cure or pharmacological treatment options for this disease, though surgical resection is available in severe cases to alleviate symptoms. CCM can arise by inherited mutations in one of three genes (CCM1, CCM2 or CCM3) and sporadically by unknown genetic loci. In familial CCM, loss of function mutations in CCM1, CCM2 or CCM3 account for at least 80% of cases, where the mutated allele is transmitted in an autosomal dominant fashion and loss of heterozygosity occurs in a subset of endothelial cells leading to the disease phenotype. While mutations in any one of these three genes results in similar histological manifestations, mutations in CCM3 are associated with the highest risk of hemorrhage. Patients with the same mutations in either one of the familial CCM genes have a range of symptoms and severity, suggesting the existence of modifier genes. Thus, understanding the biochemistry of CCM proteins and how these proteins engage their signaling pathways should not only uncover modifiers of familial disease but possibly genes that predispose to sporadic CCMs. To understand the *in vitro* and *in vivo* functions of the CCM proteins we propose to combine the powerful and complementary methods of proteomics and genetics. Biochemically, CCM1 and CCM2 associate with each other in a tight complex to control common downstream signaling events that modulate cytoskeletal function. Genetically, reports in mouse, zebrafish, and our preliminary data in *C. elegans*, indicate that CCM3 exhibits functions that are largely distinct from CCM1 and CCM2. While CCM3 can physically associate with CCM1•CCM2, results from our group and others suggest that most CCM3 protein resides in different molecular complexes in various cell types, including the newly described STRIPAK (STRiatin Interacting Phosphatase And Kinase) complex. Within STRIPAK, CCM3 is responsible for bridging kinases of the Sterile-20 family (GCKIII subfamily) to the striatin molecule, itself a regulatory subunit for the PP2A family of phosphatases. Interaction of CCM3 with the CCM1•CCM2 complex is also detected, but with lower stoichiometries than the CCM3•STRIPAK complex. Importantly, however, the GCKIII kinases were also detected by proteomics approaches in CCM1•CCM2•CCM3 complexes. Based on our functional characterization of roles for STRIPAK in cytoskeletal events such as regulation of Rho signaling and polarization, we postulate that the more severe phenotypes associated with CCM3 mutations in patients may be caused by concomitant loss of the CCM1•CCM2•CCM3 and STRIPAK•CCM3 signaling function. Consistent with this biochemical evidence, we have found that ablation of both *ccm1* and *ccm3* in *C. elegans* results in synthetic lethality, which we will exploit to screen for new components of the CCM3 pathway and the CCM regulatory network. In addition, we have found that *ccm3* and the STRIPAK complex are required for development the *C. elegans* excretory cell, a unicellular vascular structure that resembles capillaries of vertebrates.

The goals of this project are to uncover the molecular pathways that lead to CCM pathology using the powerful and complementary methods of proteomics and model organism genetics. To accomplish this we propose the following three Specific Aims:

Aim 1: Establish physical interaction maps for CCM proteins in mammals and *C. elegans*

Aim 2: Define the global genetic interaction map for CCM1 and CCM3

Aim 3: Identify substrates for GCKIII kinases

Taken together, these studies will not only greatly expand our understanding of CCM biology but potentially uncover new genes for preventive screening and the future development of therapeutics for treating patients with this disease.

GINGRAS, Anne-Claude

Operating Grant/Subvention de fonctionnement Application/Demande 2012-03-01

Lay abstract/Résumé non scientifique

Cerebral Cavernous Malformations (CCMs) are defects of the brain capillaries that can arise by inheritance of mutations in one of three 'familial' genes (CCM1, CCM2 or CCM3) or sporadically by unknown mechanisms/genes. In many ways this disease is like a ticking time bomb. Patients can live a normal life without knowing they have CCMs but, without notice, experience a range of symptoms as mild as headaches or as severe as seizures and even stroke. There are currently no therapeutic options for patients except removal of these raspberry-like lesions by invasive neurosurgery. While surgery is generally a final option it can lead to long lasting effects on balance, behaviour and memory. Because there is very little known about the molecular events that lead up to CCM disease we propose to study the basic function of these proteins using two very powerful but complementary approaches. Drs. Gingras and Derry are experts in the study of proteins and genes, respectively, and have integrated their research expertise to understand the most fundamental aspects of CCM biology. In this grant application, they propose to study how the CCM proteins communicate signals within and between cells to prevent the vascular defects that cause this disease in patients. The Gingras laboratory has discovered new components of the CCM signaling network using biochemical approaches while the Derry lab has developed a model of this disease in the tiny roundworm *C. elegans*. Together, their combined efforts will provide a much clearer picture of how the CCM1, CCM2 and CCM3 proteins work, which should uncover new non-surgical methods for the clinical management of this devastating disease in humans.

The Gingras and Derry laboratories have been working together for the past several years to better understand the molecular mechanism of action of CCM proteins. Interest in CCM in the two groups has emerged independently, initially, from the discovery of the STRIPAK complex into which the bulk of CCM3 resides in mammalian cells (*Gingras; Appendix 1*), and from studies of the role of CCM1 (*kri-1*) in *C. elegans* germ cell apoptosis (*Derry; Appendix 2*). Since then, however, the co-applicants have combined their efforts in genetics, biochemistry and proteomics. These collaborative efforts have resulted in two recent publications (also with collaborator F. Sicheri) reporting the heterodimerization of CCM3 with kinases of the GCKIII family (*Appendix 3*), and the molecular organization of the STRIPAK complex (*Appendix 4*). These reports are described in the introduction to this proposal and help to frame the future goals of this work. Importantly, and as described in more detail in the preliminary data section of the grant, our two laboratories have been working together to assess the functional significance of the association of CCM3 with the GCKIII kinases and other STRIPAK components using cell biological assays in mammalian cells and phenotypical analysis and genetic screens in the multicellular organism *C. elegans*. In particular, the Derry lab has now identified important functions for CCM3, GCKIII kinases and other STRIPAK components in osmoregulation and morphology of the *C. elegans* excretory cell, the sole vascular structure in this organism. The phenotypes reported for CCM3 and CCM1 in *C. elegans* (including a synthetic lethal interaction between the two gene) will enable our team to harness the power of genetic screens to identify additional components of the CCM signaling pathway(s). The Derry lab has a very strong expertise in this area, having conducted genetic screens and phenotypical analysis for the past 8 years (i.e., Derry *et al.*, 2007; Quevedo *et al.*, 2007; Gao *et al.*, 2008; Ito *et al.*, 2010; Ross *et al.*, 2011).

Since starting her laboratory at the Lunenfeld, AC Gingras has established herself as a proteomics expert (as evidenced by her publications, multiple invitations as a guest speaker, participation to the editorial board of the leading proteomics journal and serving on the advisory board of the UCSF proteomics centre). She has been very active in the past several years in developing reagents and procedures to facilitate generation of high quality mass spectrometry data, in particular for interaction proteomics. For example, she has developed protocols to improve the yield of affinity-purified samples (e.g. Chen and Gingras, *Methods*, 2007), but also contributed to the development and implementation of a number of bioinformatics tools. In particular, she co-developed, with A Nesvizhskii, algorithms to identify true interaction partners in affinity purification/mass spectrometry (AP-MS) experiments. The SAINT (Significance Analysis of INTeractome) statistical tool compares the quantitative information associated with the identification of each protein in a specific experiment, with the quantitative information for the same protein across all other experiments in the dataset (*Appendix 5*). This strategy is applicable to very large datasets (including the yeast kinase and phosphatase interaction network published with M Tyers; *Science* 2010), but also to much smaller datasets (see, e.g. Skarra *et al.*, *Proteomics*, 2011). In the laboratory, SAINT is supported by our robust bioinformatics pipeline ProHits which enables us to track our mass spectrometry data, annotate experiments, and view and analyze the experimental results (with M Tyers, *Nat Biotech*, 2011). We have an open source policy and are distributing both and ProHits freely to the scientific community. In the recent years, new postdoctoral fellows with expertise in identification of kinase substrates and quantitative proteomics have joined the group and a research collaboration with mass spectrometry vendor AB-SCIEX has further cemented our leadership in quantitative phosphoproteomics; this is enabling the realization of the challenging experiments proposed here.

While the Gingras and Derry labs are supported by grants from the CIHR for unrelated projects this application will support efforts to combine their distinct but complementary strengths in proteomics and genetics to define the mechanisms by which CCM proteins function.

We thank the reviewers for their insightful suggestions on the previous version of this grant, and for their very positive comments (appended to this grant). We were delighted to receive a score of 4.47 and by the fact that our grant was selected by the Institute of Genetics for bridge funding. Understanding the molecular mechanisms underlying cerebral cavernous malformations is a key focus of both our groups, and we have therefore continued to work extensively in this area since the initial submission of the grant. We also agree with most of the comments of the reviewers, and wish to address them in more detail below:

As noted by reviewer #2, the identification of substrates for the kinases in Aim 3 is our more “risky” aim, especially with regards to the proteomics approaches. We have therefore initiated experiments to test the feasibility of the method we proposed for identifying substrates of the GCKIII kinases. Using recombinantly expressed active MST4 and a cell lysate where all endogenous kinases have been inactivated by the chemical FSBA, we have been able to detect potential direct substrates for the kinase by ³²P incorporation. Furthermore, in two biological replicates of the purification (with quantitative proteomics), we have now identified a number of differentially phosphorylated proteins, one of which is a component of the STRIPAK complex, MOB3 (Fig 20). We have confirmed that MST4 can directly phosphorylate MOB3 *in vitro*, confirming the feasibility of this approach. Importantly, and for the first time, this new data has enabled us to define consensus sites for MST4, which will greatly help in prioritizing hits from the worm and proteomics screens. In a proof-of-principle experiment with a different kinase (p38), Dr. Gingras’ postdoctoral fellow James Knight introduced a modification to the kinase enrichment protocol, which has enabled more rapid identification of substrates whose phosphorylation is also downstream of the selected kinase. The work describing the methods and its application to identifying substrates for p38 has been accepted for publication (Knight et al.; *Skeletal muscle*, 2012; Gingras is co-author). Importantly, this strategy (identification of sites phosphorylated *in vitro* and dependent on the presence of the kinase *in vivo*) helps in the prioritization of hits from the phosphoproteomics screens (Fig 21). While we believe that this combination of *in vitro/in vivo* phosphorylation approach is feasible, we realize that we may encounter technical difficulties, and will continue considering alternative strategies. We contend that identification of the signaling pathways affected directly by CCM3 or the kinases is essential to the identification of additional therapeutic targets.

We have also continued characterizing interacting partners for the CCM1, CCM2 and CCM3 proteins. In collaboration with Mike Fainzilber’s group, we now show that three GCKIII kinases can associate (likely via the CCM3 bridge) with CCM2. STK25 is implicated in promoting apoptotic cell death through Trk signaling (Costa et al., *manuscript under review*). In this new paper, our collaborators also show that CCM2 is a potential substrate for the GCKIII kinases (in this case, STK25), which we propose to investigate in detail here. We have furthermore characterized a novel interaction between the uncharacterized protein c10orf47 and CCM3. Like striatins and CCM2, c10orf47 possesses an acidic region which we have demonstrated to be required for interaction with CCM3. Similar to the interaction with striatin and CCM2, the interaction of c10orf47 with CCM3 is abolished by mutation of the globular FAT domain of CCM3 (Figs. 7 and 8). These studies all confirm that a module formed of the GCKIII kinases and CCM3 can associate to *either*: 1) STRIPAK (most abundant in the cells we have looked at); 2) CCM3-CCM1-ICAP1; 3) c10orf47. This is important, as it provides molecular insight regarding the clinical differences between patients harboring CCM3 mutations, as compared to those patients with CCM1 or CCM2 mutations.

On the technical side, we have made significant progress using a label-free quantitative proteomics approach called SWATH to accurately quantify changes in interactomes (Lambert et al., *in preparation*; Fig 18). Combined with affinity purification, SWATH rapidly and accurately identifies interactome

differences; importantly, however, quantification is also accurate at the level of individual peptides, making it appropriate for quantification of phosphopeptides. This method will be used as an alternative quantification option described in Aim 3.

We regret that we were a bit vague with regards to the prioritization of the hits from both screens, especially with regards to potential therapeutic targets for treating the disease. We have tried to clarify this throughout, and added figures explaining how we will go about selecting targets most relevant to treating the disease in patients. Note that our modified strategy for the phosphoproteomics screens will in itself drastically help with prioritization. Because we are sailing uncharted waters our first priority is to first define the genetic and physical CCM interaction network. Understanding how signals are propagated through these modules will greatly facilitate prioritization of hits. Using the *C. elegans* excretory cell as a vascular model will provide an *in vivo* system for stratifying follow up analyses (i.e., inhibiting genes that restore excretory cell morphology to normal in *ccm3* mutants will be ideal candidates for future therapeutic development).

At the moment, one of our major hypotheses – which we have tried to clarify throughout the proposal – is that the GCKIII kinases are essential components of CCM signaling. It is still unclear, however, what the relationship is between their function and that of CCM3. CCM3 could work simply as an adaptor molecule, linking the GCKIII kinases to CCM3-CCM1-ICAP1, STRIPAK or other complexes and substrates. Alternatively, CCM3 could help modulating kinase activity, either globally, or towards specific substrates. Therefore, in addition to systematically identifying substrates for each of the three GCKIII kinases (Aim 3), we have established a collaboration with Geoff Hicks (U Manitoba and director of the NorCOMM, the North American Conditional Mouse Mutagenesis Project). As part of this collaboration, we will gain access to individual ES lines targeting each of the three GCKIII kinases. Importantly, however, we are also generating a CCM3 allele, which harbors mutations in the interaction site for the three kinases (as defined by us in Appendix 3). All ES cells will be employed to identify substrates for the kinases. Additionally, starting with the knock-in allele of CCM3 deficient in kinase binding, we will assess whether abrogating interaction with the GCKIII kinases, in the context of an otherwise normal CCM3 protein, recapitulates the phenotype of the mouse CCM3 null. These analyses will be initiated in Toronto, but pursued in collaboration with Dr. Murat Gunel, who has generated a CCM3 knockout mouse (the homozygote total knockout is inviable, and has striking vascular defects). If our hypothesis is correct, increasing GCKIII levels or activity may provide therapeutic avenues; while this is not proposed here as an Aim, we have initiated discussions with Jeff Wrana, director of the SMART robotics facility at the Lunenfeld, to set up assays to screen for small molecule regulators of GCKIII levels or activity in cells depleted of CCM3.

Lastly, while our view at the moment is that there is much to still be learned about the biology of the disease and that this is an absolute prerequisite to identify additional therapeutic targets, we are working closely with two of the leading clinicians in the CCM field in order to more rapidly translate our findings to patient care. Murat Gunel is chief of Neurovascular Surgery at Yale University and leading expert on CCM3 (which he discovered and for which he generated mouse models). Issam Awad is the director of the Neurovascular Surgery Program at the University of Chicago, and is currently conducting preclinical trials of ROCK inhibitors in his mouse CCM models. While he is in general optimistic about the success of ROCK inhibition, Dr. Awad fully realizes the need for alternative therapeutic targets, especially for CCM3 patients (see his appended letter). We are sharing early high-confidence hits with both of these experts. Dr Gunel is currently performing exome sequencing on his cohort of patients, and will use our hits to prioritize sequence variants to be followed up on; Dr Awad and Dr Gunel will also take the lead to test expression and/or deregulation of our candidates in their mouse models and eventually CCM patient tissue samples.

A. BACKGROUND AND SIGNIFICANCE

Cerebral cavernous malformations (CCMs) primarily occur in the central nervous system where CCM-affected capillaries have grossly dilated vascular channels lined by only a single layer of endothelium (reviewed in¹). CCM lesions do not contain any intervening neural parenchyma or identifiable mature vessel wall elements such as smooth muscle or elastin. Furthermore, gaps exist between the endothelial cells, disrupting the tight junctions that would normally create the blood-brain barrier, allowing for the leakage of blood into the surrounding brain parenchyma². Hemorrhages associated with these lesions lead to headaches, focal neurological defects, seizures and strokes in 20-30% of affected individuals, and the incidence of CCMs has been estimated to be 0.5% of the population. Recurrent seizures or strokes necessitate risky and complex excision of lesions, the only therapeutic option currently available. As lesions can be located in difficult areas to access in the brain, and patients may have multiple lesions (over 100 in more aggressive familial cases), less invasive therapeutic interventions are clearly required for managing this devastating disease³. As only the endpoint of CCMs (vascular dilatation and hemorrhage) is observed in patients, the mechanism that leads up to disease manifestation is currently unclear. Roughly 40% of CCMs are familial in origin, with single-copy germline loss-of-function mutations in one of three genes (here referred to as CCM1-3; see Fig 1 for an extended list) being responsible for the vast majority of these cases⁴⁻¹². While the histology of CCM3 vascular lesions is indistinguishable from those caused by mutations in CCM1 and 2, the risk of hemorrhage in patients with CCM3 mutations is much higher⁴. There is a great deal of debate surrounding CCM disease: do additional modifier gene(s) affect the severity of disease¹²; what is the cause of CCMs in non-familial cases (where CCM1-3 appear normal); is the loss of the second copy of CCM1-3 leading to disease in familial cases^{13,14}; and is a single molecular pathway responsible for all CCMs?

The identification of the three genes mutated in familial CCMs (CCM1-3) has led to research on possible molecular mechanisms underlying the formation of these lesions in patients. CCM1, CCM2 and CCM3 are all mediators of intracellular signaling, predominantly via the small GTPases of the Rho family¹⁵⁻¹⁷, though roles in stress signaling, apoptosis, and various other intracellular pathways have been reported, as briefly reviewed below.

CCM1 and CCM2: CCM1 and 2 contain protein interaction domains and motifs that are consistent with roles as signaling scaffolds¹⁸ (Fig 2). CCM1 contains a FERM (4.1-Ezrin-Radixin-Moesin) domain at its C-terminus implicated in membrane binding^{19,20}. Rap1A, a small GTPase interacting with CCM1 in yeast two-hybrid assays, contributes to junctional recruitment of CCM1^{20,21}. In addition, three NPxY motifs mediate interaction with the phosphotyrosine-binding (PTB) domains of CCM2²² and of ICAP1 (Integrin beta Cytoplasmic domain-Associated Protein)^{23,24}. Interestingly, CCM1 binding to ICAP1 and to CCM2 is mediated by different NPxY motifs²², enabling formation of CCM1•CCM2•ICAP1 complexes (preliminary data). CCM1 also contains a series of ankyrin repeats, for which the binding partners are not yet known. Other interaction partners and functions for CCM1 are also likely: for example, the *C. elegans* orthologue of CCM1 (*kri-1*) is required for cross-tissue signaling in promoting longevity and apoptosis^{25,26}(Appendix 2).

While the interaction between CCM1 and CCM2 occurs at high stoichiometry (the protein ICAP1 is also abundant in these complexes), CCM2 establishes additional interactions, including with the CCM3 protein²⁷, although the fraction of CCM3 that co-purifies with CCM1•CCM2 is small in all cell types we have analyzed. We recently demonstrated, together with M. Fainzilber, that the CCM2 Karet domain²⁸ mediates association with CCM3 (preliminary data). Other interactions were also reported for CCM2, including the upstream component of the p38 MAP kinase pathway MEKK3²². Regulation of Rho signaling by CCM1, CCM2 and CCM3 may involve degradation of Rho protein, and CCM2 has been shown to associate with the SMURF1 ubiquitin E3 ligase in this process¹⁷. Tissue-specific

interactions are also likely, as reported for an interaction between CCM2 (PTB domain) and TrkA, which regulates cell death in medulloblastoma and neuroblastoma cells²⁸. While we have not been able to identify an obvious CCM2 gene in *C. elegans* by homology searches, we will utilize genetics and proteomics approaches to search for a functional homologue in Aim 1.

CCM3: CCM3 was first identified through a screen for genes expressed during the induction of apoptosis in a premyeloid cell line¹². Despite its small size, CCM3 establishes multiple protein-protein interactions, and also homodimerizes via its amino terminus²⁹. However, heterodimerization with members of the germinal center kinase III (GCKIII) family³⁰ via the same region is much favored, as we recently demonstrated (Appendix 4). The interaction between CCM3 and the GCKIII kinases creates a modular unit that can be recruited to different complexes. CCM3 also contains a C-terminal globular domain bearing structural homology to the FAT (focal adhesion targeting) domain of focal adhesion kinase²⁹ which can bind phospholipids³¹, but also associates, at least *in vitro*, with an acidic peptide on paxillin²⁹. Interaction with CCM2²⁹ and the striatin component of STRIPAK (Appendix 4, see below) also occurs via the same molecular contacts, indicating that they are mutually exclusive. Lastly, other interaction partners have been reported for CCM3, most notably the VEGF receptor 2 (VEGFR2), a critical mediator of endothelial cell development that is stabilized by interaction with CCM3³², and a protein tyrosine phosphatase called PTPN13³³. How these other interaction partners are recruited to CCM3 is not currently known. The *C. elegans* CCM3 gene (*C14A4.11*) has not been characterized until now, but our preliminary data indicate that it is critical for tubulogenesis of excretory cells, which we will use as an *in vivo* model to study CCM function (see below).

GCKIII kinases: GCKIII kinases (members of the Sterile 20 kinase family) are critical mediators of CCM3 function. Three members, STK24, STK25 and MST4, are present in human cells that are characterized by a kinase domain followed by a family-defining tail that is used for heterodimerization with CCM3 (Appendix 3). They work positively with CCM3 in cell biology assays in mammalian cells (Appendix 4) and in vascular models. Overexpression of the sole worm GCKIII ortholog can restore truncated excretory canals in *ccm3* mutants to wild type lengths (preliminary data), and overexpression of the GCKIII kinase rescues vascular defects caused by depletion of CCM3 in zebrafish (I Scott, pers comm.). Collectively, these exciting results suggest that the key function of CCM3 is dependent on the kinase activity of GCKIII. How these kinases are activated remains poorly defined, but caspase cleavage has been proposed as a possible mechanism of activation³⁴. In addition, GCKIII localization is affected by oxidative stress^{34b}, activation of the tumor suppressor Lkb1, and depletion of CCM3 or striatin^{35,36} (Appendix 4). Substrates for these kinases still remain largely unknown, though STK25 was shown to phosphorylate a 14-3-3 protein³⁷, and MST4 the ezrin-radixin-moesin (ERM) proteins^{34b,35}. The GCKIII kinases are also implicated in the regulation of p38, JNK and ERK, although there is no clear consensus as to their exact function. While STK25 was reported to phosphorylate CCM3 *in vitro*³³, whether this happens in a cellular context is not known.

STRIPAK: We discovered and characterized the large molecular weight complex STRIPAK (striatin interacting phosphatase and kinase) using interaction proteomics and biochemical methods (Appendix 1), and showed that the majority of CCM3 protein resides within this complex in mammalian cells. STRIPAK possesses both kinase and phosphatase activities, and several of its components have been conserved through eukaryotic evolution (Fig 3), including its cytoskeletal functions. In *S. cerevisiae*, depletion of the STRIPAK components suppresses the lethality and actin polarization defects associated with mutations in the Target of Rapamycin complex 2 (TORC2), as we and our collaborators have recently shown³⁸. In filamentous fungi, STRIPAK promotes membrane fusion^{39,40}, a phenotype that appears conserved in mammals⁴¹. CCM3 and the GCKIII kinases only appear in metazoa, and both are present in *C. elegans*. We recently demonstrated that, like CCM3, depletion of STRIPAK components cause truncations in excretory canals, indicating CCM3 and STRIPAK are

genetically linked in early metazoans. The excretory cell in *C. elegans* will be used here as a model of vascular tube development (see below). In zebrafish embryos, depletion of the GCKIII kinases or of the STRIPAK component striatin produce the same phenotype (a grossly malformed vascular system) as depletion of CCM3⁴² (Ian Scott, pers. comm.). Lastly, experiments in cell lines by our groups and others have revealed additional roles for the STRIPAK and CCM3-associated kinases, for example in Golgi polarization and cell migration. We recently demonstrated that CCM3 and striatin oppose each other in targeting the MST4 kinase to Golgi, where it promotes Golgi polarization towards the leading edge of a wound (Appendix 4). In addition, a recent report demonstrated that PP2A inactivates MST4 via interaction with striatin^{42b} (also see Fig 17), revealing an intricate link between the phosphatase and kinase activities in mediating the biological functions of this complex.

***C. elegans* as a model for understanding CCM gene function.** Homozygous deletion of *ccm1* or *ccm2* in the mouse causes cardiovascular defects and embryonic lethality⁴³⁻⁴⁵ but mice lacking *ccm3* have distinct and more severe phenotypes^{46,47}, consistent with patients harbouring a *ccm3* mutation⁴. While *in vitro* and animal models have provided some mechanistic insight into CCMs, many key questions remain. Firstly, what signaling pathway(s) does CCM3 engage to promote vascular development and integrity? Second, do other CCM genes or modifiers of CCM gene function exist? Since patients with the same mutations present a range of symptoms, it is likely that modifier genes exist, which is one of the key advantages of using *C. elegans* to probe the genetic landscape of CCM genes. The roundworm *C. elegans* is a genetic powerhouse and many of the core signaling pathways that control development and homeostasis are highly conserved in this multicellular organism. Much of what we have learned for these pathways has been derived from unbiased whole-genome genetic screens in *C. elegans*.

Our central hypothesis is that the CCM3•kinase module may target different substrates when associated with the CCM1•CCM2•ICAP1 complex, with the STRIPAK complex or with alternative protein assemblies. We postulate that the worst outcome for CCM3 patients, as well as the distinct phenotypes for CCM1•CCM2 versus CCM3 depletion, may result from a cumulative role for the CCM3•kinase module across these different complexes. Combining worm genetics and functional proteomics will undoubtedly synergize to provide major insights into this disease and reveal new opportunities for treating CCM patients pharmacologically.

B. PRELIMINARY DATA

Our groups have made substantial contributions to understanding the biochemistry and cellular functions of CCM proteins over the past two years. We have generated high quality protein-protein interaction maps for each of the three CCM proteins, characterized the structural nature of the interactions, and identified several genes that modify the biological function of CCM proteins *in vivo*.

Protein-protein interactions: The Gingras lab has established a very solid expertise in the generation of protein-protein interaction maps using affinity purification coupled to mass spectrometry (AP-MS), which consists of the purification of a protein from a cell or tissue source using an affinity step, followed by identification of all proteins associating with the protein of interest using mass spectrometry. We have developed more sensitive biochemical approaches (see, e.g. ^{48,49}), improved tracking of mass spectrometry data⁵⁰, and most importantly, led the development and implementation of statistical tools which enable the identification of true interaction partners among a sea of contaminants⁵¹⁻⁵³. In addition, we have been working closely with our industrial partner AB-SCIEX to implement more sensitive mass spectrometry instruments and robust quantification methods, for example using the new TripleTOF 5600 (e.g. ^{54,55}). With these innovations, we now have a very robust platform dedicated to quantitative interaction proteomics (Fig 4), which has enabled us and our collaborators to make several significant discoveries (e.g. ⁵⁶⁻⁶⁰). Importantly, while we have been using this platform most often within the context of purifications from epitope-tagged proteins expressed at low levels in a model human cell (HEK293, which expresses all three CCM proteins at endogenous

levels and is now believed to be a neuronally derived cell⁶¹), the same approach can be applied to virtually any purification protocol, from tagged or endogenously expressed proteins and in any cell type (or species) we have tried thus far. We determined that the CCM3•STRIPAK interaction occurs endogenously in HEK293 and HeLa cells (Appendices 1 and 3), and in cells of endothelial origin. We performed AP-MS analysis on an allelic series of CCM3 proteins, including point mutants unable to associate with the GCKIII kinases or with STRIPAK. This helped us identify new CCM3 interaction partners, and in many cases to map the interacting regions (Fig 5). We also performed, in collaboration with Mike Fainzilber (Israel), AP-MS analysis with the full-length CCM2 protein, with a truncation mutant expressing only the PTB domain and a truncation mutant expressing only the Karet domain²⁸. This unambiguously defined the PTB domain as the region responsible for interaction with CCM1•ICAP1 and the Karet domain as responsible for the interaction with CCM3. Interestingly, a strong CCM2-kinase interaction (likely mediated by CCM3) was only apparent when the Karet domain was analyzed in isolation. Additional interaction partners for CCM2 were also detected by these approaches, and are listed in Fig 6. Importantly, we have shown that CCM3•GCKIII associates in a mutually exclusive manner with another protein, c10orf47, further expanding the characterization of the range of action of CCM3 and associated kinases (Figs 7-8). We have now also performed AP-MS analysis with CCM1, ICAP1, RAP1A, and several of the new CCM2 and CCM3 interactors; this will be continued in Aim 1.

Whole organism study of CCM function. Dr Derry's lab has developed *C. elegans* as an *in vivo* model to study *ccm1* and *ccm3* function in a multicellular setting, and demonstrated that the powerful genetics of the worm can be used to find new and conserved regulators of CCM signaling. They found that *ccm3* and GCKIII (*gck-1*) mutants recapitulate the human disease phenotype, with extensive truncations and formation of cysts that resemble cavernomas in the excretory cell, a single-celled vasculature structure in this organism (Fig 9). In collaboration, our groups have also provided important mechanistic insights into CCM1-3 function, which are briefly summarized below.

Dr. Derry's lab first identified *ccm1* (known as *kri-1* in *C. elegans*) in a screen for genes that regulate programmed cell death²⁶ (Appendix 2). Following up from this initial work his lab has found that *ccm1* and *ccm3* have distinct functions *in vivo*. Ablation of *ccm1* by mutation or RNAi causes resistance to radiation-induced apoptosis of germline stem cells²⁶ (Appendix 2) and hypersensitivity to osmotic stress (Fig 10). In contrast, ablation of *ccm3* results in truncation of the excretory cell during development, but like *ccm1*, causes hypersensitivity to osmotic stress (Fig 10 & 11). Importantly, ablation of *ccm1* and *ccm3* together results in synthetic lethality (Fig 14), providing strong evidence that these genes act in parallel signaling pathways that impinge on a common cellular process required for viability. Both the human and worm CCM3 proteins interact with all Ste20-like kinases of the GCKIII family^{30,62} (Appendix 3; Fig 12) and Dr. Derry's lab has also shown that ablation of the worm sole GCKIII gene (*gck-1*) causes identical excretory cell truncations as ablating *ccm3* (Fig 13). Furthermore, truncated excretory cells in *ccm3* mutants can be rescued by overexpressing *gck-1* (Fig 13), suggesting that CCM3 activates this kinase to promote excretory canal development/stability. This genetic evidence supports biochemical studies showing that CCM3 and GCKIII function in a common signaling pathway that is distinct from *ccm1/ccm2*. To uncover additional components of the *ccm3*/STRIPAK pathway, Dr. Derry's lab performed a pilot RNAi screen to identify more genes that cause synthetic lethality when knocked down in *ccm1* mutants. After completing a screen of chromosome 1 (~2,700 genes) they identified 35 genes that reproducibly cause synthetic lethality when knocked down in *ccm1* mutants. They refined this list of genes to four, which are required for excretory canal morphology, and thirteen genes that cause hypersensitivity to osmotic stress (Fig 15), similar to *ccm3* mutants. Ablation of the core STRIPAK genes in *C. elegans* resulted in excretory canal truncations that were indistinguishable from *ccm3* or *gck1* mutants (Fig 16), demonstrating a robust conservation of function for this pathway. Genes required for excretory cell development in *C. elegans*

that are also conserved in vertebrates (Aim 2) will be prioritized for proteomic analysis in human cells. One interesting candidate from the screen of chromosome 1 is Y71G12B.11, an open reading frame with high homology to mesoderm development candidate (*MESDC1*), an actin-binding protein also detected in our proteomics screen (Fig 5).

Substrates for the GCKIII kinases. A) *In vivo phosphorylation:* The CCM3•kinase module associates with alternative assemblies and we postulate that some of its interactors can also be substrates for the kinase(s). We therefore carried out pilot experiments to test the feasibility of performing quantitative phosphoproteomics experiments after affinity purification. By combining our AP-MS approach with phosphopeptide enrichment using Immobilized Metal Enrichment Chromatography (IMAC⁶³, Fig 17), we identified >60 phosphorylation sites on the STRIPAK core components. This allows us to monitor variations in phosphorylation, as we showed by treating cells with okadaic acid, a potent pharmacological inhibitor of PP2A enzymes⁶⁴, prior to FLAG purification, IMAC and LC-MS. While there was no drastic change in the global phosphorylation pattern of STRIPAK subunits, we found 12 phosphopeptides that were increased by >3-fold, including a phosphopeptide in the activation segment of the GCKIII kinases. Importantly, this preliminary result supports the feasibility of the *in vivo* phosphorylation experiments proposed in Aim 3. Since the previous submission of this proposal we have developed more sensitive mass spectrometry-based quantification methods (including those presented in Appendix 4) as well as MRM-HR and SWATH (Fig 18). B) *In vitro phosphorylation:* the identification of direct substrates for the GCKIII family has been hampered in part by a relatively poor definition of the consensus site(s) favored by these kinases. James Knight (Gingras lab) developed a novel approach for the identification of substrates by *in vitro* phosphorylation from a total cell lysate^{64b}. This method involves the irreversible inactivation of all kinases from the lysate using the ATP analog 5'-4-fluorosulfonylbenzoyladenosine (FSBA) followed by *in vitro* phosphorylation with an exogenously-added kinase. Because of its compatibility with both ³²P labeling and quantitative mass spectrometry, this is an excellent approach for identifying kinase substrates. We have begun applying this approach to the GCKIII kinases, starting with MST4, and identified a potential consensus motif for phosphorylation, as well as several *in vitro* substrates. Interestingly, these include the STRIPAK component MOB3, which we have validated with recombinant proteins (Figs 19-21).

C. RESEARCH PROPOSAL

In order to uncover the molecular pathways that lead to CCM pathology, we will utilize the powerful and complimentary methods of proteomics and genetics in mammalian cells and *C. elegans*. Our three Specific Aims, as described in detail below, are to:

Aim 1: Establish physical interaction maps for CCM proteins in mammals and *C. elegans*

Aim 2: Define the global genetic interaction map for CCM1 and CCM3

Aim 3: Identify substrates for GCKIII kinases

Aim 1. Establish physical interaction maps for CCM proteins in mammals and *C. elegans*

A. Refine and expand the interactome maps for CCM proteins in HEK293 cells. As mentioned above, we have generated a high-density interaction map surrounding CCM3 that has led to the identification of the STRIPAK complex into which CCM3 predominantly resides; new interactors for CCM2 and CCM3 have also been uncovered (Figs 5 and 6). **Methods and expected outcomes:** Newly discovered interactors from the proteomics screens (in years 1-2), and high confidence interactors from the genetic screens (in years 3-5; see Aim 2) will be cloned and epitope-tagged, expressed in the Flp-In T-REx human HEK293 tetracycline inducible cells (this allows for a single integration event, and tunable expression^{54,66}). These reagents will also be used as baits for AP-MS analysis (many of these proteins have already been cloned and expressed in the Flp-In T-REx cells). We have access at the

Lunenfeld to collections of full-length cDNAs that should encompass most of the discovered interactors. This strategy is routinely used in our group, and should not present major difficulties. In the case where expression of a given interaction partner proved difficult, we will employ alternative expression systems which we have done extensively in the past (e.g. ^{67,68}). In addition, as we have done for CCM3 and CCM2, mutagenesis of CCM1 will be performed to eliminate isolated protein domain-mediated interactions and attempt to provide more structural information; when appropriate, the same strategy will be undertaken for the newly identified interactors. Similar mutations will be introduced to the orthologous worm genes and expressed in the appropriate knock out strain to determine which residues are important for their *in vivo* functions. Taken together, this should expand the knowledge of the molecular context into which the CCM proteins and their genetic interactors reside. New physical interacting partners will also be functionally characterized in cells and *C. elegans* (Aim 2).

B. Investigate the CCM interaction networks in endothelial cells. Our preliminary data indicate conservation of the CCM3•kinase•STRIPAK complex across cell types; however, it is possible that we may have missed interaction partners relevant to the disease by performing our initial analyses in HEK293 cells. To address this issue, we will characterize the interaction profiles of CCM1, CCM2 and CCM3 in endothelial cells. We have already demonstrated that antibodies to endogenous proteins can be used to perform AP-Western and AP-MS (Appendices 1 and 4). **Methods:** We will use antibodies to endogenous CCM1, CCM2 and CCM3 proteins to identify interaction partners from endothelial model cell lines, including HUVEC, and bovine lymphatic, venous and aortic endothelial cells (all provided generously by D. Dumont), using protocols well established in the Gingras lab (Appendices 1,4) ^{51,55,69}. Control samples will include isotype-matched antibodies and antibodies to unrelated proteins to eliminate common contaminants and multiple affinity reagents will be used per protein analyzed.

Alternative strategy: If any endogenous protein cannot be efficiently immunoprecipitated, AP-MS will be performed using recombinant proteins expressed with lentivirus, as we recently have done⁶⁸. If endogenous antibody cross-reactivity is an issue, AP-MS will be performed after knocking down the bait protein and analyzing the resulting interactions by quantitative proteomics (as in ⁶⁶). **Expected outcomes:** we may uncover additional endothelial specific CCM interactors: orthologs in *C. elegans*

will be investigated as described in Aim 2. We also note that, while the endothelium is clearly affected in the disease, CCMs may also have a neuronal, and/or smooth muscle defect, as the SMC layer is missing from CCM lesions, and a tissue-specific knock-out of CCM3 in neurons exhibits CCM-like phenotypes⁴⁷. If no new partner for CCM is detected in endothelial cells, neuronal and smooth muscle interactors will be investigated.

C. Define the physical CCM interactome of *C. elegans*. We have not been able to identify a CCM2 orthologue in *C. elegans* by sequence searching. Given that we consistently detect strong physical interactions between CCM1 and CCM2 in mammalian cells and that CCM2 is able to bridge CCM1 and CCM3, we hypothesize that a functional orthologue of CCM2 exists in worms and binds CCM1 and/or CCM3 *in vivo*. Several proteins encoded in the *C. elegans* genome that are below the limit of detection by sequence homology have been identified and shown to exhibit structurally homology to mammalian proteins. For example, Dr. Derry was the first to identify the elusive *C. elegans* p53 protein (CEP-1) which has only ~15% sequence identity with human p53 but 74% structural homology with the DNA binding domain of human p53^{70,71}. We propose to use the available GFP-tagged transgenic lines for worm CCM1 and CCM3 (as well as negative controls) to perform AP-MS analysis.

Alternatively, we will raise polyclonal antibodies to *C. elegans* CCM1 and CCM3 to use for the purification of the endogenous proteins from cell lysate prepared from *C. elegans*⁷². Interacting proteins will be identified by mass spectrometry, as described above. **Alternative strategy and expected outcomes:** Given that our proteomics methods have worked well, we anticipate no major drawbacks in *C. elegans*, and we expect to identify not only a CCM2 ortholog, but also additional binding partners for worm CCM1 and CCM3 (these may or may not be the orthologs of the binding partners identified

in mammalian cells). As an alternative strategy to identify CCM2, we will use RNAi to knock down the expression of the thirteen *C. elegans* proteins that contain phosphotyrosine binding (PTB) domains (the most conserved feature of the vertebrate CCM2 protein as well as the ICAP1 protein for which no worm ortholog can be detected, with the possible exception of Y45F10D.10) and determine if they are synthetically lethal with CCM3, or required for CCM1/*kri-1*-dependent apoptosis (see Aim 2). Note that as the genetic screens described in Aim 2 progress, we may also identify a CCM2 ortholog on the basis of genetic interaction with CCM3. If the putative CCM2 ortholog is detected by genetic means, the first step of validation will be to determine whether it can physically associate with worm CCM1 and/or CCM3, both by co-immunoprecipitation/immunoblotting and via the use of recombinant proteins expressed in bacteria (e.g. Appendix 3). If we uncover new partners not detected in mammalian cell lines, interaction between the human orthologs will also be assessed. This work will set the stage for future work testing the therapeutic potential of these proteins for suppressing the phenotypes associated with loss of CCM gene function.

D. Analyze regulated interactions for the CCM proteins. As knowledge of the signaling pathways leading to CCM signaling expands, we will revisit which of the interactions are regulated; this aim will be integrated with the phosphorylation analysis described below. **Methods:** We already have cell lines expressing tagged CCM1, CCM2, CCM3, ICAP1 and the three GCKIII kinases. Each cell line will be subjected to a number of treatments known to affect CCM signaling. Briefly, the tagged proteins will be purified in parallel, and analyzed either by IP-western using antibodies to the known partners, or by quantitative proteomics using label-free quantification as in Appendix 4. For the characterization by IP-Western, we will establish time-course and dose-dependence curves. Because of the reported role of the GCKIII kinases (and CCM3) in stress pathways, we will first explore oxidative stress (using H₂O₂⁷³⁻⁷⁵), osmotic stress (400mM sorbitol), chemical anoxia (sodium cyanide and 2-deoxyglucose⁷⁶) and staurosporine³⁴. In addition, we will investigate whether stimulation of endothelial cells with vascular endothelial growth factor (VEGF)³² or of neurons with nerve growth factor (NGF)²⁸ alters the interactions. **Alternative strategy:** In our hands, the label free quantitation has been working well for identifying regulated protein interactions, but if this was not successful here, we would employ the SILAC (stable isotopic labeling with amino acids in cell culture⁷⁷) approach which has been optimized at our institute⁷⁸ (see ⁷⁹ for a review). **Expected outcomes:** We expect that one or more of the interactions will be regulated by selected treatments. Post-translational modifications detected by mass spectrometry are also anticipated. Once we identify regulated interactions, we will focus on their characterization: 1) are the interactions regulated by other physiologically relevant treatments? 2) do these interactions require post-translational modifications? 3) what are the consequences of abrogating the interaction, or of generating a constitutive interaction?

E. Assess the organization of the CCM interaction network. As shown in Appendices 3 and 4, we have been able to identify at the molecular level how interactions between STRIPAK, CCM3 and the GCKIII kinases occur. Given the relevance of CCM proteins and their binding partners in CCMs, we will pursue this work with the newly identified physical and genetic interaction partners of CCM proteins. **Methods:** Truncation analysis followed by immunoblotting or mass spectrometry (as in Appendix 4, Fig 1) will be performed to uncover the regions of each of the proteins mediating interactions (focusing on regulated interactions). We will also, when appropriate, deplete selected proteins by RNA interference and monitor the recovery of binding partners after immunoprecipitation and immunoblotting (or MS), as in Appendix 4. Taken together with quantitative proteomics information, this will help us narrow down direct interactors. As we did in Appendices 3 and 4, we will then express the proteins in bacteria (or the baculovirus expression system), and monitor direct interactions. Lastly, we will refine the mapping of the direct protein-protein interactions by mutagenesis and binding assays, as we are doing routinely e.g. ^{49,55,80}, and by peptide array strategies as in Appendix 4. This work will be performed in a continued collaboration with F. Sicheri (letter

attached). **Expected outcomes:** We do not anticipate any major conceptual difficulty with this aim, but technical difficulties may arise. Some of the proteins or protein fragments may be difficult to express, or exhibit poor solubility, for example. In this case, we typically adopt different expression systems (e.g. baculovirus or *in vitro* transcription/translation⁶⁷), or alter the construct boundaries or the species used (e.g. ⁸¹). Silencing the expression of a given protein may in itself alter the expression or stability of its binding partners (as we observed in ⁴⁹), which would complicate the analysis of the silencing experiment. Despite these difficulties, we should be able to provide a much clearer picture of the molecular assembly of the CCM pathway components. As we identify substrates and interactors in Aims 1-3, the information regarding post-translational modifications (and especially phosphorylation) will be interpreted within the context of this binding site mapping.

Aim 2: Defining the CCM genetic interaction network

A. Phenotypic assessment for physical interaction partners and potential substrates: As we have done for the STRIPAK components (preliminary data), we will test each of the interaction partners detected in Aim 1 and the high confidence potential substrates from Aim 3 for CCM1- and CCM3-associated functions in human cell lines and in *C. elegans*. **Method 1:** In *C. elegans*, confirmed binding partners (or orthologs of human partners) will be analyzed for CCM1 (*kri-1*)-related functions by assaying for resistance to germline apoptosis as we have described (i.e. ^{26,82-84}) and hypersensitivity to osmotic stress (Fig 10). To determine CCM3-related functions, we will ablate candidates by RNAi and look for truncations and cyst formation in excretory cells of living animals (Fig 11). **Method 2:** Interaction partners and substrates identified above will be knocked down by RNAi to determine their role in a) localizing MST4 at the Golgi and affecting Golgi polarization (Appendix 4), b) modulating the expression of Rho proteins¹⁷, c) protecting from or promoting apoptosis⁸⁵, and d) signaling through MAP kinase pathways³⁰. As new biological readouts become available (including through Aim 1D), new assays will also be implemented. **Expected outcomes:** The advantage of these functional validation approaches is that they are scalable, enabling us to test dozens of candidates in parallel. While we do not expect all of them to generate a clear phenotype across all readouts, this strategy will help us prioritize hits to follow up in depth.

B. Genetic modifier screen in *C. elegans* to uncover novel CCM3 signaling proteins: Genes operate in signaling pathways that control all biological processes, and most developmental processes require collaboration between distinct signaling pathways to ensure robustness. The key advantages of using *C. elegans* as model system to understand how genes collaborate during development and in disease states are its amenability to genetic manipulation, the ability to study genes in a multicellular setting, and the high degree of conservation in gene structure and function with humans⁸⁶. We hypothesize that delineating genetic interactions with *ccm1* and *ccm3* in *C. elegans* will uncover conserved pathways in vertebrates relevant to the pathology of CCMs. **Methodology:** *C. elegans* use bacteria as a source of food and growing these animals on bacteria that produce double-stranded RNA to worm genes result in potent and specific knock down of the endogenous gene in these animals and their progeny^{86b}. This RNAi approach allows for rapid, whole-genome screens^{86c, 86d}. We found that knocking down via RNAi the *C. elegans* *ccm3* gene in *ccm1* mutant animals results in synthetic lethality (Fig 14), suggesting that these genes function in parallel signaling pathways. Furthermore, ablation of *ccm3* by RNAi or mutation causes a severe truncation of the excretory cell (Fig 11), the only vasculature structure present in *C. elegans*. We hypothesize that other genes that cause synthetic lethality in *ccm1* mutants will reveal additional components of the *ccm3* pathway. To achieve this goal, we will first systematically knock down worm genes in *ccm1* mutants by the RNAi feeding method as we have previously described⁸²⁻⁸⁴. Genes that cause synthetic lethality when knocked down in *ccm1* mutants will be examined for defects in development of the excretory cell. Briefly, transgenic lines that express *pes-6::GFP* in the excretory cell (Fig 9C) will be grown on bacteria producing double-stranded RNA to

genes that exhibit synthetic lethal interactions with *ccm1*. The effect of inhibiting these genes on excretory cell length and morphology will be monitored over a period of 1 week and quantified in staged young adult animals. From a pilot RNAi screen of chromosome 1 we identified 35~2,700 genes that exhibit synthetic lethality in *ccm1* mutants, of which four are required for proper excretory cell development (Fig 14-15). In addition, since we have identified a role for *ccm1* and *ccm3* in osmoregulation we will also evaluate this for candidate genes by growing animals on bacterial RNAi plates containing 400 mM NaCl then quantifying viability (Fig 10). We anticipate that it will take approximately 24 months to complete the rest of the genome. Analysis of excretory cell lengths, osmotic stress, and other phenotypes (i.e., apoptosis) will take an additional 12-24 months, depending on the number of positive hits obtained in the genome-wide screen. Based on the number of genes identified on chromosome 1 we anticipate uncovering 25-50 more genes (5-10 genes per chromosome – *C. elegans* has five autosomes and one sex chromosome) that function in the *ccm3* pathway to regulate excretory cell morphology. Prioritization of potential *ccm3* pathway genes will be as follows: (i) reproducible synthetic lethal interactions with *ccm1*, (ii) defects in excretory cell development (when knocked down alone or in *ccm1* mutants), and (iii) conservation of interacting genes in vertebrates. Genes that fulfill all three of these criteria will be prioritized for future analysis of vascular phenotypes in mouse models with our collaborator Dr. Murat Gunel (see letter of collaboration) and pipelined for identification of physical interaction partners for mammalian orthologs (Aim 1)

C. Expression patterns and tissue-specific requirements for CCM3 signaling proteins.

To determine where the novel CCM pathway genes are expressed we will clone their promoters and open reading frames and generate GFP fusions. These constructs will be injected into worms to generate transgenic lines in order to visualize their spatiotemporal expression patterns throughout development, which is routinely carried out in the Derry lab. The expression constructs will also be used to rescue excretory cell defects and other phenotypes in strains carrying loss-of-function mutations in candidate genes. Combined, the *C. elegans* knockout consortium and Million Mutation Project has generated over 9,000 null alleles, and the list is growing (D. Moerman, pers comm.). If a knockout does not exist for the top hits identified in our RNAi screen we will make our own deletion by standard mutagenesis and PCR screening, as we have previously done⁷⁰. Once we establish the tissues in which these genes are required we will attempt to rescue the various phenotypes (excretory canal truncations, osmotic stress, etc) by cloning the gene into tissue-specific expression vectors. This will be critical for understanding their biological functions in a multicellular setting since CCM proteins have important roles in cross-tissue signaling, as we demonstrated for the worm *ccm1* gene, *kri-1* (Appendix 2). We are currently generating tissue-specific promoters driving *kri-1* or *ccm3* only in the excretory cell (*pes-6* promoter), the intestine (*elt-2* promoter), and other tissues to determine the tissue of focus for excretory cell morphology, apoptosis, and osmotic tolerance. These experiments will set the stage for understanding how CCM proteins collaborate with their binding partners to control their various biological functions through autonomous and/or non-autonomous signaling.

Aim 3: Identify substrates for GCKIII kinases

Very few substrates have been uncovered for the GCKIII family members, and a consensus site for phosphorylation is not yet clearly defined. We propose a comprehensive approach to identify *bona fide* substrates using active versions of each kinase (Appendix 3) and cell lines expressing FLAG-tagged versions of each kinase, including point mutants that abolish their catalytic activity.

A. Candidate approach. We postulate that one or more of the interaction partners for CCM3•kinase pairs may be a substrate for the GCKIII kinases. Even though kinase-substrate interactions have not been generally regarded as stable enough to withstand biochemical purification, there has been an increasingly high number of interactions pairs confirmed to be enzyme-substrate partners. Re-analysis of our yeast kinome data⁵¹ by computational biologists revealed a statistically significant enrichment in

the interaction partners for consensus motifs associated with each kinase (P.M. Kim, pers comm.), and preliminary data in Mike Fainzilber's laboratory has identified CCM2 as a putative target for STK25. We therefore propose to test whether components of the CCM1•CCM2•ICAP1 complex, STRIPAK, or new interaction partners (identified genetically or physically) can be substrates for any of the three kinases. **Methods:** Active and dead kinases will be incubated with recombinantly expressed proteins in the presence of γ -³²P-ATP and incorporation monitored by autoradiography. We will purify previously reported substrates of these kinases (14-3-3zeta, ezrin) to serve as positive controls. Once a putative substrate is identified, phosphorylation reactions will be performed in the absence of ³²P, and sites identified by mass spectrometry. As a final level of confirmation, we will perform alanine substitution and test for phosphorylation, as we have described⁸⁷⁻⁸⁹. **Caveats and expected outcomes:** This approach will be limited to those proteins that we can express recombinantly, though expression of our constructs in other systems (e.g. in the transient mammalian T7/vaccinia hybrid expression system⁹⁰) could also be performed. *In vivo* phosphorylation mapping will be attempted as described below.

B. Global *in vitro/in vivo* analysis. In order to complement the candidate approach described above, we will exploit an unbiased approach for the identification of kinase substrates (Fig 19). **Methods:** Endothelial cell lysates will be treated with the ATP analog FSBA to inactivate all endogenous kinases, and desalted lysates will be incubated with one of the GCKIII kinases (active or dead). After optimization of the conditions using radioactive assays, we will scale up the reactions and couple them with quantitative mass spectrometry using isotopic based labeling (we have used dimethyl-labeling for the preliminary data showed in Fig 20, but will alternatively employ the widely used stable isotope labeling with amino acids in cell culture; SILAC^{77,79,78}). We will perform biological replicates analysis, permuting the kinases and isotopic labels. After phosphorylation assays, the kinases will be inactivated, lysates subjected to proteolysis and phosphopeptide enrichment with titanium dioxide and IMAC. The phosphopeptides will be identified and quantified using high mass accuracy mass spectrometers. Statistically significant changes in phosphorylation will be analyzed to identify potential phosphorylation motifs. *In vitro* phosphorylation may not be fully representative of the situation *in vivo*, and a modification of the substrate screening approach has been developed to emphasize substrates more likely to be biologically relevant (Fig 19, 21). This approach exploits a parallel mapping of sites dependent on the presence of a kinase *in vivo*, and those which can be directly targeted *in vitro*. When kinase inhibitors are available, they will be used; however, in the case of the GCKIII kinases, we will employ cells in which individual kinases have been depleted by RNAi knock-down. Alternatively, in collaboration with Geoff Hicks (U Manitoba) we are generating mouse ES knockout lines for each of the three kinases as well as a knock-in line in which the kinase binding site of CCM3 has been deleted. Each of these cell lines will be compared to wild-type in phosphorylation mapping experiments. **Caveats and expected outcomes:** We have performed a preliminary substrate identification analysis for MST4 in HEK293 cells lysate, and found several possible targets, including the STRIPAK component MOB3, which we have validated. As an alternative approach to the FSBA method (in case it does not work as well with STK24 or STK25), we would investigate the use of a gatekeeper-mutated kinase and bulky-ATP analog (i.e. the Shokat kinases⁹¹). It is also possible that pre-phosphorylation of the sites in the lysate may occlude the effect of the kinases. If this is the case, we will pre-treat the lysate with a phosphatase prior to adding the kinase or use lysate deficient in the GCKIII kinases. Lastly, while we believe that isotope-based approaches are the simplest for this strategy, if necessary we will consider other quantitative mass spectrometry methods, including SRM⁹², TRAQ labeling⁹³, or the SWATH technique that we recently implemented in the lab (Fig 18). While we will initially attempt the phosphoproteomics experiments using mouse ES cells, they will be repeated after differentiation into endothelial/neuronal lineages (and in co-cultures).

C. Validation of the substrates *in vitro* and *in vivo*. **Methods:** Candidates substrates identified in Aims 3A and 3B will be validated as follows: 1) for substrates for which we already have stable cell lines,

quantitative phosphoproteomics will be performed following depletion of individual kinases (or all three kinases, simultaneously) by RNAi and immunoprecipitation of the FLAG-tagged bait protein (similar to what we have done with STRIPAK components following treatment with okadaic acid in Fig 17, using our newer more accurate quantification methods). Phosphorylation events that can be recapitulated in cells will be further investigated (see below). 2) For substrates identified in Aim 3B, we will first validate the phosphorylation *in vitro* as in 3A; validated sites will be analyzed in cells and in *C. elegans*, as above. 3) We will perform site-directed mutagenesis to confirm the identification of the phosphorylation site and the kinase-substrate relationship; these mutants will also be used to address the physiological consequences of phosphorylation. 4) For sites of particular interest (e.g. those in MOB3, CCM2, etc.), we will raise phosphospecific antibodies^{87,88} to examine in details signaling through the CCM proteins. **Expected outcomes:** We have already identified a number of phosphorylation targets of MST4, including MOB3 for which we have initiated validation. Other highly modulated putative substrates, and substrates biologically linked to CCM signaling will be pursued for validation studies, as below. Our plan for hit prioritization is depicted in Fig 21.

Alternative strategies. Forward genetic screen in *C. elegans ccm3* mutants. While we expect that our RNAi screen may uncover some direct targets of the GCKIII kinases, forward mutagenesis screens have identified kinase substrates in *C. elegans*. One advantage of a mutagenesis screen compared with RNAi-based screening is that rare gain-of-function alleles can be identified, which is important if the target of the kinase becomes activated by phosphorylation. For example, gain-of-function mutations in the *pdk-1* and *akt-1* genes were identified from mutagenesis screen carried out in *age-1*/PI3K loss-of-function mutants⁹⁷. The *pdk-1* gene is directly downstream of *age-1*/PI3K and the AKT-1 kinase is phosphorylated and activated by PDK-1. There are many more examples of how forward genetics has uncovered kinase substrates and signaling pathways in *C. elegans*, so we expect this to be a fruitful alternative to the proteomics approaches. **Expected outcomes:** These screens are routinely carried out in the Derry lab and we anticipate no major problems with this method. Top candidates will be prioritized based on how well they restore excretory cell morphology in *ccm3* mutants, then pipelined for kinase assays, as described above.

D. PERSPECTIVES.

The proposed studies in this application are the result of collaborative work initiated two years ago between Anne-Claude Gingras and Brent Derry. The serendipitous discoveries of new biological roles and binding partners for CCM proteins presented a unique opportunity to combine our strengths to understand the molecular mechanisms that underlie this devastating disease. The two papers we recently published in JBC are a testament of our commitment to work together in this new and emerging area. We will exploit the complimentary tools of proteomics and genetics to understand how the CCM3/STRIPAK pathway contributes to vascular integrity in *C. elegans* and discover new components of this network. We have assembled a team of outstanding collaborators with expertise in all facets of this project, including Dr. Frank Sicheri (structural biology), Dr. Geoff Hicks (ES knockouts, knock-ins), and Dr. Ian Scott (zebrafish models of CCM). This project represents a new direction of research for Dr. Derry and Dr. Gingras, and is independent of their other CIHR-funded work. While we are still at the discovery phase of the molecular mechanisms of CCMs, the proposed project is performed in close collaboration and consultation with Dr. Murat Gunel, a neurosurgeon and CCM expert, who will follow-up on candidates detected in this study to determine if the corresponding genes are mutated in patient samples. We are also communicating our results to Dr. Issam Awad, another leading CCM clinician who is currently performing pre-clinical trials for ROCK inhibitors in CCM mouse models and is seeking other therapeutic targets. We anticipate that this work will uncover new proteins that can be targeted for the clinical treatment of CCM disease in humans, which will offer hope for patients.

E. REFERENCES:

1. K. M. Krisht, K. J. Whitehead, T. Niazi et al., *Neurosurg Focus* 29 (3), E2 (2010).
2. R. E. Clatterbuck, C. G. Eberhart, B. J. Crain et al., *J Neurol Neurosurg Psychiatry* 71 (2), 188 (2001).
3. S. Yadla, P. M. Jabbour, R. Shenkar et al., *Neurosurg Focus* 29 (3), E4 (2010).
4. C. Denier, P. Labauge, F. Bergametti et al., *Ann Neurol* 60 (5), 550 (2006).
5. S. Stahl, S. Gaetzner, K. Voss et al., *Hum Mutat* 29 (5), 709 (2008).
6. P. Labauge, C. Denier, F. Bergametti et al., *Lancet Neurol* 6 (3), 237 (2007).
7. S. Laberge-le Couteulx, H. H. Jung, P. Labauge et al., *Nat Genet* 23 (2), 189 (1999).
8. T. Sahoo, E. W. Johnson, J. W. Thomas et al., *Hum Mol Genet* 8 (12), 2325 (1999).
9. C. L. Liquori, M. J. Berg, A. M. Siegel et al., *Am J Hum Genet* 73 (6), 1459 (2003).
10. C. Denier, S. Goutagny, P. Labauge et al., *Am J Hum Genet* 74 (2), 326 (2004).
11. B. Guclu, A. K. Ozturk, K. L. Pricola et al., *Neurosurgery* 57 (5), 1008 (2005).
12. F. Bergametti, C. Denier, P. Labauge et al., *Am J Hum Genet* 76 (1), 42 (2005).
13. J. Gault, R. Shenkar, P. Recksiek et al., *Stroke* 36 (4), 872 (2005).
14. A. L. Akers, E. Johnson, G. K. Steinberg et al., *Hum Mol Genet* 18 (5), 919 (2009).
15. R. A. Stockton, R. Shenkar, I. A. Awad et al., *J Exp Med* 207 (4), 881 (2010).
16. A. L. Borikova, C. F. Dibble, N. Sciaky et al., *J Biol Chem* 285 (16), 11760 (2010).
17. L. E. Crose, T. L. Hilder, N. Sciaky et al., *J Biol Chem* 284 (20), 13301 (2009).
18. T. Pawson and P. Nash, *Science* 300 (5618), 445 (2003).
19. S. Beraud-Dufour, R. Gautier, C. Albiges-Rizo et al., *FEBS J* 274 (21), 5518 (2007).
20. A. Glading, J. Han, R. A. Stockton et al., *J Cell Biol* 179 (2), 247 (2007).
21. I. Serebriiskii, J. Estojak, G. Sonoda et al., *Oncogene* 15 (9), 1043 (1997).
22. J. S. Zawistowski, L. Stalheim, M. T. Uhlik et al., *Hum Mol Genet* 14 (17), 2521 (2005).
23. J. Zhang, R. E. Clatterbuck, D. Rigamonti et al., *Hum Mol Genet* 10 (25), 2953 (2001).
24. J. S. Zawistowski, I. G. Serebriiskii, M. F. Lee et al., *Hum Mol Genet* 11 (4), 389 (2002).
25. J. R. Berman and C. Kenyon, *Cell* 124 (5), 1055 (2006).
26. S. Ito, S. Greiss, A. Gartner et al., *Curr Biol* 20 (4), 333 (2010).
27. T. L. Hilder, M. H. Malone, S. Bencharit et al., *J Proteome Res* 6 (11), 4343 (2007).
28. L. Harel, B. Costa, M. Tcherpakov et al., *Neuron* 63 (5), 585 (2009).
29. X. Li, R. Zhang, H. Zhang et al., *J Biol Chem* 285 (31), 24099 (2010).
30. X. Ma, H. Zhao, J. Shan et al., *Mol Biol Cell* 18 (6), 1965 (2007).
31. C. F. Dibble, J. A. Horst, M. H. Malone et al., *PLoS One* 5 (7), e11740 (2010).
32. Y. He, H. Zhang, L. Yu et al., *Sci Signal* 3 (116), ra26 (2010).
33. K. Voss, S. Stahl, E. Schleider et al., *Neurogenetics* 8 (4), 249 (2007).
34. C. Y. Huang, Y. M. Wu, C. Y. Hsu et al., *J Biol Chem* 277 (37), 34367 (2002).
- 34b. M. Fidalgo, A. Guerrero, M. Fraile et al., *J Biol Chem*, *in press*, PMID:22291017 (2012)
35. J. P. ten Klooster, M. Jansen, J. Yuan et al., *Dev Cell* 16 (4), 551 (2009).
36. B. M. Filippi, P. de los Heros, Y. Mehellou et al., *EMBO J* 30 (9), 1730 (2011).
37. C. Preisinger, B. Short, V. De Corte et al., *J Cell Biol* 164 (7), 1009 (2004).
38. A. Baryshnikova, M. Costanzo, Y. Kim et al., *Nat Methods* 7 (12), 1017 (2010).
39. A. R. Simonin, C. G. Rasmussen, M. Yang et al., *Fungal Genet Biol* 47 (10), 855 (2010).
40. Q. Xiang, C. Rasmussen, and N. L. Glass, *Genetics* 160 (1), 169 (2002).
41. R. M. Guzzo, J. Wigle, M. Salih et al., *Biochem J* 381 (Pt 3), 599 (2004).
42. X. Zheng, C. Xu, A. Di Lorenzo et al., *J Clin Invest* 120 (8), 2795 (2010).
- 42b. J. Gordon, J. Hwang, K.J. Carrier et al., *BMC Biochem* 12, 54 (2011)
43. K. J. Whitehead, N. W. Plummer, J. A. Adams et al., *Development* 131 (6), 1437 (2004).
44. N. W. Plummer, C. J. Gallione, S. Srinivasan et al., *Am J Pathol* 165 (5), 1509 (2004).
45. N. W. Plummer, T. L. Squire, S. Srinivasan et al., *Mamm Genome* 17 (2), 119 (2006).

46. A. C. Chan, S. G. Drakos, O. E. Ruiz et al., *J Clin Invest* 121 (5), 1871 (2011).
47. A. Louvi, L. Chen, A. M. Two et al., *Proc Natl Acad Sci U S A* 108 (9), 3737 (2011).
48. G. I. Chen and A. C. Gingras, *Methods* 42 (3), 298 (2007).
49. G. I. Chen, S. Tisayakorn, C. Jorgensen et al., *J Biol Chem* 283 (43), 29273 (2008).
50. G. Liu, J. Zhang, B. Larsen et al., *Nat Biotechnol* 28 (10), 1015 (2010).
51. A. Breitkreutz, H. Choi, J. R. Sharom et al., *Science* 328 (5981), 1043 (2010).
52. H. Choi, B. Larsen, Z. Y. Lin et al., *Nat Methods* 8 (1), 70 (2011).
53. D. V. Skarra, M. Goudreault, H. Choi et al., *Proteomics* 11 (8), 1508 (2011).
54. W. H. Dunham, B. Larsen, S. Tate et al., *Proteomics* 11 (13), 2603 (2011).
55. M. J. Kean, D. F. Ceccarelli, M. Goudreault et al., *J Biol Chem* 286 (28), 25065 (2011).
56. Z. Li, F. J. Vizeacoumar, S. Bahr et al., *Nat Biotechnol* 29 (4), 361 (2011).
57. L. O'Donnell, S. Panier, J. Wildenhain et al., *Mol Cell* 40 (4), 619 (2010).
58. S. Nakada, I. Tai, S. Panier et al., *Nature* 466 (7309), 941 (2010).
59. M. Costanzo, A. Baryshnikova, J. Bellay et al., *Science* 327 (5964), 425 (2010).
60. S. Lawo, M. Bashkurov, M. Mullin et al., *Curr Biol* 19 (10), 816 (2009).
61. G. Shaw, S. Morse, M. Ararat et al., *FASEB J* 16 (8), 869 (2002).
62. S. Li, C. M. Armstrong, N. Bertin et al., *Science* 303 (5657), 540 (2004).
63. T. E. Thingholm and O. N. Jensen, *Methods Mol Biol* 527, 47 (2009).
64. J. J. Fernandez, M. L. Cadenas, M. L. Souto et al., *Curr Med Chem* 9 (2), 229 (2002).
- 64b. J. R. Knight, R. Tian, R.E.C. Lee et al., *Skeletal Muscle*, *in press* (2012).
65. J. T. Murray, D. G. Campbell, M. Peggie et al., *Biochem J* 384 (Pt 3), 489 (2004).
66. T. Glatter, A. Wepf, R. Aebersold et al., *Mol Syst Biol* 5, 237 (2009).
67. A. C. Gingras, M. Caballero, M. Zarske et al., *Mol Cell Proteomics* 4 (11), 1725 (2005).
68. A. B. Mak, Z. Ni, J. A. Hewel et al., *Mol Cell Proteomics* 9 (5), 811 (2010).
69. M. Goudreault, L. M. D'Ambrosio, M. J. Kean et al., *Mol Cell Proteomics* 8 (1), 157 (2009).
70. W. B. Derry, A. P. Putzke, and J. H. Rothman, *Science* 294 (5542), 591 (2001).
71. Y. Huyen, P. D. Jeffrey, W. B. Derry et al., *Structure* 12 (7), 1237 (2004).
72. T. F. Duchaine, J. A. Wohlschlegel, S. Kennedy et al., *Cell* 124 (2), 343 (2006).
73. C. B. Chen, J. K. Ng, P. H. Choo et al., *Biosci Rep* 29 (6), 405 (2009).
74. C. M. Pombo, J. V. Bonventre, A. Molnar et al., *EMBO J* 15 (17), 4537 (1996).
75. J. Zhou, Z. Shao, R. Kerkela et al., *Mol Cell Biol* 29 (15), 4167 (2009).
76. E. Nogueira, M. Fidalgo, A. Molnar et al., *J Biol Chem* 283 (23), 16248 (2008).
77. S. E. Ong, B. Blagoev, I. Kratchmarova et al., *Mol Cell Proteomics* 1 (5), 376 (2002).
78. C. Jorgensen, A. Sherman, G. I. Chen et al., *Science* 326 (5959), 1502 (2009).
79. A. C. Gingras, M. Gstaiger, B. Raught et al., *Nat Rev Mol Cell Biol* 8 (8), 645 (2007).
80. D. F. Ceccarelli, R. C. Laister, V. K. Mulligan et al., *J Biol Chem* 286 (28), 25056 (2011).
81. J. Marcotrigiano, A. C. Gingras, N. Sonenberg et al., *Cell* 89 (6), 951 (1997).
82. M. X. Gao, E. H. Liao, B. Yu et al., *Cell Death Differ* 15 (6), 1054 (2008).
83. C. Quevedo, D. R. Kaplan, and W. B. Derry, *Curr Biol* 17 (3), 286 (2007).
84. A. J. Ross, M. Li, B. Yu et al., *Cell Death Differ* 18 (7), 1140 (2011).
85. I. Dan, S. E. Ong, N. M. Watanabe et al., *J Biol Chem* 277 (8), 5929 (2002).
86. E. M. Jorgensen and S. E. Mango, *Nat Rev Genet* 3 (5), 356 (2002).
- 86b. L. Timmons and A. Fire, *Nature* 395 (6705), 854 (1998).
- 86c. A.G. Fraser, R.S. Kamath, P. Zipperlen et al., *Nature* 408 (6810), 325 (2000).
- 86d. R.S. Kameth, A.G. Fraser, Y. Dong et al., *Nature* 421 (6920), 231 (2003).
87. A. C. Gingras, S. P. Gygi, B. Raught et al., *Genes Dev* 13 (11), 1422 (1999).
88. A. C. Gingras, B. Raught, S. P. Gygi et al., *Genes Dev* 15 (21), 2852 (2001).
89. S. G. Whalen, A. C. Gingras, L. Amankwa et al., *J Biol Chem* 271 (20), 11831 (1996).
90. T. R. Fuerst, E. G. Niles, F. W. Studier et al., *Proc Natl Acad Sci U S A* 83 (21), 8122 (1986).

91. K. Shah, Y. Liu, C. Deirmengian et al., *Proc Natl Acad Sci U S A* 94 (8), 3565 (1997).
92. N. Bisson, D. A. James, G. Ivosev et al., *Nat Biotechnol* 29 (7), 653 (2011).
93. Y. Zhang, A. Wolf-Yadlin, P. L. Ross et al., *Mol Cell Proteomics* 4 (9), 1240 (2005).
94. B. Bodenmiller, S. Wanka, C. Kraft et al., *Sci Signal* 3 (153), rs4 (2010).
95. H. R. Horvitz, *Biosci Rep* 23 (5-6), 239 (2003).
96. P. W. Sternberg, *Genetics* 172 (2), 727 (2006).
97. S. Paradis and G. Ruvkun, *Genes Dev* 12 (16), 2488 (1998).

<i>Human name used here</i>	<i>Official human gene name</i>	<i>Human aliases</i>	<i>C. elegans ortholog</i>
CCM1	<i>KRIT1</i>	Krev-interaction trapped 1	<i>kri-1</i>
CCM2	<i>CCM2</i>	OSM; C7orf22; MGC4067; malcavernin	None identified
CCM3	<i>PDCD10</i>	programmed cell death 10; TFAR15	<i>C14A4.11</i> (renamed <i>ccm-3</i>)
ICAP1	<i>ITGB1BP1</i>	Integrin beta 1 binding protein 1; ICAP-1alpha	Possibly <i>Y45F10D.10</i>
MST4	<i>MST4</i>	Mst3 and SOK1-related kinase; MASK	<i>gck-1</i>
STK24	<i>STK24</i>	MST3; STK3	
STK25	<i>STK25</i>	SOK1; YSK1	
PP2Acat	<i>PPP2CA</i> ; <i>PPP2CB</i>	PP2A catalytic subunit	<i>let-92</i>
PP2AA	<i>PPP2R1A</i> ; <i>PPP2R1B</i>	PP2A A scaffolding subunit; PR65	<i>paa-1</i>
Striatins	<i>STRN</i> ; <i>STRN3</i> ; <i>STRN4</i>	Zinedin; SG2NA	<i>cash-1</i>
MOB3	<i>MOBKL3</i>	Phocean; PREI3; Mob1	<i>C30A5.3</i>
MESDC1	<i>MESDC1</i>	mesoderm development candidate 1	<i>Y71G12B.11</i>

Figure 1. Protein naming convention. For simplicity, we have used throughout the grant a single name to refer to both a protein its corresponding gene. Official human gene names (as per NCBI Entrez Gene) are listed, followed by other aliases used in the literature to designate the human protein/gene. *C. elegans* orthologs for the listed proteins are also shown. All other proteins listed in the figures follow the NCBI Entrez Gene convention.

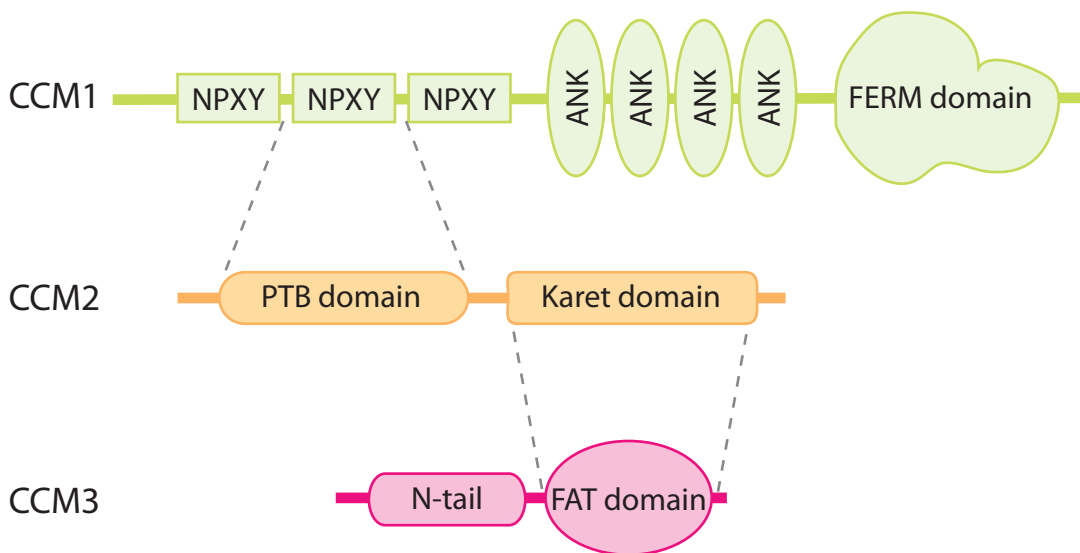


Figure 2. Schematic of binding topology of the CCM1•CCM2•CCM3 complex. CCM1 is comprised of three NPXY motifs (which normally mediate interactions with PTB domain containing proteins in a phosphorylation-dependent manner), followed by several ankyrin repeats and a FERM domain (the FERM domain is responsible for membrane targeting). CCM2 contains at its N-terminus a PTB domain and at its C terminus a new domain referred to as “Karet” (which we have identified as being responsible for interaction with CCM3). CCM3 contains an amino-terminal region that is similar to the C-terminal tail of the GCKIII kinases and used for heterodimerization with the GCKIII kinases (Appendix 3) and a C-terminal Focal Adhesion Targeting (FAT) domain. Association between CCM1 and CCM2 is provided by a NPXY peptide-PTB interaction while interaction between CCM2 and CCM3 is provided by an acidic peptide-FAT domain interaction (see Appendix 4). Note that the FAT domain of CCM3 also interacts (using the same mode of binding) with the striatin component of STRIPAK; in vitro, interactions with paxillin also occur through the same region. Also, as defined in the preliminary data, additional interactions for each protein have also been uncovered.

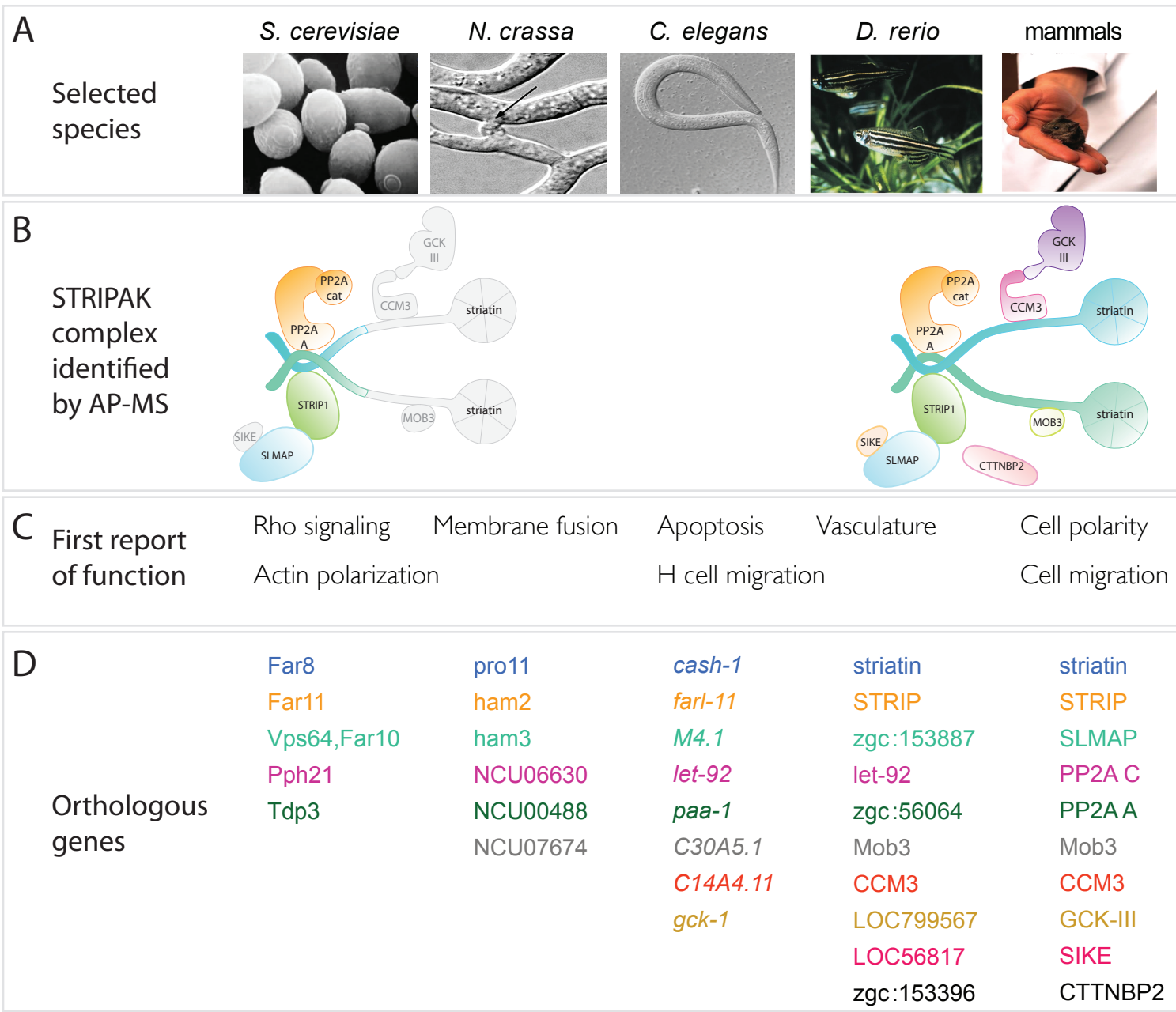
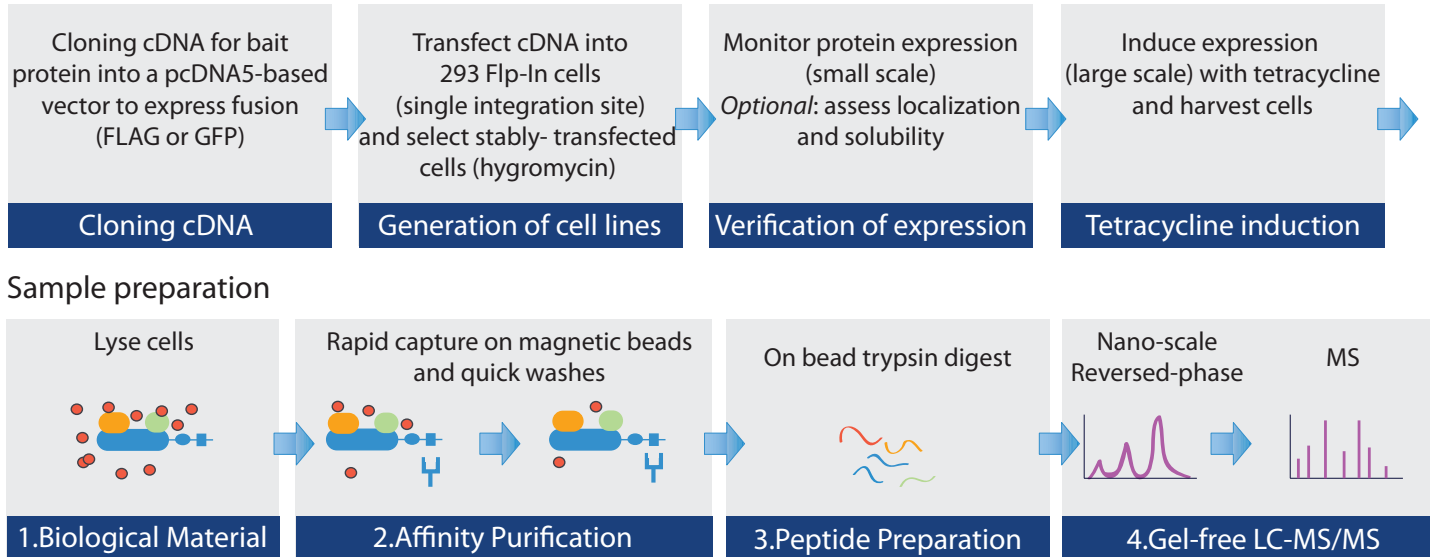


Figure 3. Evolution of the STRIPAK complex in which most of CCM3 resides. A) list of the selected species. B) Composition of the STRIPAK complex in the yeast *S. cerevisiae* and in mammals, as determined by AP-MS analysis (note that a Far3, 7-11 complex containing many of the STRIPAK components was first reported by Kemp and Sprague, Mol Cell Biol, 2003). The greyed out proteins (or protein domains) in the yeast complex indicates that there is no identified ortholog (or orthologous domain) in yeast for the mammalian STRIPAK components. C) New functions from the STRIPAK complex are being characterized across eukaryotic evolution. In most cases, when a function appears, it is maintained throughout evolution, as new complex components and new functions are added. D) orthologous genes to the human STRIPAK components (paralogous families are shown for the mammalian STRIPAK; 20 genes in total). The orthologs are color-coded to match the human paralogous groups. CCM3 and the GCKIII kinases first appear in the nematode *C. elegans*.

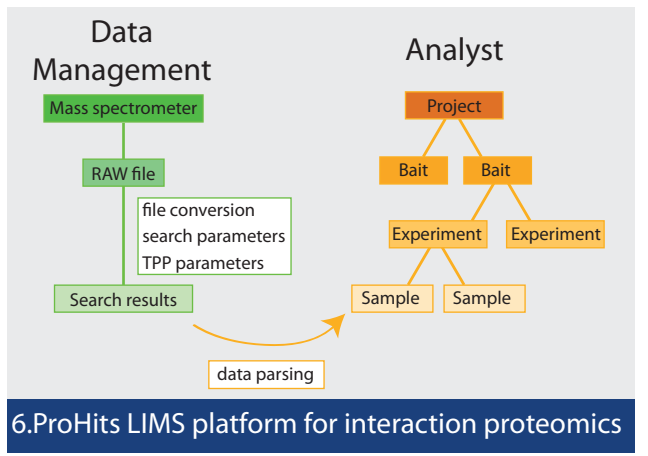
A

Generation of the inducible cell lines



B

Robust bioinformatics platform



C

Computational approaches to distinguish true interactors and protein complexes

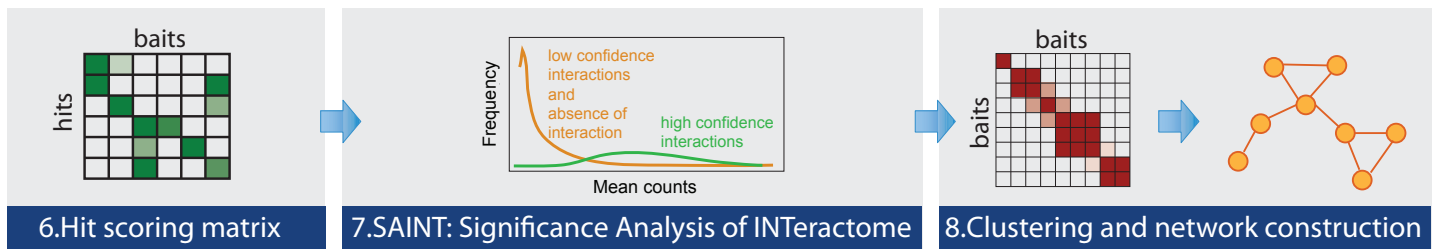


Figure 4. Current affinity-purification coupled to mass spectrometry platform. A) In most cases, we now perform AP-MS using a tetracycline-inducible system from Invitrogen called Flp-In T-Rex. In this system, integration of the recombinant tagged protein to a single cellular locus is mediated by Flp recombinase. Integrants are selected with hygromycin, and expression is induced by adding tetracycline to the cell culture medium. We have generated several expression vectors compatible with this system that enable fusion to epitope tags, including FLAG and GFP (vectors are available for Gateway or ligase-mediated cloning) (e.g. Dunham et al., *Proteomics*, 2011). Once the cells are induced, they are harvested, lysed, and subjected to a single affinity purification step (most often on magnetic beads coupled to the anti-tag antibody; Breitkreutz et al., *Science*, 2010); after on-beads digestion, the proteins are proteolyzed and subjected to LC-MS/MS. B) All data is recorded in our interaction-specific protein database called ProHits (Liu et al., *Nature Biotech*, 2010; Liu et al., 2012, *submitted*). C) It is critical to distinguish true interactors from background contaminants. We have developed new statistical tools called SAINT (for Significance Analysis of INTERactome) to assist in this process (references: Breitkreutz et al., *Science*, 2010; Choi et al., *Mol Sys Biol* 2010 and *Nature Methods* 2011; Skarra et al., *Proteomics*, 2011; Choi et al., 2012, *submitted*). See Appendix 5.

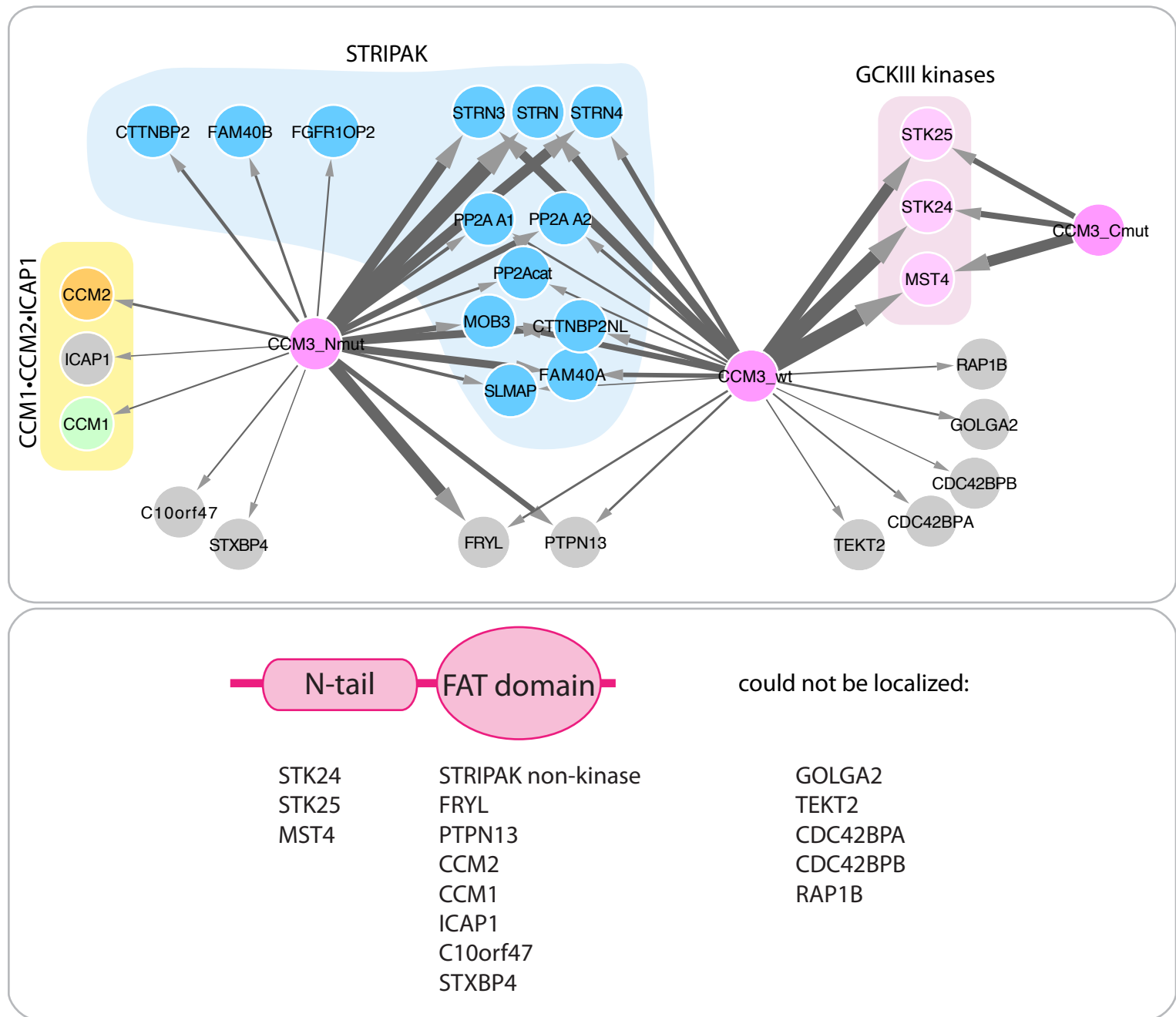


Figure 5. Current CCM3 interaction network. *Top:* CCM3 wt, a point mutant in the N-terminal heterodimerization domain (Appendix 3) and a point mutant in the C-terminal FAT domain (Appendix 4) were expressed as GFP fusion proteins in the Flp-In T-Rex system from Invitrogen (see Figure 4). AP-MS analysis on GFP-Trap beads (Chromotek) was performed on biological duplicates. An empty vector control as well as several unrelated proteins were used as negative controls. All data was analyzed using the SAINT statistical tools (as in Skarra et al., *Proteomics*, 2011). Only high confidence interactions (Averaged SAINT between the two biological replicates ≥ 0.8) are reported. The thickness of the arrows indicates the number of peptides detected for each protein in the mass spectrometer (indicating both abundance and confidence in the interactions). Non-kinase components of STRIPAK, shown in blue, interact with both the wt and the N-terminal mutant (Nmut). Similarly, CCM1•CCM2•ICAP1 associate with the wt and Nmut, as are four other binding partners for CCM3: FRYL, PTPN13, STXBP4 and c10orf47 (note that the interaction between PTPN13 and CCM3 was previously reported by yeast two hybrid; the other interactions are new). On the other hand, the GCKIII kinases associate readily with the wt CCM3 and the mutant in the FAT domain (Cmut). Lastly, some proteins interacted only with the wt protein in our assay. As we previously reported (Appendices 1 and 4), STRIPAK components, and especially the GCKIII kinases, are the main interactors for CCM3wt (look at cumulative thickness of the arrows).

Bottom. Summary of the interactions identified, with mapped interaction regions indicated when possible.

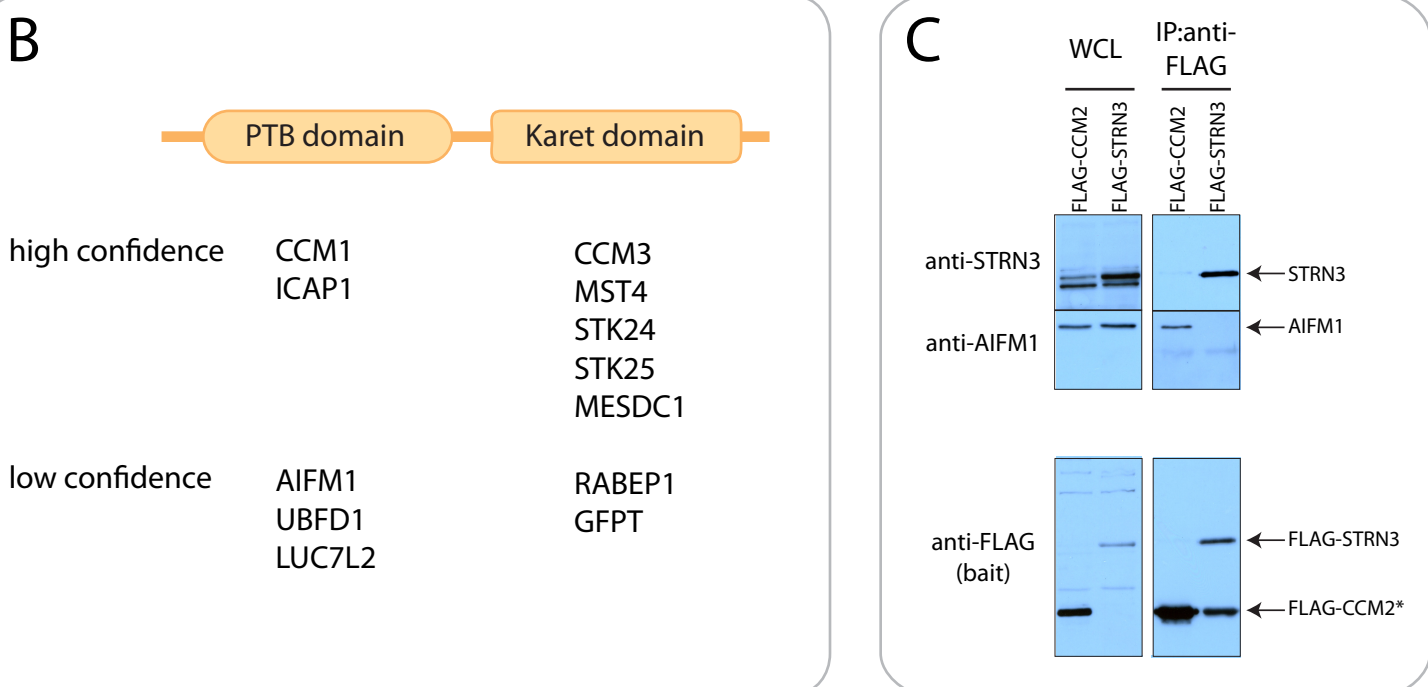
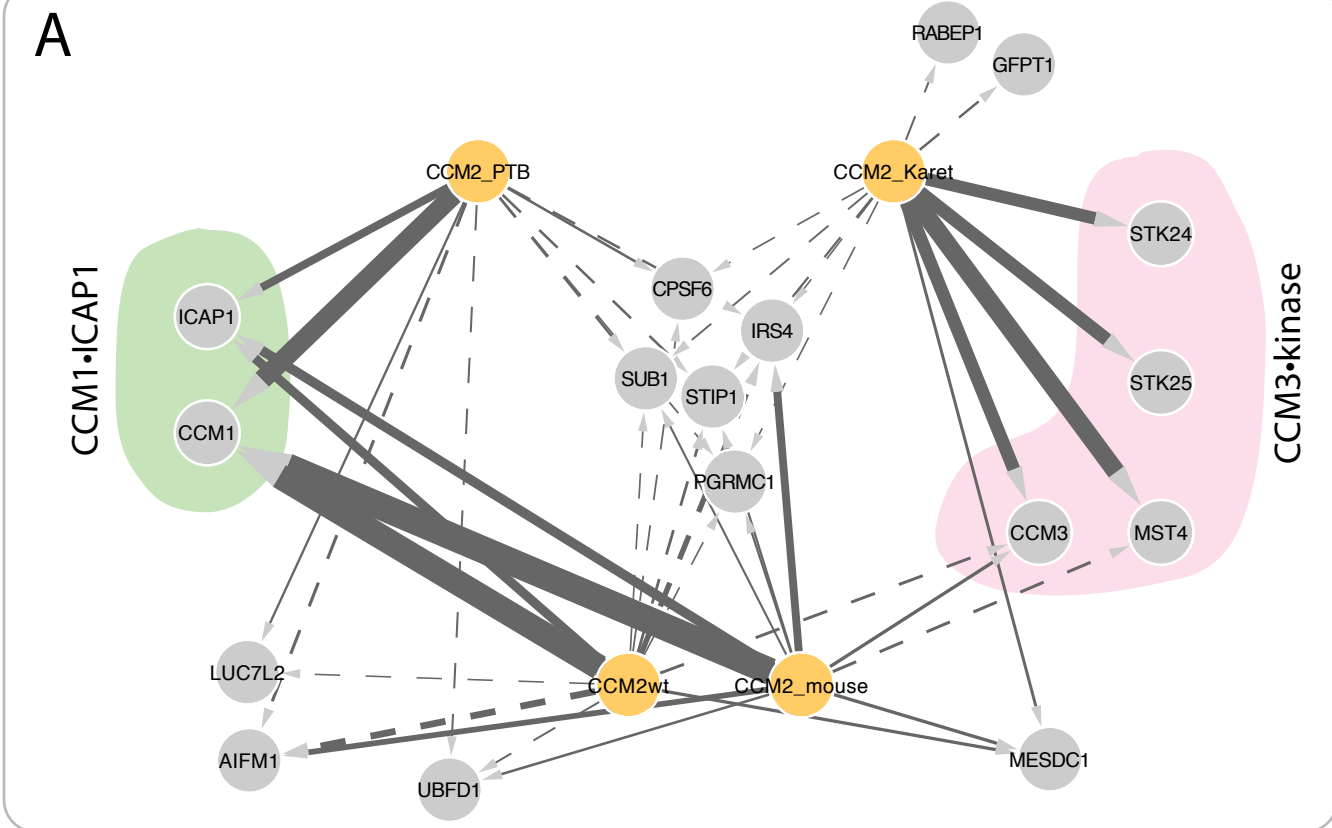
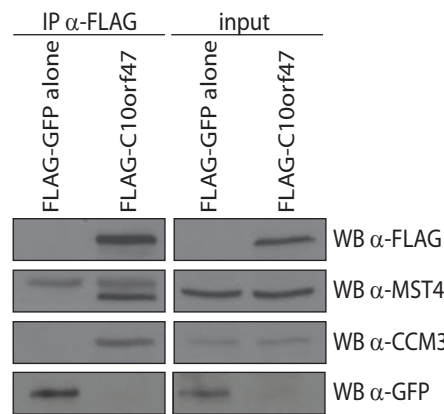


Figure 6. Current CCM2 interactome. A) Human CCM2 full length (CCM2wt), mouse CCM2 full length (CCM2_mouse), or truncations of human CCM2 expressing only the PTB domain (CCM2_PTB) or only the Karet domain (CCM2_Karet) were used for AP-MS analysis in at least biological duplicates. Interaction partners detected with high confidence (using the SAINT statistical tool; threshold of 0.8 for full lines, 0.5 for dashed lines) are indicated. The thickness of the arrows is proportional to the number of peptides for each interactor detected by mass spectrometry. CCM1 and ICAP1 are the most abundant interaction partners for full-length CCM2 and CCM2_PTB; CCM3 and the GCKIII kinases are the most abundant partners of CCM2_Karet. B) Summary of the interactions mapped unambiguously (high confidence) or likely mapped (low confidence) to the PTB and Karet domains of CCM2, respectively. Like the CCM3 protein with which it shares limited homology, MESDC1 interacts via the Karet domain. C) Validation of the interaction between endogenous AIFM1 (a member of the Hsp90 interaction network, Taipale *et al.*, *in prep*) and FLAG-CCM2 by IP-Western. Note that FLAG-STRN3, used here as a negative control, does not interact with AIFM1.

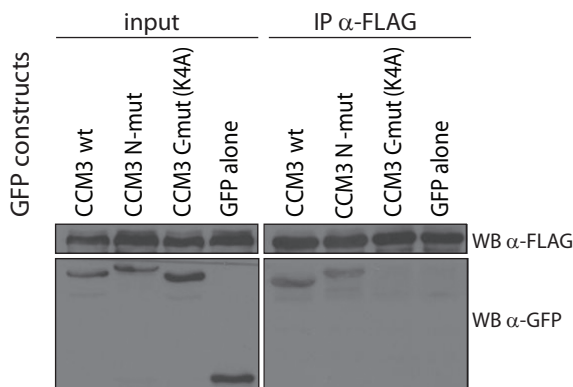
A

	sample 1	sample 2
CCM3	69	60
STK24	65	60
MST4	63	74
c10orf47 (bait)	59	51
STK25	46	67

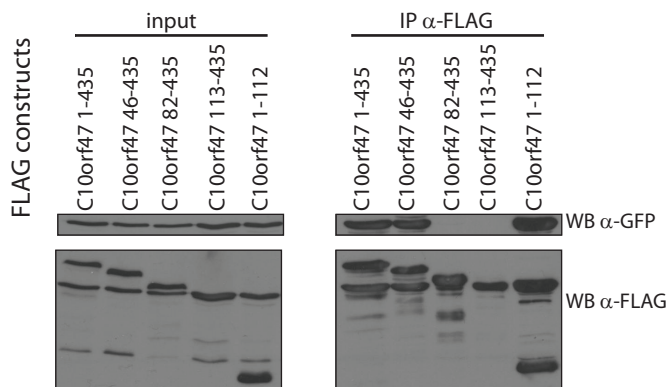
B



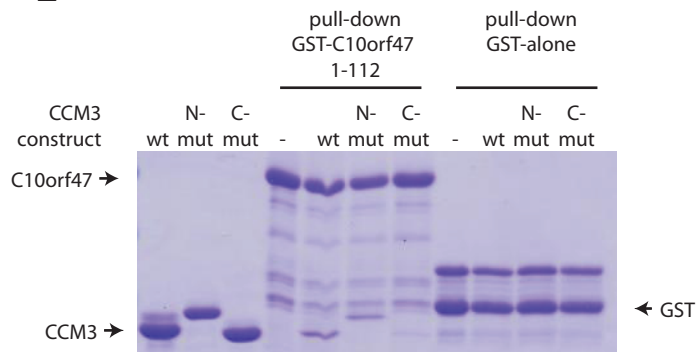
C



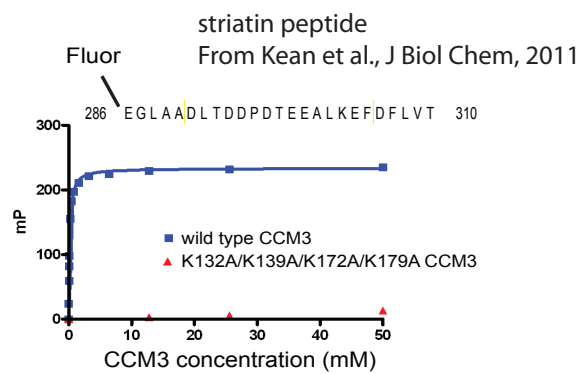
D



E



F

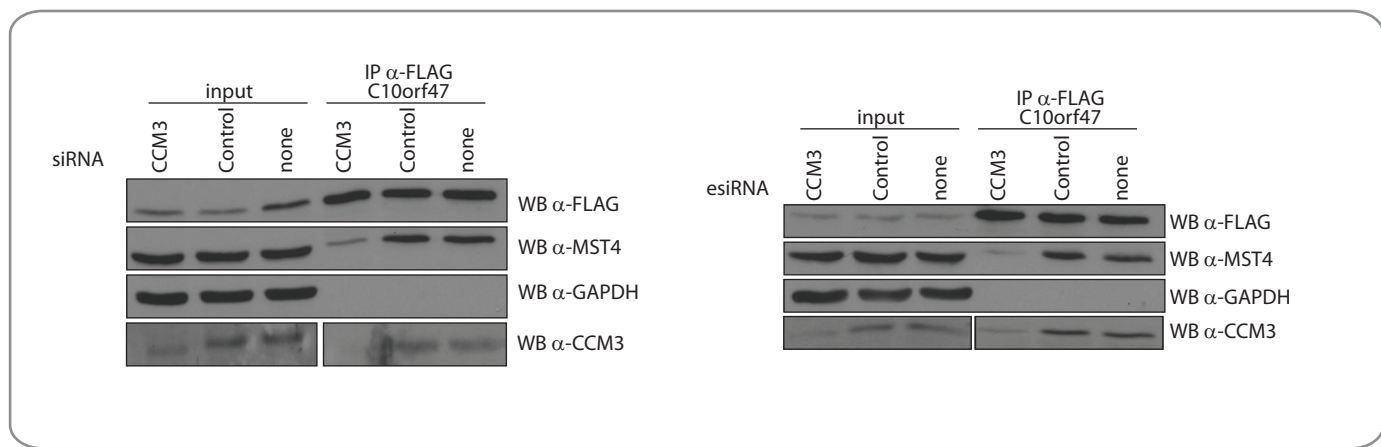


G

LDDESLKYLTTHEEKDVLLFFETIDSLDEDFEEPVLCDGGVCC LCSPSLEESTSSPSEPEDVIDLVQ (c10orf47)

Figure 7. c10orf47 specifically interacts with CCM3 and all three GCKIII kinases. A) Results of AP-MS analysis of stable cells expressing FLAG-tagged c10orf47; the number of spectra for each of the indicated proteins across two biological replicates is indicated. No other protein was detected with high-confidence. B) Confirmation of the MS results by immunoprecipitation followed by immunoblotting from the FLAG-c10orf47 expressing cells (a cell line expressing a FLAG-GFP fusion is used as a control). C) c10orf47 interacts with wt CCM3 and a quadruple point mutant at its N-terminus that abrogates interaction with the GCKIII kinases. Interaction is abrogated with a quadruple point mutant in the CCM3 C-terminal FAT domain. D) Mapping of the interaction region on c10orf47 that interacts with CCM3: amino acids 1-46 and 113-435 are dispensable for the interaction. E) c10orf47 amino acids 1-112 interact directly with CCM3. F) Sequence of the minimal peptide derived from striatin which we previously demonstrated to interact with CCM3. G) The c10orf47 region 46-112 contains two stretches of acidic residues resembling the striatin peptide interacting with CCM3.

A



B

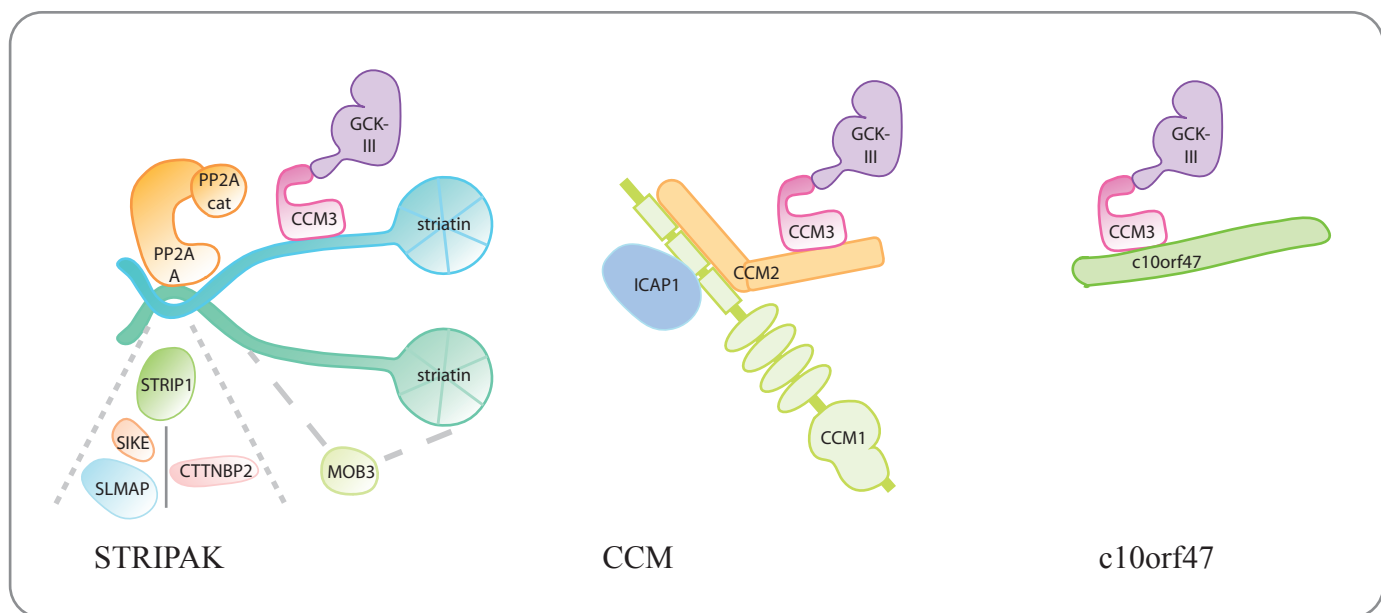


Figure 8. CCM3 acts as a bridge between the GCKIII kinases and mutually alternative complexes. A) Interaction of c10orf47 with the GCKIII kinase MST4 is bridged by CCM3. Depletion of CCM3 by chemically-synthesized siRNA pools (left) or endoribonuclease-prepared esiRNAs (right) drastically reduce the recovery of endogenous MST4 with FLAG-c10orf47. **B)** The CCM3-GCKIII can interact with alternative assemblies. CCM3 and its associated kinases is able to associate with *either* the STRIPAK complex (Goudreault et al., Mol Cell Proteomics, 2009; Kean et al., J Biol Chem, 2011), the CCM2-CCM3-ICAP complex (Costa et al., submitted) or the protein c10orf47 (Goudreault et al., in prep) via similar interfaces.

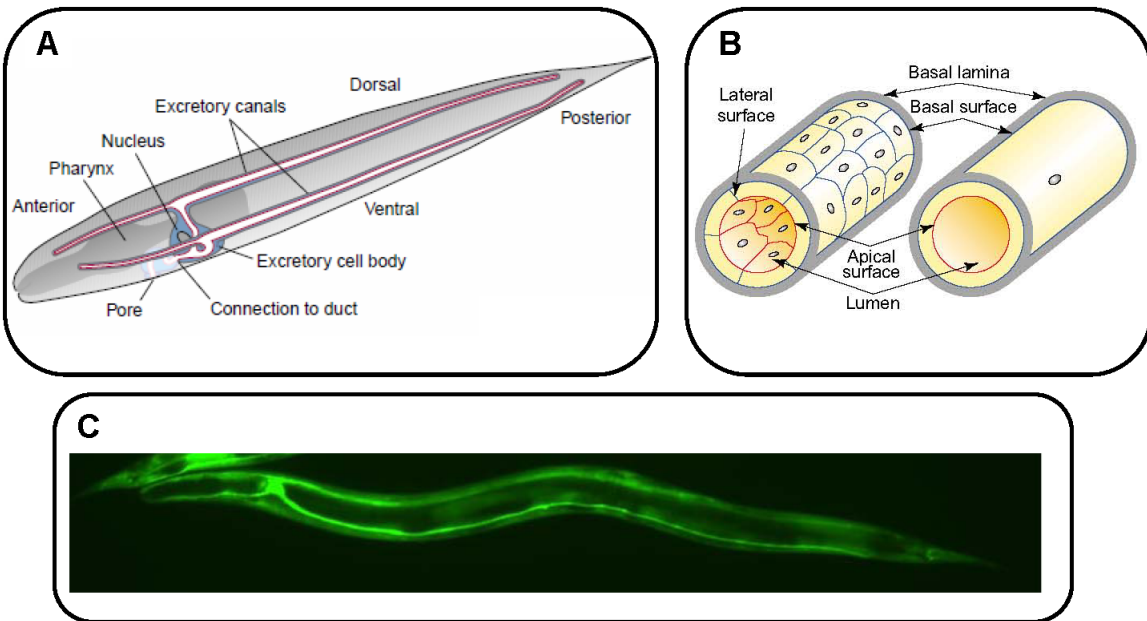


Figure 9: The *C. elegans* excretory system. **A**, Lateral schematic of an adult hermaphrodite showing the large H-shaped excretory cell where canals run down both sides of the animal from anterior to posterior end of the body. The large excretory cell is the largest in the worm. Fluid is excreted into the environment through the pore cell. The excretory system is required for regulation of osmotic stress and ion balance. **B**, Schematic depiction of a multicellular capillary tube in vertebrate animals (left) compared with the unicellular excretory canal tube of *C. elegans* (right). **C**, Transgenic *C. elegans* hermaphrodite expressing GFP under the control of the *pes-6* promoter in the excretory cell. Both multicellular and unicellular tubes have apical and basal surfaces and both tubes transport fluids in the lumen. Figures A and B from Buechner (2002) *Trends in Cell Biology*, 12: 479-484.

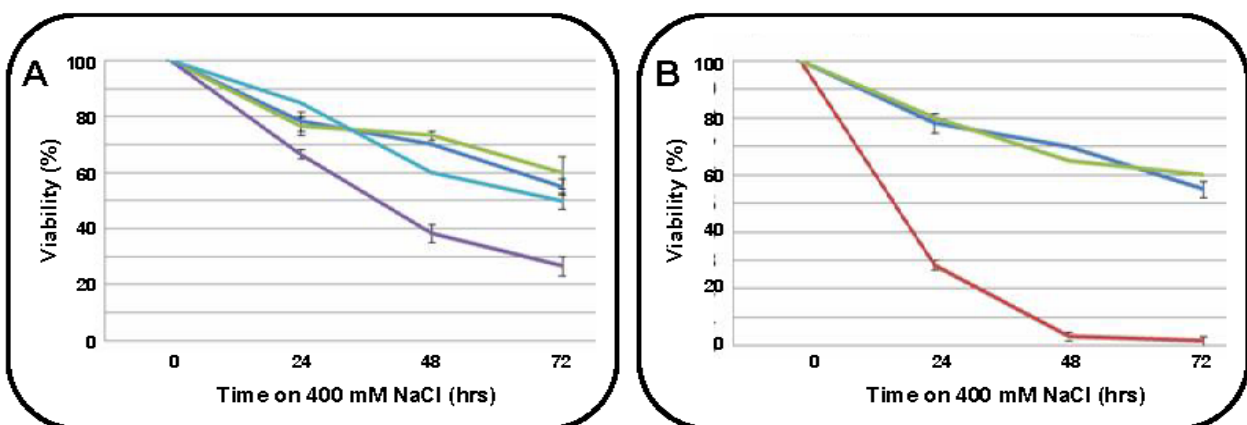


Figure 10: CCM mutants are hypersensitive to osmotic stress. **A**, Homozygous *ccm-3(lf)* mutants (purple line) are more sensitive to 400 mM NaCl than WT (dark blue line) or *ccm-3(lf)/+* (light blue line). Expression of a wild-type copy of *ccm-3* from an extrachromosomal array in *ccm-3(lf)* homozygotes (green line) rescues sensitivity to osmotic stress. **B**, Homozygous *kri-1(lf)* mutants (red line) are hypersensitive to 400 mM NaCl compared with WT (dark blue line). Expression of a wild-type copy of *kri-1* from an extrachromosomal array in *kri-1(lf)* homozygotes (green line) rescues sensitivity to osmotic stress.

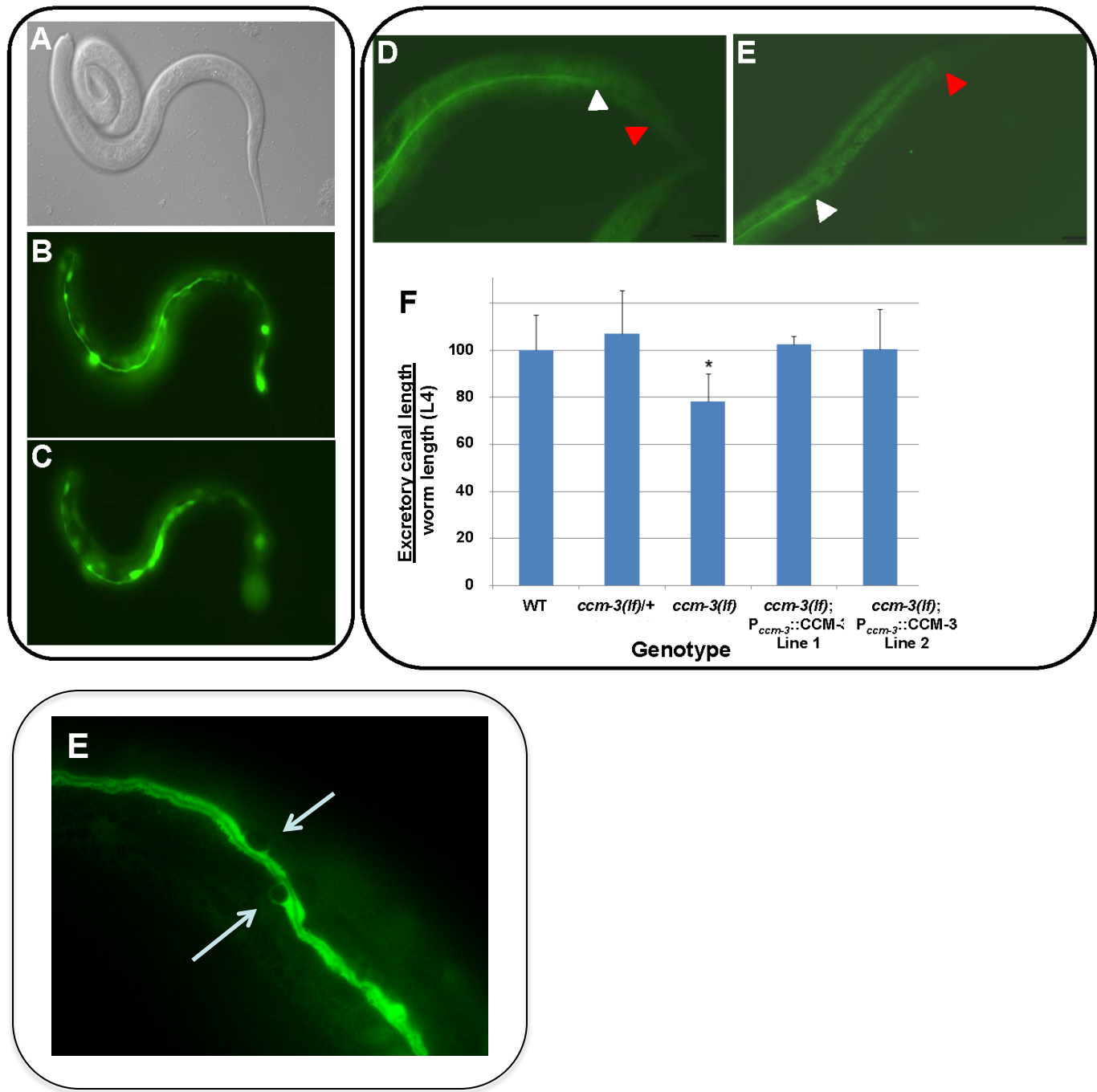


Figure 11: CCM3 is expressed in excretory cell and required for its proper development. **A**, bright field micrograph of transgenic worm expressing CCM-3::GFP, which is expressed in the excretory cell (**B**) and intestine (**C**). Wild-type worm expressing *pes-6*::GFP in excretory cell of wild type (**D**) and *ccm-3(lf)* mutants (**E**), which have truncated excretory canals compared to wild type controls in **D**. White arrow heads mark posterior end of excretory canal. Red arrow heads indicate position of anus. **F**, quantification of excretory canal length relative to body length in wild type (WT), *ccm-3* heterozygotes (*ccm-3(lf)/+*), *ccm-3* homozygotes (*ccm-3(lf)*) and two rescue lines expressing *ccm3(+)* from an extrachromosomal array. **G**, example of cyst formation along truncated excretory canal (arrows) of *ccm-3(lf)* mutant.

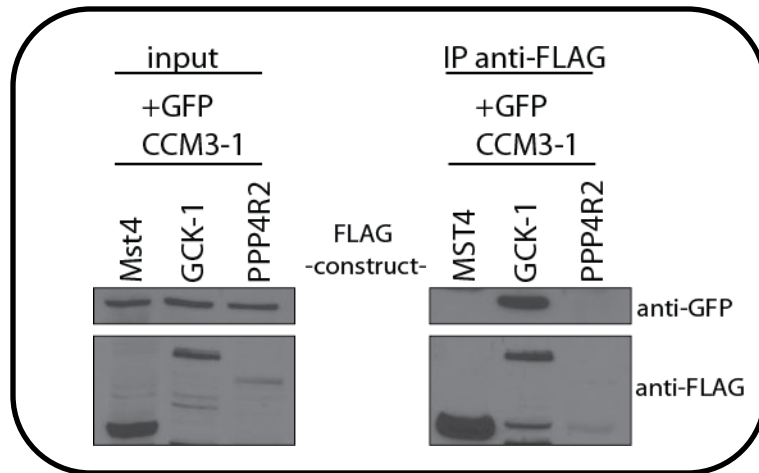


Figure 12: Physical interaction between *C. elegans* GCK-1 and CCM-3. Coding sequences for human (MST4) or worm (GCK-1) GCKIII kinase and worm CCM3 (CCM3-1) were subcloned in epitope-tagged vectors for expression in mammalian cells. Human PPP4R2 is used as a negative control. FLAG immunoprecipitation was followed by detection of both FLAG and GFP-tagged proteins by immunoblotting. GFP-CCM3-1 was readily detected in the purifications of FLAG-GCK-1 but not of FLAG-MST4 or FLAG-PPP4R2.

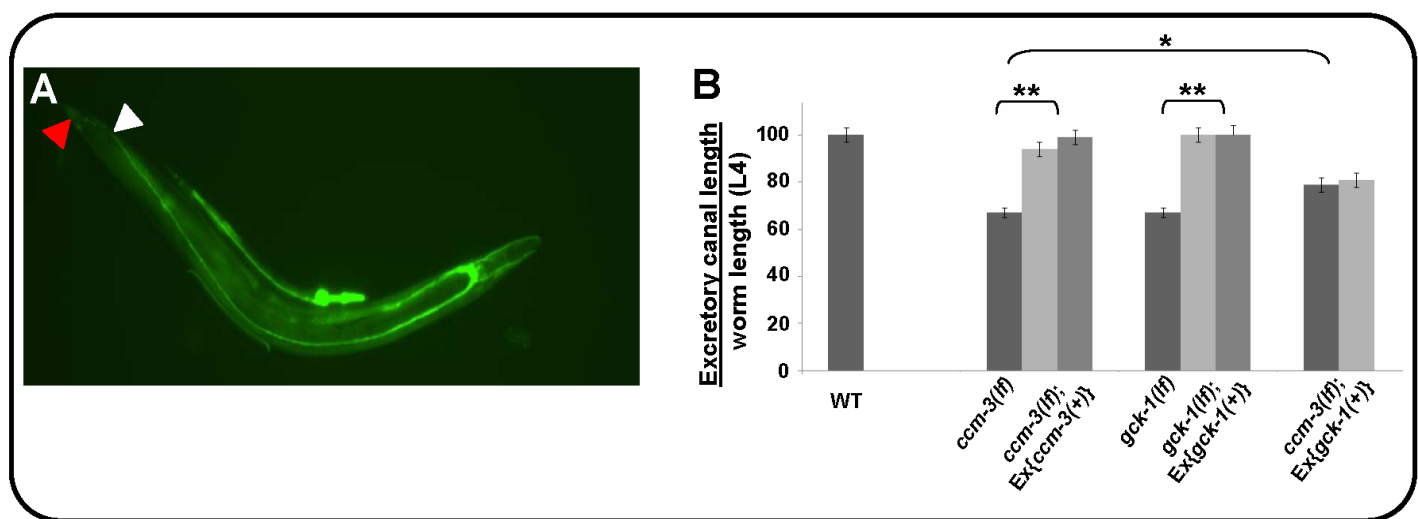


Figure 13: Expression of wild type GCK-1 can rescue excretory cell truncations in *ccm-3* mutants. **A,** *ccm-3(lf)* mutant worm overexpressing wild type *gck-1*. *pes-6::GFP* marks the excretory cell (in green). White arrowhead marks the posterior end of the excretory canal and the red arrow head indicates the anus. In this example the excretory canals are restored to wild type lengths. **B,** quantification of excretory canal length relative to body length in wild type (WT), *ccm-3(lf)*, two rescue lines expressing wild type *ccm3* from an extrachromosomal array, *gck-1* homozygous mutants (*gck-1(lf)*), two independent lines expressing wild type *gck-1* from an array, and *ccm-3* homozygous mutants expressing wild type *gck-1* from an extrachromosomal array. * P = 0.05, ** P= 0.0001 (Student's t-test).

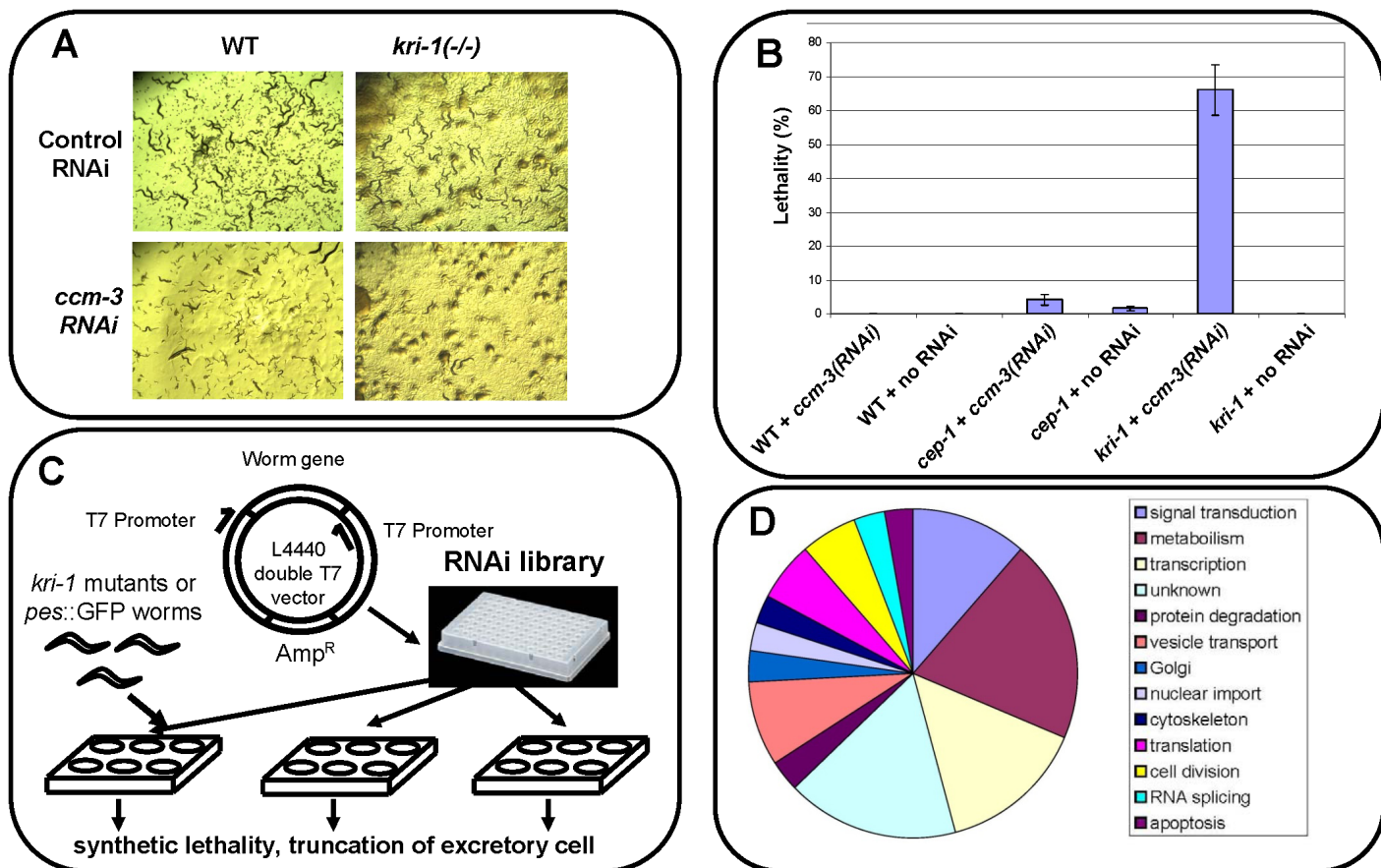


Figure 14: Rationale and strategy for synthetic lethal RNAi screen. **A**, The population of *kri-1* mutants reduced when grown on *ccm-3*(RNAi) compared with a control RNAi. **B**, *ccm-3* and *kri-1* exhibit synthetic lethality when both genes are ablated. Error bars = S.D. **C**, strategy for RNAi screen of *ccm-3* pathway components. *kri-1*(*lf*) mutant worms grown on plates of bacteria expressing dsRNA to individual *C. elegans* genes will be screened for lethality. **D**, Summary of results from pilot screen. Of the ~2,700 genes on chromosome 1, 35 were synthetic lethal with *kri-1*, and these genes represent a range of protein classes (side bar). 4/35 genes cause truncations in the excretory cell when ablated by RNAi (see Fig. 12).

	RNAi Phenotypes		
Worm gene	Survival on 400mM NaCl (24 Hour Post treatment)	Truncation of Excretory Cell (Level I – III)	Description/Function
<i>gsa-1</i>	25%	NO	G protein, Subunit Alpha
<i>ZC123.3</i>	15%	NO	homeobox protein / transcription
<i>F49B2.6</i>	15%	YES (II)	aminopeptidase
<i>ekl-4</i>	0%	YES (II)	DNA methyltransferase 1-associated protein-1
<i>abtm-1</i>	20%	NO	ABC Transporter, Mitochondrial
<i>lpd-3</i>	20%	NO	LiPid Depleted
<i>cogc-1</i>	20%	NO	Conserved oligomeric Golgi complex subunit 1
<i>Y65B4BR.5</i>	30%	NO	Transcription factor containing NAC and TS-N domains
<i>Y71F9AL1.17</i>	33%	NO	Vesicle coat complex COPI, alpha subunit
<i>C53H9.2</i>	20%	NO	GTP binding proteins / translation
<i>rnp-6</i>	7%	NO	Polypyrimidine tract-binding protein (RNA splicing)
<i>exoc-8</i>	47%	YES (II)	Exocyst complex component 8
<i>grh-1</i>	7%	YES (II)	Isoform 2 of Grainyhead-like protein 2 homolog
<i>srw-111</i>	13.3%	NO	Serpentine type 7TM GPCR chemoreceptor Srw
Control	60%	NO	N/A

Figure 15: Summary of genes from RNAi screen that affect excretory cell morphology and/or sensitivity to osmotic stress.

A

Worm orthologue	Human gene	RNAi Phenotypes	
		Survival on 400mM NaCl (72 Hour Post-treatment)	Truncation of Excretory Cell
<i>C30A5.3</i>	MOB3	53%	NO
<i>farl-11</i>	STRIP1/2	73%	YES
<i>cash-1</i>	Striatin	92%	YES
<i>C49H3.6</i>	CTTNBP2/NL	80%	YES
(<i>HT115</i>) -ve control	N/A	75%	NO

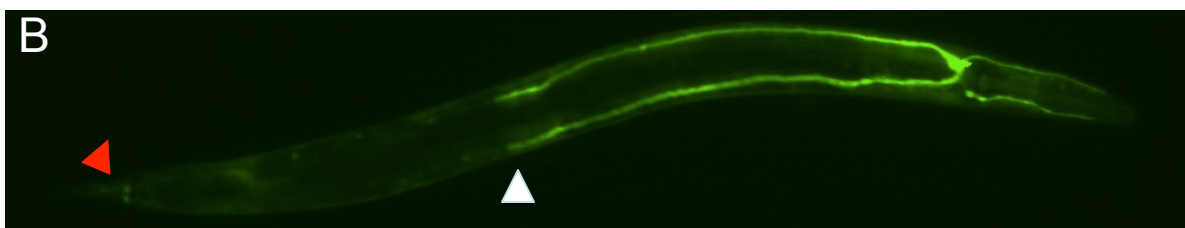
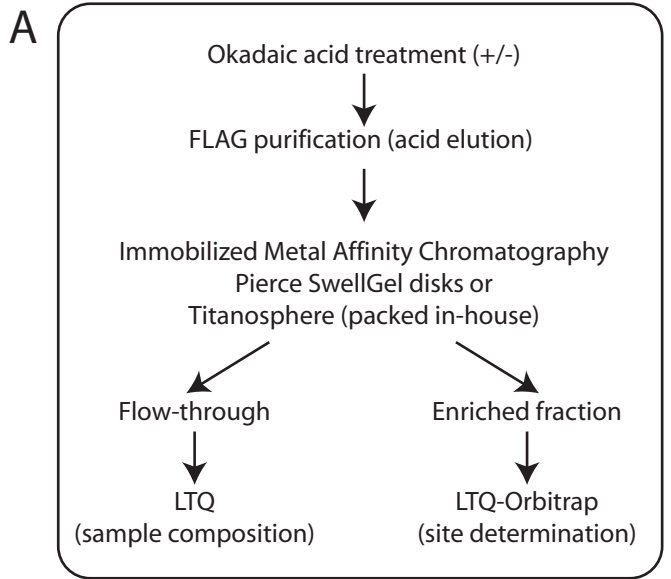
B

Figure 16: STRIPAK depletion phenotypes resemble those of *ccm-3* depletion.

A, Summary of RNAi phenotypes for *C. elegans* STRIPAK genes. B, Ablation of the the *C. elegans* striatin orthologue *cash-1* by RNAi causes excretory canal truncations that resemble *ccm-3*(lf) mutants (see Fig 11E). Shown is an example of a wild-type worm expressing the *pes-6*::GFP reporter after 3 days of growth on bacteria expressing double stranded RNA to *cash-1*. A white arrow head marks the posterior end of excretory canal and a red arrow head indicates the position of anus.



B

Number of IMAC AP/MS analyses	10
Number of phosphopeptide spectra	1276
Number of unique sites	60
Global enrichment with okadaic acid	1.2
Number of phosphosites increased > 3-fold	12
Fold enrichment in GCK-III A-loop	9

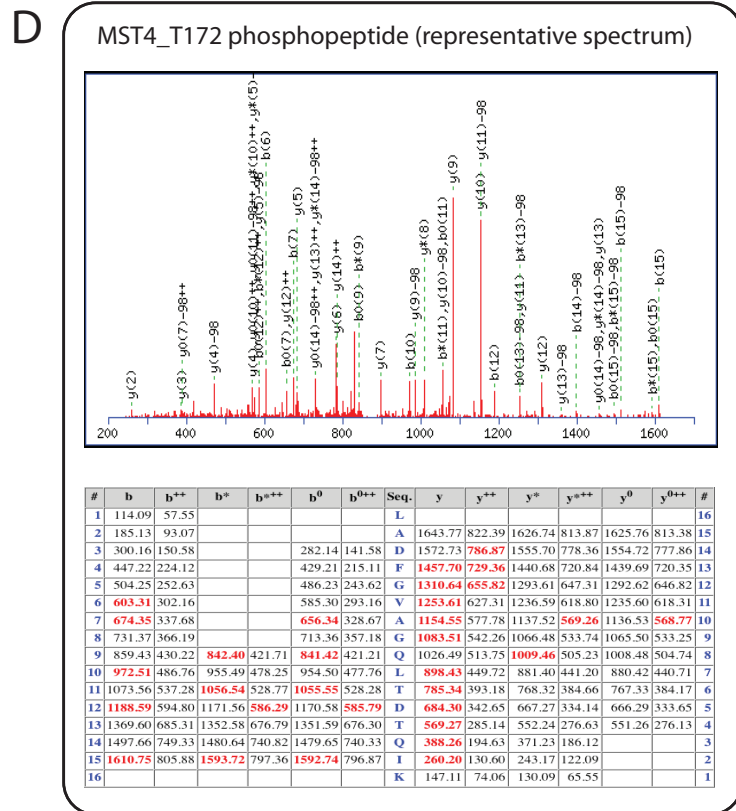
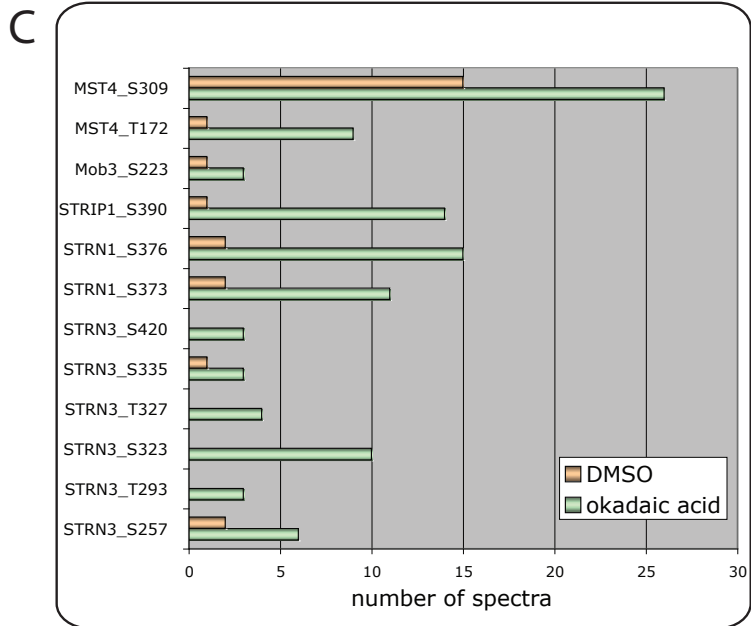
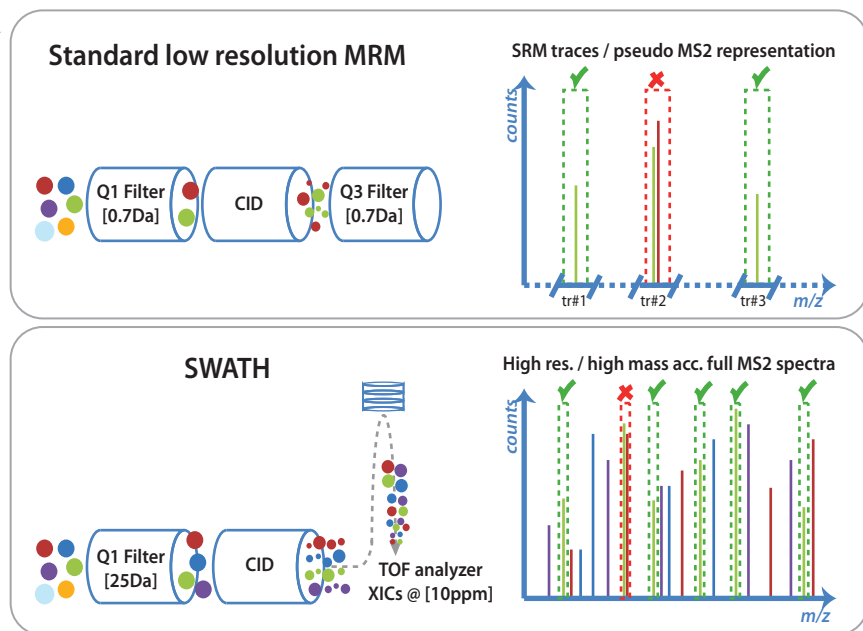
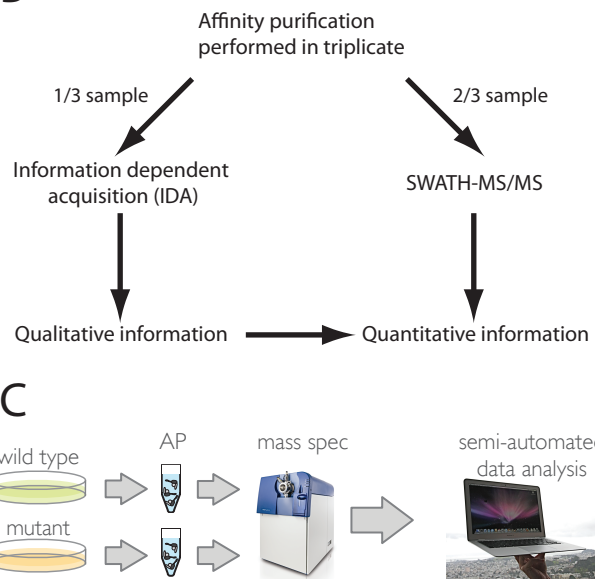


Fig. 17. Establishment of a platform for mapping *in vivo* phosphorylation sites and application to the analysis of the phosphorylation status of STRIPAK core components. A) Schematic representation of the experimental workflow for phosphorylation site analysis. Cells stably expressing STRIPAK core components (STRN3, CCM3 and Mob3) were treated with or without okadaic acid, and FLAG-purification followed by proteolysis with trypsin was followed by phosphopeptide enrichment and LC-MS/MS/MS analysis on a LTQ-Orbitrap. B) Summary of the quantitative parameters generated for our pilot experiment: note that we only focused on the phosphorylation sites detected on core STRIPAK components (we have also detected multiple sites on other interacting proteins, particularly CTTNBP2NL). C) Spectral count distributions for the 12 phosphopeptides affected by >3-fold by okadaic acid treatment. D) Representative annotated spectrum for the MST4 activation loop phosphopeptide. Note that this peptide is absolutely conserved in STK24 and STK25 (and thus we cannot resolve the precise source of the peptide).

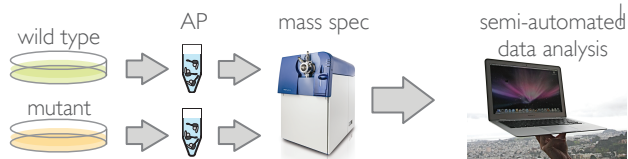
A



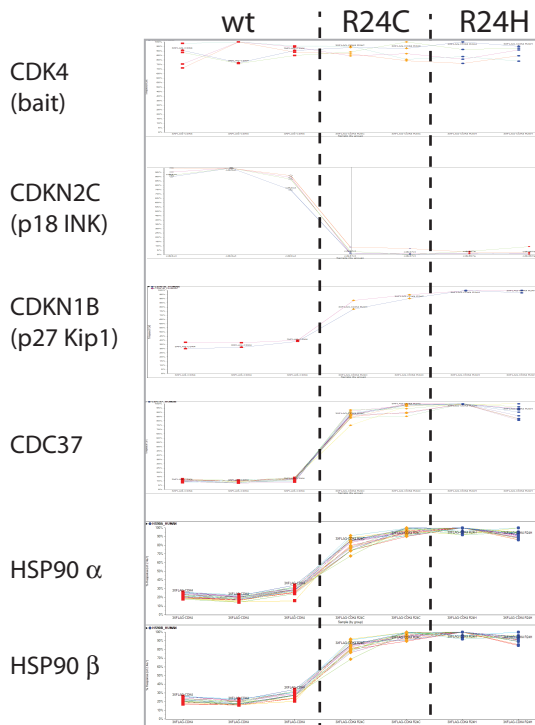
B



C



D



E

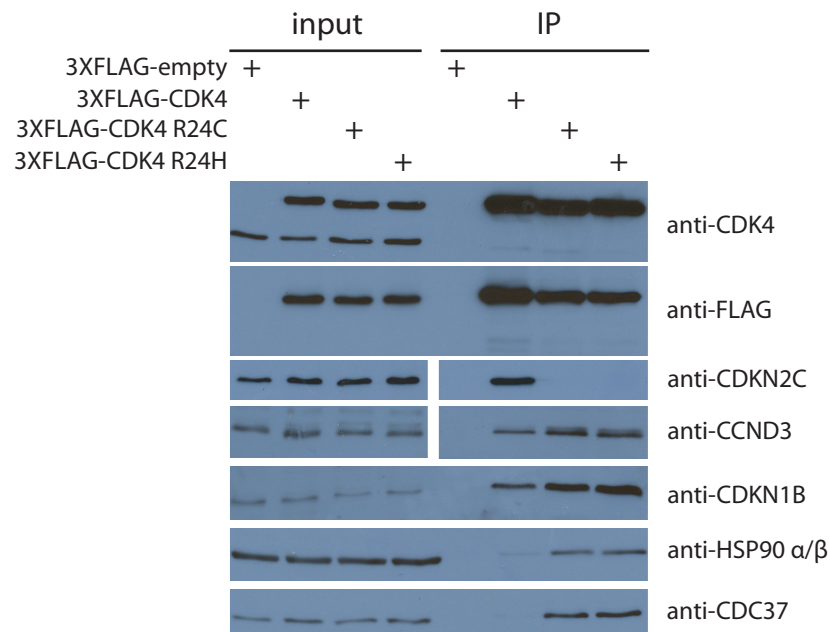
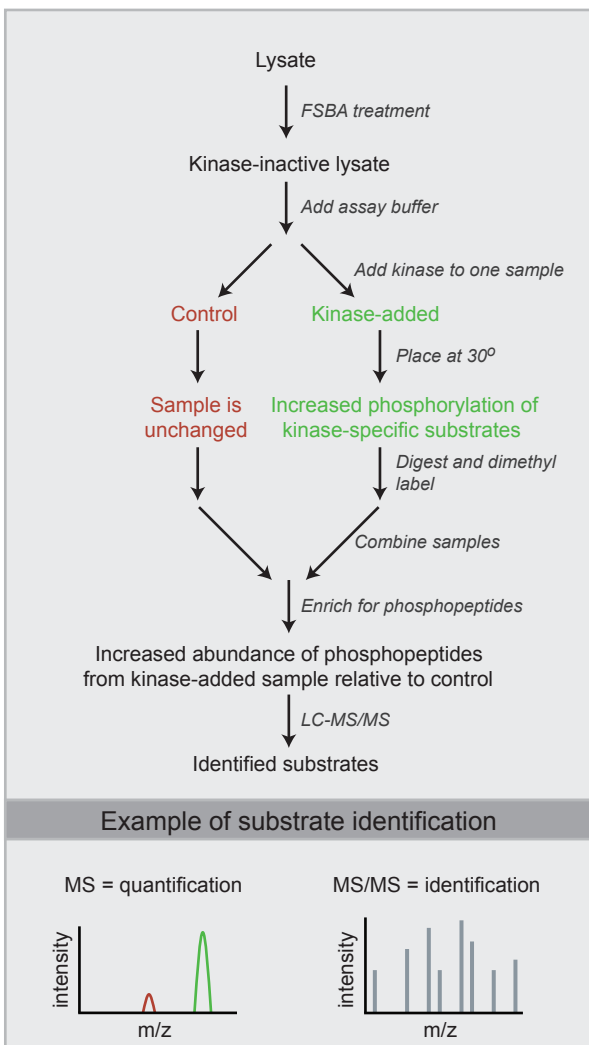
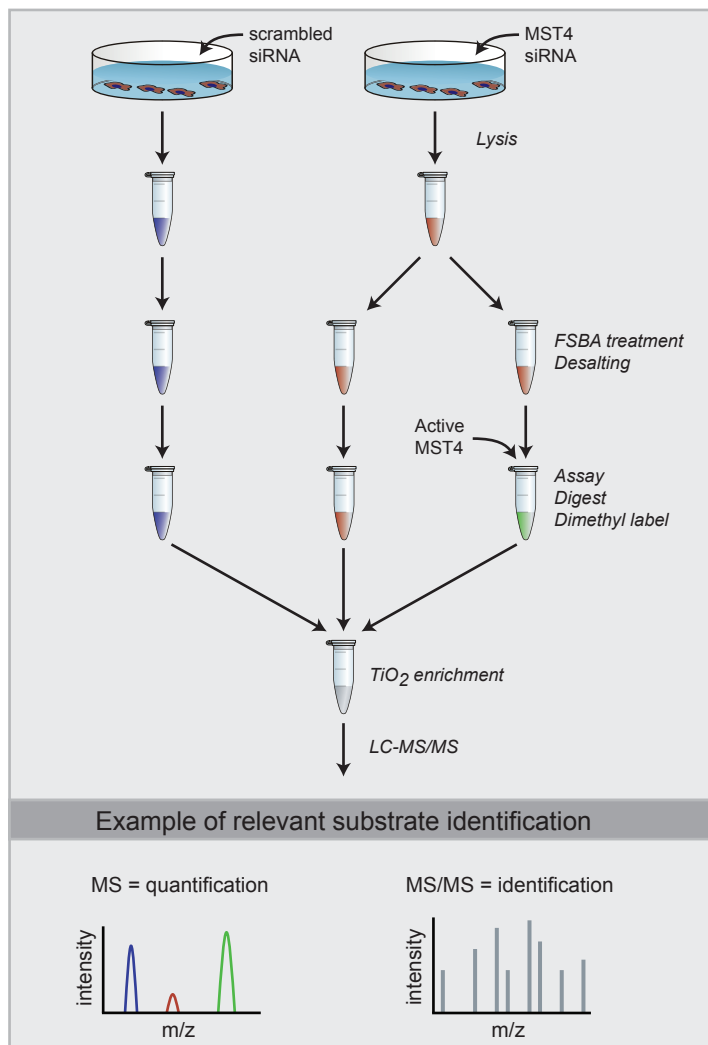


Figure 18. Quantitative approaches using MS2 quantification for the analysis of affinity-purified samples. A) The SWATH methodology is related to standard MRM (or SRM): In a first step, ions of a given mass are let through a filter, and then fragmented by CID. Masses of the fragment ions are recorded and quantification is performed. In standard MRM, the masses of the precursor ions to isolate are predetermined, and the isolation of the precursor and the detection of the product ions are at low resolution (~1 Da). By contrast, SWATH-MS does not require predetermined isolation of the precursor masses: the entire m/z range is progressively fragmented in 25 amu “swaths”; the loss of accuracy in peptide isolation is compensated by ppm level precision in MS2. B) Because the spectra associated to SWATH-MS data are most often mixed, a spectral library search strategy needs to be employed. For AP-MS samples, we generate the spectral library from the same samples that would be quantified by SWATH-MS and on the same instrument. C) Experimental design for AP-SWATH. Cell lines expressing similar levels of a wild-type and mutant bait protein are processed in parallel by affinity purification and mass spectrometry; several replicates are analyzed for each sample. The data is analyzed using a semi-automated pipeline, as described in Bisson et al., Nature Biotech, 2011. D) Results of AP-SWATH for the bait CDK4 and two dominant point mutants implicated in melanoma; three replicates of the wild type and two replicates of each of the two point mutants were analyzed. Extracted peptide intensity for selected prey proteins shows a tight correlation (all intensities – on the vertical axis – are within a narrow range of each other). This indicates that the AP-SWATH approach can – like standard MRM/SRM – provide accurate peptide-level quantification. Normalization to the averaged bait levels in the wt runs was applied to all samples. E) Validation of the AP-SWATH quantification results by IP/Western. As previously reported, CDKN2C (also known as p18 INK) is unable to associate – and hence to repress – the CDK4 mutants. By contrast, other proteins, and in particular HSP90 and its kinase-specific co-chaperone CDC37 associate preferentially with the mutants.

A



B



C

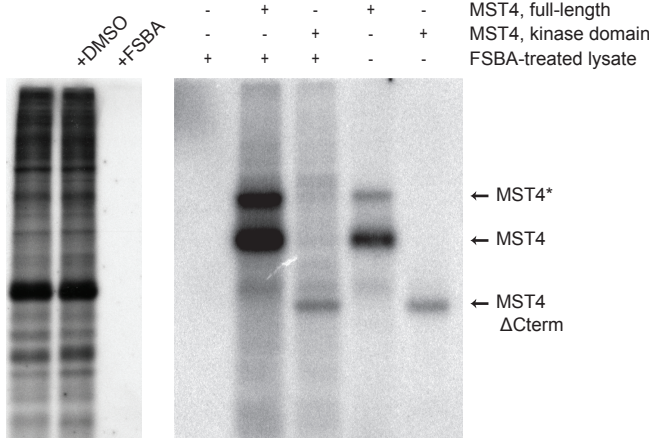


Figure 19. Strategy for identification of enzymatic substrates for GCKIII kinases.

A) Procedure for the identification of *in vitro* substrates. After cell harvesting, lysate is treated with the ATP analog FBSA to irreversibly inhibit all endogenous kinases. A kinase to be tested is then added to one of the samples. After the kinase assay has been performed, samples are combined, digested with trypsin, followed by isotopomeric dimethyl labeling and phosphopeptide enrichment. Identification of the phosphopeptides and relative quantification is performed in a high mass accuracy mass spectrometer (see inset for the theoretical identification of a substrate for active kinase [green] based on the higher intensity in MS).

B) Procedure for the identification of relevant “*in vivo*” substrates. By using lysate derived from control (scrambled) or GCKIII kinase knockdown cells (in this case MST4), *in vitro* sites modulated by the kinase *in vivo* can be identified. Relevant substrates for the kinase of interest are identified based on the higher phosphopeptide intensity in MS for both the control (scrambled, blue) and kinase-added (green) samples. A higher phosphopeptide abundance in MS for the control (blue) sample relative to the knockdown (red) sample indicates a phosphorylation site downstream of the kinase of interest *in vivo*. A higher phosphopeptide abundance for the kinase-added (green) sample relative to the knockdown (red) sample indicates a phosphorylation site directly targeted by the kinase *in vitro*. C) Autoradiography displaying the efficiency of FBSA to inhibit all endogenous kinases (left, compare the DMSO to the FBSA lanes), and the effect of re-addition of an exogenous kinase (here MST4) on the phosphorylation of endogenous proteins. Autophosphorylation of MST4 is indicated by arrows. The * indicates GST-tagged MST4 (tag failed to fully cleave during purification); MST4 ΔCterm is the kinase domain of MST4 alone.

A

Gene Name	Protein Name	Phosphorylation Site(s)	Dimethyl Ratio MST4/Control	PTM Score
ACTB	Actin, cytoplasmic 1	S323,T324	59.807	176.42
ANXA2	Annexin A2	S22	16.753	83.758
TAGLN2	Transgelin-2	T180	33.94	199.82
CFL1	Cofilin-1	T70	14.544	270
MOB3	Mob1 homolog 3	T7	9.2966	143.96
CSRP2	Cysteine and glycine-rich protein 2	T79	14.308	168.5
DOCK3	Dedicator of cytokinesis protein 3	S836	3.9688	84.359
NME1	Nucleoside diphosphate kinase A	T103	12.296	165.66
HNRNPK	Heterogeneous nuclear ribonucleoprotein K	S75	3.9852	142.39
HSPA8	Heat shock cognate 71 kDa protein	T163	34.739	125.53
HSP90AA1	Heat shock protein HSP 90-alpha	T109	16.402	188.09
IDH1	Cytosolic NADP-isocitrate dehydrogenase	T311	11.173	155.08
LAP2	Lamina-associated polypeptide 2	T137	28.011	150.49
LMNA	70 kDa lamin	S22	3.9989	81.526
PSMD7	26S proteasome non-ATPase reg.sub. 7	T186	146.54	153.12
MYL3	Myosin light chain 3	T147	4.2375	179.5
NAP1L4	Nucleosome assembly protein 1-like 4	T261, T264	30.556	155.84
RPS19	40S ribosomal protein S19	T36	4.4339	132.79
TPI	Triosephosphate isomerase	T65	26.175	194.77
VIM	Vimentin	T63	7.3298	158.52

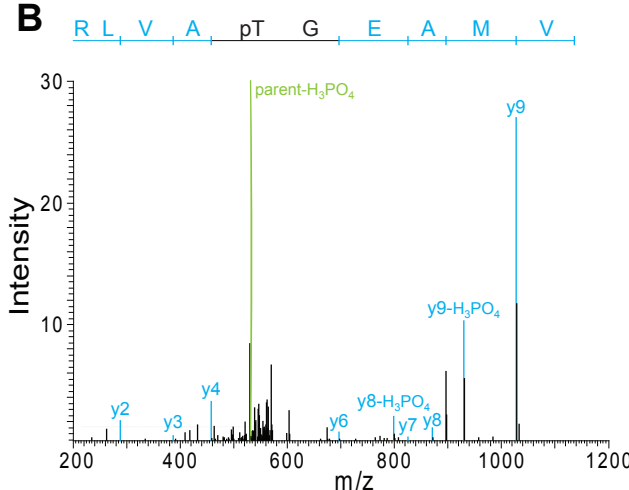
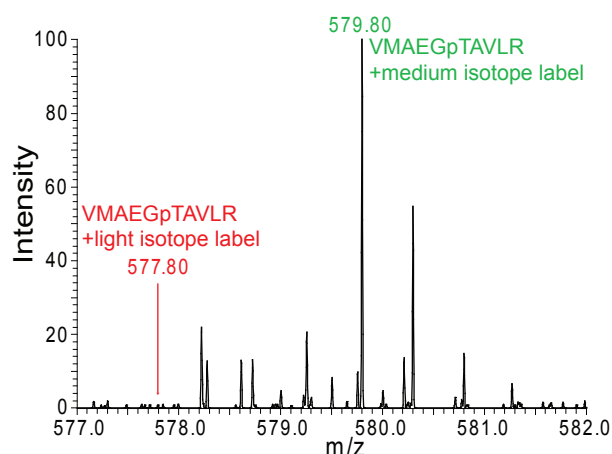
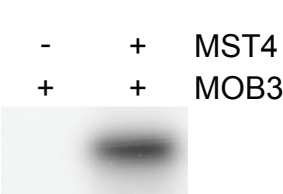
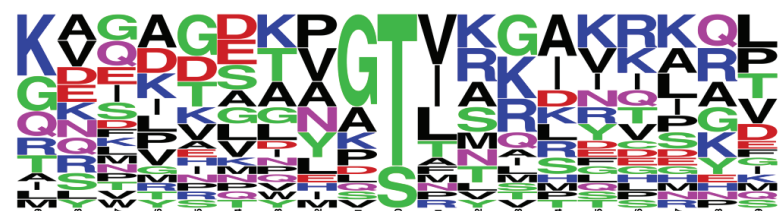
B**C****D****E**

Figure 20. In vitro MST4 substrates. **A)** Twenty-two *in vitro* substrate phosphorylation sites were identified for MST4 using the FSBA approach outlined in Figure 19. HEK293 lysate was used as a substrate pool. Each protein is listed with the site of phosphorylation, the dimethyl ratio indicating the enrichment of the corresponding phosphopeptide relative to control (unlabeled) lysate, and the post-translational modification score from the MaxQuant software. **B)** MS/MS spectra for the phosphopeptide VMAEGpTAVLR identified from MOB3. **C)** MS spectra showing the relative abundance of the MOB3 phosphopeptide from the control (red, light isotope label) and MST4-labeled (green, medium isotope label) lysate samples. **D)** *In vitro* validation of MOB3 as an MST4 substrate. Recombinant MOB3 was incubated with recombinant MST4 and a radiolabeling buffer (32P-ATP). The labeling of MOB3 in the presence of MST4 confirms it as a substrate. **E)** The twenty-two substrate phosphorylation sites were aligned and a sequence logo generated using Weblogo. The consensus phosphorylation motif for MST4 is G[S/T]a, where a is an aliphatic residue.

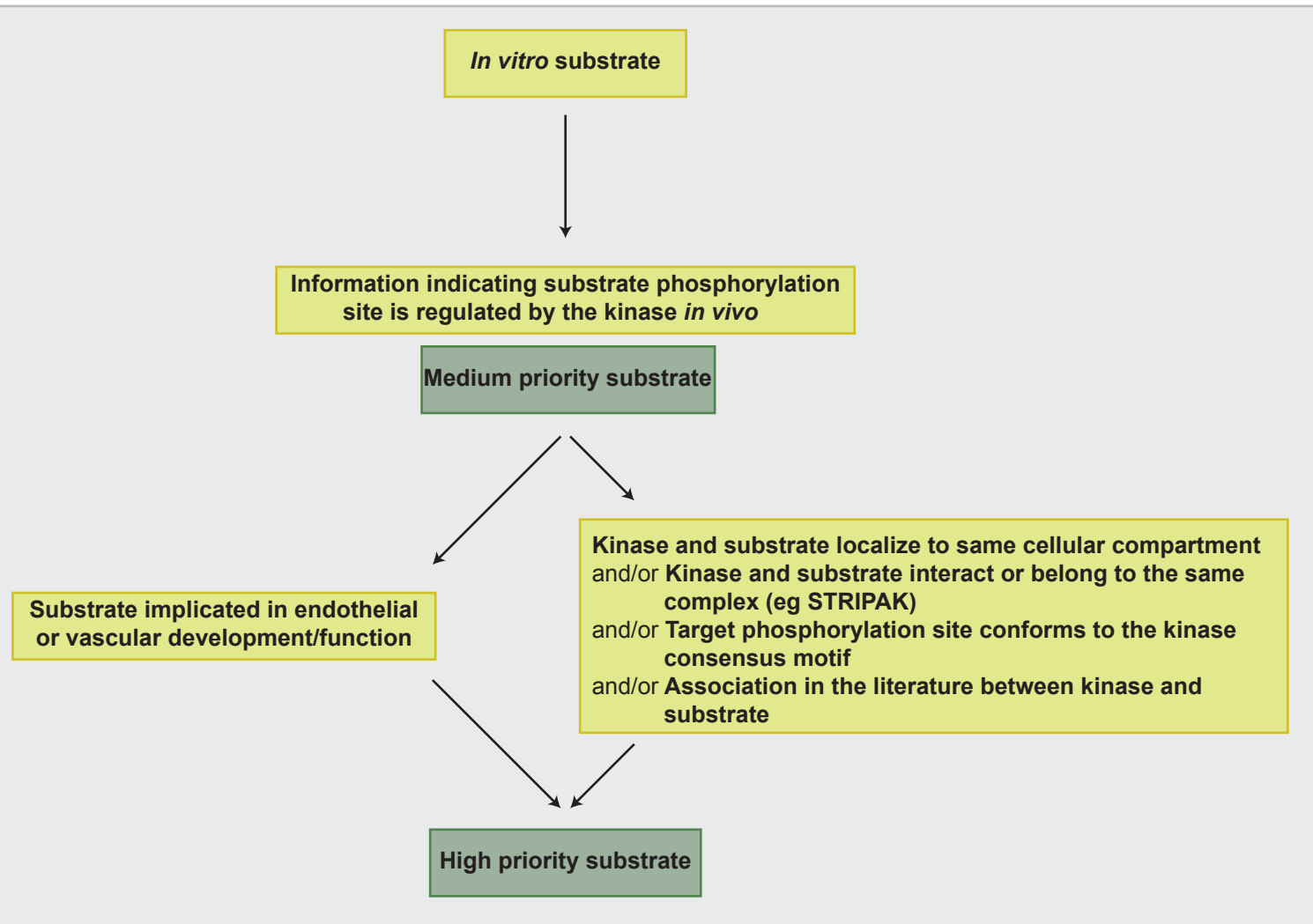


Figure 21. Strategy for prioritization of GCKIII kinase substrates. Following identification of *in vitro* substrates for the GCKIII kinases, *in vivo* information will be sought to determine if the substrate is downstream of the kinase *in vivo*. Such substrates will be labeled as “medium priority”. Substrates will be labeled as “high priority” if there is additional information available indicating they play critical roles in endothelial cell function or vascular development. As not all substrates will have been studied in endothelial or vascular contexts, we will also label substrates as “high priority” if they satisfy other criteria indicating there is a high-likelihood of biological relevance.

A PP2A Phosphatase High Density Interaction Network Identifies a Novel Striatin-interacting Phosphatase and Kinase Complex Linked to the Cerebral Cavernous Malformation 3 (CCM3) Protein^{*S}

Marilyn Goudreault,^{a,b} Lisa M. D'Ambrosio,^{a,b,c} Michelle J. Kean,^{a,c,d}
 Michael J. Mullin,^{a,e} Brett G. Larsen,^a Amy Sanchez,^f Sidharth Chaudhry,^{c,g}
 Ginny I. Chen,^{a,c,h} Frank Sicheri,^{a,c} Alexey I. Nesvizhskii,ⁱ Ruedi Aebersold,^{f,j}
 Brian Raught,^k and Anne-Claude Gingras^{a,c,l}

The serine/threonine protein phosphatases are targeted to specific subcellular locations and substrates in part via interactions with a wide variety of regulatory proteins. Understanding these interactions is thus critical to understanding phosphatase function. Using an iterative affinity purification/mass spectrometry approach, we generated a high density interaction map surrounding the protein phosphatase 2A catalytic subunit. This approach recapitulated the assembly of the PP2A catalytic subunit into many different trimeric complexes but also revealed several new protein-protein interactions. Here we define a novel large multiprotein assembly, referred to as the striatin-interacting phosphatase and kinase (STRIPAK) complex. STRIPAK contains the PP2A catalytic (PP2Ac) and scaffolding (PP2A A) subunits, the striatins (PP2A regulatory B'' subunits), the striatin-associated protein Mob3, the novel proteins STRIP1 and STRIP2 (formerly FAM40A and FAM40B), the cerebral cavernous malformation 3 (CCM3) protein, and members of the germinal center kinase III family of Ste20 kinases. Although the function of the CCM3 protein is unknown, the CCM3 gene is mutated in familial cerebral cavernous malformations, a condition associated with seizures and strokes. Our proteomics survey indicates that a large portion of the CCM3 protein resides within the STRIPAK complex, opening the way for

further studies of CCM3 biology. The STRIPAK assembly establishes mutually exclusive interactions with either the CTTNBP2 proteins (which interact with the cytoskeletal protein cortactin) or a second subcomplex consisting of the sarcolemmal membrane-associated protein (SLMAP) and the related coiled-coil proteins suppressor of IKK ϵ (SIKE) and FGFR1OP2. We have thus identified several novel PP2A-containing protein complexes, including a large assembly linking kinases and phosphatases to a gene mutated in human disease. *Molecular & Cellular Proteomics* 8:157–171, 2009.

Protein phosphatase 2A (PP2A)¹ is a major eukaryotic serine/threonine phosphatase that has been implicated in the control of cell growth, proliferation, and differentiation (1–4). The catalytic subunit of PP2A is represented by two genes in humans (gene names are in the supplemental materials; gene products here are referred to as PP2Ac α and PP2Ac β) sharing 97% identity at the protein level (5). Many mutually exclusive protein complexes containing the PP2A family catalytic subunits have been characterized biochemically (3, 6). The PP2A catalytic (PP2Ac) subunit binds directly to the PP2A A scaf-

From the ^aSamuel Lunenfeld Research Institute at Mount Sinai Hospital, Toronto, Ontario M5G 1X5, Canada, ^bDepartment of Molecular Genetics, University of Toronto, Toronto, Ontario M5S 1A8, Canada ^cInstitute for Systems Biology, Seattle, Washington 98103, ^dDepartment of Pathology and Center for Computational Medicine and Biology, University of Michigan, Ann Arbor, Michigan 48109, ^eInstitute of Molecular Systems Biology, ETH Zurich, Competence Center for Systems Physiology and Metabolic Diseases, and Faculty of Science, University of Zurich, CH-8093 Zurich, Switzerland, and ^fOntario Cancer Institute and McLaughlin Centre for Molecular Medicine, Toronto, Ontario M5G 1L7 Canada

Received, June 16, 2008, and in revised form, August 21, 2008

Published, MCP Papers in Press, September 8, 2008, DOI 10.1074/mcp.M800266-MCP200

¹ The abbreviations used are: PP2A, protein phosphatase 2A; PP2Ac, PP2A catalytic; STRIPAK, striatin-interacting phosphatase and kinase; STRIP1, striatin-interacting protein 1 (formerly FAM40A); STRIP2, striatin-interacting protein 2 (formerly FAM40B); GCK-III, germinal center kinase, subgroup III; CCM, cerebral cavernous malformation; AP, affinity purification; TAP, tandem affinity purification; SIKE, suppressor of IKK ϵ ; IKK ϵ , I κ B kinase ϵ ; SLMAP, sarcolemmal membrane-associated protein; IP, immunoprecipitation; IPI, International Protein Index; HA, hemagglutinin; CCT, chaperonin-containing TCP1; FOP, fibroblast growth factor receptor 1 oncogene partner; CTTNBP2, cortactin-binding protein 2; CTTNBP2NL, cortactin-binding protein 2, N-terminal-like; aa, amino acid(s); FHA, forkhead-associated; FGFR1, fibroblast growth factor receptor 1; CaMKIV, calcium-calmodulin-dependent kinase IV; STRN, striatin. See supplemental materials for gene names; LTQ, linear trapquadrupole; XML, eXtensible Markup Language.

folding subunit (two 85% identical proteins, PP2A A α and PP2A A β , are present in human cells), to form the so-called PP2A dimeric core (7–9). The core serves as a platform for the association of a regulatory or B subunit to generate a trimeric complex important for substrate recruitment and subcellular targeting. Four families of B subunits exist in human cells (B, B', B'', and B'''; the B''' members are commonly known as striatins), altogether coded for by at least 15 genes (for reviews, see Refs. 2, 3, and 6; for trimer structure, see Refs. 10 and 11). Several splice variants and post-translational modifications have been described for components of the PP2A holoenzyme, adding another level of complexity to the regulation and specificity of the phosphatases. Non-trimeric PP2A family-containing complexes have also been reported (in addition to the dimeric core of PP2Ac·PP2A A (12)). For example, the antiapoptotic protein alpha4 can interact directly with the PP2A catalytic subunit in the absence of the scaffolding subunit (13, 14). In addition, Mob3, a small molecular weight protein of the Mob family (also known as phocean or preimplantation antigen 3), stably assembles with striatin (B'') molecules, PP2Ac, and PP2A A in a complex containing at least four proteins (15, 16). Recent studies have highlighted the role of the regulatory subunits as key determinants of specificity and biological activity. For example, PP2A B' δ targets the Cdc25 protein for dephosphorylation during mitosis (17, 18). In addition, the PP2A B' γ subunit was demonstrated to be targeted by the small T antigen of SV40 in human cell transformation (19). Intracellular localization is also important, and a splice variant of PP2A B β 2, containing an N-terminal mitochondrial localization signal, assembles a holoenzyme involved in neuronal survival signaling (20).

Given the relevance of the composition of protein complexes in the biological functions of PP2A, it is important to devise approaches to characterize the many PP2A-containing molecular assemblies. Affinity purification coupled to mass spectrometry (AP-MS) is a powerful method to identify and characterize interaction partners (21–26). However, although a single AP-MS can successfully identify multiple interactors, this method is uninformative regarding the relationships between components of multiple multiprotein complexes containing a protein of interest. For example, AP-MS of PP2Ac or PP2A A would yield identification of both B and B' proteins in the same purification, yet B and B' proteins are mutually exclusive binding partners of the PP2Ac·PP2A A core and are never found in the same complex (2). Generating a high density interaction map in which most, and ideally all, interacting partners are purified in parallel experiments consisting of reciprocal purifications can help to resolve the components of individual complexes. The strategy utilized here is depicted in Fig. 1A. Briefly the protein of interest is epitope-tagged and stably expressed in human cells. The protein and its interacting partners are purified, subjected to proteolytic digestion, and identified using mass spectrometry (gel-free method). High confidence interactors are in turn cloned, expressed,

and purified, and their interacting partners are identified. The process may be repeated in an iterative fashion to generate high density local interactomes centered around proteins of interest. The high density of the interactions allows for a more precise understanding of the multitude of alternative complexes containing a particular protein of interest, a problem not always addressed in lower density global interaction studies (27–30).

Here we utilized tandem affinity purification (TAP) and FLAG affinity purification (31, 32) to produce a high density interaction map surrounding the PP2A catalytic subunit (we previously reported on the same approach used to study PP4c (33)). Our map recapitulated previously characterized assemblies for PP2A but also allowed the discovery of a large complex surrounding the previously characterized PP2Ac·PP2A A·striatin-Mob3 assembly. This complex, which we refer to as striatin-interacting phosphatase and kinase (STRIPAK), contains the uncharacterized proteins FAM40A/FAM40B, which we have renamed striatin-interacting proteins 1 and 2 (STRIP1 and STRIP2). In addition, STRIPAK contains all members of the GCK-III subfamily of Ste20 protein kinases (STK24, STK25, and MST4) as well as cerebral cavernous malformation 3 (CCM3; gene name PDCD10), a protein encoded by a gene mutated in familial cases of cerebral cavernous malformations (34, 35). In addition, we present evidence that STRIPAK can establish mutually exclusive interactions with the cortactin-binding proteins cortactin-binding protein 2 (CTTNBP2)/cortactin-binding protein 2, N-terminal-like (CTTNBP2NL) or with an assembly of sarcolemmal membrane-associated protein (SLMAP) and the related proteins SIKE/FGFR1OP2.

EXPERIMENTAL PROCEDURES

cDNA and Stable Cell Lines—Constructs used in this study are described in supplemental Table S2; all inserts were sequenced in their entirety. Briefly, coding sequences for proteins of interest were amplified by PCR using *Pfu* Ultra (or other high fidelity polymerases) from a HeLa cell cDNA library (Stratagene) or cDNA clones from the mammalian gene collection or IMAGE collection. Whenever human cDNAs were available they were used; in some cases, the mouse ORF was utilized instead. Our original clone for mouse Fam40A/STRIP1 lacked the initiator methionine and a glutamic acid codon as compared with the longest mouse cDNA (GenBank™ accession number NM_153563). A full-length construct of mFam40A/STRIP1 was therefore generated by adding coding sequences for methionine and glutamic acid in the PCR primer. The resulting sequence corresponds to GenBank accession number NM_153653 (coding sequence). Inserts were cloned in-frame into pcDNA3-FLAG, pcDNA3-3HA, or pcDNA3-NTAP vectors. Constructs were sequenced and found to match the sequence of the original cDNAs with the exception of MST4, which carried a single amino acid substitution (Ile-356 to Thr; no wild type clones were obtained). These constructs were stably expressed in low passage HEK293 cells as described previously (33), and pools of selected cell lines were generated. Expression was monitored by Western blotting using normal rabbit serum (for TAP-tagged constructs) or an antiserum directed against the FLAG epitope, respectively. To determine the approximate percentage of the FLAG-tagged proteins solubilized in our extraction pro-

cedure, we separately analyzed the pellet and supernatant following lysis; in each case, at least half of the protein was extracted, consistent with the previous annotation of many of the complex components as distributed in both membrane-associated and soluble compartments.

Antibodies—Rabbit anti-GST-alpha4 (rabbit 2972, a kind gift from Dr. N. Sonenberg) recognizes a single major band in HEK293 cell extract (not shown). Commercial antibodies were as follows (catalog numbers are in parentheses): anti-PP2Ac α (610555), anti-striatin (610838), and anti-MST4 (612684) were from BD Transduction Laboratories; anti-PP2A A was from Upstate Biotechnology (07-250); anti-SG2NA (STRN3) was from Cell Signaling Technology (S68); anti-PP4R2 was from Bethyl Laboratories (A300-838A), anti-FLAG was from Sigma (F3165); and anti-HA was from Covance Research Products (MMS-101P). Secondary antibodies for immunoblotting were donkey anti-mouse IgG and donkey anti-rabbit IgG, both conjugated to horseradish peroxidase (GE Healthcare). For the IP/Western of MST4 in Fig. 3A, the anti-mouse IgG TrueBlot Ultra horseradish peroxidase conjugate from eBioscience (88-8817-31) was used as a secondary antibody.

Tandem Affinity Purification and Mass Spectrometric Analysis—Tandem affinity purification was performed essentially as described previously (33), and proteins were eluted by incubation in 25 mM EGTA in 50 mM ammonium bicarbonate, pH 8. Sequencing grade modified trypsin (0.5–1 μ g; Promega) was added directly to the eluate. Digestion was performed overnight at 37 °C. Following digestion, the sample was lyophilized and then resuspended in reversed-phase HPLC buffer A1 (20 μ l; 0.4% AcOH, 0.005% heptafluorobutyric anhydride in H₂O). Prior to loading onto the reversed-phase column, the sample was centrifuged at 13,000 rpm for 10 min, and the supernatant was transferred to a fresh tube. Microcapillary reversed-phase columns (75- μ m inner diameter, 363- μ m outer diameter; Polymicro Technology) were cut to a final length of 15–20 cm, and spray tips were pulled in-house by hand. Columns were packed in-house (12 cm) with Magic C₁₈ 100-Å, 5- μ m silica particles (Michrom) using a pressure bomb. Prior to loading the sample, columns were equilibrated in HPLC buffer A1. Half of the sample was applied to the column using a pressure bomb and then washed off line in buffer A1 + 5% acetonitrile for 30–60 min. The LC column was then placed in front of a Finnigan LCQ mass spectrometer programmed for data-dependent MS/MS acquisition (one survey scan, three MS/MS of the most abundant ions). After sequencing the same *m/z* species (\pm 3 Da) three times, it was placed on an exclusion list for 3 min. Peptides were eluted from the reversed-phase column using a multiphasic elution gradient (5–14% acetonitrile over 5 min, 14–40% over 60 min, and 40–80% over 10 min). The remaining half of the sample was processed in the same manner. To prevent cross-contamination, each sample was analyzed on a freshly prepared reversed-phase column. The MS searches were performed as in Gingras *et al.* (33) such that the results are directly comparable: raw files generated by Xcalibur (Finnigan) were converted to the mzXML format (36), and combined runs (from the same sample) were searched using SEQUEST against the human International Protein Index (IPI) database, version 3.01 (55,140 entries were searched). SEQUEST searches were performed without constraining for the number of tryptic termini, with a mass tolerance on the precursor ion of \pm 2, and with methionine oxidation (+16) as a variable modification. SEQUEST html output was analyzed with PeptideProphet (37) and ProteinProphet (38) using the default parameters of each program. Supplemental Table S4 contains the experimental data; supplemental Tables S6 and S7 list the proteins identified on the basis of a single peptide together with additional evidence for the interaction. Supplemental Fig. S7 presents the annotated spectra of those proteins identified by a single unique peptide.

FLAG Affinity Purification, Immunoprecipitation Using Antibodies to Endogenous Proteins, and Mass Spectrometric Analysis—FLAG affinity purification was performed essentially as described previously (32) with the following modifications. Detergent concentration in the lysis buffer was 0.5% Nonidet P-40, the lysis buffer was added at 4 ml/g of wet cell pellet, and cells were subjected to passive lysis (30 min) followed by one freeze-thaw cycle. For the AP-MS of endogenous proteins, 0.3 mg of cell pellet from untransfected HEK293 cells was resuspended in 2.7 ml of lysis buffer, and cell extract was prepared as above. For each IP, 7 mg of crude lysate was used. The lysate was subjected to two preclearing steps: one on 20 μ l of packed protein G beads for 1 h and one on 20 μ l of packed protein G beads preincubated with 4 μ g of anti-HA antibody for 1 h. IP was performed by adding anti-MST4 (16 μ l), anti-striatin (8 μ l), or anti-FLAG (8 μ l) antibodies and protein G-Sepharose (25 μ l of packed beads) to the precleared lysate and incubating for 2 h. Beads were washed three times in lysis buffer and three times in 50 mM ammonium bicarbonate. Samples (from the FLAG or endogenous immunoprecipitations) were eluted with ammonium hydroxide, lyophilized in a SpeedVac, resuspended in 50 mM ammonium bicarbonate (pH 8–8.3), and incubated at 37 °C with trypsin overnight. The ammonium bicarbonate was evaporated, and the samples were resuspended in HPLC buffer A2 (2% acetonitrile, 0.1% formic acid) and then directly loaded onto capillary columns packed in-house with Magic 5 μ m, 100 Å, C₁₈AQ. MS/MS data were acquired in data-dependent mode (over a 2-h acetonitrile 2–40% gradient) on a ThermoFinnigan LTQ or a ThermoFinnigan LTQ-Orbitrap equipped with a Proxeon NanoSource and an Agilent 1100 capillary pump. mzXML files were generated from ThermoFinnigan *.RAW files using the ReAdW tool available in the TransProteomic Pipeline platform. The searched database contained the human IPI fasta sequence file (version 3.38; 70,856 entries plus the same number in reverse were searched) and common contaminants and was appended with a reversed version of the same IPI database. mzXML files were searched with X!Tandem (39) with *k*-score plug-in (40) using the following parameters: b- and y-ion series, partial trypsin digestion, allowing for one missed cleavage site, and methionine oxidation and N-terminal acetylation specified as variable modifications. The fragment mass tolerance was 0.8 Da (monoisotopic mass), and the mass window for the precursor was from –1 to 4 Da (average mass) in the case of LTQ data and from –100 to 100 ppm (monoisotopic) in the case of LTQ-Orbitrap data.

Search results were converted into pepXML format using Tandem2XML. PeptideProphet (37) was run on each result set, generating probability scores for each search result that are added to the pepXML documents. In the case of Orbitrap data, the high mass accuracy option was used. The resulting lists of peptides were assembled into proteins using ProteinProphet (38). ProteinProphet files were parsed and exported into a local Mysql database for further analysis and extraction of spectral count information.

Data were exported into Excel files and manually curated. Biological replicates were analyzed for FLAG-PP2Ac (*n* = 3) and FLAG alone (*n* = 3) to verify the reproducibility of the procedure (not shown). To generate lists of high confidence specific interactors, proteins detected in any of the FLAG alone samples were subtracted from the final list. Only those proteins that were detected with spectral counts >20 with at least two of the baits are reported. The error rate is 0% as measured by both ProteinProphet and using decoy scores. Supplemental Table S5 contains the experimental data; supplemental Tables S6 and S7 list the proteins identified on the basis of a single peptide together with additional evidence for the interaction. Supplemental Fig. S7 presents the annotated spectra of those proteins identified by a single unique peptide. Supplemental Table S8 contains the MS data for the endogenous IPs along with the annotated spectra for those proteins identified on the basis of a single unique peptide.

High confidence interactions reported here were submitted to the BioGrid (41).

Immunoprecipitation/Western Blot—Lysates from stable cell lines (prepared as above) were incubated with FLAG M2-agarose beads for 1.5 h, washed as above, and directly eluted by boiling in Laemmli or Criterion XT sample buffer. Alternatively lysates from untransfected HEK293 cells were incubated with protein G-Sepharose (GE Health-care) and antibodies to endogenous striatin (5 μ L), striatin3 (2.5 μ L), MST4 (2.5 μ L), PP4R2 (5 μ L), or the FLAG epitope (2.5 μ L) for 2 h and washed three times in lysis buffer and once in PBS prior to elution in 25 μ L of 2 \times Laemmli sample buffer. Precipitated proteins were separated via SDS-PAGE, transferred to nitrocellulose, and detected with antibodies directed against the FLAG or HA epitopes or endogenous proteins.

RESULTS

A PP2A High Density Interaction Network—The catalytic subunits of PP2A (PP2Ac α and PP2Ac β) were cloned in-frame C-terminal to a TAP cassette and stably expressed in HEK293 cells. Cells were lysed, and proteins recovered following dual purification were analyzed by mass spectrometry as described previously (33). After background subtraction (as in Ref. 33), we identified high confidence interactors for these catalytic subunits (Table I). Several of the interactors (alpha4 and the multisubunit CCT chaperonin complex) were detected previously with PP4c (note that we previously detected PP2Ac, PP4c, and PP6c peptides in immunoprecipitates from another protein, hTip41, but that we have not detected peptides for hTip41 in purifications of the catalytic subunits) (33). All other interactors were specific for PP2Ac α and PP2Ac β . The two PP2A catalytic subunits yielded essentially the same interactors as expected from previous studies (42, 43).

To characterize phosphatase complex organization, we generated a high density interaction network surrounding these phosphatases. To this end, we cloned into the TAP vector and stably expressed in HEK293 cells several of our identified interactors (alpha4, PP2A B α , PP2A B' α , the PP2A B'' striatin4, and Mob3; gene names are in supplemental Table S1). TAP and mass spectrometric analysis of these interactors yielded a detailed map of the interactions surrounding the PP2A catalytic subunits (Table I and Fig. 1B). We identified several different prototypical trimeric complexes containing the PP2Ac catalytic subunit, the PP2A A scaffolding subunit, and regulatory B, B', or B'' (striatin4) subunits. Note that we did not detect association with the B'' family in this set of experiments, but we did see these in subsequent purifications using FLAG affinity purification (supplemental Table S5). Each regulatory subunit associated specifically with the PP2Ac-PP2A A core and did not associate with other families of regulatory subunits (see below for discussion of striatin dimerization). Overall this experiment recapitulated the known organization of the PP2A trimers, which are composed of one catalytic protein, a single scaffolding protein, and a single regulatory molecule (for the B and B' families; Fig. 1C). In addition, we recapitulated alpha4 interaction with PP2Ac in the absence of PP2A A, representing an apparently mutually

exclusive interaction between alpha4 and the PP2A A and B subunits. These results indicate that our approach can successfully identify complexes described previously by biochemical approaches and that this type of analysis can be extended to identify potentially novel interactions.

In addition to the classical PP2A family trimers, a number of additional proteins were also detected in our network. For example, several peptides for liprin α (PPFIA1) were identified in PP2A A α purifications (and a few in PP2Ac purifications). Liprins are multidomain scaffolding proteins first identified as interactors of the leukocyte antigen-related (protein tyrosine phosphatase, receptor type F) tyrosine phosphatase (40) linked to synaptic functions in several organisms (40, 44). A recent publication reported the interaction of liprin α with the B'' PP2A regulatory subunit (45). Another interaction partner for PP2Ac β is FOP (also see supplemental Table S5), a protein associated with CAP350, required for microtubule anchoring to the centrosome (46). FOP was initially discovered as a fusion partner for fibroblast growth factor receptor 1 (FGFR1) in stem cell myeloproliferative disorders and confers dimerization (and constitutive activation) to FGFR1 (47–49). Other than the liprins and FOP, all other new PP2A interactors co-purified with striatin4 and Mob3; these interactors are described in more detail below. FOP and liprins did not associate with Mob3 and striatin4 and will be the topic of a separate follow-up study.

PP2A, Striatins, and Mob3 Stably Associate with Novel Components—We were particularly intrigued by an apparent higher order complex containing the catalytic and scaffolding PP2A subunits, the regulatory B'' molecule striatin4, and the Mob3 protein. Three striatin proteins exist in humans (gene names STRN, STRN3, and STRN4). Striatin expression levels are highest in brain where it has been implicated in synaptic functions (50–54). Earlier co-precipitation studies (16) identified the small Mob3 protein (referred to in the initial publications as phocean or hMob1, gene name MOBKL3 (15, 55)) as a striatin-interacting partner. Multiple Mob-like proteins exist in higher eukaryotes that appear to regulate the related nuclear DumbBell forming (Dbf)2-related and large tumor suppressor family of kinases through direct binding (56). Other striatin interactors detected in these earlier studies by co-immunoprecipitation and two-dimensional gel electrophoresis remained uncharacterized (16).

Our TAP tagging and AP-MS analysis of striatin4 and Mob3 (as well as PP2Ac and PP2A A) yielded many peptides corresponding to two different protein families: 1) FAM40A/FAM40B, which we have renamed STRIP1 and STRIP2 (also see below), and 2) CTTNBP2NL/CTTNBP2 (Fig. 1, B and D; lower amounts of peptides for additional unrelated proteins were also detected). STRIP1 and STRIP2 are highly related proteins (68% identity; supplemental Fig. S1) of unknown function with no significant homology to other proteins in the human genome and no recognizable sequence motifs. However, the STRIP1/2 proteins bear 13% identity with the yeast

TABLE I
Human PP2A-type phosphatase interaction network

Common names for the bait and prey proteins are listed alongside the spectral counts (PeptideProphet probability value >0.9; PEPT) and sequence coverage (% COVER) for the prey proteins. Results were sorted according to decreasing prey protein coverage. Preys in bold are STRIP1 and STRIP2 as well as CTTNBP2 and CTTNBP2NL, which are studied further in Fig. 2. For identifications based on a single unique peptide, a list of the experimental evidence is presented in supplemental Tables S6 and S7; annotated spectra are shown in supplemental Fig. S7.

BAIT	PREY	PEPT	% COVER	BAIT	PREY	PEPT	% COVER	BAIT	PREY	PEPT	% COVER
PP2Aα	PP2AA α	112	63.2	PP2AAα	PP2AA α	124	55.0	Mob3	dynein	6	62.9
	PP2AC $\alpha\beta$	77	55.3		PP2AB δ	39	45.5		Mob3	27	50.3
	PP2AB α	64	55.1		PP2AB α	33	44.9		striatin	63	46.4
	alpha4	37	51.3		PP2A $\alpha\beta$	36	42.7	STRIP1		55	45.0
	PP2AB δ	29	37.0		striatin 3	6	28.5	CTTNBP2NL		45	44.5
	PP2AB δ	11	27.5		PP2AB γ	7	27.2	PP2AA α		37	44.3
	Mob3	4	22.8		Mob3	6	22.8	PP2AC $\alpha\beta$		15	44.3
	striatin 3	9	15.8		PP2AB δ	7	20.1	striatin 4		44	42.2
	PP2AB ϵ	10	14.6	STRIP1		13	15.5	striatin 3		78	58.5
	PP2AA β	11	14.4		liprin A1	24	14.7	FGFR1OP2		2	15.0
STRIP1		4	12.3		striatin 4	8	14.2	PP2AA β		12	10.9
	PP2AB γ	4	12.2		striatin	9	9.9	SLMAP		5	9.1
	CCT2	2	7.9	CTTNBP2NL		5	8.4	STRIP2		12	7.2
	TCP1	2	5.6	PP2ABγ	CCT2	49	56.4	CTTNBP2		2	1.3
	striatin	2	4.5		TCP1	56	54.1	striatin4	striatin 4	175	58.8
	PP2AB α	2	3.7		CCT7	39	53.8		Mob3	52	53.8
	striatin 4	2	3.2		CCT4	35	47.4		striatin 3	107	47.8
PP2A$\epsilon\beta$	PP2AA α	69	46.3		CCT3	32	47.1		CCT3	30	46.0
	PP2AC β	60	45.6		CCT5	41	46.0		PP2AA α	80	43.0
	PP2AA β	60	44.0		PP2AB γ	51	44.7		striatin	70	36.3
	striatin	55	39.7		PP2AA α	44	44.4	CTTNBP2NL		49	31.0
	STRIP1	41	38.8		CCT8	33	39.4	TCP1		22	30.0
	striatin 3	22	34.3		CCT6	42	37.2	CCT4		24	29.8
	striatin 4	30	33.9		PP2A $\alpha\beta$	16	28.8	STRIP1		57	28.7
	TCP1	22	31.1		PP2AA β	10	9.1	PP2AC $\alpha\beta$		18	27.8
	CCT2	20	30.5	PP2ABα	PP2A $\alpha\beta$	18	38.8	CCT7		25	24.3
	alpha4	12	28.6		PP2AB α	20	29.6	CCT5		13	23.8
	PP2AB α	10	26.7		PP2AA α	36	28.2	CCT2		27	19.5
	Mob3	12	22.8					CCT6A		30	18.5
	CCT4	8	22.6					CCT8		26	15.0
	CCT3	12	21.3					FGFR1OP2		2	13.5
	CCT6A	14	19.8					dynein		6	12.4
	CCT5	12	19.6					PP2AA β		2	11.3
	CCT8	9	16.6								
CTTNBP2NL		14	15.2								
	FOP	3	14.2								
	PP2AB δ	2	9.1								

protein Far11, which has been linked to pheromone signaling, and 21% identity with the *Neurospora crassa* HAM-2 gene product, which is implicated in hyphal fusion (supplemental Fig. S1). CTTNBP2 and CTTNBP2NL are also related; the N terminus of CTTNBP2 is 38% identical and 53% similar to CTTNBP2NL over 649 aa (supplemental Fig. S2). This N-terminal portion is predicted to contain a ~200-aa stretch of coiled-coil motifs. A shorter variant of CTTNBP2 (also known

as CBP90), corresponding to the N-terminal 630 aa, was first identified as a protein interacting with the Src homology 3 domain of cortactin (cortical actin-binding protein) in an overlay assay and GST pulldown (57). This interaction is apparently mediated by a proline-rich region at the C terminus of CTTNBP2 that is conserved in CTTNBP2NL (supplemental Fig. S2). Note that we did not detect cortactin in any of our interaction studies.

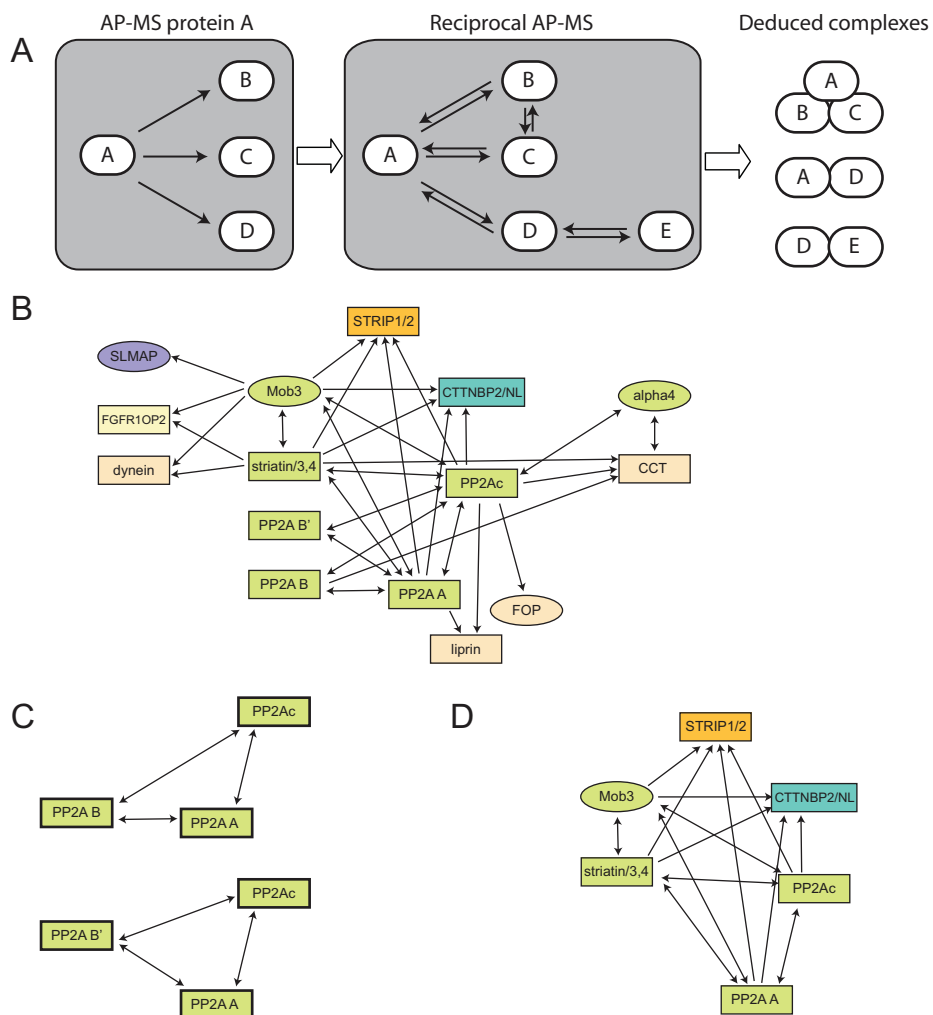


FIG. 1. TAP interaction network for PP2A phosphatases. *A*, iterative TAP tagging approach to identify protein complexes. Protein A is stably expressed in HEK293 cells, and interaction partners B, C, and D are detected by LC-MS/MS. Proteins B, C, and D are in turn cloned and stably expressed, and their interactors are identified. Here proteins B and C only interacted with each other and with protein A. Protein D interacted with the new protein E, which was in turn tested by TAP tagging. The mass spectrometric data for this high density network suggest the association of A in two mutually exclusive complexes: (a) a trimer with B and C or (b) a dimer with D. The association of protein D in a dimer with A is likely to be mutually exclusive with its association with protein E in a separate complex. *B*, phosphatase interaction network for PP2A detected by TAP tagging. The proteins used as baits are shown in green. For display purposes (and because we have not detected evidence for paralog-specific interactions with TAP tagging), proteins belonging to the same paralogy group (defined in supplemental Table S3) are collapsed into a single node (in this case, they are represented by rectangles, whereas proteins without paralogs are shown as ovals). The directionality of the arrows represents the bait to prey relationship. *C*, classical PP2A trimers detected by reciprocal TAP tagging. D, PP2Ac, PP2A A, striatin4, and Mob3 interact with two novel protein families, STRIP1/STRIP2 (orange) and CTTNBP2/CTTNBP2NL (blue).

Because we obtained many more peptides for STRIP1 (FAM40A) and CTTNBP2NL than for their respective paralogs in the TAP experiments, we used these two proteins for subsequent IP/Western validation studies. STRIP1 and CTTNBP2NL were cloned into the pcDNA3-FLAG vector (see “Experimental Procedures”) and stably expressed in HEK293 cells. Lysates were subjected to immunopurification using FLAG M2-agarose beads followed by immunoblotting using antibodies directed against endogenous striatin and PP2Ac (the interaction of STRIP1 with PP2A A α is shown in supplemental Fig. S3). As a control, cells were transfected with the FLAG vector alone or FLAG-alpha4 (according to our MS

results, alpha4 interacts with PP2Ac but not with striatin). As shown in Fig. 2 (and despite the low expression of FLAG-CTTNBP2NL) STRIP1 and CTTNBP2NL co-precipitated striatin and PP2Ac, although the percentage of PP2Ac (and PP2A A; supplemental Fig. S3) co-precipitated was low. This is consistent with our MS results in which the number of STRIP1 and CTTNBP2NL peptides was highest in striatin4 and Mob3 purifications. The relatively low abundance of STRIP1 and CTTNBP2NL peptides in PP2Ac and PP2A A purifications (13 each with PP2Ac) may be accounted for by alternate complexes containing the same PP2Ac and PP2A A subunits (2–4).

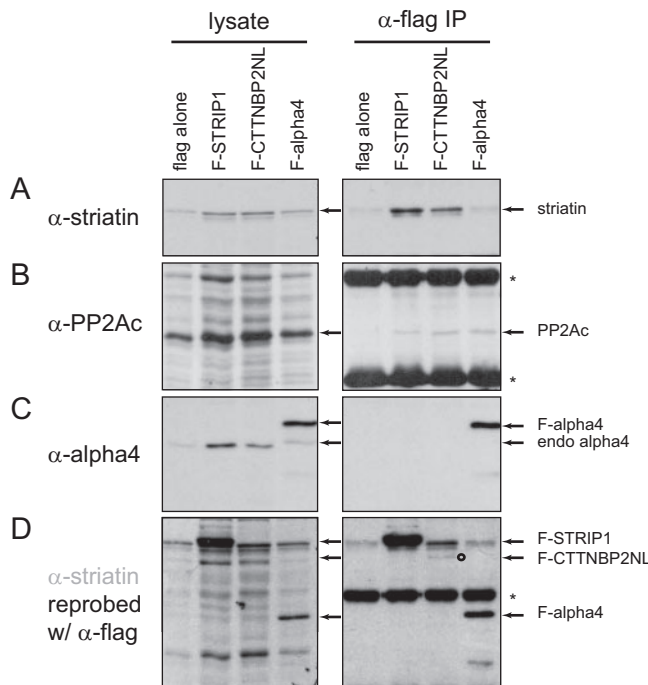


Fig. 2. Association of STRIP and CTTNBP2NL with PP2Ac and striatin. Extracts were prepared from pools of cells stably expressing FLAG alone, FLAG-STRIP1, FLAG-CTTNBP2NL, or FLAG-alpha4, and FLAG purification on M2-agarose beads was performed on 300 μ g of lysate per condition (whole cell lysate was 25 μ g). Proteins were eluted directly in Laemmli sample buffer, separated by SDS-PAGE, transferred to nitrocellulose, and detected by immunoblotting with antibodies to the endogenous striatin (A), PP2Ac (B), alpha4 (C), or FLAG tag (D). The position of the proteins is indicated by an open arrow, and asterisks denote the IgG heavy and light chains. FLAG-tagged CTTNBP2NL is expressed at very low levels, and its position is indicated by an open circle.

Interaction Partners for STRIP1 and CTTNBP2NL—We next focused on the characterization of proteins associating with STRIP1 and CTTNBP2NL. To increase throughput and potentially enrich for weaker interactors, we utilized a purification strategy using a single N-terminal FLAG epitope. Although this approach yielded a significant increase in background contaminants (32, 58), it also allowed us to obtain significantly increased peptide coverage for each of the proteins in our complex. FLAG-tagged STRIP1 and CTTNBP2NL stably expressed in HEK293 cells (as in Fig. 2) were used for AP-MS, and contaminant proteins were subtracted as described under “Experimental Procedures” to generate an annotated list of interactors (Table II and supplemental Table S5).

As shown in Table II, purification of the FLAG-tagged mouse STRIP1 protein efficiently recovered PP2A catalytic and scaffolding subunits as well as all three striatins and Mob3, confirming these interactions (Fig. 1). CTTNBP2NL and CTTNBP2 were also detected in STRIP1 AP-MS, indicating that these proteins can be present within the same complex as STRIP1. Additional proteins were also confidently identified by several peptides (Table III and text below for a brief de-

TABLE II
Matrix distribution of spectral counts across FLAG pulldowns (columns) for one representative experiment

Hits are listed in rows; horizontal lines separate groups of paralogs. Dark gray shading indicates spectral counts for the bait. A complete table is presented in the supplemental materials. When multiple entry numbers matched the same gene, only the top entry is reported.

	F-CTTNBP2	F-CTTNBP2NL	F-striatin	F-striatin3	F-Mob3	F-STRIP1	F-TRAFIP3	F-SIKE	F-CCM3	F-STK24	F-STK25	F-mmMst4	F-PP2AA α	F-PP2AA β
CTTNBP2	122		7	24	51	7	..	3	1*	
CTTNBP2NL	7	108	28	52	107	19			10	44	46	33	3	13
striatin	52	88	845	56	308	104	85	69	31	113	229	89	9	34
striatin3	96	107	51	212	260	143	73	55	23	84	153	68	27	37
striatin4	66	75	123	69	396	100	64	33	10	43	32	28	10	10
Mob3	26	69	59	52	179	42	29	16	9	22	33	29	10	
STRIP1	71	62	93	99	164	424	62	40	13	55	33	52	8	13
STRIP2	18	26	13	18	28	34	16	..	13	5	8			
SLMAP			59	51	104	17		37	17	41	48	33	2	1*
TRAF3IP3						60		..						
FGFR1OP2			30	17	29	11	30	26	8	9	12	13		
SIKE			12	20	50	5	39	218	5	16	2	11		
PDCD10	4	15	25	6	33	20	7	6	218	81	63	97		
STK24	47	..	59	..	8	4	209	322		
STK25	..	10	10	195	..	577	3		
MST4	3	8	36	26	294	..	16	555		
PP2AA α	43	43	76	52	111	25	37	30	19	63	40	39	548	345
PP2AA β	..	8	16	..	32	17	11	..	2	57
PP2Ac (α/β)	15	22	29	32	28	17	15	11	6	10	9	14	121	124

• For identifications based on a single unique peptide, a list of the experimental evidence is presented in supplemental Tables S6 and S7; annotated spectra are shown in supplemental Fig. S7.

•• ProteinProphet detected spectra corresponding to this protein, but no spectrum could uniquely be assigned to this entry.

scription of these proteins), including SLMAP; two small related proteins, SIKE and FGFR1OP2; members of the GCK-III subfamily of the Ste20 kinases (STK24, STK25, and MST4); and the CCM3 protein. Purification of CTTNBP2NL also recovered all of these proteins (including STRIP1/FAM40A and STRIP2/FAM40B) with the exception of SLMAP, FGFR1OP2, and SIKE (Figs. 3 and 4). A brief description of each of these interactors follows.

SLMAP was initially identified as a component of the cardiac sarcolemma involved in myoblast fusion and muscle contraction (59–61). Four SLMAP splicing variants have been studied; all encode a putative transmembrane domain toward the C terminus as well as two putative leucine zippers but vary in their N termini: one of the longest isoforms encodes a putative FHA domain and localizes to the centrosome (62).

SIKE is a small coiled coil-containing protein first characterized as an interaction partner for the kinases TBK1 and IKK ϵ and as a negative regulator of the interferon pathway (63). SIKE is 50% identical to another co-precipitating protein, FGFR1OP2. SIKE and FGFR1OP2 orthologs have been detected throughout metazoa, but no functions have been ascribed to these proteins in model organisms (supplemental Fig. S4). Interestingly FGFR1OP2 is implicated in the 8p11 myeloproliferative syndrome, a rare and aggressive

STRIPAK Links Phosphatases and Kinases to CCM3

TABLE III
STRIPAK components

STRIPAK and associating partners comprise 10 protein families (paralogy groups) and 20 proteins. The percentage of identity between the most distant family members (%ID) is indicated as well as structural motifs and biological functions assigned to each of the proteins. See text and the supplemental material for more details. N/A, not applicable.

Protein or paralogy group	%ID	Protein name	Structural motifs	Biological role
1	97	PP2A α	Phosphatase catalytic, PP2A family	Protein dephosphorylation; multiple substrates
		PP2A β	Phosphatase catalytic, PP2A family	Protein dephosphorylation; multiple substrates
2	85	PP2AA α	HEAT repeats, PP2A scaffold	Phosphatase scaffold; multiple substrates
		PP2AA β	HEAT repeats, PP2A scaffold	Phosphatase scaffold; multiple substrates
3	46	striatin	WD40, coiled-coil, PP2A regulatory	Protein binding; calcium signalling; synaptic functions
		striatin3	WD40, coiled-coil, PP2A regulatory	Protein binding; calcium signalling; synaptic functions
		striatin4	WD40, coiled-coil, PP2A regulatory	Protein binding; calcium signalling; synaptic functions
4	N/A	Mob3	Mob domain	Suggested roles in trafficking, synaptic functions
5	68	STRIP1	None detected	Not determined
		STRIP2	None detected	Not determined
6	36	CTTNBP2NL	Coiled-coil, Proline-rich	Not determined
		CTTNBP2	Coiled-coil, Proline-rich, ankyrin repeats	Binds the cytoskeletal protein cortactin
7	20	SLMAP	Coiled-coil, FHA, leucine zipper, hydrophobic membrane anchor	Myoblast fusion, muscle contraction
		TRAF3IP3	Coiled-coil	Binds TRAF3; activates stress pathway
8	47	SIKE	Coiled-coil	Binds IKK ϵ , TBK1; negatively regulates interferon pathway
		FGFR1OP2	Coiled-coil	Fusion partner for FGFR1 in myeloproliferative syndrome
9	N/A	CCM3	None detected	Gene mutated in cerebral cavernous malformations
10	66	STK24	Ste20 kinase, GCK-III subgroup	Protein phosphorylation; putative involvement in proliferation, apoptosis, stress response
		STK25	Ste20 kinase, GCK-III subgroup	Protein phosphorylation; putative involvement in proliferation, apoptosis, stress response
		MST4	Ste20 kinase, GCK-III subgroup	Protein phosphorylation; putative involvement in proliferation, apoptosis, stress response

hematological malignancy characterized by the fusion of unrelated genes to the FGFR1, resulting in the dimerization and activation of FGFR1 in a ligand-independent manner. The FGFR1OP2 fusion involves two coiled-coil domains from FGFR1OP2 that likely promote dimerization of the FGFR1OP2-FGFR1 protein (64).

The CCM3 protein is encoded by the gene *PDCD10*, mutations of which are found in families with cerebral cavernous malformations (34, 35, 65). Cerebral cavernous malformations are a type of angioma affecting 0.5–1% of the population (66–68). Although most individuals are asymptomatic, roughly 30% will develop symptoms ranging from headaches to seizures, strokes, and even death. The CCM3 protein was demonstrated previously to interact with the GCK-III subgroup of Ste20 family kinases both in yeast two-hybrid assays (where the interaction was first reported) and by co-immunoprecipitation followed by Western blotting (69, 70). Consistent with this, several peptides for these three Ste20 kinases (STK24, STK25, and MST4) were found in association with STRIP1 and CTTNBP2NL in our study. These three kinases

define a subgroup of the germinal center kinases (GCK-III) characterized by an N-terminal kinase domain followed by a C-terminal tail of unknown function. The GCK-III kinases have been linked to proliferation, apoptosis, and stress response, but the substrates and molecular mechanism of action remain largely unknown (71–77).

The interaction of STRIP1 and CTTNBP2NL with endogenous MST4 was confirmed by immunoprecipitation/immuno-blotting (Fig. 3A); FLAG-alpha4, which was used as a negative control, failed to co-precipitate MST4. We also monitored the interactions among endogenous proteins. Antisera directed against MST4, striatin, and striatin3 (but not anti-PP4R2 or anti-FLAG) all recovered striatin and striatin3 from untransfected HEK293 cells (Fig. 3B), indicating that the interaction detected between the MST4 kinase and striatins is not due to the presence of an epitope tag or mild overexpression. We also subjected the anti-MST4 and anti-striatin3 immunoprecipitates to mass spectrometry and were able to recover many of the binding partners also seen in FLAG AP-MS (supplemental Table S8).

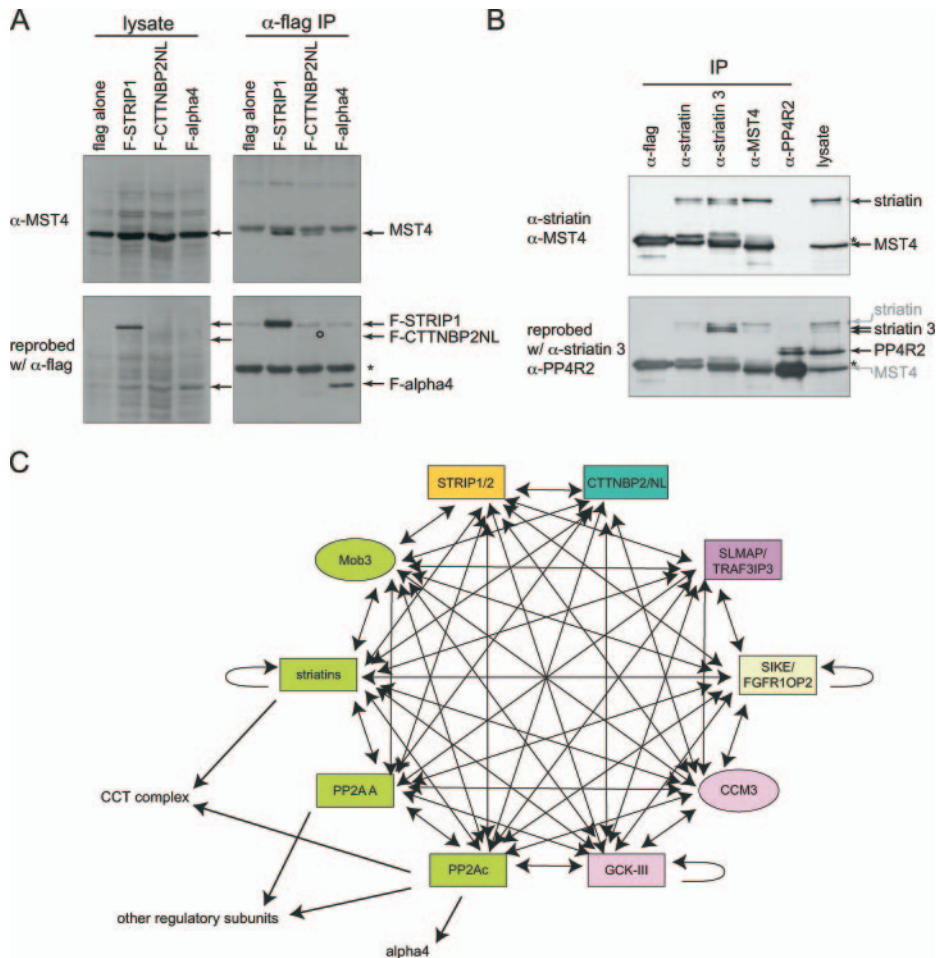


FIG. 3. STRIPAK complex interactions. *A*, interaction of MST4 with STRIPAK. FLAG purification was performed as in Fig. 2, and detection of endogenous MST4 in immunoprecipitates was performed. *B*, validation of the interactions among endogenous proteins. Lysate from untransfected HEK293 cells (1 mg per IP) was used for immunoprecipitation using the indicated antibodies and protein G-Sepharose (whole cell lysate = 30 μ g). Proteins were directly eluted in Laemmli sample, separated by SDS-PAGE, transferred to nitrocellulose, and detected by immunoblotting with specified antibodies. PP4R2 is a PP4c-interacting protein used here as a negative control. *C*, summary of the interactions detected by AP-MS with FLAG-tagged proteins. Green nodes represent the previously characterized association between PP2Ac, PP2A A, striatins, and Mob3; pink indicates previously characterized interactions between CCM3 and the Ste20 kinases of the CGK-III subgroup. The directionality of the arrows represents the bait to prey relationship. When evidence of self-interaction within a protein family exists, self-pointing arrows are depicted.

In summary, AP-MS of STRIP1 and CTTNBP2NL confirmed the interactions with PP2Ac, PP2A A, striatins, and Mob3 but also revealed that these proteins are capable of interacting with each other. In addition, SLMAP, SIKE, FGFR1OP2, CCM3, and the GCK-III subfamily of kinases were able to interact with these proteins and are putative components of this complex (Figs. 3 and 4).

Reciprocal Interactions among Complex Components—To further characterize the many newly detected protein-protein interactions, FLAG-PP2Ac α , FLAG-PP2Ac β , FLAG-PP2A A α , FLAG-striatin, FLAG-striatin3, FLAG-STK24, FLAG-STK25, FLAG-CTTNBP2, and FLAG-SIKE were stably expressed in HEK293 cells for a second round of interaction studies. We could not express SLMAP in HEK293 cells (supplemental Fig. S6 and data not shown) and therefore cloned and expressed

the only related family member of SLMAP, namely TRAF3IP3 (supplemental Fig. S5). SLMAP and TRAF3IP3 share 22% identity at the amino acid level (a stretch of 343 amino acids exhibits 28% identity and 50% similarity), and both proteins contain predicted coiled-coil regions. TRAF3IP3, initially cloned as a TRAF3 interactor involved in signaling via the c-Jun N-terminal kinase (JNK) pathway, is normally restricted to cells of lymphoid origin and is not endogenously expressed in HEK293 cells. At the onset of these studies (and because the similarity between SLMAP and TRAF3IP3 is fairly low) we did not know whether TRAF3IP3 would interact with the same partners as SLMAP. With the inclusion of FLAG-TRAF3IP3, the list of baits represents at least one member for each of the paralogous protein families detected in our STRIP1 and CTTNBP2NL AP-MS analyses.

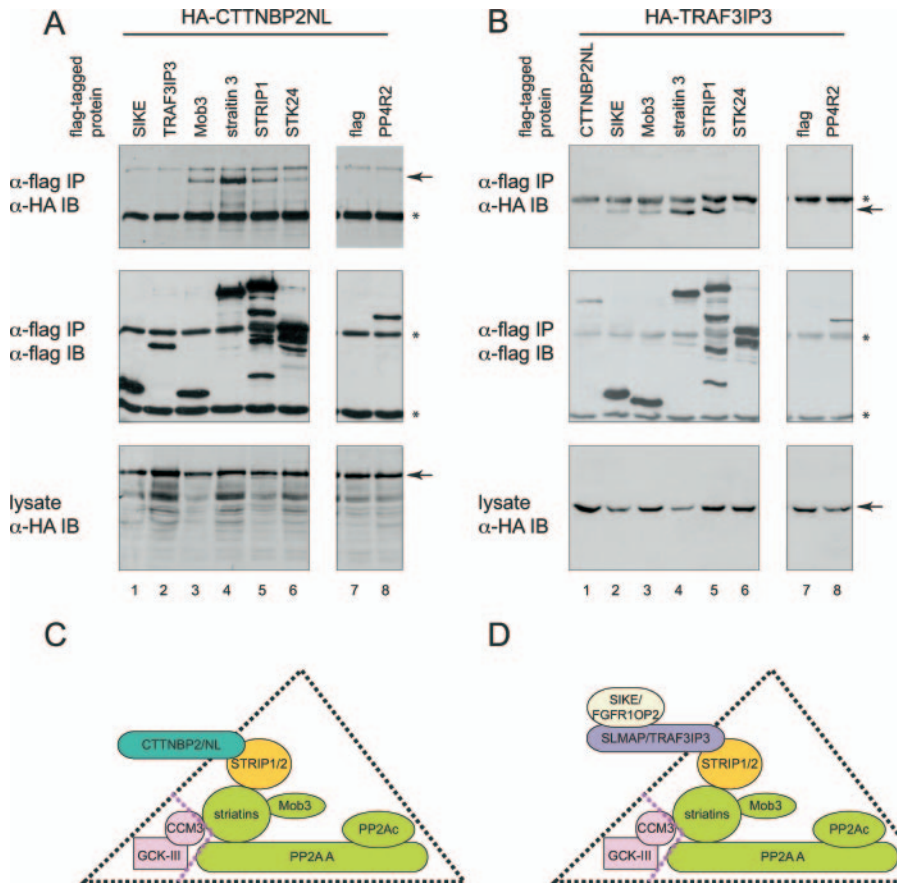


Fig. 4. Mutually exclusive associations with STRIPAK. A and B, STRIPAK assembles with CTTNBP2NL or TRAF3IP3 in a mutually exclusive manner. Immunoprecipitation on anti-FLAG-Sepharose beads was performed on lysate from HEK293 cells transiently co-expressing the indicated FLAG- and HA-tagged constructs. To monitor specificity of the interactions, negative controls included FLAG alone as well as FLAG-PP4R2. Immune complexes were resolved by SDS-PAGE followed by transfer to nitrocellulose. Co-precipitation of HA-tagged proteins was detected by immunoblotting (*IB*) for the HA epitope (*top panels*; position of the tagged protein is indicated by an arrow. Asterisks indicate the heavy chains.). The precipitated FLAG-tagged protein was detected with anti-FLAG antibodies (*middle panels*). The expression of the HA-tagged protein in all samples is comparable (*bottom panels*). C and D, model for mutually exclusive interactions with STRIPAK. Our data suggest that STRIP proteins (orange) associate with the striatins, Mob3, and the phosphatases (green) in a stable complex. Associated with this complex are the CCM3 and GCK-III kinases (pink); these are likely to be more weakly associated as they were not recovered in TAPs. This core complex, STRIPAK, may associate with CTTNBP2 family proteins (C) or with a second complex containing SLMAP and SIKE family proteins (D).

The interaction of each of these proteins with endogenous striatin was confirmed by IP/Western from each of the FLAG-tagged stable cell lines (supplemental Fig. S6 and data not shown). AP-MS for each of the FLAG-tagged proteins was also performed to detect their associations with each other (Table II; a complete list of the MS data is in supplemental Table S5; interactions of some of these proteins with STK24 were reported previously by Ewing *et al.* (78), but the low density of the data did not allow determination of complex composition). Striatins as well as the Mob3 protein, the PP2A scaffolding subunit, CCM3, and the Ste20 kinases of the GCK-III group co-precipitated every other protein in this large group, indicating that these proteins have the ability to form interactions with each member of the complex. In addition, as shown above and as reported previously, we observed that the striatins can asso-

ciate with each other; striatin brought down unique peptides for striatin3 and striatin4 and vice versa. The PP2Ac·PP2A A·striatin·Mob3·STRIP·CCM3·GCK-III proteins thus form a large multiprotein complex *in vivo* that we refer to as the STRIPAK complex.

Interestingly AP of CTTNBP2 (as with CTTNBP2NL above) did not contain detectable amounts of SLMAP, SIKE, or FGFR1OP2. Conversely immunoprecipitates of the SLMAP-related protein TRAF3IP3 did not yield detectable amounts of CTTNBP2 or CTTNBP2NL but did yield large quantities of SIKE and FGFR1OP2. SIKE immunoprecipitates contained a large number of SLMAP and FGFR1OP2 peptides but no detectable CTTNBP2 or CTTNBP2NL peptides. These data suggest that the association of CTTNBP2NL or CTTNBP2 with the remainder of the STRIPAK complex may preclude the association of SLMAP/TRAF3IP3 and SIKE/FGFR1OP2 and

vice versa; *i.e.* these interactions appear to be mutually exclusive. To validate these findings, transient transfections of either an HA-tagged version of CTTNBP2NL or of TRAF3IP3 with a panel of FLAG-tagged proteins (SIKE, Mob3, striatin3, STRIP1, STK24, CTTNBP2NL, TRAF3IP3, PP4R2, or FLAG alone) was performed. Recombinant FLAG-tagged proteins were immunoprecipitated, and the co-precipitation of the HA-tagged proteins was detected by immunoblotting with an antibody against the HA epitope. As expected, both HA-CTTNBP2NL and HA-TRAF3IP3 were efficiently recovered in Mob3, striatin3, STRIP1, and STK24 pulldowns but not in the negative controls (FLAG alone and PP4R2; Fig. 4, A and B). In agreement with our mass spectrometry results, however, HA-CTTNBP2NL was not detectable in SIKE or TRAF3IP3 pull-downs (Fig. 4A, *top panel*, lanes 1 and 2). Conversely HA-TRAF3IP3 was not detectable in CTTNBP2NL pulldowns but was easily detected in SIKE pulldowns (Fig. 4B, lanes 1 and 2) consistent with the notion that SIKE/FGFR1OP2 and SLMAP/TRAF3IP3 can be present in the same complex but do not co-exist with CTTNBP2NL/CTTNBP2.

Taken together, our data highlight a stable, core complex containing PP2A catalytic and scaffolding subunits, striatin(s), Mob3, and STRIP (Fig. 4, C and D). Because we did not detect CCM3 and the Ste20 kinases in our TAP experiments, they are not likely to be necessary for the formation of this core complex and may be associated with it more loosely to form the STRIPAK complex. The STRIPAK assembly appears to associate either with a member of the CTTNBP2 family or with SLMAP/TRAF3IP3 in combination with SIKE/FGFR1OP2.

DISCUSSION

CCM3 and Its GCK-III Kinase Subfamily Partners Are Physically Associated with PP2A Complexes—Here we report the identification of a large molecular assembly (STRIPAK) that links the *PDCD10* gene product CCM3 and associated GCK-III kinases to a PP2A-striatin-Mob3-STRIP complex. Mutations in the CCM1, CCM2, and CCM3 genes account for nearly all cases of familial cerebral cavernous malformations (68). Previous proteomics studies detected an interaction between CCM3, CCM1, and CCM2, suggesting a common mode of action for all three proteins (70, 79). However, here we demonstrate that (at least in HEK293 cells) CCM3 preferentially associates with GCK-III kinases and our newly defined PP2A-striatin-Mob3-STRIP complex. No CCM1 or CCM2 peptides were detected in our analyses either with CCM3 or with other STRIPAK components. However, we did obtain evidence for an interaction between CCM3 and CCM2 when performing AP-MS using CCM2 (rather than CCM3) as a bait. In that case, FLAG-tagged CCM2 pulldowns yielded numerous peptides for CCM1; yet a small number of CCM3 peptides were also detected (not shown). These data suggest that CCM1 and CCM2 form an abundant complex that likely associates with CCM3 in substoichiometric amounts, whereas a large portion of CCM3 is

associated with the STRIPAK complex. Hence we posit that members of the PP2A-striatin-Mob3-STRIP complex should be analyzed for their involvement in non-familial cases of CCM where the genetic basis for the disease is unknown (mutations in CCM1–3 only account for 60% of sporadic cases (68)).

Interactions between GCK-III Kinases and PP2A—It is intriguing that the STRIPAK complex contains both phosphatase and kinase components. Associations between PP2A and several other kinases have been reported previously. Casein kinase II, the ribosomal S6 protein kinase (S6K1), the calcium-calmodulin-dependent kinase IV (CaMKIV), and the Raf protein were all described as interactors for the catalytic subunit of PP2A (80–83) but were not identified as interaction partners for PP2A in this study. This apparent discrepancy may be due to differences in the biological system used (for example the initial identification of the CaMKIV-PP2A interaction was performed in T cells (80)) or more likely due to the differential sensitivity of the methods of analysis used. Previous studies detected interactions by affinity purification of one component (usually the kinase) followed by immunoblotting for the other factor (PP2A). By contrast, we relied on immunoprecipitation of the PP2A phosphatase coupled to direct MS analysis. Because PP2A is a highly abundant protein and is capable of interacting with multiple binding partners, the fraction of PP2A complexed with a specific protein may be below the detection limits of our method. In this regard, even the interactions of PP2Ac with the Ste20 kinases were not detected in every analysis; co-precipitation of the GCK-III kinases was much more readily detected when starting from striatin or other complex components that reside predominantly in STRIPAK.

The presence of the GCK-III kinases and the PP2A phosphatase within a single complex raises the intriguing question of the enzyme/substrate relationships. Are the kinases regulating the phosphatases or vice versa? Are the substrates for these two enzymes the other STRIPAK components, or are the substrates yet to be identified? Interestingly many of the STRIPAK components are phosphoproteins (16, 70, 76, 84, 85); known phosphopeptides are displayed in supplemental Figs. S1, S2, and S4. In addition, the striatins and the Mob3 protein were previously suggested to be PP2A targets as their phosphorylation (as detected by mobility shift on SDS-PAGE and by ³²P labeling) increased following treatment with the PP2A inhibitor okadaic acid (16). Phosphorylation sites were identified on each of the three striatins and are located at amino acids Ser-245, Ser-229, and Ser-206, respectively (86–90). Further studies will be aimed at defining the dependence of these phosphorylation events on the phosphatases and kinases associated to STRIPAK.

What Is the Function of STRIPAK?—Although our study allowed us to define a macromolecular complex(es) in which a large fraction of the CCM3 protein resides, the function of this complex remains to be elucidated. Several of the complex

components are localized to both the cytosol and intracellular membranes, and reports have linked them to intracellular trafficking in mammalian cells. For example, Mob3 (phocean) shares limited homology to clathrin adaptors and can interact with Eps15 (a protein involved in clathrin-mediated endocytosis) and the nucleoside-diphosphate kinase (whose product, GTP, is required for dynamin-dependent synaptic vesicle recycling) (91, 92). Similarly an IP/MS experiment with a peripheral endosome protein, GIPC, recently identified both STRN and STRN3 as binding partners (93). This is significant as GIPC regulates endocytosis and trafficking of the nerve growth factor receptor TrkA.

Interestingly STRIP1/2 orthologs are conserved from yeasts to humans; the budding yeast STRIP ortholog, Far11 (pheromone arrest 11) is a component of a protein complex (Far3–11) implicated in cell cycle arrest following pheromone signaling (94). Some sequence similarity can be detected between an additional Far protein, Far8, and the striatins (although the WD domain is not present in Far8). Limited sequence similarity is also detected between Far9/Vps64 and Far10 with SLMAP. Finally a link between the PP2A A ortholog (Tpd3) and Far11 was detected by both yeast two-hybrid assay (95) and TAP-MS,² indicating that portions of the STRIPAK assembly are conserved throughout evolution.

Two of the STRIPAK components (STRIP and striatin) have orthologs that have been isolated independently by forward genetics screens in filamentous fungi. The only *Sordaria macrospora* striatin ortholog, PRO11 regulates fungal cell differentiation and is required for fertility and fruiting body formation (96). The human striatin cDNA can functionally replace the PRO11 gene product, indicating functional conservation (96). The only STRIP ortholog in *Neurospora crassa*, HAM-2 has also been cloned from a genetic screen: HAM-2 mutants are female sterile, are slow growing, have short hyphae, and have a pronounced defect in hyphal fusion (97). Importantly directed mutations in the striatin homolog HAM-3 and the SLMAP/VPS64 homolog HAM-4, which has an FHA domain, result in strains with a fusion phenotype identical to that of HAM-2 mutants.³ These results indicate that components of the STRIPAK complex share similar functions in mediating hyphal fusion. As hyphal fusion may be a model system to study membrane fusion events, it is tempting to speculate that the STRIPAK complex may affect cell fusion in other systems. Consistent with this possibility, overexpression of SLMAP prevents the myoblast to myotube transition in C2C12 cells without precluding the expression of differentiation markers (61).

Although this study highlighted the composition of STRIPAK, the topology of this large multiprotein complex remains to be defined. For example, the striatins were shown to dimerize (or

perhaps multimerize) (Ref. 16 and Tables I and II), raising the possibility that the STRIPAK complex may be asymmetric. The presence of so many paralogous protein species may indicate that subcomplexes containing different paralogs perform slightly different functions. For example, the functions of the three Ste20 kinases found in STRIPAK are likely very different: STK25 and to a lesser extent MST4 but not STK24 have been found associated with the Golgi apparatus and are required for Golgi integrity (84). An in-depth analysis will be required to further elucidate the function of the various paralogs within this complex.

Acknowledgments—We are grateful to Dr. N Sonenberg for the kind gift of anti-alpha4 antibody; D. Fermin and G. Liu for programming assistance; and Drs. L. Hood, K. Colwill, and T. Pawson for access to the mammalian gene collection clones. We thank A. Simonin, C. G. Rasmussen, Dr. N. L. Glass, and A. B. Mak for sharing unpublished data. We are grateful to Dr. D. Ceccarelli for critical reading of the manuscript and to Dr. S. Angers for helpful discussions.

* This work was supported, in whole or in part, by National Institutes of Health Grant N01-HV-28179 from the NHLBI (to R. A.). This work was also supported by Canadian Institute for Health Research Grants MOP-84314 (to A.-C. G.) and MOP-81268 (to B. R.). The costs of publication of this article were defrayed in part by the payment of page charges. This article must therefore be hereby marked “advertisement” in accordance with 18 U.S.C. Section 1734 solely to indicate this fact.

^a The on-line version of this article (available at <http://www.mcponline.org>) contains supplemental material.

^b Both authors contributed equally to this work.

^c Supported by an Ontario Graduate Scholarship award.

^d Supported by an Early Researcher Award (to A. C. G.).

^e Present address: Banting and Best Dept. of Medical Research, University of Toronto, Toronto, Ontario M5S 3E1, Canada.

^f Supported by a studentship from the Ontario Students Opportunity Trust Fund.

^g Holds the Canada Research Chair in Functional Proteomics. To whom correspondence should be addressed: Samuel Lunenfeld Research Inst. at Mount Sinai Hospital, 600 University Ave., Rm. 992, Toronto, Ontario M5G 1X5, Canada. Tel.: 416-586-5027; Fax: 416-586-8869; E-mail: gingras@lunenfeld.ca.

REFERENCES

- Van Hoof, C., and Goris, J. (2004) PP2A fulfills its promises as tumor suppressor: which subunits are important? *Cancer Cell* **5**, 105–106
- Janssens, V., Goris, J., and Van Hoof, C. (2005) PP2A: the expected tumor suppressor. *Curr. Opin. Genet. Dev.* **15**, 34–41
- Virshup, D. M. (2000) Protein phosphatase 2A: a panoply of enzymes. *Curr. Opin. Cell Biol.* **12**, 180–185
- Mumby, M. (2007) PP2A: unveiling a reluctant tumor suppressor. *Cell* **130**, 21–24
- Stone, S. R., Hofsteenge, J., and Hemmings, B. A. (1987) Molecular cloning of cDNAs encoding two isoforms of the catalytic subunit of protein phosphatase 2A. *Biochemistry* **26**, 7215–7220
- Goldberg, Y. (1999) Protein phosphatase 2A: who shall regulate the regulator? *Biochem. Pharmacol.* **57**, 321–328
- Hemmings, B. A., Adams-Pearson, C., Maurer, F., Muller, P., Goris, J., Merlevede, W., Hofsteenge, J., and Stone, S. R. (1990) α - and β -forms of the 65-kDa subunit of protein phosphatase 2A have a similar 39 amino acid repeating structure. *Biochemistry* **29**, 3166–3173
- Mumby, M. C., and Walter, G. (1993) Protein serine/threonine phosphatases: structure, regulation, and functions in cell growth. *Physiol. Rev.* **73**, 673–699

² A. B. Mak, unpublished data.

³ A. Simonin, C. G. Rasmussen, and N. L. Glass, personal communication.

9. Xing, Y., Xu, Y., Chen, Y., Jeffrey, P. D., Chao, Y., Lin, Z., Li, Z., Strack, S., Stock, J. B., and Shi, Y. (2006) Structure of protein phosphatase 2A core enzyme bound to tumor-inducing toxins. *Cell* **127**, 341–353
10. Xu, Y., Xing, Y., Chen, Y., Chao, Y., Lin, Z., Fan, E., Yu, J. W., Strack, S., Jeffrey, P. D., and Shi, Y. (2006) Structure of the protein phosphatase 2A holoenzyme. *Cell* **127**, 1239–1251
11. Cho, U. S., and Xu, W. (2007) Crystal structure of a protein phosphatase 2A heterotrimeric holoenzyme. *Nature* **445**, 53–57
12. Kremmer, E., Ohst, K., Kiefer, J., Brewis, N., and Walter, G. (1997) Separation of PP2A core enzyme and holoenzyme with monoclonal antibodies against the regulatory A subunit: abundant expression of both forms in cells. *Mol. Cell. Biol.* **17**, 1692–1701
13. Murata, K., Wu, J., and Bratigan, D. L. (1997) B cell receptor-associated protein alpha displays rapamycin-sensitive binding directly to the catalytic subunit of protein phosphatase 2A. *Proc. Natl. Acad. Sci. U. S. A.* **94**, 10624–10629
14. Chen, J., Peterson, R. T., and Schreiber, S. L. (1998) Alpha 4 associates with protein phosphatases 2A, 4, and 6. *Biochem. Biophys. Res. Commun.* **247**, 827–832
15. Baillat, G., Moqrich, A., Castets, F., Baude, A., Bailly, Y., Benmerah, A., and Monneron, A. (2001) Molecular cloning and characterization of phoelein, a protein found from the Golgi complex to dendritic spines. *Mol. Biol. Cell* **12**, 663–673
16. Moreno, C. S., Lane, W. S., and Pallas, D. C. (2001) A mammalian homolog of yeast MOB1 is both a member and a putative substrate of striatin family-protein phosphatase 2A complexes. *J. Biol. Chem.* **276**, 24253–24260
17. Margolis, S. S., Perry, J. A., Forester, C. M., Nutt, L. K., Guo, Y., Jardim, M. J., Thomenius, M. J., Freil, C. D., Darbandi, R., Ahn, J. H., Arroyo, J. D., Wang, X. F., Shenolikar, S., Nairn, A. C., Dunphy, W. G., Hahn, W. C., Virshup, D. M., and Kornbluth, S. (2006) Role for the PP2A/B56δ phosphatase in regulating 14-3-3 release from Cdc25 to control mitosis. *Cell* **127**, 759–773
18. Forester, C. M., Maddox, J., Louis, J. V., Goris, J., and Virshup, D. M. (2007) Control of mitotic exit by PP2A regulation of Cdc25C and Cdk1. *Proc. Natl. Acad. Sci. U. S. A.* **104**, 19867–19872
19. Chen, W., Possemato, R., Campbell, K. T., Plattner, C. A., Pallas, D. C., and Hahn, W. C. (2004) Identification of specific PP2A complexes involved in human cell transformation. *Cancer Cell* **5**, 127–136
20. Dagda, R. K., Zaucha, J. A., Wadzinski, B. E., and Strack, S. (2003) A developmentally regulated, neuron-specific splice variant of the variable subunit B β targets protein phosphatase 2A to mitochondria and modulates apoptosis. *J. Biol. Chem.* **278**, 24976–24985
21. Gingras, A. C., Gstaiger, M., Raught, B., and Aebersold, R. (2007) Analysis of protein complexes using mass spectrometry. *Nat. Rev. Mol. Cell Biol.* **8**, 645–654
22. Gingras, A. C., Aebersold, R., and Raught, B. (2005) Advances in protein complex analysis using mass spectrometry. *J. Physiol.* **563**, 11–21
23. Bauer, A., and Kuster, B. (2003) Affinity purification-mass spectrometry: Powerful tools for the characterization of protein complexes. *Eur. J. Biochem.* **270**, 570–578
24. Dziembowski, A., and Seraphin, B. (2004) Recent developments in the analysis of protein complexes. *FEBS Lett.* **556**, 1–6
25. Chang, I. F. (2006) Mass spectrometry-based proteomic analysis of the epitope-tag affinity purified protein complexes in eukaryotes. *Proteomics* **6**, 6158–6166
26. Vasilescu, J., and Figgeys, D. (2006) Mapping protein-protein interactions by mass spectrometry. *Curr. Opin. Biotechnol.* **17**, 394–399
27. Ho, Y., Gruhler, A., Heilbut, A., Bader, G. D., Moore, L., Adams, S. L., Millar, A., Taylor, P., Bennett, K., Bouliier, K., Yang, L., Wolting, C., Donaldson, I., Schandorff, S., Shewnarane, J., Vo, M., Taggart, J., Goudreault, M., Muskat, B., Alfarano, C., Dewar, D., Lin, Z., Michalickova, K., Willems, A. R., Sassi, H., Nielsen, P. A., Rasmussen, K. J., Andersen, J. R., Johansen, L. E., Hansen, L. H., Jespersen, H., Podtelejnikov, A., Nielsen, E., Crawford, J., Poulsen, V., Sorensen, B. D., Matthiesen, J., Hendrickson, R. C., Gleeson, F., Pawson, T., Moran, M. F., Durocher, D., Mann, M., Hogue, C. W., Figgeys, D., and Tyers, M. (2002) Systematic identification of protein complexes in *Saccharomyces cerevisiae* by mass spectrometry. *Nature* **415**, 180–183
28. Gavin, A. C., Aloy, P., Grandi, P., Krause, R., Boesche, M., Marzioch, M., Rau, C., Jensen, L. J., Bastuck, S., Dompelfeld, B., Edelmann, A., Heu-
tier, M. A., Hoffman, V., Hoeft, C., Klein, K., Hudak, M., Michon, A. M., Schelder, M., Schirle, M., Remor, M., Rudi, T., Hooper, S., Bauer, A., Bouwmeester, T., Casari, G., Drewes, G., Neubauer, G., Rick, J. M., Kuster, B., Bork, P., Russell, R. B., and Superti-Furga, G. (2006) Proteome survey reveals modularity of the yeast cell machinery. *Nature* **440**, 631–636
29. Gavin, A. C., Bosche, M., Krause, R., Grandi, P., Marzioch, M., Bauer, A., Schultz, J., Rick, J. M., Michon, A. M., Cruciat, C. M., Remor, M., Hofert, C., Schelder, M., Brajenovic, M., Ruffner, H., Merino, A., Klein, K., Hudak, M., Dickson, D., Rudi, T., Gnau, V., Bauch, A., Bastuck, S., Huhse, B., Leutwein, C., Heurtier, M. A., Copley, R. R., Edelmann, A., Querfurth, E., Rybin, V., Drewes, G., Raida, M., Bouwmeester, T., Bork, P., Seraphin, B., Kuster, B., Neubauer, G., and Superti-Furga, G. (2002) Functional organization of the yeast proteome by systematic analysis of protein complexes. *Nature* **415**, 141–147
30. Krogan, N. J., Cagney, G., Yu, H., Zhong, G., Guo, X., Ignatchenko, A., Li, J., Pu, S., Datta, N., Tikuvisis, A. P., Punna, T., Peregrin-Alvarez, J. M., Shales, M., Zhang, X., Davey, M., Robinson, M. D., Paccanaro, A., Bray, J. E., Sheung, A., Beattie, B., Richards, D. P., Canadien, V., Lalev, A., Mena, F., Wong, P., Starostine, A., Canete, M. M., Vlasblom, J., Wu, S., Orsi, C., Collins, S. R., Chandran, S., Haw, R., Rilstone, J. J., Gandhi, K., Thompson, N. J., Musso, G., St Onge, P., Ghanny, S., Lam, M. H., Butland, G., Altaf-Ul, A. M., Kanaya, S., Shilatifard, A., O'Shea, E., Weissman, J. S., Ingles, C. J., Hughes, T. R., Parkinson, J., Gerstein, M., Wodak, S. J., Emili, A., and Greenblatt, J. F. (2006) Global landscape of protein complexes in the yeast *Saccharomyces cerevisiae*. *Nature* **440**, 637–643
31. Rigaut, G., Shevchenko, A., Rutz, B., Wilm, M., Mann, M., and Seraphin, B. (1999) A generic protein purification method for protein complex characterization and proteome exploration. *Nat. Biotechnol.* **17**, 1030–1032
32. Chen, G. I., and Gingras, A. C. (2007) Affinity-purification mass spectrometry (AP-MS) of serine/threonine phosphatases. *Methods* **42**, 298–305
33. Gingras, A. C., Caballero, M., Zarske, M., Sanchez, A., Hazbun, T. R., Fields, S., Sonenberg, N., Hafen, E., Raught, B., and Aebersold, R. (2005) A novel, evolutionarily conserved protein phosphatase complex involved in cisplatin sensitivity. *Mol. Cell. Proteomics* **4**, 1725–1740
34. Guclu, B., Ozturk, A. K., Pricola, K. L., Bilguvar, K., Shin, D., O'Roak, B. J., and Gunel, M. (2005) Mutations in apoptosis-related gene, PDCD10, cause cerebral cavernous malformation 3. *Neurosurgery* **57**, 1008–1013
35. Bergametti, F., Denier, C., Labauge, P., Arnoult, M., Boetto, S., Clenet, M., Coubes, P., Echenne, B., Ibrahim, R., Irthum, B., Jacquet, G., Lonjon, M., Moreau, J. J., Neau, J. P., Parker, F., Tremoulet, M., and Tournier-Lasserre, E. (2005) Mutations within the programmed cell death 10 gene cause cerebral cavernous malformations. *Am. J. Hum. Genet.* **76**, 42–51
36. Pedrioli, P. G., Eng, J. K., Hubley, R., Vogelzang, M., Deutsch, E. W., Raught, B., Pratt, B., Nilsson, E., Angeletti, R. H., Apweiler, R., Cheung, K., Costello, C. E., Hermjakob, H., Huang, S., Julian, R. K., Kapp, E., McComb, M. E., Oliver, S. G., Omenn, G., Paton, N. W., Simpson, R., Smith, R., Taylor, C. F., Zhu, W., and Aebersold, R. (2004) A common open representation of mass spectrometry data and its application to proteomics research. *Nat. Biotechnol.* **22**, 1459–1466
37. Keller, A., Nesvizhskii, A. I., Kolker, E., and Aebersold, R. (2002) Empirical statistical model to estimate the accuracy of peptide identifications made by MS/MS and database search. *Anal. Chem.* **74**, 5383–5392
38. Nesvizhskii, A. I., Keller, A., Kolker, E., and Aebersold, R. (2003) A statistical model for identifying proteins by tandem mass spectrometry. *Anal. Chem.* **75**, 4646–4658
39. Craig, R., and Beavis, R. C. (2004) TANDEM: matching proteins with tandem mass spectra. *Bioinformatics* **20**, 1466–1467
40. MacLean, B., Eng, J. K., Beavis, R. C., and McIntosh, M. (2006) General framework for developing and evaluating database scoring algorithms using the TANDEM search engine. *Bioinformatics* **22**, 2830–2832
41. Breitkreutz, B. J., Stark, C., Reguly, T., Boucher, L., Breitkreutz, A., Livstone, M., Oughtred, R., Lackner, D. H., Bahler, J., Wood, V., Dolinski, K., and Tyers, M. (2008) The BioGRID Interaction Database: 2008 update. *Nucleic Acids Res.* **36**, D637–D640
42. Zhou, J., Pham, H. T., and Walter, G. (2003) The formation and activity of PP2A holoenzymes do not depend on the isoform of the catalytic subunit. *J. Biol. Chem.* **278**, 8617–8622
43. Ikebara, T., Shinjo, F., Ikebara, S., Imamura, S., and Yasumoto, T. (2006) Baculovirus expression, purification, and characterization of human pro-

- tein phosphatase 2A catalytic subunits α and β . *Protein Expr. Purif.* **45**, 150–156
44. Spangler, S. A., and Hoogenraad, C. C. (2007) Liprin- α proteins: scaffold molecules for synapse maturation. *Biochem. Soc Trans.* **35**, 1278–1282
45. Arroyo, J. D., Lee, G. M., and Hahn, W. C. (2008) Liprin $\alpha 1$ interacts with PP2A B56 γ . *Cell Cycle* **7**, 525–532
46. Yan, X., Habedanck, R., and Nigg, E. A. (2006) A complex of two centrosomal proteins, CAP350 and FOP, cooperates with EB1 in microtubule anchoring. *Mol. Biol. Cell.* **17**, 634–644
47. Mikolajka, A., Yan, X., Popowicz, G. M., Smialowski, P., Nigg, E. A., and Holak, T. A. (2006) Structure of the N-terminal domain of the FOP (FGFR1OP) protein and implications for its dimerization and centrosomal localization. *J. Mol. Biol.* **359**, 863–875
48. Popovici, C., Zhang, B., Gregoire, M. J., Jonveaux, P., Lafage-Pochitaloff, M., Birnbaum, D., and Pebusque, M. J. (1999) The t(6;8)(q27;p11) translocation in a stem cell myeloproliferative disorder fuses a novel gene, FOP, to fibroblast growth factor receptor 1. *Blood* **93**, 1381–1389
49. Guasch, G., Delaval, B., Arnoulet, C., Xie, M. J., Xerri, L., Sainty, D., Birnbaum, D., and Pebusque, M. J. (2004) FOP-FGFR1 tyrosine kinase, the product of a t(6;8) translocation, induces a fatal myeloproliferative disease in mice. *Blood* **103**, 309–312
50. Moreno, C. S., Park, S., Nelson, K., Ashby, D., Hubalek, F., Lane, W. S., and Pallas, D. C. (2000) WD40 repeat proteins striatin and S/G(2) nuclear autoantigen are members of a novel family of calmodulin-binding proteins that associate with protein phosphatase 2A. *J. Biol. Chem.* **275**, 5257–5263
51. Castets, F., Rakitina, T., Gaillard, S., Moqrich, A., Mattei, M. G., and Monneron, A. (2000) Zinedin, SG2NA, and striatin are calmodulin-binding, WD repeat proteins principally expressed in the brain. *J. Biol. Chem.* **275**, 19970–19977
52. Castets, F., Bartoli, M., Barnier, J. V., Baillat, G., Salin, P., Moqrich, A., Bourgeois, J. P., Denizot, F., Rougon, G., Calothy, G., and Monneron, A. (1996) A novel calmodulin-binding protein, belonging to the WD-repeat family, is localized in dendrites of a subset of CNS neurons. *J. Cell Biol.* **134**, 1051–1062
53. Bartoli, M., Ternaux, J. P., Forni, C., Portalier, P., Salin, P., Amalric, M., and Monneron, A. (1999) Down-regulation of striatin, a neuronal calmodulin-binding protein, impairs rat locomotor activity. *J. Neurobiol.* **40**, 234–243
54. Benoit, M., Gaillard, S., and Castets, F. (2006) The striatin family: a new signaling platform in dendritic spines. *J. Physiol. (Paris)* **99**, 146–153
55. Baily, Y. J., and Castets, F. (2007) Phoein: a potential actor in vesicular trafficking at Purkinje cell dendritic spines. *Cerebellum* **23**, 1–9
56. Hergovich, A., Cornils, H., and Hemmings, B. A. (2008) Mammalian NDR protein kinases: from regulation to a role in centrosome duplication. *Biochim. Biophys. Acta* **1784**, 3–15
57. Ohoka, Y., and Takai, Y. (1998) Isolation and characterization of cortactin isoforms and a novel cortactin-binding protein, CBP90. *Genes Cells* **3**, 603–612
58. Chen, G. I., Tisayakorn, S., Jorgensen, C., D'Ambrosio, L. M., Goudreault, M., and Gingras, A.-C. (2008) PP4R4/KIAA1622 forms a novel stable cytosolic complex with phosphoprotein phosphatase 4. *J. Biol. Chem.* **283**, 29273–29284
59. Wigle, J. T., Demchysyn, L., Pratt, M. A., Staines, W. A., Salih, M., and Tuana, B. S. (1997) Molecular cloning, expression, and chromosomal assignment of sarcolemmal-associated proteins. A family of acidic amphiphatic alpha-helical proteins associated with the membrane. *J. Biol. Chem.* **272**, 32384–32394
60. Wielowieyski, P. A., Sevinc, S., Guzzo, R., Salih, M., Wigle, J. T., and Tuana, B. S. (2000) Alternative splicing, expression, and genomic structure of the 3' region of the gene encoding the sarcolemmal-associated proteins (SLAPs) defines a novel class of coiled-coil tail-anchored membrane proteins. *J. Biol. Chem.* **275**, 38474–38481
61. Guzzo, R. M., Wigle, J., Salih, M., Moore, E. D., and Tuana, B. S. (2004) Regulated expression and temporal induction of the tail-anchored sarcolemmal-membrane-associated protein is critical for myoblast fusion. *Biochem. J.* **381**, 599–608
62. Guzzo, R. M., Sevinc, S., Salih, M., and Tuana, B. S. (2004) A novel isoform of sarcolemmal membrane-associated protein (SLMAP) is a component of the microtubule organizing centre. *J. Cell Sci.* **117**, 2271–2281
63. Huang, J., Liu, T., Xu, L. G., Chen, D., Zhai, Z., and Shu, H. B. (2005) SIKE is an IKK epsilon/TBK1-associated suppressor of TLR3- and virus-triggered IRF-3 activation pathways. *EMBO J.* **24**, 4018–4028
64. Grand, E. K., Grand, F. H., Chase, A. J., Ross, F. M., Corcoran, M. M., Oscier, D. G., and Cross, N. C. (2004) Identification of a novel gene, FGFR1OP2, fused to FGFR1 in 8p11 myeloproliferative syndrome. *Genes Chromosomes Cancer* **40**, 78–83
65. Craig, H. D., Gunel, M., Cepeda, O., Johnson, E. W., Ptacek, L., Steinberg, G. K., Ogilvy, C. S., Berg, M. J., Crawford, S. C., Scott, R. M., Steichen-Gersdorf, E., Sabroe, R., Kennedy, C. T., Mettler, G., Beis, M. J., Fryer, A., Awad, I. A., and Lifton, R. P. (1998) Multilocus linkage identifies two new loci for a mendelian form of stroke, cerebral cavernous malformation, at 7p15–13 and 3q25.2–27. *Hum. Mol. Genet.* **7**, 1851–1858
66. Plummer, N. W., Zawistowski, J. S., and Marchuk, D. A. (2005) Genetics of cerebral cavernous malformations. *Curr. Neurol. Neurosci. Rep.* **5**, 391–396
67. Revencu, N., and Viikku, M. (2006) Cerebral cavernous malformation: new molecular and clinical insights. *J. Med. Genet.* **43**, 716–721
68. Labauge, P., Denier, C., Bergametti, F., and Tournier-Lasserre, E. (2007) Genetics of cavernous angiomas. *Lancet Neurol.* **6**, 237–244
69. Ma, X., Zhao, H., Shan, J., Long, F., Chen, Y., Chen, Y., Zhang, Y., Han, X., and Ma, D. (2007) PDCD10 interacts with Ste20-related kinase MST4 to promote cell growth and transformation via modulation of the ERK pathway. *Mol. Biol. Cell.* **18**, 1965–1978
70. Voss, K., Stahl, S., Schleider, E., Ullrich, S., Nickel, J., Mueller, T. D., and Felbor, U. (2007) CCM3 interacts with CCM2 indicating common pathogenesis for cerebral cavernous malformations. *Neurogenetics* **8**, 249–256
71. Lin, J. L., Chen, H. C., Fang, H. I., Robinson, D., Kung, H. J., and Shih, H. M. (2001) MST4, a new Ste20-related kinase that mediates cell growth and transformation via modulating ERK pathway. *Oncogene* **20**, 6559–6569
72. Osada, S., Izawa, M., Saito, R., Mizuno, K., Suzuki, A., Hirai, S., and Ohno, S. (1997) YSK1, a novel mammalian protein kinase structurally related to Ste20 and SPS1, but is not involved in the known MAPK pathways. *Oncogene* **14**, 2047–2057
73. Dan, I., Ong, S. E., Watanabe, N. M., Blagoev, B., Nielsen, M. M., Kajikawa, E., Kristiansen, T. Z., Mann, M., and Pandey, A. (2002) Cloning of MASK, a novel member of the mammalian germinal center kinase III subfamily, with apoptosis-inducing properties. *J. Biol. Chem.* **277**, 5929–5939
74. Qian, Z., Lin, C., Espinosa, R., LeBeau, M., and Rosner, M. R. (2001) Cloning and characterization of MST4, a novel Ste20-like kinase. *J. Biol. Chem.* **276**, 22439–22445
75. Zhou, T. H., Ling, K., Guo, J., Zhou, H., Wu, Y. L., Jing, Q., Ma, L., and Pei, G. (2000) Identification of a human brain-specific isoform of mammalian STE20-like kinase 3 that is regulated by cAMP-dependent protein kinase. *J. Biol. Chem.* **275**, 2513–2519
76. Pombo, C. M., Bonventre, J. V., Molnar, A., Kyriakis, J., and Force, T. (1996) Activation of a human Ste20-like kinase by oxidant stress defines a novel stress response pathway. *EMBO J.* **15**, 4537–4546
77. Pombo, C. M., Force, T., Kyriakis, J., Nogueira, E., Fidalgo, M., and Zalvide, J. (2007) The GCK II and III subfamilies of the STE20 group kinases. *Front. Biosci.* **12**, 850–859
78. Ewing, R. M., Chu, P., Elisma, F., Li, H., Taylor, P., Climie, S., McBroom-Cerajewski, L., Robinson, M. D., O'Connor, L., Li, M., Taylor, R., Dharsee, M., Ho, Y., Heilbut, A., Moore, L., Zhang, S., Ornatsky, O., Buhkman, Y. V., Ethier, M., Sheng, Y., Vasilescu, J., Abu-Farha, M., Lambert, J. P., Duewel, H. S., Stewart, II, Kuehl, B., Hogue, K., Colwill, K., Gladwish, K., Muskat, B., Kinach, R., Adams, S. L., Moran, M. F., Morin, G. B., Topaloglu, T., and Figeys, D. (2007) Large-scale mapping of human protein-protein interactions by mass spectrometry. *Mol. Syst. Biol.* **3**, 89
79. Hilder, T. L., Malone, M. H., Bencharit, S., Colicelli, J., Haystead, T. A., Johnson, G. L., and Wu, C. C. (2007) Proteomic identification of the cerebral cavernous malformation signaling complex. *J. Proteome Res.* **6**, 4343–4355
80. Westphal, R. S., Anderson, K. A., Means, A. R., and Wadzinski, B. E. (1998) A signaling complex of Ca^{2+} -calmodulin-dependent protein kinase IV and protein phosphatase 2A. *Science* **280**, 1258–1261
81. Westphal, R. S., Coffee, R. L., Jr., Marotta, A., Pelech, S. L., and Wadzinski, B. E. (1999) Identification of kinase-phosphatase signaling modules composed of p70 S6 kinase-protein phosphatase 2A (PP2A) and p21-activated kinase-PP2A. *J. Biol. Chem.* **274**, 687–692
82. Heriche, J. K., Lebrin, F., Rabillo, T., Leroy, D., Chambaz, E. M., and Goldberg, Y. (1997) Regulation of protein phosphatase 2A by direct

- interaction with casein kinase 2 α . *Science* **276**, 952–955
83. Abraham, D., Podar, K., Pacher, M., Kubicek, M., Welzel, N., Hemmings, B. A., Dilworth, S. M., Mischak, H., Kolch, W., and Baccarini, M. (2000) Raf-1-associated protein phosphatase 2A as a positive regulator of kinase activation. *J. Biol. Chem.* **275**, 22300–22304
84. Preisinger, C., Short, B., De Corte, V., Bruyneel, E., Haas, A., Kopajtich, R., Gettemans, J., and Barr, F. A. (2004) YSK1 is activated by the Golgi matrix protein GM130 and plays a role in cell migration through its substrate 14-3-3 ζ . *J. Cell Biol.* **164**, 1009–1020
85. Schinkmann, K., and Blenis, J. (1997) Cloning and characterization of a human STE20-like protein kinase with unusual cofactor requirements. *J. Biol. Chem.* **272**, 28695–28703
86. Munton, R. P., Tweedie-Cullen, R., Livingstone-Zatchej, M., Weinandy, F., Waidelich, M., Longo, D., Gehrig, P., Potthast, F., Rutishauser, D., Gerrits, B., Panse, C., Schlapbach, R., and Mansuy, I. M. (2007) Qualitative and quantitative analyses of protein phosphorylation in naïve and stimulated mouse synaptosomal preparations. *Mol. Cell. Proteomics* **6**, 283–293
87. Trinidad, J. C., Thalhammer, A., Specht, C. G., Lynn, A. J., Baker, P. R., Schoepfer, R., and Burlingame, A. L. (2008) Quantitative analysis of synaptic phosphorylation and protein expression. *Mol. Cell. Proteomics* **7**, 684–696
88. Ballif, B. A., Villen, J., Beausoleil, S. A., Schwartz, D., and Gygi, S. P. (2004) Phosphoproteomic analysis of the developing mouse brain. *Mol. Cell. Proteomics* **3**, 1093–1101
89. Villen, J., Beausoleil, S. A., Gerber, S. A., and Gygi, S. P. (2007) Large-scale phosphorylation analysis of mouse liver. *Proc. Natl. Acad. Sci. U. S. A.* **104**, 1488–1493
90. Beausoleil, S. A., Villen, J., Gerber, S. A., Rush, J., and Gygi, S. P. (2006) A probability-based approach for high-throughput protein phosphorylation analysis and site localization. *Nat. Biotechnol.* **24**, 1285–1292
91. Baillat, G., Gaillard, S., Castets, F., and Monneron, A. (2002) Interactions of phecein with nucleoside-diphosphate kinase, Eps15, and Dynamin I. *J. Biol. Chem.* **277**, 18961–18966
92. Krishnan, K. S., Rikhy, R., Rao, S., Shivalkar, M., Mosko, M., Narayanan, R., Etter, P., Estes, P. S., and Ramaswami, M. (2001) Nucleoside diphosphate kinase, a source of GTP, is required for dynamin-dependent synaptic vesicle recycling. *Neuron* **30**, 197–210
93. Varsano, T., Dong, M. Q., Niesman, I., Gacula, H., Lou, X., Ma, T., Testa, J. R., Yates, J. R., III, and Farquhar, M. G. (2006) GIPC is recruited by APPL to peripheral TrkA endosomes and regulates TrkA trafficking and signaling. *Mol. Cell. Biol.* **26**, 8942–8952
94. Kemp, H. A., and Sprague, G. F., Jr. (2003) ar3 and five interacting proteins prevent premature recovery from pheromone arrest in the budding yeast *Saccharomyces cerevisiae*. *Mol. Cell. Biol.* **23**, 1750–1763
95. Uetz, P., Giot, L., Cagney, G., Mansfield, T. A., Judson, R. S., Knight, J. R., Lockshon, D., Narayan, V., Srinivasan, M., Pochart, P., Qureshi-Emili, A., Li, Y., Godwin, B., Conover, D., Kalbfleisch, T., Vijayadamodar, G., Yang, M., Johnston, M., Fields, S., and Rothberg, J. M. (2000) A comprehensive analysis of protein-protein interactions in *Saccharomyces cerevisiae*. *Nature* **403**, 623–627
96. Poggeler, S., and Kuck, U. (2004) A WD40 repeat protein regulates fungal cell differentiation and can be replaced functionally by the mammalian homologue striatin. *Eukaryot. Cell* **3**, 232–240
97. Xiang, Q., Rasmussen, C., and Glass, N. L. (2002) The ham-2 locus, encoding a putative transmembrane protein, is required for hyphal fusion in *Neurospora crassa*. *Genetics* **160**, 169–180

ONLINE SUPPLEMENTAL MATERIAL

LIST OF SUPPLEMENTAL TABLES AND FIGURES

Supplemental Table S1

Protein names, gene names and aliases

Supplemental Table S2

Constructs used in this study

Supplemental Table S3

Paralogy groups

Supplemental Table S4

Detailed mass spectrometry data, Tandem Affinity Purification

Supplemental Table S5

Detailed mass spectrometry data, flag immunoprecipitation

Supplemental Table S6

Evidence for the proteins identified on the basis of a single unique peptide

Supplemental Table S7

Peptide statistics for single peptide identifications

Supplemental Table S8

MS results for endogenous immunoprecipitations

Supplemental Figure S1

STRIP1/STRIP2 sequence analysis

Supplemental Figure S2

CTTNBP2/CTTNBP2NL sequence analysis

Supplemental Figure S3

Interaction of flag-STRIP1 with endogenous PP2A components

Supplemental Figure S4

SIKE/FGFR1OP2 sequence analysis

Supplemental Figure S5

SLMAP/TRAF3IP3 sequence analysis

Supplemental Figure S6

Confirmation of the association between proteins of the STRIPAK and endogenous striatin

Supplemental Figure S7

Annotated spectra for the proteins identified on the basis of a single unique peptide

SUPPLEMENTAL REFERENCES

¹ *ClustalW*: Larkin MA et al. (2007), "Clustal W and Clustal X version 2.0", Bioinformatics. 23:2947; BLOSUM62: Henikoff S and Henikoff JG (1993), "Performance evaluation of amino acid substitution matrices.", Proteins, 17:49.

² *Phosphosite*: www.phosphosite.org

³ *Rat CBP90*: Ohoka Y and Takai Y (1998), "Isolation and characterization of cortactin isoforms and a novel cortactin-binding protein, CBP90", Genes Cells, 3: 603.

⁴ *CDD reference*: Marchler-Bauer A et al. (2007), "CDD: a conserved domain database for interactive domain family analysis", Nucleic Acids Res.35(D)237-240

⁵ *Paircoil reference*: A.V. McDonnell, T. Jiang, A.E. Keating, B. Berger, "Paircoil2: Improved prediction of coiled coils from sequence", Bioinformatics Vol. 22(3) (2006).

SUPPLEMENTAL TABLE S1. PROTEIN AND GENE NAMES.

PROTEIN NAME ¹	GENE NAME ²	FULL PROTEIN NAME	ALIASES
calcineurin	PPP3CA	protein phosphatase 3 (formerly 2B), catalytic subunit, alpha isoform	CALNA, CCN1, CNA1, PP2B
CCT2	CCT2	chaperonin containing TCP1, subunit 2 (beta)	CCTB, PRO1633, TCPB
CCT3	CCT3	chaperonin containing TCP1, subunit 3 (gamma)	CCTG, PIG48, TCGP, TRIC5
CCT4	CCT4	chaperonin containing TCP1, subunit 4	CCTD, TCPD, SRB
CCT5	CCT5	chaperonin containing TCP1, subunit 5 (epsilon)	CCTE, KIAA0098, TCPE
CCT6A	CCT6A	chaperonin containing TCP1, subunit 6A (zeta 1)	CCTZ1, MoDP-2, TCPZ
CCT7	CCT7	chaperonin containing TCP1, subunit 7 (eta)	CCTH, Nip7-1, TCPH
Cdc25C	CDC25C	cell division cycle 25 homolog C	CDC25
CTTNBP2	CTTNBP2	Cortactin binding protein 2	c7orf8, CORTBP2, KIAA1758
CTTNBP2NL	CTTNBP2NL	CTTNBP2 N-terminal like	KIAA1433
dynein	DYNC1H1	dynein, cytoplasmic 1, heavy chain 1	DHC1; DNCL; DYHC
STRIP1	FAM40A	FAM40A	KIAA1761
STRIP2	FAM40B	FAM40B	KIAA1170
FGFR1OP2	FGFR1OP2	FGFR1 oncogene partner 2	HSPC123
Mob3	MOBKL3	Mps one binder kinase activator-like 3	PREI3, phocein
MST4	MST4	serine/threonine protein kinase MST4	MASK, EC 2.7.11.1
CCM3	PDCD10	Programmed cell death protein 10	CCM3, TFAR15
PP1c	PPP1CA	protein phosphatase 1, catalytic subunit, alpha isoform	PP-1A, PPP1A
PP2Ac α	PPP2CA	protein phosphatase 2 catalytic subunit, alpha isoform	PP2A-alpha, EC 3.1.3.16
PP2Ac β	PPP2CB	protein phosphatase 2 catalytic subunit, beta isoform	PP2A-beta, EC 3.1.3.16
PP2AA α	PPP2R1A	protein phosphatase 2 65kDa regulatory subunit A alpha isoform	PP2A A, PR65 alpha
PP2Aa β	PPP2R1B	protein phosphatase 2 65kDa regulatory subunit A beta isoform	PP2A A, PR65 beta
PP2AB α	PPP2R2A	protein phosphatase 2, regulatory subunit B, alpha isoform	B55A, PR52A, PR55A
PP2AB β	PPP2R2B	protein phosphatase 2, regulatory subunit B, gamma isoform	B55G, IMYPNO, PR52, PR55G
PP2AB δ	PPP2R2D	protein phosphatase 2, regulatory subunit B, delta isoform	
PP2AB' α	PPP2R5A	protein phosphatase 2, regulatory subunit B', alpha isoform	B56A, PR61A
PP2AB' γ	PPP2R5C	protein phosphatase 2, regulatory subunit B', gamma isoform	B56G, PR61G
PP2AB' δ	PPP2R5D	protein phosphatase 2, regulatory subunit B', delta isoform	B56D, PR61D
PP2AB' ϵ	PPP2R5E	protein phosphatase 2, regulatory subunit B', epsilon isoform	B56E, PR61E
PP4c	PPP4C	protein phosphatase 4 (formerly X), catalytic subunit	PP4, PPH3, PPX
PP6c	PPP6C	protein phosphatase 6, catalytic subunit	
PP7	PPEF1	protein phosphatase, EF-hand calcium binding domain 1	PP7, PPEF, PPP7C
liprin A1	PPFIA1	PTPRF interacting protein (liprin) alpha 1	LIP.1, LIP1, LIPRIN
liprin A3	PPFIA3	PTPRF interacting protein (liprin) alpha 3	KIAA0654, LPNA3
SIKE	SIKE	Suppressor of IKK-epsilon	FLJ21168
SLMAP	SLMAP	Sarcolemmal membrane-associated protein	SLAP, KIAA1601
STK24	STK24	serine/threonine protein kinase 24	MST3, STK3
STK25	STK25	serine/threonine protein kinase 25	SOK, YSK1
striatin	STRN	striatin	
striatin3	STRN3	striatin-3	cell cycle autoantigen SG2NA, GS2NA
striatin4	STRN4	striatin-4	zinedin, ZIN
TCP1	TCP1	t-complex 1	CCTA, CCT1, D6S230E, TCPA
TRAF3IP3	TRAF3IP3	TRAF3-interacting JNK-activating modulator	T3JAM

¹ Protein names used in this publication² Gene name as per HUGO (ncbi Gene)

SUPPLEMENTAL TABLE S2: CONSTRUCTS USED IN THIS STUDY

PROTEIN ¹	GENE NAME ²	SPECIES	SOURCE ³	ACCESSION	FLAG SITES ⁴	FLAG PUB ⁵	TAP SITES ⁶	TAP PUB ⁷
alpha4	IGBP1	human	Kim Arndt	NM_001551	BamHI/NotI	Gingras 05	Pmel/Pacl	Gingras 05
CTTNBP2	CTTNBP2	human	MGC	BC106000	EcoRI/NotI	this study	N/A	N/A
CTTNBP2NL	CTTNBP2NL	human	MGC	BC016029	EcoRI/NotI	this study	N/A	N/A
STRIP1	FAM40A	mouse	MGC	BC023952	EcoRV/NotI	this study	N/A	N/A
TIP41	TIP41RL	human	Hela library	NM_152902	N/A	N/A	Pmel/Pacl	Gingras 05
Mob3	MOBKL3	human	MGC	BC005237	EcoRI/NotI	this study	Pmel/Pacl	this study
MST4	MST4	mouse	MGC	BC005708	Ascl/NotI	this study	N/A	N/A
CCM3	PDCD10	human	MGC	BC002506	Ascl/NotI	this study	N/A	N/A
PP2Ac α	PPP2CA	human	Hela library	NM_002715	EcoRI/Not	Gingras 05	Pmel/Pacl	this study
PP2Ac β	PPP2CB	human	Hela library	NM_004156	EcoRI/Not	Gingras 05	Pmel/Pacl	this study
PP2AA α	PPP2R1A	human	MGC	BC001537	Ascl/NotI	this study	Pmel/Pacl	Chen 08
SIKE	SIKE	human	MGC	BC005934	EcoRI/Xhol	this study	N/A	N/A
STK24	STK24	human	MGC	BC035578	Ascl/NotI	this study	N/A	N/A
STK25	STK25	human	MGC	BC007852	EcoRI/NotI	this study	N/A	N/A
striatin	STRN	mouse	MGC	BC090968	Ascl/NotI	this study	N/A	N/A
striatin3	STRN3	human	MGC	BC126221	EcoRI/NotI	this study	N/A	N/A
striatin4	STRN4	human	Origene	NM_013403	N/A	N/A	Pmel/Pacl	this study
TRAF3IP3	TRAF3IP3	human	MGC	BC110302	EcoRI/NotI	this study	NA	N/A

¹ Protein name as used in this publication² Gene name as per HUGO (ncbi Gene)³ Source of the original cDNAs used for cloning (MGC: mammalian gene collection)⁴ Restriction sites used to clone into pcDNA3-flag or pcDNA3-3HA⁵ Original reference for the pcDNA3-flag construct: (Gingras 05: Gingras, AC *et al*, Mol Cell Proteomics, 2005, 4: 1725-40)⁶ Restriction sites used to clone into pcDNA3-NTAP⁷ Original reference for the pcDNA3-NTAP construct (Chen 08: Chen, GI *et al*, 2008, submitted)

SUPPLEMENTAL TABLE S3. PARALOGY GROUPS

NODE NAME ¹	PROT 1 ²	PROT 2	PROT 3	PROT 4	PROT 5	PROT 6	PROT 7	PROT 8	MIN ID ³
CCT	TCP1	CCT2	CCT3	CCT4	CCT5	CCT6A	CCT7	CCT7	23%
CTTNBP2/NL	CTTNBP2	CTNBP2NL							36%
STRIP1/2	STRIP1/ FAM40A	STRIP2/ FAM40B							68%
liprin	liprin A1	liprin A3							61%
PP2A A	PP2A A α	PP2A A β							85%
PP2A B	PP2A B α	PP2A B β	PP2A B γ	PP2A B δ					80%
PP2A B'	PP2A B' α	PP2A B' β	PP2A B' γ	PP2A B' δ	PP2A B' ϵ				57%
PP2Ac	PP2Ac α	PP2Ac β							97%
SIKE/ FGFR1OP2	SIKE	FGFR1OP2							47%
SLMAP/ TRAF3IP3	SLMAP	TRAF3IP3							20%
striatins	striatin	striatin3	striatin4						46%
GCK-III	STK24	STK25	MST4						66%

¹ Name used on Figures 1, 3 and 4 to represent the paralogous protein families.² Members of the paralogy group³ Lowest percentage of identity (amino acid sequence) amongst components of the paralogy group.
Percentage ID calculated from Clustal alignments with BLOSUM 62 matrix, using the longest protein isoform deposited in RefSeq.

SUPPLEMENTAL TABLE S4

Detailed mass spectrometry data for TAP interactions. "Prophet" indicates the ProteinProphet p value, "%cover" is the coverage of each of the proteins, "npeps" is the number of unique peptides, "nspecs" is the total number of spectra assigned to the protein, "Ratio cover" is the percentage coverage of the interactor relative to the bait. **Red** denotes components of the PP2Ac-PP2A A core phosphatase, **green** represents the known PP2A B regulatory subunits (including the striatins), and **blue** indicates the detection of STRIP1/2 and CTTNBP2/NL in the pull-downs. The highlighted numbers are for proteins identified on the basis of a single unique peptide: the corresponding peptide annotation and annotated spectra are presented in Sup Table S6 and Sup Fig S7.

Bait name	Gene name	Protein name	RefSeq	Prophet	%cover	npeps	nspecs	Ratio cover
TAP-PP2AA α	PPP2R1A	PP2A A α	NP_055040	1	55	54	124	1.00
TAP-PP2AA α	PPP2R5D	PP2A B' δ	NP_006236	1	45.5	23	39	0.83
TAP-PP2AA α	PPP2CA/B	PP2Ac α/β	NP_002706, NP_004147	1	42.7	15	36	0.78
TAP-PP2AA α	PPP2R2A	PP2A B α	NP_002708	1	44.9	16	33	0.82
TAP-PP2AA α	PPFIA1	liprin A1	NP_003617	1	14.7	13	24	0.27
TAP-PP2AA α	FAM40A	STRIP1	XP_042708	1	15.5	7	13	0.28
TAP-PP2AA α	STRN	striatin	NP_003153	1	9.9	5	9	0.18
TAP-PP2AA α	STRN3	striatin 3	NP_001077362	1	31.9	5	9	0.58
TAP-PP2AA α	STRN4	striatin 4	NP_037535	1	14.2	5	8	0.26
TAP-PP2AA α	PPP2R2D	PP2A B δ	NP_006236	1	20.1	4	7	0.37
TAP-PP2AA α	PPP2R5C	PP2A B' γ	NP_002710	1	27.2	6	7	0.49
TAP-PP2AA α	MOBKL3	Mob3	NP_056202	1	22.8	2	6	0.41
TAP-PP2AA α	CTTNBP2NL	CTTNBP2NL	NP_061174	1	8.4	4	5	0.15
TAP-PP2Ac α	PPP2R1A	PP2A A α	NP_055040	1	63.2	41	112	1.14
TAP-PP2Ac α	PPP2CA/B	PP2Ac α/β	NP_002706, NP_004147	1	55.3	23	77	1.00
TAP-PP2Ac α	PPP2R2A	PP2A B α	NP_002708	1	55.1	27	64	1.00
TAP-PP2Ac α	IGBP1	alpha4	NP_001542	1	51.3	20	37	0.93
TAP-PP2Ac α	PPP2R5D	PP2A B' δ	NP_006236	1	37	15	29	0.67
TAP-PP2Ac α	PPP2R1B	PP2A A β	NP_002707	1	14.4	5	11	0.26
TAP-PP2Ac α	PPP2R2D	PP2A B δ	NP_006236	1	27.5	5	11	0.50
TAP-PP2Ac α	PPP2R5E	PP2A B' ϵ	NP_006237	1	14.6	4	10	0.26
TAP-PP2Ac α	STRN3	striatin 3	NP_055389	1	15.8	7	9	0.29
TAP-PP2Ac α	FAM40A	STRIP1	NP_149079	1	12.3	4	4	0.22
TAP-PP2Ac α	MOBKL3	Mob3	NP_056202	1	22.8	2	4	0.41
TAP-PP2Ac α	PPP2R5C	PP2A B' γ	NP_002710	1	12.2	2	4	0.22
TAP-PP2Ac α	STRN	striatin	NP_003153	1	4.5	2	2	0.08
TAP-PP2Ac α	CCT2	CCT2	NP_006422	1	7.9	2	2	0.14
TAP-PP2Ac α	TCP1	TCP1	NP_110379	1	5.6	2	2	0.10
TAP-PP2Ac α	STRN4	striatin 4	NP_037535	1	3.2	2	2	0.06
TAP-PP2Ac α	PPFIA3	liprin A3	NP_003651	0.99	2.4	1	1	0.04
TAP-PP2Ac α	PPFIA1	liprin A1	NP_003617	0.99	2.5	1	1	0.05
TAP-PP2Ac α	CTTNBP2NL	CTTNBP2NL	NP_061174	0.92	2.8	1	1	0.05
TAP-PP2Ac β	PPP2R1A	PP2A A α	NP_055040	1	46.3	33	69	1.02
TAP-PP2Ac β	PPP2CB	PP2Ac β	NP_004147	1	45.6	19	60	1.00
TAP-PP2Ac β	STRN	striatin	NP_003153	1	39.7	29	55	0.87
TAP-PP2Ac β	FAM40A	STRIP1	XP_042708	1	38.8	22	41	0.85
TAP-PP2Ac β	STRN4	striatin 4	NP_037535	1	33.9	14	30	0.74
TAP-PP2Ac β	STRN3	striatin 3	NP_001077362	1	37.5	10	27	0.82
TAP-PP2Ac β	TCP1	TCP1	NP_110379	1	31.1	14	22	0.68
TAP-PP2Ac β	CCT2	CCT2	NP_006422	1	30.5	10	20	0.67
TAP-PP2Ac β	CCT6A	CCT6A	NP_001753	1	19.8	7	14	0.43
TAP-PP2Ac β	CTTNBP2NL	CTTNBP2NL	NP_061174	1	15.2	8	14	0.33
TAP-PP2Ac β	MOBKL3	Mob3	NP_056202	1	22.8	4	12	0.50
TAP-PP2Ac β	CCT3	CCT3	NP_005989	1	21.3	9	12	0.47
TAP-PP2Ac β	CCT5	CCT5	NP_036205	1	19.6	9	12	0.43
TAP-PP2Ac β	IGBP1	alpha4	NP_001542	1	28.6	8	12	0.63
TAP-PP2Ac β	PPP2R2A	PP2A B α	NP_002708	1	26.7	8	10	0.59
TAP-PP2Ac β	CCT8	CCT8	NP_006576	1	16.6	8	9	0.36
TAP-PP2Ac β	CCT7	CCT7	NP_006420	1	14	5	8	0.31
TAP-PP2Ac β	CCT4	CCT4	NP_006421	1	22.6	7	8	0.50
TAP-PP2Ac β	FGFR1OP	FOP	NP_008976,	1	14.2	3	3	0.31

TAP-PP2Ac β	PPP2R5D	PP2A B' δ	NP_006236, NP_219499	1 0.94	9.1 3.8	2 1	2 1	0.20 0.08
TAP-PP2AB γ	TCP1	TCP1	NP_110379	1	54.1	32	56	1.21
TAP-PP2AB γ	PPP2R2C	PP2A B γ	NP_065149	1	44.7	5	51	1.00
TAP-PP2AB γ	CCT2	CCT2	NP_006422	1	56.4	31	49	1.26
TAP-PP2AB γ	PPP2R1A	PP2A A α	NP_055040	1	43.5	27	49	0.97
TAP-PP2AB γ	CCT6A	CCT6A	NP_001753	1	37.3	25	42	0.83
TAP-PP2AB γ	CCT5	CCT5	NP_036205	1	46	26	41	1.03
TAP-PP2AB γ	CCT7	CCT7	NP_006420	1	53.8	25	39	1.20
TAP-PP2AB γ	CCT4	CCT4	NP_006421	1	47.4	20	35	1.06
TAP-PP2AB γ	CCT8	CCT8	NP_006576	1	39.4	23	33	0.88
TAP-PP2AB γ	CCT3	CCT3	NP_005989	1	47.1	23	32	1.05
TAP-PP2AB γ	PPP2CA/B	PP2Ac α/β	NP_002706,NP_004147	1	28.8	9	16	0.64
TAP-PP2AB γ	PPP2R1B	PP2A A β	NP_002707	1	9.1	3	10	0.20
TAP-PP2AB' α	PPP2R1A	PP2A A α	NP_055040	1	28.2	18	36	0.95
TAP-PP2AB' α	PPP2R5A	PP2A B' α	NP_006234	1	29.6	14	20	1.00
TAP-PP2AB' α	PPP2CA/B	PP2Ac α/β	NP_002706,NP_004147	1	38.8	10	18	1.31
TAP-PP2AB' α	PPP2R1B	PP2A A β	NP_002707	0.99	4.9	1	3	0.17
TAP-striatin4	STRN4	striatin 4	NP_037535	1	58.8	50	175	1.00
TAP-striatin4	STRN3	striatin 3	NP_001077362	1	47.8	28	107	0.81
TAP-striatin4	PPP2R1A	PP2A A α	NP_055040	1	43	27	80	0.73
TAP-striatin4	STRN	striatin	NP_003153	1	36.3	26	70	0.62
TAP-striatin4	FAM40A	STRIP1	NP_149079	1	28.7	20	57	0.49
TAP-striatin4	MOBKL3	Mob3	NP_056202	1	53.8	11	53	0.91
TAP-striatin4	CTTNBP2NL	CTTNBP2NL	NP_061174,	1	31	17	49	0.53
TAP-striatin4	CCT3	CCT3	NP_005989	1	46	17	30	0.78
TAP-striatin4	CCT6A	CCT6A	NP_001753	1	18.5	9	30	0.31
TAP-striatin4	CCT2	CCT2	NP_006422	1	19.5	8	27	0.33
TAP-striatin4	CCT5	CCT5	NP_006576	1	31.2	15	26	0.53
TAP-striatin4	CCT7	CCT7	NP_006420	1	24.3	10	25	0.41
TAP-striatin4	CCT4	CCT4	NP_006421	1	29.8	11	24	0.51
TAP-striatin4	TCP1	TCP1	NP_110379	1	30	11	22	0.51
TAP-striatin4	PPP2CA/B	PP2Ac α/β	NP_002706,NP_004147	1	27.8	5	18	0.47
TAP-striatin4	CCT5	CCT5	NP_036205	1	23.8	8	13	0.40
TAP-striatin4	DNCL	dynein	NP_003737,NP_542408	0.97	12.4	1	6	0.21
TAP-striatin4	SIKE	SIKE	NP_079349	0.99	13.5	2	2	0.23
TAP-striatin4	PPP2R1B	PP2A A β	NP_002707,NP_859050	0.99	11.3	1	2	0.19
TAP-Mob3	STRN3	striatin 3	NP_001077362	1	58.5	18	78	1.16
TAP-Mob3	STRN	striatin	NP_003153	1	46.4	34	63	0.92
TAP-Mob3	FAM40A	STRIP1	NP_149079	1	45	34	55	0.89
TAP-Mob3	CTTNBP2NL	CTTNBP2NL	NP_061174	1	44.5	32	45	0.88
TAP-Mob3	STRN4	striatin 4	NP_037535	1	42.2	23	44	0.84
TAP-Mob3	PPP2R1A	PP2A A α	NP_055040	1	44.3	20	37	0.88
TAP-Mob3	MOBKL3	Mob3	NP_056202	1	50.3	13	27	1.00
TAP-Mob3	PPP2CA/B	PP2Ac a/b	NP_002706,NP_004147	1	44.3	10	15	0.88
TAP-Mob3	PPP2R1B	PP2A A b	NP_002707	1	10.9	3	12	0.22
TAP-Mob3	FAM40B	STRIP1	NP_065755	1	7.2	6	12	0.14
TAP-Mob3	DNCL	dynein	NP_003737	1	62.9	4	6	1.25
TAP-Mob3	SLMAP	SLMAP	NP_009090	1	9.1	4	5	0.18
TAP-Mob3	SIKE	SIKE	NP_079349	1	15	2	2	0.30
TAP-Mob3	CTTNBP2	CTTNBP2	NP_219499	1	1.3	2	2	0.03

SUPPLEMENTAL TABLE S5.

Detailed mass spectrometric data for flag interactions. The gene name for each prey (or "hit") is indicated; for protein names, refer to Sup Table S1. The accession numbers (protid) are from the International Protein Index (IPI). ProtLen is the length of the protein in amino acids and the GeneSymbol is from HUGO. Pw is the ProteinProphet probability, taking into account all peptides, regardless of the weight (based on shared peptides); Pfull is the ProteinProphet probability calculated without taking the weight into account. Npeps is the number of unique peptide ions; Nspecs is the number of matched spectra; Nspecswt95 is the number of spectra assigned with a weight of 0.95 or more to a given protein. Npepswt95 is the number of peptides with a weight >0.95. Ewing score is the interaction probability value reported by Ewing et al. (2007) Mol. Syst Biol, 3:89, when applicable (STK24 as a bait). Only proteins absent from flag alone purifications and detected with >20 spectra in at least two different AP-MS are reported. The exception to the 20 peptide rule consists in previously-reported interactions, such as those involving PP2Ac, PP2AA and PP2A B subunits; in this case, all hits are reported. Note that STRN3, SIKE and SLMAP are represented by two entries; the highest spectral count is used in Table II. The highlighted numbers are proteins identified on the basis of a single peptide: the corresponding peptide annotation and annotated spectra are presented in Sup Table S6 and Sup Fig S7. Red denotes components of the PP2Ac•PP2A A core phosphatase, green represents the known PP2A B regulatory subunits (including the striatins), and blue indicates the detection of STRIP1/2 and CTTNBP2/NL in the pull-downs

BAIT	protid	protLen	GeneSymbol	Protein name	Pw	Pfull	Npeps	Nspecs	Nspecswt95	Npepswt95	Ewing score
PP2A A α	IPI00554737	589	PPP2R1A	PP2A A α	1	1	126	548	548	134	
	IPI00008380	309	PPP2CA	PP2A C α	1	1	36	121	4	1	
	IPI00332511	447	PPP2R2A	PP2A B α	1	1	37	108	50	18	
	IPI00014456	780	STRN	striatin	1	1	4	9	9	4	
	IPI00549766	837	FAM40A	STRIP1	1	1	6	8	8	6	
	IPI00879459	797	STRN3	striatin 3	1	1	14	27	4	3	
	IPI00477001	713	STRN3	striatin 3	1	1	13	25	2	1	
	IPI00000030	602	PPP2R5D	PP2A B' δ	1	1	33	73	58	28	
	IPI00294178	601	PPP2R1B	PP2A A β	0	1	36	208	2	1	
	IPI00003016	753	STRN4	striatin 4	1	1	7	10	10	7	
	IPI00012834	524	PPP2R5C	PP2A B' γ	1	1	23	47	25	12	
	IPI00470920	453	PPP2R2D;ACTG1	PP2A B δ	1	1	29	75	17	8	
	IPI00442098	540	PPP2R5C	PP2A B' γ	0	1	22	44	0	0	
	IPI00007694	386	PPME1	PME1	1	1	14	27	27	14	
	IPI00514311	639	CTTNBP2NL	CTTNBP2NL	0.9999	0.9999	2	3	3	4	
	IPI00002853	467	PPP2R5E	PP2A B' ϵ	1	1	17	31	24	13	
	IPI00163496	1202	PPFIA1	lpirin A1	1	1	15	24	24	16	
	IPI00793853	433	SLMAP	SLMAP	0.809	0.809	1	2	2	1	
	IPI00014978	486	PPP2R5A	PP2A B' α	1	1	7	11	10	6	
	IPI00845329	575	PPP2R3B	PP2A B' β	1	1	2	3	3	2	
	IPI00289271	1259	PPFIA2	lpirin A2	0	0.9959	4	6	0	0	
	IPI00014980	497	PPP2R5B	PP2A B' β	0	0.7772	2	2	0	0	
BAIT	protid	protLen	GeneSymbol	Protein name	Pw	Pfull	Npeps	Nspecs	Nspecswt95	Npepswt95	Ewing score
PP2Ac α	IPI00554737	589	PPP2R1A	PP2A A α	1	1	58	345	310	56	
	IPI00008380	309	PPP2CA	PP2A C α	1	1	32	124	124	40	
	IPI00332511	447	PPP2R2A	PP2A B α	1	1	35	162	96	23	
	IPI00014456	780	STRN	striatin	1	1	14	34	32	14	
	IPI00549766	837	FAM40A	STRIP1	1	1	7	13	13	8	
	IPI00879459	797	STRN3	striatin 3	1	1	14	33	1	1	
	IPI00477001	713	STRN3	striatin 3	1	1	14	37	5	1	
	IPI00000030	602	PPP2R5D	PP2A B' δ	1	1	39	144	100	33	
	IPI00294178	601	PPP2R1B	PP2A A β	1	1	20	57	22	12	
	IPI00003016	753	STRN4	striatin 4	1	1	8	10	10	9	
	IPI00012834	524	PPP2R5C	PP2A B' γ	0	1	13	42	0	0	
	IPI00470920	453	PPP2R2D;ACTG1	PP2A B δ	1	1	27	88	22	14	
	IPI00442098	540	PPP2R5C	PP2A B' γ	1	1	17	48	12	6	
	IPI00386122	225	MOBLK3	Mob3	1	1	4	10	10	4	
	IPI00007694	386	PPME1	Pme1	1	1	18	51	51	19	
	IPI00514311	639	CTTNBP2NL	CTTNBP2NL	1	1	8	13	13	9	
	IPI00002853	467	PPP2R5E	PP2A B' ϵ	1	1	9	26	24	10	
	IPI00163496	1202	PPFIA1	lpirin A1	1	1	32	79	72	28	
	IPI00019148	339	IGBP1	alpha4	1	1	11	39	39	11	
	IPI00793853	433	SLMAP	SLMAP	0.2292	0.2292	1	1	1	1	
	IPI00297779	535	CCT2	CCT2	1	1	8	18	18	8	
	IPI00784090	548	CCT8	CCT8	1	1	17	35	35	18	
	IPI00103869	1663	CTTNBP2	CTTNBP2	0.9627	0.9627	1	1	1	1	
	IPI00553185	545	CCT3	CCT3	1	1	11	20	20	12	
	IPI00290566	556	TCP1	TCP1	1	1	17	30	29	17	
	IPI00010720	541	CCT5	CCT5	1	1	5	11	11	6	
	IPI00027626	531	CCT6A	CCT6A	1	1	7	11	11	7	
	IPI00018465	543	CCT7	CCT7	1	1	7	19	19	7	
	IPI00398364	1194	PPFIA3	lpirin A3	1	1	21	35	28	18	
	IPI00014978	486	PPP2R5A	PP2A B' α	1	1	7	20	20	7	
	IPI000302927	539	CCT4	CCT4	1	1	8	18	17	7	
	IPI00845329	575	PPP2R3B	PP2A B' β	1	1	10	19	19	10	
	IPI00289271	1259	PPFIA2	lpirin A2	0	1	10	21	0	0	
	IPI00013076	399	FGFR1OP	FOP	1	1	4	6	6	4	
	IPI00014980	497	PPP2R5B	PP2A B' β	0	0.9996	2	3	1	1	
BAIT	protid	protLen	GeneSymbol	Protein name	Pw	Pfull	Npeps	Nspecs	Nspecswt95	Npepswt95	Ewing score
striatin	IPI00554737	589	PPP2R1A	PP2A A α	1	1	29	76	62	25	
	IPI00008380	309	PPP2CA	PP2A C α	1	1	7	29	29	7	
	IPI00014456	780	STRN	striatin	1	1	68	845	844	70	
	IPI00549766	837	FAM40A	STRIP1	1	1	34	93	90	33	
	IPI00879459	797	STRN3	striatin 3	1	1	24	51	5	3	
	IPI00477001	713	STRN3	striatin 3	0.9997	1	22	47	1	1	
	IPI00292827	416	RP6-213H19.1	MST4	1	1	14	37	14	8	
	IPI00294178	601	PPP2R1B	PP2A A β	0.9998	1	7	16	2	2	

BAIT	protid	protLen	GeneSymbol	Protein name	Pw	Pfull	Npeps	Nspecs	Nspecswt95	Npepswt95	Ewing score
striatin3	IPI0003016	753	STRN4	striatin 4	1	1	26	123	122	25	
	IPI00012093	426	STK25	STK25	0	1	4	9	0	0	
	IPI00872754	484	STK24	STK24	0	1	16	47	0	0	
	IPI00386122	225	MOBKL3	Mob3	1	1	10	59	59	11	
	IPI00298558	212	PDCD10	CCM3	1	1	16	25	25	16	
	IPI00514311	639	CTTNBP2NL	CTTNBP2NL	1	1	18	28	28	18	
	IPI00640464	207	SIKE	SIKE	1	1	9	12	12	9	
	IPI00305186	211	SIKE	SIKE	0	1	8	10	0	0	
	IPI0067651	893	FAM40B	STRIP2	1	1	8	13	10	7	
	IPI00793853	433	SLMAP	SLMAP	0	1	24	59	0	0	
	IPI00297779	535	CCT2	CCT2	1	1	8	14	14	8	
	IPI00784090	548	CCT8	CCT8	1	1	7	11	11	7	
	IPI00103869	1663	CTTNBP2	CTTNBP2	1	1	3	7	7	3	
	IPI00553185	545	CCT3	CCT3	1	1	8	11	11	8	
	IPI00290566	556	TCP1	TCP1	1	1	10	13	13	10	
	IPI00010720	541	CCT5	CCT5	1	1	13	23	23	13	
	IPI00014903	253	FGFR1OP2	FGFR1OP2	1	1	8	30	30	8	
	IPI00027626	531	CCT6A	CCT6A	1	1	7	12	12	7	
	IPI00018465	543	CCT7	CCT7	1	1	9	15	15	9	
	IPI00302927	539	CCT4	CCT4	1	1	7	9	9	7	
	IPI00788882	94	SLMAP	SLMAP	0.8869	1	4	19	1	1	
	IPI00220656	530	CCT6B	CCT6B	0	0.9887	2	2	0	0	
BAIT	protid	protLen	GeneSymbol	Protein name	Pw	Pfull	Npeps	Nspecs	Nspecswt95	Npepswt95	Ewing score
striatin3	IPI00554737	589	PPP2R1A	PP2A A α	1	1	34	52	52	37	
	IPI00008380	309	PPP2CA	PP2A $\alpha\alpha$	1	1	12	32	32	12	
	IPI00014456	780	STRN	striatin	1	1	34	56	52	32	
	IPI00549766	837	FAM40A	STRIP1	1	1	45	99	91	47	
	IPI00879459	797	STRN3	striatin 3	1	1	72	212	11	9	
	IPI00477001	713	STRN3	striatin 3	0.9998	1	64	203	2	1	
	IPI00292827	416	RP6-213H19.1	MST4	1	1	8	8	4	4	
	IPI00294178	601	PPP2R1B	PP2A A β	0	1	6	10	0	0	
	IPI00003016	753	STRN4	striatin 4	1	1	39	69	65	36	
	IPI00012093	426	STK25	STK25	0	1	5	5	0	0	
	IPI00872754	484	STK24	STK24	0	1	7	7	0	0	
	IPI00386122	225	MOBKL3	Mob3	1	1	10	52	52	12	
	IPI00298558	212	PDCD10	CCM3	1	1	5	6	6	5	
	IPI00514311	639	CTTNBP2NL	CTTNBP2NL	1	1	35	52	52	36	
	IPI00640464	207	SIKE	SIKE	1	1	18	20	20	19	
	IPI00305186	211	SIKE	SIKE	0	1	16	18	0	0	
	IPI0067651	893	FAM40B	STRIP2	1	1	12	18	10	9	
	IPI008793853	433	SLMAP	SLMAP	1	1	37	51	1	1	
	IPI00297779	535	CCT2	CCT2	1	1	17	18	18	17	
	IPI00784090	548	CCT8	CCT8	1	1	10	10	10	10	
	IPI00103869	1663	CTTNBP2	CTTNBP2	1	1	21	24	24	21	
	IPI00553185	545	CCT3	CCT3	1	1	16	19	19	18	
	IPI00290566	556	TCP1	TCP1	1	1	16	16	15	15	
	IPI00010720	541	CCT5	CCT5	1	1	14	14	14	14	
	IPI00014903	253	FGFR1OP2	FGFR1OP2	1	1	14	17	17	14	
	IPI00027626	531	CCT6A	CCT6A	1	1	11	12	12	11	
	IPI00018465	543	CCT7	CCT7	1	1	8	8	8	8	
	IPI00302927	539	CCT4	CCT4	1	1	8	8	7	7	
	IPI00788882	94	SLMAP	SLMAP	0	0.9998	3	4	0	0	
BAIT	protid	protLen	GeneSymbol	Protein name	Pw	Pfull	Npeps	Nspecs	Nspecswt95	Npepswt95	Ewing score
Mob3	IPI00554737	589	PPP2R1A	PP2A A α	1	1	45	111	89	38	
	IPI00008380	309	PPP2CA	PP2A $\alpha\alpha$	1	1	11	28	28	11	
	IPI00014456	780	STRN	striatin	1	1	72	308	302	72	
	IPI00549766	837	FAM40A	STRIP1	1	1	54	164	157	51	
	IPI00879459	797	STRN3	striatin 3	1	1	65	260	30	13	
	IPI00477001	713	STRN3	striatin 3	0.9997	1	53	232	2	1	
	IPI00292827	416	RP6-213H19.1	MST4	1	1	15	36	19	5	
	IPI00294178	601	PPP2R1B	PP2A A β	1	1	15	32	10	8	
	IPI00003016	753	STRN4	striatin 4	1	1	56	396	393	56	
	IPI00012093	426	STK25	STK25	0.9705	1	6	10	1	1	
	IPI00872754	484	STK24	STK24	0	1	25	59	0	0	
	IPI00386122	225	MOBKL3	Mob3	1	1	16	179	179	17	
	IPI00298558	212	PDCD10	CCM3	1	1	19	33	33	19	
	IPI00514311	639	CTTNBP2NL	CTTNBP2NL	1	1	39	107	107	39	
	IPI00640464	207	SIKE	SIKE	1	1	18	50	50	20	
	IPI00305186	211	SIKE	SIKE	0	1	17	48	0	0	
	IPI0067651	893	FAM40B	STRIP2	1	1	20	28	21	16	
	IPI008793853	433	SLMAP	SLMAP	1	1	49	104	0	0	
	IPI00297779	535	CCT2	CCT2	1	1	6	7	7	6	
	IPI00784090	548	CCT8	CCT8	1	1	10	16	16	10	
	IPI00103869	1663	CTTNBP2	CTTNBP2	1	1	33	51	51	33	
	IPI00553185	545	CCT3	CCT3	1	1	7	8	8	7	
	IPI00290566	556	TCP1	TCP1	1	1	9	9	9	9	
	IPI00010720	541	CCT5	CCT5	1	1	5	7	7	5	
	IPI00014903	253	FGFR1OP2	FGFR1OP2	1	1	17	29	29	17	
	IPI00027626	531	CCT6A	CCT6A	1	1	6	8	8	6	
	IPI00018465	543	CCT7	CCT7	1	1	5	7	7	5	
	IPI00302927	530	CCT6B	CCT6B	0	0.6419	2	2	0	0	
BAIT	protid	protLen	GeneSymbol	Protein name	Pw	Pfull	Npeps	Nspecs	Nspecswt95	Npepswt95	Ewing score
STRIP1	IPI00554737	589	PPP2R1A	PP2A A α	1	1	14	25	25	15	
	IPI00008380	309	PPP2CA	PP2A $\alpha\alpha$	1	1	9	17	17	9	

BAIT	protid	protLen	GeneSymbol	Protein name	Pw	Pfull	Npeps	Nspecs	Nspecswt95	Npepswt95	Ewing score
CTTNBP2NL	IPI00554737	589	PPP2R1A	PP2A A α	1	1	20	43	43	20	
	IPI00008380	309	PPP2CA	PP2A $\alpha\epsilon$	1	1	10	22	22	10	
	IPI00014456	780	STRN	striatin	1	1	34	88	82	37	
	IPI00549766	837	FAM40A	STRIP1	1	1	23	62	41	25	
	IPI00879459	797	STRN3	striatin 3	1	1	27	107	16	6	
	IPI00477001	713	STRN3	striatin 3	0.9998	1	22	95	4	1	
	IPI00292827	416	RP6-213H19.1	MST4	0	1	8	16	0	0	
	IPI00294178	601	PPP2R1B	PP2A A β	0	1	4	8	0	0	
	IPI00003016	753	STRN4	striatin 4	1	1	21	75	75	22	
	IPI00012093	426	STK25	STK25	0	1	5	10	1	1	
	IPI00872754	484	STK24	STK24	0	1	5	9	0	0	
	IPI00386122	225	MOBKL3	Mob3	1	1	10	69	69	12	
	IPI00298558	212	PDCD10	CCM3	1	1	7	15	15	7	
	IPI00514311	639	CTTNBP2NL	CTTNBP2NL	1	1	26	108	108	26	
	IPI00607651	893	FAM40B	STRIP2	1	1	4	26	5	3	
BAIT	protid	protLen	GeneSymbol	Protein name	Pw	Pfull	Npeps	Nspecs	Nspecswt95	Npepswt95	Ewing score
CTTNBP2	IPI00554737	589	PPP2R1A	PP2A A α	1	1	30	43	43	30	
	IPI00008380	309	PPP2CA	PP2A $\alpha\epsilon$	1	1	10	15	15	11	
	IPI00014456	780	STRN	striatin	1	1	35	52	50	35	
	IPI00549766	837	FAM40A	STRIP1	1	1	45	71	65	44	
	IPI00879459	797	STRN3	striatin 3	1	1	44	96	9	7	
	IPI00477001	713	STRN3	striatin 3	0.9998	1	38	90	3	1	
	IPI00292827	416	RP6-213H19.1	MST4	0	1	3	3	1	1	
	IPI00294178	601	PPP2R1B	PP2A A β	0	1	4	4	0	0	
	IPI00003016	753	STRN4	striatin 4	1	1	32	66	66	34	
	IPI00012093	426	STK25	STK25	0	0.9602	2	2	0	0	
	IPI00872754	484	STK24	STK24	0	0.9948	4	4	0	0	
	IPI00386122	225	MOBKL3	Mob3	1	1	12	26	26	12	
	IPI00298558	212	PDCD10	CCM3	1	1	4	4	4	4	
	IPI00514311	639	CTTNBP2NL	CTTNBP2NL	1	1	7	7	7	8	
	IPI00607651	893	FAM40B	STRIP2	1	1	14	18	12	10	
	IPI00297779	535	CCT2	CCT2	0.9998	0.9998	2	2	2	2	
	IPI00784090	548	CCT8	CCT8	0.9998	1	2	2	2	2	
	IPI00103869	1663	CTTNBP2	CTTNBP2	1	1	42	122	122	47	
	IPI00553185	545	CCT3	CCT3	1	1	3	5	5	4	
	IPI00290566	556	TCP1	TCP1	1	1	3	4	4	3	
	IPI00010720	541	CCT5	CCT5	1	1	2	2	2	2	
	IPI00027626	531	CCT6A	CCT6A	0.9999	0.9999	2	2	2	2	
BAIT	protid	protLen	GeneSymbol	Protein name	Pw	Pfull	Npeps	Nspecs	Nspecswt95	Npepswt95	Ewing score
CCM3	IPI00554737	589	PPP2R1A	PP2A A α	1	1	18	19	19	18	
	IPI00008380	309	PPP2CA	PP2A $\alpha\epsilon$	1	1	6	6	6	6	
	IPI00014456	780	STRN	striatin	1	1	31	31	31	33	
	IPI00549766	837	FAM40A	STRIP1	1	1	13	13	13	15	
	IPI00879459	797	STRN3	striatin 3	1	1	20	23	1	1	
	IPI00477001	713	STRN3	striatin 3	1	1	20	23	1	1	
	IPI00292827	416	RP6-213H19.1	MST4	1	1	79	294	104	54	
	IPI00294178	601	PPP2R1B	PP2A A β	0	0.9933	2	2	0	0	
	IPI00003016	753	STRN4	striatin 4	1	1	9	10	10	9	
	IPI00012093	426	STK25	STK25	1	1	37	195	28	24	
	IPI00872754	484	STK24	STK24	1	1	56	209	120	36	
	IPI00386122	225	MOBKL3	Mob3	1	1	7	9	9	7	
	IPI00298558	212	PDCD10	CCM3	1	1	89	218	218	96	
	IPI00514311	639	CTTNBP2NL	CTTNBP2NL	1	1	10	10	10	10	
	IPI00640464	207	SIKE	SIKE	1	1	5	5	5	5	
	IPI00305186	211	SIKE	SIKE	1	1	5	5	5	5	
	IPI00793853	433	SLMAP	SLMAP	1	1	16	17	0	0	
	IPI00103869	1663	CTTNBP2	CTTNBP2	0.9865	0.9865	1	1	1	1	
	IPI00014903	253	FGFR1OP2	FGFR1OP2	1	1	8	8	8	8	
	IPI00788882	94	SLMAP	SLMAP	1	1	2	2	0	0	
BAIT	protid	protLen	GeneSymbol	Protein name	Pw	Pfull	Npeps	Nspecs	Nspecswt95	Npepswt95	Ewing score
MST4	IPI00554737	589	PPP2R1A	PP2A A α	1	1	29	39	39	29	
	IPI00008380	309	PPP2CA	PP2A $\alpha\epsilon$	1	1	8	14	14	8	
	IPI00014456	780	STRN	striatin	1	1	39	89	87	42	
	IPI00549766	837	FAM40A	STRIP1	1	1	33	52	49	30	
	IPI00879459	797	STRN3	striatin 3	1	1	31	68	8	5	
	IPI00477001	713	STRN3	striatin 3	0.9998	1	27	63	3	1	

BAIT	protid	protLen	GeneSymbol	Protein name	Pw	Pfull	Npeps	Nspecs	Nspecswt95	Npepswt95	Ewing score
STK24	IPI00292827	416	RP6-213H19.1	MST4	1	1	95	555	328	86	
	IPI00294178	601	PPP2R1B	PP2A A β	0	1	6	10	0	0	
	IPI0003016	753	STRN4	striatin 4	1	1	16	28	28	16	
	IPI0012093	426	STK25	STK25	1	1	25	230	3	3	
	IPI00872754	484	STK24	STK24	0	1	20	169	0	3	
	IPI00386122	225	MOBL3	Mob3	1	1	10	29	29	10	
	IPI00298558	212	PDCD10	CCM3	1	1	36	97	97	38	
	IPI00514311	639	CTTNBP2NL	CTTNBP2NL	1	1	26	33	33	26	
	IPI00640464	207	SIKE	SIKE	1	1	10	11	11	10	
	IPI00305186	211	SIKE	SIKE	0	1	9	10	0	0	
	IPI00607651	893	FAM40B	STRIP2	1	1	8	8	5	5	
	IPI00793853	433	SLMAP	SLMAP	1	1	27	33	0	0	
	IPI00103869	1663	CTTNBP2	CTTNBP2	1	1	3	3	3	3	
	IPI00014903	253	FGFR1OP2	FGFR1OP2	1	1	10	13	13	10	
	IPI00788882	94	SLMAP	SLMAP	0	0.9998	2	3	0	0	
BAIT	protid	protLen	GeneSymbol	Protein name	Pw	Pfull	Npeps	Nspecs	Nspecswt95	Npepswt95	Ewing score
STK24	IPI00554737	589	PPP2R1A	PP2A A α	1	1	33	63	47	26	0.51
	IPI00008380	309	PPP2CA	PP2A C α	0.9989	1	7	10	1	1	0.42
	IPI00014456	780	STRN	striatin	1	1	57	113	113	59	0.521
	IPI00549766	837	FAM40A	STRIP1	1	1	36	55	50	33	0.426
	IPI00879459	797	STRN3	striatin 3	1	1	41	84	12	5	0.559
	IPI00477001	713	STRN3	striatin 3	0.9997	1	37	74	2	1	
	IPI00292827	416	RP6-213H19.1	MST4	0	1	13	79	0	0	
	IPI00294178	601	PPP2R1B	PP2A A β	0.9868	1	8	17	1	1	
	IPI0003016	753	STRN4	striatin 4	1	1	23	43	43	24	
	IPI0012093	426	STK25	STK25	0	1	6	64	0	0	0.444
	IPI00872754	484	STK24	STK24	0	1	52	322	0	0	
	IPI00386122	225	MOBL3	Mob3	1	1	11	22	22	11	0.446
	IPI00298558	212	PDCD10	CCM3	1	1	39	81	81	40	0.462
	IPI00514311	639	CTTNBP2NL	CTTNBP2NL	1	1	28	44	44	28	
	IPI00640464	207	SIKE	SIKE	1	1	12	16	16	12	
	IPI00305186	211	SIKE	SIKE	0	1	11	15	0	0	
	IPI00607651	893	FAM40B	STRIP2	1	1	12	13	8	8	
	IPI00793853	433	SLMAP	SLMAP	1	1	28	41	0	0	0.377
	IPI00297779	535	CCT2	CCT2	1	1	3	3	3	3	
	IPI00784090	548	CCT8	CCT8	1	1	4	4	4	4	
	IPI00103869	1663	CTTNBP2	CTTNBP2	1	1	6	7	7	6	
	IPI00553185	545	CCT3	CCT3	1	1	7	11	11	7	
	IPI00290566	556	TCP1	TCP1	1	1	6	6	6	6	
	IPI00010720	541	CCT5	CCT5	1	1	3	3	3	3	
	IPI00014903	253	FGFR1OP2	FGFR1OP2	1	1	8	9	9	8	
	IPI00027626	531	CCT6A	CCT6A	1	1	3	4	4	3	
	IPI00018465	543	CCT7	CCT7	1	1	4	5	5	4	
	IPI00302927	539	CCT4	CCT4	1	1	3	4	4	3	
	IPI00788882	94	SLMAP	SLMAP	1	1	3	5	0	0	
BAIT	protid	protLen	GeneSymbol	Protein name	Pw	Pfull	Npeps	Nspecs	Nspecswt95	Npepswt95	Ewing score
STK25	IPI00554737	589	PPP2R1A	PP2A A α	1	1	21	40	30	16	
	IPI00008380	309	PPP2CA	PP2A C α	1	1	5	9	9	5	
	IPI00014456	780	STRN	striatin	1	1	50	229	154	49	
	IPI00549766	837	FAM40A	STRIP1	1	1	24	33	31	22	
	IPI00879459	797	STRN3	striatin 3	1	1	34	153	13	8	
	IPI00477001	713	STRN3	striatin 3	0.9998	1	27	142	2	1	
	IPI00292827	416	RP6-213H19.1	MST4	1	1	22	387	16	11	
	IPI00294178	601	PPP2R1B	PP2A A β	0.9998	1	6	11	1	1	
	IPI0003016	753	STRN4	striatin 4	1	1	17	32	32	17	
	IPI0012093	426	STK25	STK25	1	1	42	577	206	33	
	IPI00872754	484	STK24	STK24	0	1	14	149	0	0	
	IPI00386122	225	MOBL3	Mob3	1	1	9	33	33	9	
	IPI00298558	212	PDCD10	CCM3	1	1	29	63	63	30	
	IPI00514311	639	CTTNBP2NL	CTTNBP2NL	1	1	17	46	46	17	
	IPI00640464	207	SIKE	SIKE	1	1	2	2	2	3	
	IPI00305186	211	SIKE	SIKE	1	1	2	2	2	3	
	IPI00607651	893	FAM40B	STRIP2	1	1	5	5	3	3	
	IPI00793853	433	SLMAP	SLMAP	1	1	16	48	0	0	
	IPI00103869	1663	CTTNBP2	CTTNBP2	0.992	0.992	1	1	1	1	
	IPI00290566	556	TCP1	TCP1	1	1	3	3	3	3	
	IPI00014903	253	FGFR1OP2	FGFR1OP2	1	1	9	12	12	9	
	IPI00788882	94	SLMAP	SLMAP	1	1	3	4	0	0	
BAIT	protid	protLen	GeneSymbol	Protein name	Pw	Pfull	Npeps	Nspecs	Nspecswt95	Npepswt95	Ewing score
SIKE	IPI00554737	589	PPP2R1A	PP2A A α	1	1	16	30	30	17	
	IPI00008380	309	PPP2CA	PP2A C α	1	1	6	11	11	6	
	IPI00014456	780	STRN	striatin	1	1	30	69	69	35	
	IPI00549766	837	FAM40A	STRIP1	1	1	25	40	40	25	
	IPI00879459	797	STRN3	striatin 3	1	1	27	55	4	3	
	IPI00477001	713	STRN3	striatin 3	0.9957	1	25	52	1	1	
	IPI00294178	601	PPP2R1B	PP2A A β	0	0.9761	3	7	0	0	
	IPI0003016	753	STRN4	striatin 4	1	1	15	33	32	16	
	IPI00872754	484	STK24	STK24	0.9999	0.9999	2	4	4	2	
	IPI00386122	225	MOBL3	Mob3	1	1	8	16	16	9	
	IPI00298558	212	PDCD10	CCM3	1	1	4	6	6	4	
	IPI00640464	207	SIKE	SIKE	1	1	35	218	218	41	
	IPI00305186	211	SIKE	SIKE	0	1	32	209	0	0	
	IPI00607651	893	FAM40B	STRIP2	0	0.9184	2	5	0	1	
	IPI00793853	433	SLMAP	SLMAP	1	1	16	37	0	0	

	IPI00014903	253 FGFR1OP2	FGFR1OP2	Pw	1	1	10	26	26	11	Ewing score
BAIT	protid	protLen	GeneSymbol	Protein name	Pfull	Npeps	Nspecs	Nspecswt95	Npepswt95		
TRAF3IP3	IPI00554737	589 PPP2R1A	PP2A A α	PP2A A α	1	1	31	37	37	33	
	IPI00008380	309 PPP2CA	PP2A $\text{C}\alpha$	PP2A $\text{C}\alpha$	1	1	10	15	15	10	
	IPI00014456	780 STRN	striatin	striatin	1	1	42	85	84	45	
	IPI00549766	837 FAM40A	STRIP1	STRIP1	1	1	38	62	55	34	
	IPI00879459	797 STRN3	striatin 3	striatin 3	1	1	41	73	72	42	
	IPI00477001	713 STRN3	striatin 3	striatin 3	0	1	34	63	0	0	
	IPI00292827	416 RP6-213H19.1	MST4	MST4	0	1	3	3	0	0	
	IPI00294178	601 PPP2R1B	PP2A A β	PP2A A β	0	1	4	4	0	0	
	IPI00003016	753 STRN4	striatin 4	striatin 4	1	1	33	64	64	35	
	IPI00012093	426 STK25	STK25	STK25	0	0.997	2	2	0	1	
	IPI00872754	484 STK24	STK24	STK24	1	1	6	8	8	6	
	IPI00386122	225 MOBKL3	Mob3	Mob3	1	1	9	29	29	10	
	IPI00298558	212 PDCD10	CCM3	CCM3	1	1	7	7	7	7	
	IPI00640464	207 SIKE	SIKE	SIKE	1	1	21	39	4	2	
	IPI00305186	211 SIKE	SIKE	SIKE	0.9798	1	20	36	1	1	
	IPI00607651	893 FAM40B	STRIP2	STRIP2	1	1	12	16	9	9	
	IPI00784090	548 CCT8	CCT8	CCT8	0.9995	0.9995	2	2	2	3	
	IPI00553185	545 CCT3	CCT3	CCT3	0.591	0.591	2	2	2	2	
	IPI00290566	556 TCP1	TCP1	TCP1	0.9999	0.9999	2	2	2	2	
	IPI00010720	541 CCT5	CCT5	CCT5	1	1	2	3	3	2	
	IPI00014903	253 FGFR1OP2	FGFR1OP2	FGFR1OP2	1	1	19	30	30	20	
	IPI00719170	551 TRAF3IP3	TRAF3IP3	TRAF3IP3	1	1	23	60	60	23	
	IPI00019329	89 DYNLL1	DYNLL1	DYNLL1	0.9997	0.9998	2	5	5	2	

SUPPLEMENTAL TABLE S6.

List of proteins identified by a unique peptide. For the bait, F = flag-tag, T = TAP tag. The number of unique peptides (npeps) and spectra (nspecs) are indicated. The sequence of the identified peptide is shown. "Direct additional evidence" for the interaction indicates that the interaction was also detected between the same two proteins in an independent experiment (e.g. in the other tag system, or in a reciprocal AP-MS experiment in which the hit or prey is now tagged). "Indirect additional evidence" indicates that an interaction has been independently detected between paralogs of one or the two proteins.

bait	hit	npeps	nspecs	peptide	direct additional evidence	indirect additional evidence
F-PP2A α	SLMAP	1	2	DEILLLHQAAAK		reciprocal flag MS with paralog
F-PP2A α	SLMAP	1	1	IIEALQADNDFTNER		reciprocal flag MS with paralog
F-PP2A α	CTTNBP2	1	1	APEDAAGAAAEEAK	TAP MS, reciprocal flag MS	paralogy to CTTNBP2NL
T-striatin4	dynein	1	6	NFGSYVTTHETK		flag MS with paralogs
T-striatin4	PP2A β	1	2	AAGGDGDDSLYPIAVLIDELR	published	flag MS with paralogs, reciprocal flag MS with paralog
T-PP2A α	liprin A3	1	1	DSSSLAGTPSDETLATDPLGLAK	flag MS	
T-PP2A α	liprin A1	1	1	TLTDGVLDINHEQENTPSTSGK	flag MS	
T-PP2A α	CTTNBP2NL	1	1	MNTTGLPGPATPAYSYAK	flag MS, reciprocal flag MS	flag MS with paralog, reciprocal flag MS with paralog
T-PP2A β	CTTNBP2	1	1	VAANTPSMYSQUELFQLSQYLQEALHR	flag MS, reciprocal flag MS	flag MS with paralog, reciprocal flag MS with paralog
T-PP2AB' α	PP2A β	1	3	AAGGDGDDSLYPIAVLIDELR	published	

SUPPLEMENTAL TABLE S7.

Peptide statistics for single peptide identifications. For the bait, F = flag-tag, T = TAP tag. The number of unique peptides (npeps) and spectra (nspecs) are indicated. The sequence of the identified peptide is shown. "ntt" is the number of tryptic termini, "missed" the number of missed cleavages", "charge" is the charge state of the parent ion, "parent mass" is the theoretical mass of the parent ion, "error" is the calculated error on the mass of the parent ion, "matched" id the proportion of match ions, and "PeptideProphet" is the statistical value assigned to the peptide by PeptideProphet. Software-specific scoring results (X!Tandem, SEQUEST) are indicated.

A) flag-tag experiments. Instrument: ThermoFinnigan LTQ. Searches performed with X!Tandem

bait	hit	npeps	nspecs	peptide	ntt	missed	charge	parent mass	error	matched	hyperscore	nextscore	expect		PeptideProphet
F-PP2A α	SLMAP	1	2	DEILLHQAAAK	2	0	2	1321.7	-0.2	19/22	491	353	0.046		0.9977
F-PP2A α	SLMAP	1	1	I EALQADNDFTNER	2	0	2	1635.8	-0.1	21/26	351	312	1.4		0.9589
F-PP2A α	CTTNBP2	1	1	APEDAAGAAAEEAK	2	0	2	1242.6	-0.3	20/26	357	287	0.11		0.9905

B) TAP-tag experiments. Instrument: ThermoFinnigan LCQ. Searches performed with SEQUEST

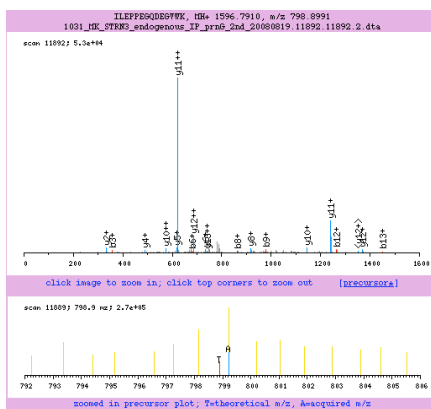
bait	hit	npeps	nspecs	peptide	ntt	missed	charge	parent mass	error	matched	Xcorr	delCN	Sp	RSp	PeptideProphet
T-striatin4	dynein	1	6	NFGSYVTHETK	2	0	2	1283.4	0.1	15/20	3.16	0.357	798	1	1
T-striatin4	PP2A A β	1	2	AAGGGDDDSLPIAVLIDELR	1	0	3	2161.4	-1.2	36/80	4.89	0.196	1526.6	1	0.99
T-PP2A α	liprin A3	1	1	DSSSLAGTPSDET LATDPLGLAK	2	0	2	2247.4	0.9	23/44	4.31	0.4	864.9	1	0.99
T-PP2A α	liprin A1	1	1	TLTDGVLDINHEQENTPSTSGK	2	0	2	2357.5	-0.9	18/42	3.5426	0.421	734.2	1	1
T-PP2A β	CTTNBP2NL	1	1	MNTGLPGPATPAYSYAK	2	0	2	1841.1	-0.1	15/34	2.0184	0.276	190.3	5	0.99
T-PP2A β	CTTNBP2	1	1	VAANTPSMYSQELFQLSQYLQEALHR	2	0	3	3026.4	1.8	28/100	3.35	0.369	387.2	1	1
T-PP2AB α	PP2A A β	1	3	AAGGGDDDSLPIAVLIDELR	1	0	3	2161.4	-1.5	33/80	4.72	0.253	1197.8	1	1

SUPPLEMENTAL TABLE S7.

Mass spectrometric data for interactions with endogenous MST4 and striatin 3. Immunoprecipitation/mass spectrometry was performed as described in Experimental Procedures. The accession numbers (protid) for each of the identified proteins are from the International Protein Index (IPI). ProtLen is the length of the protein in amino acids and the GeneSymbol is from HUGO. The number of unique peptides in the MST4 and Striatin 3 IPs (MST4 Npeps, Striatin3 Npeps) is indicated, along with the total number of spectra in each IP (MST4 Nspecs, Striatin3 Nspecs). The ProteinProphet probability was >0.99 in all cases, except for Mob3 in the Striatin3 IP (0.9796) and MST4 in the Striatin3 IP (0.9790). The numbers highlighted in purple correspond to proteins identified on the basis of a single unique peptide: the corresponding annotated spectra are presented below. • indicates that peptides were detected, but that they fell below the ProteinProphet cutoff value (0.8). •• indicates that peptides were detected, but that they were all shared with different entries. Red denotes components of the PP2Ac•PP2A A core phosphatase, green represents the known PP2A B regulatory subunits (including the striatins), and blue indicates the detection of STRIP1/2 and CTTNBP2/NL in the pull-downs

protid	protLen	GeneSymbol	Protein name	MST4 Npeps	MST4 Nspecs	Striatin3 Npeps	striatin3 Nspecs
IPI00298558	212	PDCD10	CCM3	25	97	3	3
IPI00103869	1663	CTTNBP2	CTTNBP2	2	3	••	••
IPI00514311	639	CTTNBP2NL	CTTNBP2NL	9	12	16	23
IPI00386122	225	MOBKL3	Mob3	2	8	1	2
IPI00292827	416	RP6-213H19.1	MST4	45	219	1	2
IPI00554737	589	PPP2R1A	PP2A Aa	5	8	11	20
IPI00008380	309	PPP2CA/B	PP2Aca/b	2	2	3	7
IPI00793853	433	SLMAP	SLMAP	3	3	•	•
IPI00014456	780	STRN	striatin	11	22	••	••
IPI00879459	797	STRN3	striatin 3	11	20	16	31
IPI00003016	753	STRN4	striatin 4	3	5	10	16
IPI00549766	837	FAM40A	STRIP1	•	•	9	17
IPI00607651	893	FAM40B	STRIP2	••	••	•	•

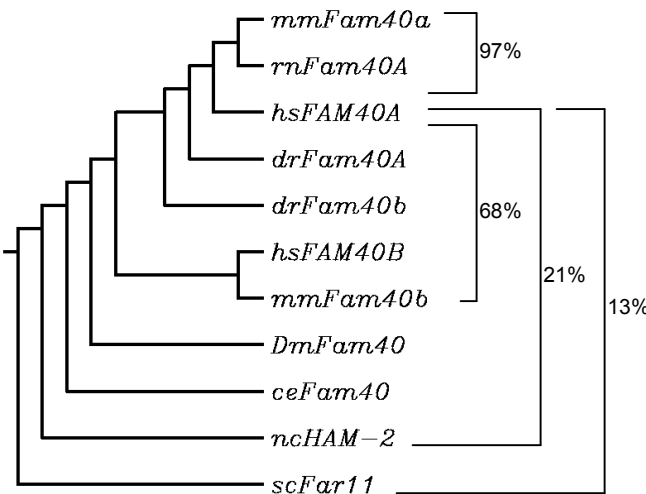
Detection of Mob3 in Striatin3 IP



SUPPLEMENTAL FIGURE S1

A

hsSTRIP1	1	MEPAVGGPGPLIVNNKQPQQPPPPPPAAQPPPGAPRAAAGLLPGKGKAREFNRNQRKDSEGYESPDLFEFYADTDKWAA
hsSTRIP2	1	-----MEDPAAPGTGGPPANGNCNGGGKGKQAAPKCREAFRSQRRESEGSVDCPTLEFEYGDADGHAA
hsSTRIP1	81	ELSELYSYTEGPPEELMNRKCFEEDFRIHVTDKKWTEDLTNQHRTHAMRRLLDGLEVTAREKRLKVARAILYVAQGTFGECS
hsSTRIP2	64	ELSELYSYTENIEETTNNRRCFEEDFRKTQVQCKEWLEEEDAQKAYIMGLLDRLEVVSRERRLKVARAVLYLAQGTFGECD
hsSTRIP1	161	SEAEVQSWMRYNIFLILLEVGTFTNALVELLNMEIDNSAACSSAVRKPAVSLADSTDLRVVILIMYLIVETVHOECFGDKAE
hsSTRIP2	144	SEVDVLHWSRYNCFLLYQMGTFTSFLLELLHMEIDNSAACSSALRKPAVSLADSTELRVVLSVMYLMVENIRLERETDPCG
hsSTRIP1	241	WRTMRQTFRAELGSPLYNNEPFAIMLFGMVTKFCSGAPHFPMKKVLLLWKTVLCTLGGFELQSMKAEKRSILGLPPL
hsSTRIP2	224	WRTARETFRTTELFSFSMHNEEPFALLFESMVTKFCSGAPHFPIKKVLLLWKVVMTLGGFELQTLKVQKRABLGLPPL
hsSTRIP1	321	PEDSIKVIRNMRAASPPASASDLIEQQQK-----RGRREHKALIKQDNLDAFNERDPYKADDSEEEEN---DDDN
hsSTRIP2	304	AEDSIQVVKSMRAASPPSYTLDIGPSQLAPPSKLRCRGSRBQLITKQDSLDIYNERDLKTEEFPATEEFFESAGDGER
hsSTRIP1	390	SLEGETFPPLERDEVMPPPLQHP--QTDRLTCPKGLPWAKPVREKDIEMFLESSRSKFIGYTLGSDTNTVVGTPRPIHESI
hsSTRIP2	384	TLDGELDLLEQDPLVPPPPSQAPLSAERVAFPKGLPWAKVRQKDIEMHLEMRSRKFIGFTLGQDTDTLVGLPRPIHESV
hsSTRIP1	468	KTLKQHKYTSIAEVQAQMEEEYLSPISGGEEEVEQVBAETLYQGLLPSLPQYMIALLKILLAAAPTSKAKTDSINILAD
hsSTRIP2	464	KTLKQHKYTSIAEVQIKNEEELEKCPMSLGEVVPETBCEILYQGVLYSLPQYMIALLKILLAAAPTSKAKTDSINILAD
hsSTRIP1	548	VLPPEMPITVLIQSMKMLGVDVNRHKEIVVKAISAVALLLLLKHFKLNHVYQFEYMAOHLVFAHCPLILKFFNQNINSYITA
hsSTRIP2	544	VLPPEMPITVLIQSMKMLGIDVNRHKEIVKSISTLLLLLKHFKLNHIVYQFEYVSOHLVFAHCPLILKFFNQNINSYITA
hsSTRIP1	628	KNSISVLDYPHQVWHELPETAESLEAGDSNQFCWRNLFSCINLLRILNKLTWKHSRTMMLVVFKSAPILKRALVKQAA
hsSTRIP2	624	KNSISVLDYPCCTIQDPLPELTETESLEAGDSNQFCWRNLFSCINLLRILNKLTWKHSRTMMLVVFKSAPILKRALVKQAA
hsSTRIP1	708	MQLYVLKLLKQTKYLGRQWRKSNMKTMSAIYQKVRHRLNDDWAYGNEDARPWDFQAEETLRANIERFNSRRYDRAH
hsSTRIP2	704	MQLYVLKLLKQTKYLGRQWRKSNMKTMSAIYQKVRHRMNDWAYGNEDARPWDFQAEETLRANIEAFNSRRYDRPQ
hsSTRIP1	788	SNPDFLPVDNCNLQSVLGQRVDLPEDEQMNYDLWLEREVFSKPISSWEELLQ--
hsSTRIP2	784	DS-EFSPVVDNCNLQSVLGQRVDLPEDEHYSYELWLEREVFSQPICWEELLQNH

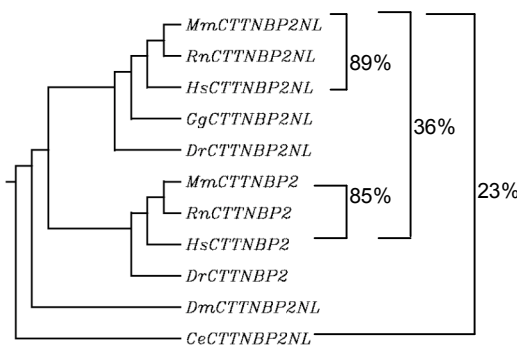
B

A) Sequence alignment between human STRIP1 (FAM40A) and STRIP2 (FAM40B). Alignment performed with BLOSUM62 (ClustalW¹). Identical residues are highlighted in BLACK; conservative substitutions in GREY. Phosphorylation sites (in either the mouse or human protein; Phosphosite²) are in orange. **B) Phylogenetic tree of the STRIP (FAM40A/FAM40B) orthology groups.** Percentage identity between selected pairs of sequences is indicated on the right. Accession numbers used are hsFAM40A, NP_149079.2; mmFam40a, NP_705791.1; rnFam40A, XP_342312.3; drFam40a, NP_998686.1; dmFam40, NP_647806.2; hsFAM40B, NP_065755.1; mmFam40b, NP_796178.2; drFam40b, XP_684274.2; ceFam40, NP_495467.1; scFar11, NP_014272.1; ncHAM-2, XP_961503.2. Species names are Hs, *Homo sapiens*; Mm, *Mus musculus*; Rn, *Rattus norvegicus*; Dr, *Danio rerio*; Dm, *Drosophila melanogaster*; Ce, *Caenorhabditis elegans*; Nc, *Neurospora crassa*; Sc, *Saccharomyces cerevisiae*.

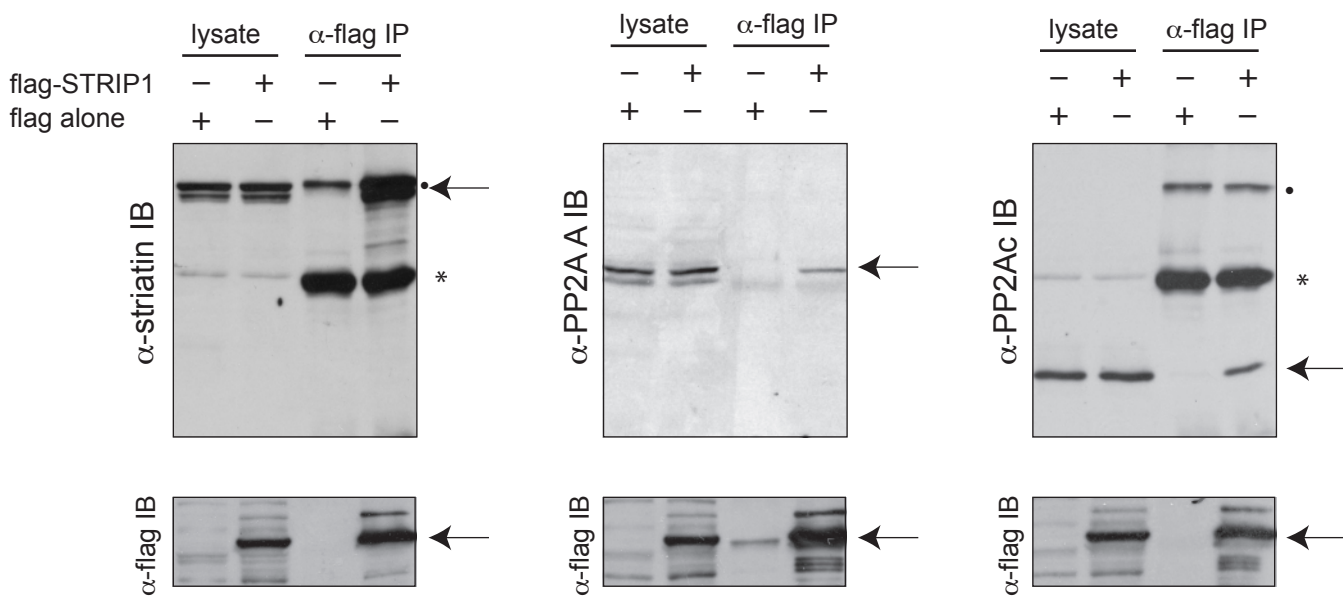
SUPPLEMENTAL FIGURE S2

A

B



A) Sequence alignment between human CTTNBP2, rat CBP90 and human CTTNBP2NL. The published CBP90 rat protein (AF053768) is orthologous to human CTTNBP2, but represents a shorter variant³. Underlining indicates a CDD (Conserved domain database)⁴-predicted chromosome segregation ATPase region (1e-08 on CTTNBP2, 3e-07 on CTTNBP2NL); the region in blue corresponds to predicted ankyrin repeats (CDD 3e-31). Red on CBP90 indicates a proline-rich region, postulated to be required for binding to the cortactin SH3 domain. The residues in green are predicted to form coiled-coils (paircoil2, 0.03 p-score cut-off⁵). Orange indicates phosphorylation sites detected in mouse or human species (Phosphosite²). **B) Phylogeny of the CTTNBP2NL and CTTNBP2 families.** Percentage identity between the aligned regions of selected pairs is indicated on the right (Matrix BLOSUM62). hsCTTNBP2NL, NP_061174.1; mmCtnbp2nl, NP_084525.1; rnCtnbp2nl, XP_227556.2; drCtnbp2nl, NP_001070839.1; dmCtnbp2nl (CG10915), NP_611299.2; ceCtnbp2nl (C49H3.6a), NP_501315.1; hsCTTNBP2, NP_219499.1; mmCtnbp2, NP_525024.1; rnCtnbp2, XP_347231.3; drCtnbp2, XP_683573.2.



Confirmation of the interaction between stably-expressed flag-STRIP1 and endogenous PP2A components. Immunoprecipitation (IP) on α -flag M2 agarose beads was conducted on lysate from HEK293 cells stably expressing flag-STRIP1 or flag alone. Immune complexes were resolved by SDS-PAGE, followed by transfer to nitrocellulose. Co-precipitation of endogenous striatin (top left), PP2AA (top middle) and PP2Ac (top right) was monitored using antibodies to the endogenous proteins. Arrows indicate the position of each protein. A contaminating band is visible in the flag alone lane on the α -striatin IB and α -PP2Ac blots (indicated by a dot); this band comigrates with the striatin protein. Note that a doublet corresponding to endogenous striatin is present in much higher amounts in the flag-STRIP1 sample. Asterisks denote the antibody heavy chain. The bottom panels show the reprobing of each membrane with α -flag antibodies for detection of flag-STRIP1 protein.

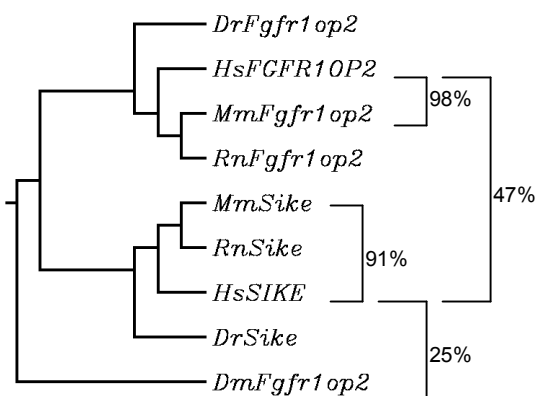
SUPPLEMENTAL FIGURE S4

A

The figure displays a sequence alignment between HsSIKE and HsFGFR1OP2. The alignment shows high conservation of amino acid residues across the entire protein length. Key features include:

- Top Row (HsSIKE):** MSCTIEKILTDAKTLLERLREHDAAAESLVDQSAALHRRVAAMREAGTALPDQVRQRYQEADASDMKDMSKYKPHI**LISQEE**
- Second Row (HsFGFR1OP2):** MSCTIE**EKA**LA**DAKA**L**VERL**RHD**AAE**S**LV**Q**TALN**KR**VEAM**QY**-----**Q**E**E**I**Q**E**LN**E**VA**R**H**R**P**R****S**T**I**V**M**G**I**Q**Q**E
- Third Row (HsSIKE):** NTQIR**E**LQ**QENR**E**LI**W**S**LEE**H**Q**D**A**E**L**I**M**S**KY**R**Q**M**QL**O**LM**V**AK**K**A**V**D**A**E**P**V**I**K**A**Q**H**SH**S**
- Fourth Row (HsFGFR1OP2):** N**R**Q**I**R**E**L**Q**Q**E**N**R**E**LI**R**T**S**LE**E**H**Q**S**A**L**E**I**M**S**KY**R**E**Q**M**F**R**L**N**A**S**K**K**D**P**G**I**IN**K**I**K**E**Q**H**SK**I**D**M**V**H**R**N**K**S**E**G****F****L**D**A**R**H**I
- Fifth Row (HsSIKE):** -----A**E**I**E**S**Q**I**D**R**I**C**E**M**G**E**V**M**R**K**A****Y****Q****V****D****D****D****O****F****C****K****I****Q****E****K****I****A****Q****L****E****N****K****E****L****R****E****I****L****S****I****S****E****S****L****Q****A****R****E****N****S**
- Sixth Row (HsFGFR1OP2):** LEAPQHG**LERR**H**LEAN**Q**N**E**Q**A**H**V**D****Q**I**T****E****M****A****V****M****R****K****A****E****R****D****E****QQ****G****C****K****E****Q****E****R****I****F****O****L****E****Q****E****N****K****G****L****R****E****D****Q****I****T****R****E****S****F****L****N****L****K****D**
- Seventh Row (HsSIKE):** 203 MDTAS**QAIK**-----
- Eighth Row (HsFGFR1OP2):** 233 A**S**E**S****T****S**LS**AL**VT**N**SD**L**SL**R**K**S**

B

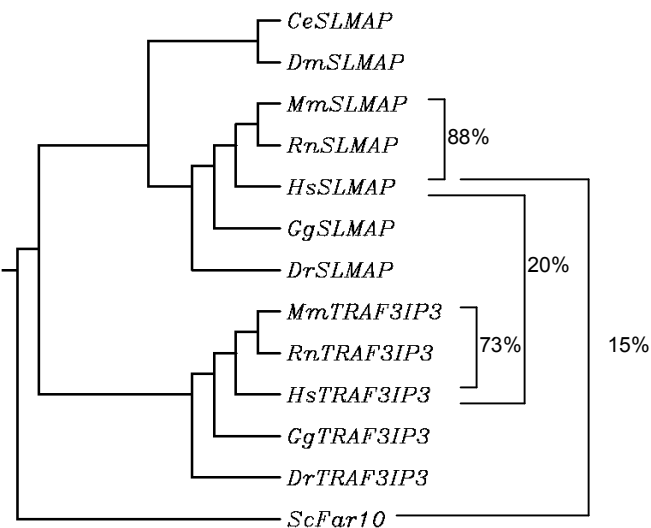


A) Sequence alignment between human SIKE and human FGFR1OP2. Alignment performed with BLOSUM62 (ClustalW¹). Identical residues are highlighted in **BLACK**; conservative substitutions in **GREY**. Phosphorylation sites (detected in either the mouse or human protein; Phosphosite²) are in **orange**. The residues in **green** are predicted to form coiled-coils (paicoil2⁵, 0.3 p-score cut-off). **B) Phylogenetic tree of the SIKE/FGFR1OP2 orthology groups.** Percentage identity between selected pairs of sequences is indicated on the right. Accession numbers used are HsSIKE, NP_001095866.1; MmSike, NP_079955.1; RnSike, NP_001012182.1; DrSike, XP_696578.2; HsFgfr1op2, NP_056448.1; MmFgfr1op2, NP_080494.1; RnFgfr1op2, NP_958824.1; DrFgfr1op2, NP_956249.1; DmFgfr1op2, NP_609084.1.

SUPPLEMENTAL FIGURE S5

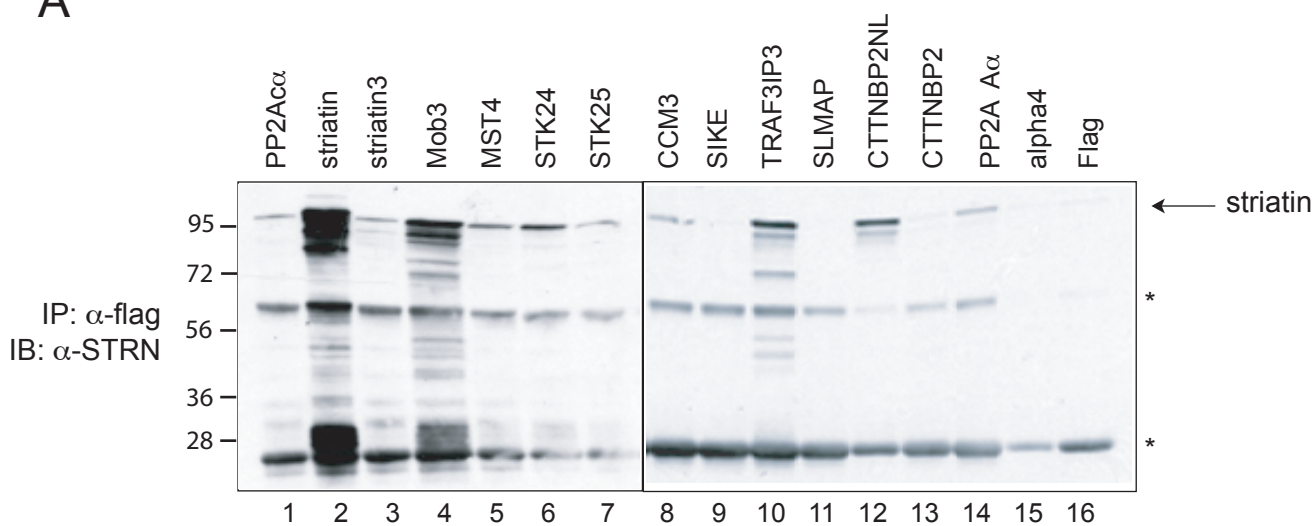
A

HsSLMAP	1	-----MPSALAI FTC RPN SHPFQERIVYLDPEPIKIGRSVARCRPAQNNATFDCKVLSRNHA DVWF <small>DHRTGKFYI</small> QDTKSS
HsTRAF3IP3	1	MISPDPRPSPG IAR WAESYEAKCER QE IRESRRCRPNVTCRQVGKTLRIQ RE QLQRARLQQFFRRR-NLELE E KGKA
HsSLMAP	76	NGTFINS DRISR -GSEESP <small>PCE</small> ILS <u>C</u> DIIQFG--vDVTENTRKVTHG <small>CIVSTIK</small> FLEDGMEARLRSDVIAHAP <small>PSPV</small>
HsTRAF3IP3	80	QHPQAREQGP <small>SRRP</small> GQVTGTSSE <u>M</u> FPAQHPPPSGICRDLSDHLSQAGGLPPQDTP <u>I</u> KKPPKHHRGTO <u>T</u> KAEGPT <u>I</u> KNDA
HsSLMAP	151	DKVAANTPS <u>MYSQELFQLSOYI</u> CEA LHREOMLEOKIATLQRLIAITOBASDTSWQALIDEDRILLSRLEV MG <small>NQI</small> QACSKN
HsTRAF3IP3	160	SQQTNYGVAVLDKE <u>I</u> IQLSDYI KEALQRELVLKQKMVILOQDLLSTLIQASDSSWKGQ <u>N</u> EDKLKGKLRS <u>E</u> ENQIYTCTQK
HsSLMAP	231	<u>QTEDSLRKELIAI</u> QEDKHNYETTA <u>AKESLRRV</u> LOEKIEVVRKLS EVERSISNTEDECTHLMEMNERTQEE IRE <u>L</u> ANKYNGA
HsTRAF3IP3	240	YSPWG <small>MKKV</small> ILLE <u>MEDQKNSYEQ</u> AKESLQKVLEEKMNAEQQLQ <u>STORS</u> IALAEQKCEEWS <u>SQYEA</u> KEDWRT <u>L</u> G <u>T</u> QHREL
HsSLMAP	311	VNEIK <u>DLSDKIZKVAEGKQEEIQQQKGQAEKKELCHK</u> DEMEKE <u>C</u> ELQAKIEALQADNDFTNERLTAL <u>Q</u> EHLLSKSGGD <u>O</u>
HsTRAF3IP3	320	ESQLHVLQSKLQGADS <u>R</u> D-----LQMNA <u>Q</u> IRFLEN <u>H</u> QOLQAKIE <u>C</u> LOGDR <u>D</u> LC <u>S</u> LD <u>T</u> Q <u>D</u> Q <u>L</u> Q <u>K</u> RSEAE <u>K</u> L <u>T</u>
HsSLMAP	391	<u>FTHQFIECOKKU</u> IVEGH <u>I</u> TKAVE <u>E</u> TKL <u>S</u> KENQTRAKESDFSDT <u>L</u> SPSKEKSSDDTT <u>DA</u> QMDE <u>Q</u> DLNE <u>PLAKV</u> SL <u>K</u> DD <u>Q</u>
HsTRAF3IP3	389	LVTRVQQLOG-L <u>L</u> QNQSL <u>Q</u> LQEQ <u>E</u> KL <u>L</u> TKKD-----
HsSLMAP	471	<u>GAQSEIEAKQEI</u> QHLRKELIAQ <u>E</u> ARTSKQKC <u>E</u> IQ <u>A</u> LL <u>E</u> ER <u>K</u> A <u>T</u> R <u>N</u> Q <u>V</u> E <u>E</u> ST <u>K</u> Q <u>I</u> Q <u>V</u> L <u>Q</u> QL <u>Q</u> RL <u>H</u> ID <u>T</u> EN <u>L</u> REE <u>K</u> D
HsTRAF3IP3	419	-----Q <u>A</u> LP <u>V</u> W <u>S</u> P <u>K</u> S <u>E</u> P <u>N</u> E <u>V</u> E <u>P</u> -----
HsSLMAP	551	<u>SEITSTRDELLSARDE</u> ILLHQAAAKV <u>A</u> SER <u>D</u> IASL <u>Q</u> EELKKVRAE <u>E</u> LERWR <u>K</u> A <u>ASE</u> YE <u>E</u> KEITS <u>L</u> Q <u>N</u> S <u>F</u> QL <u>R</u> C <u>Q</u> QC <u>E</u> <u>D</u> <u>Q</u>
HsTRAF3IP3	436	----------EGT-----
HsSLMAP	631	<u>Q</u> REE <u>EATR</u> IQGBELERLKRKEWNALETECHSILKRENVL<u>S</u>SEL<u>Q</u>RO<u>E</u>KE<u>H</u>NS<u>Q</u>K<u>Q</u>S<u>L</u>ETSDILSILQMSRKELENQVGSIKE
HsTRAF3IP3	439	GKEKDWDLRDQLQKKTQLQ <u>Q</u> AKE <u>E</u> CRE <u>L</u> H <u>S</u> ELDN <u>L</u> S <u>D</u> EY <u>L</u> S <u>C</u> L <u>R</u> <u>K</u> <u>I</u> QHCR-----
HsSLMAP	711	<u>Q</u> HLRDSADLK <u>TLL</u> SKA <u>N</u> QAKDV <u>Q</u> KEY <u>E</u> KT <u>Q</u> TV <u>L</u> SEL <u>K</u> L <u>F</u> EM <u>T</u> QE <u>K</u> Q <u>S</u> <u>I</u> T <u>E</u> <u>L</u> <u>K</u> <u>O</u> <u>C</u> <u>K</u> <u>N</u> <u>N</u> <u>I</u> <u>K</u> <u>L</u> <u>L</u> <u>R</u> <u>E</u> <u>K</u> <u>G</u> <u>NN</u> <u>K</u> P <u>WEWMPML</u>
HsTRAF3IP3	490	-----EELNQS <u>Q</u> -LPPRRQCG-----RWLPVL-----
HsSLMAP	791	<u>A</u> <u>A</u> <u>I</u> <u>V</u> <u>A</u> <u>T</u> <u>A</u> <u>T</u> <u>V</u> <u>L</u> <u>Y</u> <u>V</u> <u>P</u> <u>G</u> <u>L</u> <u>A</u> <u>R</u> <u>A</u> <u>S</u> <u>P</u>
HsTRAF3IP3	512	MV <u>V</u> <u>I</u> <u>A</u> <u>A</u> <u>A</u> <u>L</u> <u>A</u> <u>V</u> <u>FL</u> <u>A</u> <u>N</u> <u>D</u> <u>N</u> <u>L</u> <u>M</u> <u>I</u> -

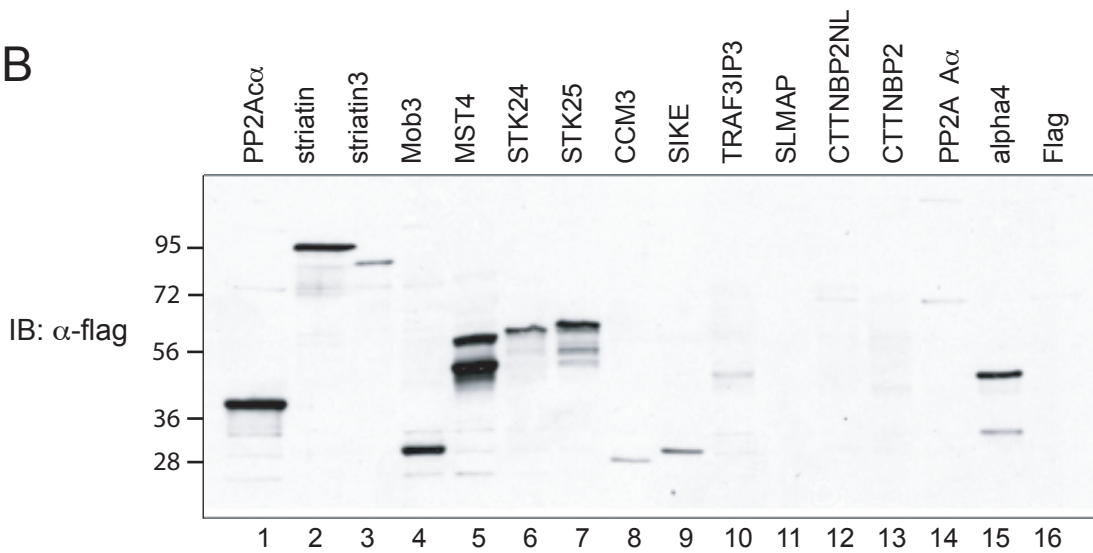
B

A) Sequence alignment between human SLMAP and human TRAF3IP3. Red lettering indicates potential leucine zippers and blue lettering represents potential hydrophobic membrane anchor (Wiggle 1997), in pink is an FHA domain (Conserved domain database, CDD; 4e-12); italicics indicates a chromosome segregation ATPase region (5e-13). On TRAF3IP3, the underlined region corresponds to the CDD COG4372, myosin-like (5e-06). **B) Phylogenetic tree of the SLMAP and TRAF3IP3 families.** Percentage identity between the aligned regions of selected pairs is indicated on the right (Matrix BLOSUM62).

A



B



Confirmation of the association between flag-tagged proteins and endogenous striatin.

(A) Immunoprecipitation (IP) on α -flag M2 agarose beads was performed on lysate from HEK293 cells stably expressing the indicated flag-tagged constructs. To ensure specificity of the interactions, IPs were also performed from lysate of flag alone and flag-alpha4 stable cell lines. The immune complexes were resolved by SDS-PAGE, followed by transfer onto nitrocellulose. Co-precipitation of endogenous striatin was detected by immunoblotting (α -STRN; position indicated by arrow). Upon prolonged exposure, striatin was also detected in the CTTNBP2 sample. (B) Recombinant protein expression detected in whole cell lysate from HEK293 cells stably expressing the indicated flag-tagged proteins. Upon prolonged exposure, TRAF3IP3, CTTNBP2NL, CTTNBP2, PP2AA α are visible. The antibody heavy and light chains are identified by asterisks (*).

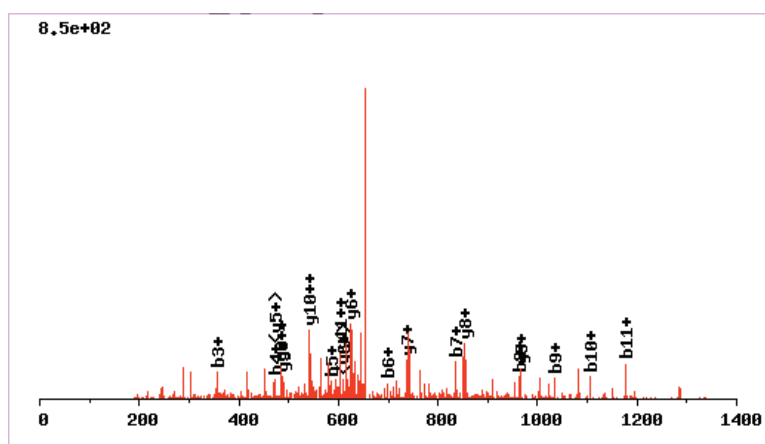
SUPPLEMENTAL FIGURE S7. page1

Goudreault et al.

page 21

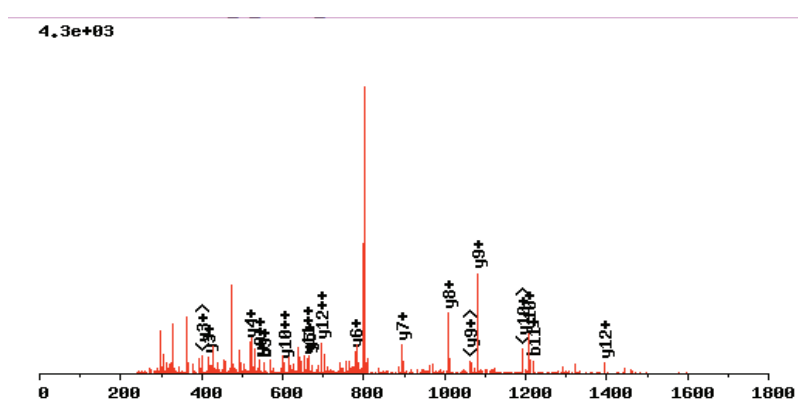
Annotated spectra for proteins identified on the basis of a single peptide.

bait	hit	npeps	nspecs	peptide
F-PP2AA α	SLMAP	1	2	DEILLLHQAAAK



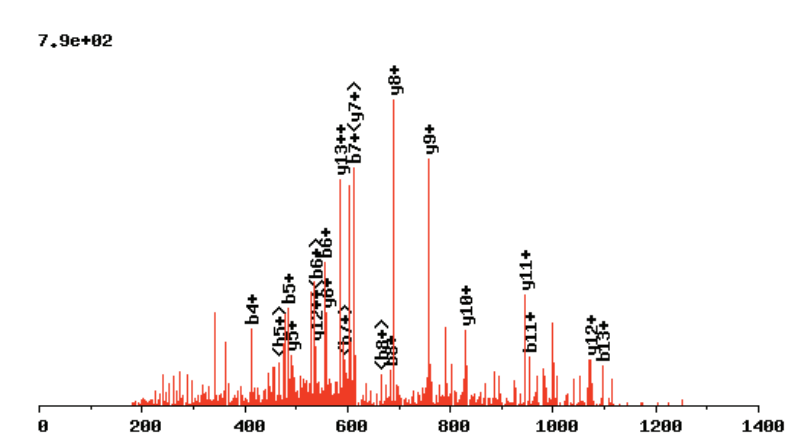
b ⁺	#	AA	#	y ⁺	y ²⁺
116.0348	1	D	12		
245.0774	2	E	11	1206.7210	603.8644
358.1614	3	I	10	1077.6784	539.3431
471.2455	4	L	9	964.5944	482.8011
584.3296	5	L	8	851.5103	426.2591
697.4136	6	L	7	738.4262	369.7170
834.4725	7	H	6	625.3422	313.1750
962.5311	8	Q	5	488.2833	244.6455
1033.5682	9	A	4	360.2247	180.6163
1104.6053	10	A	3	289.1876	145.0977
1175.6424	11	A	2	218.1505	109.5791
	12	K	1	147.1134	74.0606

F-PP2Ac α SLMAP 1 1IEALQADNDFTNER



b ⁺	#	AA	#	y ⁺	y ²⁺
114.0919	1	I	14		
243.1345	2	E	13	1522.6774	761.8426
314.1716	3	A	12	1393.6348	697.3213
427.2557	4	L	11	1322.5977	661.8028
555.3142	5	Q	10	1209.5136	605.2607
626.3513	6	A	9	1081.4550	541.2314
741.3783	7	D	8	1010.4179	505.7129
855.4212	8	N	7	895.3910	448.1994
970.4482	9	D	6	781.3481	391.1779
1117.5166	10	F	5	666.3211	333.6645
1218.5643	11	T	4	519.2527	260.1303
1332.6072	12	N	3	418.2050	209.6064
1461.6498	13	E	2	304.1621	152.5850
	14	R	1	175.1195	88.0637

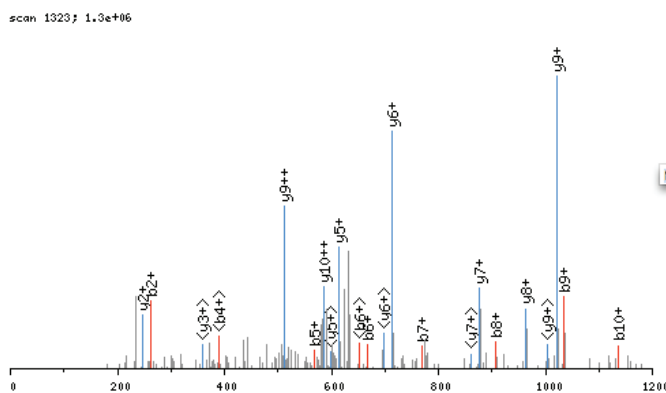
F-PP2Aca CTTNBP2 1 1 APFDAAGAAAFAAK



b ⁺	#	AA	#	y ⁺	y ²⁺
72.0449	1	A	14		
169.0977	2	P	13	1171.5595	586.2837
298.1403	3	E	12	1074.5067	537.7573
413.1672	4	D	11	945.4641	473.2360
484.2044	5	A	10	830.4372	415.7225
555.2415	6	A	9	759.4001	380.2040
612.2629	7	G	8	688.3630	344.6854
683.3000	8	A	7	631.3415	316.1747
754.3372	9	A	6	560.3044	280.6561
825.3743	10	A	5	489.2673	245.1376
954.4169	11	E	4	418.2302	209.6190
1025.4540	12	A	3	289.1876	145.0977
1096.4911	13	A	2	218.1505	109.5791
	14	K	1	147.1134	74.0606

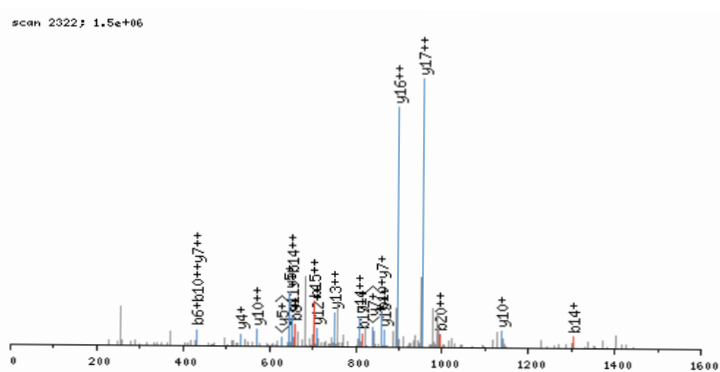
Annotated spectra for proteins identified on the basis of a single peptide.

bait	hit	npeps	nspecs	peptide
T-striatin4	dynein	1	6	NFGSYVTTHETK



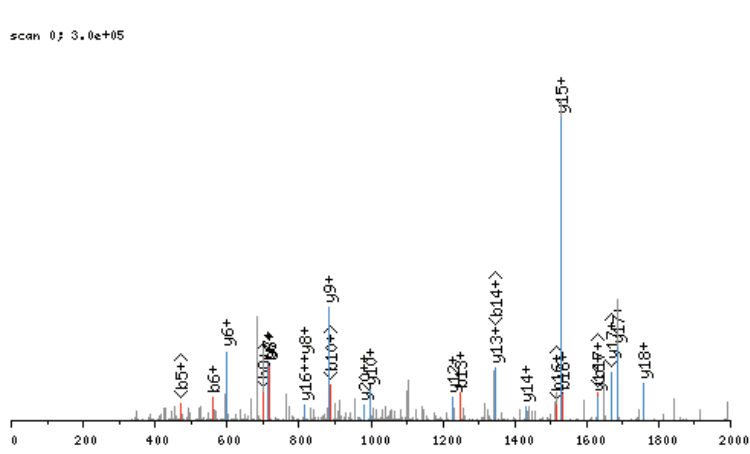
b ⁺	#	AA	#	y ⁺	y ²⁺
115.1118	1	N	11		
262.2883	2	F	10	1169.2792	585.1436
319.3403	3	G	9	1022.1027	511.5553
406.4185	4	S	8	965.0507	483.0293
569.5944	5	Y	7	877.9725	439.4902
668.7270	6	V	6	714.7966	357.9023
769.8321	7	T	5	615.6640	308.3360
906.9731	8	H	4	514.5589	257.7834
1036.0886	9	E	3	377.4179	189.2129
1137.1937	10	T	2	248.3024	124.6552
	11	K	1	147.1973	74.1026

bait	hit	npeps	nspecs	peptide	scans
T-striatin4	PP2A A β	1	2	AAGGDGDDSLYPIAVLIDELR	2



b ⁺	b ²⁺	#	AA	#	y ⁺	y ²⁺	y ³⁺
72.0867	36.5473	1	A	21			
143.1655	72.0867	2	A	20	2090.2945	1045.6512	697.4368
200.2175	100.6127	3	G	19	2019.2157	1010.1118	673.7439
257.2694	129.1387	4	G	18	1962.1638	981.5859	654.7266
372.3580	186.6830	5	D	17	1905.1119	953.0599	635.7093
429.4099	215.2089	6	G	16	1790.0233	895.5156	597.3464
544.4985	272.7532	7	D	15	1732.9714	866.9897	578.3291
659.5871	330.2975	8	D	14	1617.8828	809.4454	539.9662
746.6653	373.8366	9	S	13	1502.7942	751.9011	501.6034
859.8247	430.4163	10	L	12	1415.7160	708.3620	472.5773
1023.0007	512.0043	11	Y	11	1302.5565	651.7822	434.8575
1120.1174	560.5627	12	P	10	1139.3806	570.1943	380.4655
1233.2768	617.1424	13	I	9	1042.2639	521.6359	348.0933
1304.3556	652.6818	14	A	8	929.1045	465.0562	310.3734
1403.4882	702.2481	15	V	7	858.0257	429.5168	286.6805
1516.6476	758.8278	16	L	6	758.8931	379.9505	253.6363
1629.8071	815.4075	17	I	5	645.7337	323.3708	215.9165
1744.8957	872.9518	18	D	4	532.5742	266.7911	178.1967
1874.0111	937.5095	19	E	3	417.4856	209.2468	139.8338
1987.1706	994.0893	20	L	2	288.3701	144.6890	96.7953
		21	R	1	175.2107	88.1093	59.0755

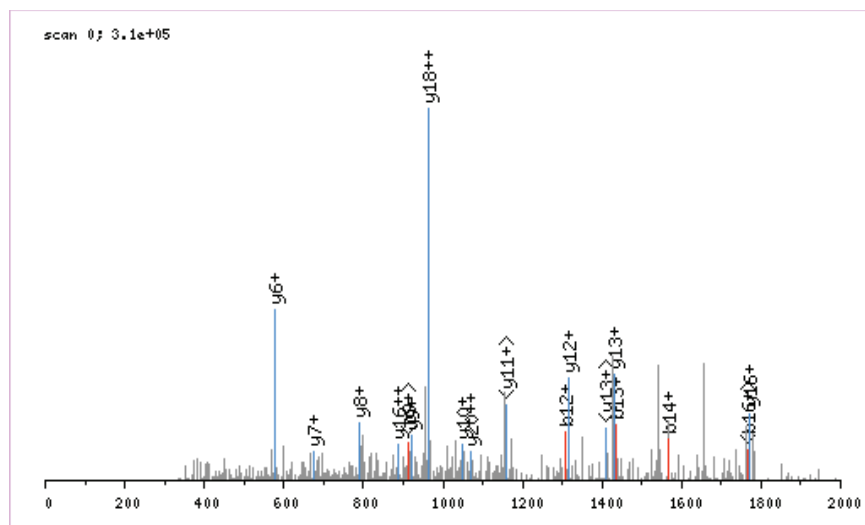
bait	hit	npeps	nspecs	peptide	scans
T-PP2Ac α	liprin A3	1	1	DSSSLAGTPSDETLATDPLGLAK	



b ⁺	#	AA	#	y ⁺	y ²⁺
116.0965	1	D	23		
203.1747	2	S	22	2132.3294	1066.6687
290.2529	3	S	21	2045.2512	1023.1296
377.3311	4	S	20	1958.1730	979.5905
490.4906	5	L	19	1871.0948	936.0514
561.5694	6	A	18	1757.9353	879.4716
618.6213	7	G	17	1686.8565	843.9322
719.7264	8	T	16	1629.8046	815.4063
816.8431	9	P	15	1528.6995	764.8537
903.9213	10	S	14	1431.5829	716.2954
1019.0099	11	D	13	1344.5047	672.7563
1148.1253	12	E	12	1229.4161	615.2120
1249.2304	13	T	11	1100.3006	550.6543
1362.3899	14	L	10	999.1955	500.1017
1433.4687	15	A	9	886.0361	443.5220
1534.5737	16	T	8	814.9573	407.9826
1649.6623	17	D	7	713.8522	357.4301
1746.7790	18	P	6	598.7636	299.8858
1859.9385	19	L	5	501.6469	251.3274
1916.9904	20	G	4	388.4875	194.7477
2030.1498	21	L	3	331.4355	166.2217
2101.2286	22	A	2	218.2761	109.6420
	23	K	1	147.1973	74.1026

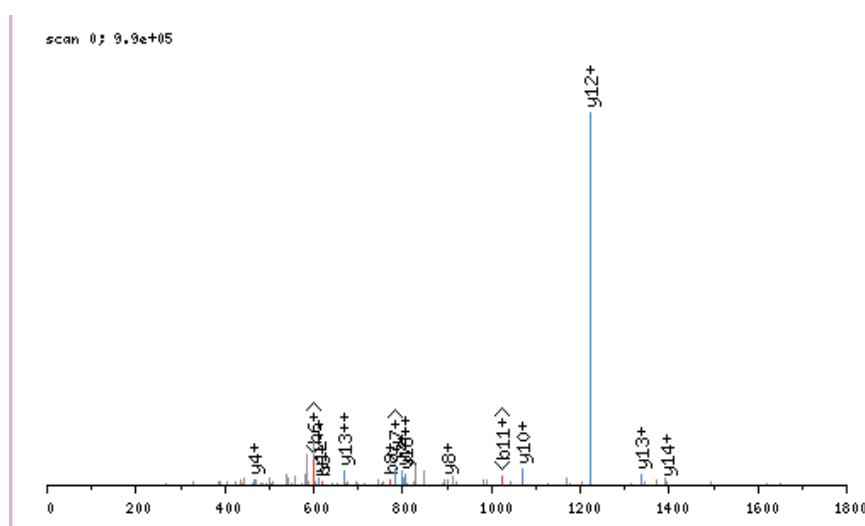
Annotated spectra for proteins identified on the basis of a single peptide.

bait	hit	npeps	nspecs	peptide
T-PP2Ac α	liprin A1	1	1	TLTDGVLDINHEQENTPSTSGK



b ⁺	#	AA	#	y ⁺	y ²⁺
102.1130	1	T	22		
215.2725	2	L	21	2256.3880	1128.6980
316.3775	3	T	20	2143.2285	1072.1182
431.4661	4	D	19	2042.1235	1021.5657
488.5181	5	G	18	1927.0349	964.0214
587.6506	6	V	17	1869.9829	935.4954
700.8101	7	L	16	1770.8504	885.9292
815.8987	8	D	15	1657.6909	829.3494
929.0581	9	I	14	1542.6023	771.8051
1043.1619	10	N	13	1429.4429	715.2254
1180.3030	11	H	12	1315.3391	658.1735
1309.4185	12	E	11	1178.1980	589.6030
1437.5492	13	Q	10	1049.0825	525.0452
1566.6647	14	E	9	920.9518	460.9799
1680.7685	15	N	8	791.8363	396.4221
1781.8736	16	T	7	677.7325	339.3702
1878.9903	17	P	6	576.6274	288.8177
1966.0685	18	S	5	479.5107	240.2593
2067.1736	19	T	4	392.4325	196.7202
2154.2518	20	S	3	291.3274	146.1677
2211.3037	21	G	2	204.2492	102.6286
	22	K	1	147.1973	74.1026

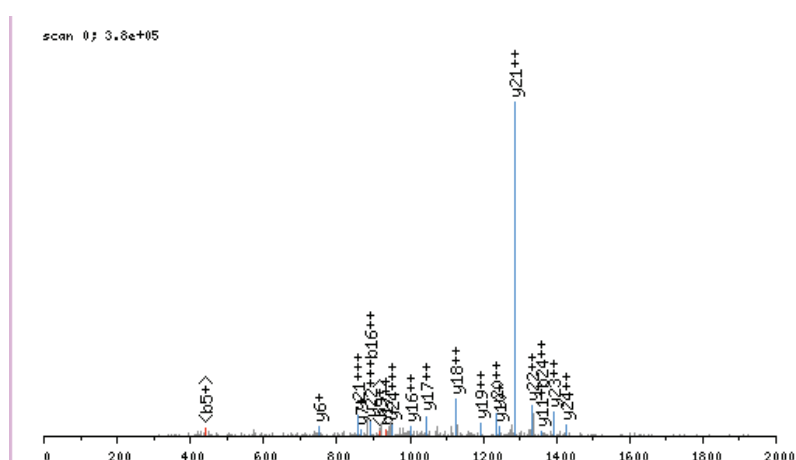
bait	hit	npeps	nspecs	peptide
T-PP2Ac α	CTTNBP2NL	1	1	MTNTGLPGPATPAYSYAK



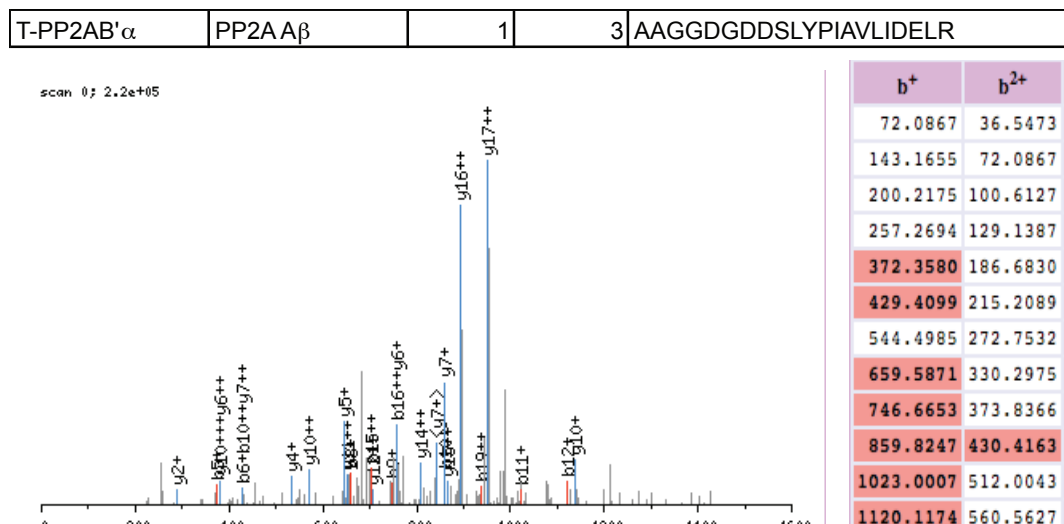
b ⁺	#	AA	#	y ⁺	y ²⁺
132.2005	1	M	18		
233.3056	2	T	17	1709.8962	855.4521
347.4094	3	N	16	1608.7911	804.8995
448.5145	4	T	15	1494.6873	747.8476
505.5664	5	G	14	1393.5822	697.2951
618.7259	6	L	13	1336.5303	668.7691
715.8425	7	P	12	1223.3709	612.1894
772.8945	8	G	11	1126.2542	563.6311
870.0111	9	P	10	1069.2023	535.1051
941.0899	10	A	9	972.0856	486.5468
1042.1950	11	T	8	901.0068	451.0074
1139.3117	12	P	7	799.9017	400.4548
1210.3905	13	A	6	702.7850	351.8965
1373.5665	14	Y	5	631.7062	316.3571
1460.6447	15	S	4	468.5303	234.7691
1623.8206	16	Y	3	381.4521	191.2300
1694.8994	17	A	2	218.2761	109.6420
	18	K	1	147.1973	74.1026

Annotated spectra for proteins identified on the basis of a single peptide.

bait	hit	npeps	nspecs	peptide
T-PP2Ac β	CTTNBP2	1	1	VAANTPSMYSQELFQLSQYLQEALHR



b ⁺	b ²⁺	# AA	#	y ⁺	y ²⁺	y ³⁺
100.1405	50.5742	1	V	26		
171.2193	86.1136	2	A	25	2927.2610	1464.1345
242.2981	121.6530	3	A	24	2856.1822	1428.5951
356.4019	178.7049	4	N	23	2785.1034	1393.0557
457.5070	229.2575	5	T	22	2670.9996	1336.0038
554.6237	277.8158	6	P	21	2569.8945	1285.4512
641.7019	321.3549	7	S	20	2472.7778	1236.8929
772.8945	386.9512	8	M	19	2385.6996	1193.3538
936.0704	468.5392	9	Y	18	2254.5071	1127.7575
1023.1486	512.0783	10	S	17	2091.3311	1046.1695
1151.2793	576.1436	11	Q	16	2004.2529	1002.6304
1280.3948	640.7014	12	E	15	1876.1222	938.5651
1393.5543	697.2811	13	L	14	1747.0067	874.0073
1540.7308	770.8694	14	F	13	1633.8473	817.4276
1668.8615	834.9347	15	Q	12	1486.6707	743.8393
1782.0210	891.5145	16	L	11	1358.5400	679.7740
1869.0992	935.0536	17	S	10	1245.3805	623.1942
1997.2299	999.1189	18	Q	9	1158.3023	579.6551
2160.4059	1080.7069	19	Y	8	1030.1716	515.5898
2273.5653	1137.2866	20	L	7	866.9957	434.0018
2401.6960	1201.3520	21	Q	6	753.8362	377.4221
2530.8115	1265.9097	22	E	5	625.7055	313.3567
2601.8903	1301.4491	23	A	4	496.5900	248.7990
2715.0497	1358.0288	24	L	3	425.5112	213.2596
2852.1908	1426.5994	25	H	2	312.3518	156.6799
		26	R	1	175.2107	88.1093
					59.0755	



b ⁺	b ²⁺	# AA	#	y ⁺	y ²⁺	y ³⁺
72.0867	36.5473	1	A	21		
143.1655	72.0867	2	A	20	2090.2945	1045.6512
200.2175	100.6127	3	G	19	2019.2157	1010.1118
257.2694	129.1387	4	G	18	1962.1638	981.5859
372.3580	186.6830	5	D	17	1905.1119	953.0599
429.4099	215.2089	6	G	16	1790.0233	895.5156
544.4985	272.7532	7	D	15	1732.9714	866.9897
659.5871	330.2975	8	D	14	1617.8828	809.4454
746.6653	373.8366	9	S	13	1502.7942	751.9011
859.8247	430.4163	10	L	12	1415.7160	708.3620
1023.0007	512.0043	11	Y	11	1302.5565	651.7822
1120.1174	560.5627	12	P	10	1139.3806	570.1943
1233.2768	617.1424	13	I	9	1042.2639	521.6359
1304.3556	652.6818	14	A	8	929.1045	465.0562
1403.4882	702.2481	15	V	7	858.0257	429.5168
1516.6476	758.8278	16	L	6	758.8931	379.9505
1629.8071	815.4075	17	I	5	645.7337	323.3708
1744.8957	872.9518	18	D	4	532.5742	266.7911
1874.0111	937.5095	19	E	3	417.4856	209.2468
1987.1706	994.0893	20	L	2	288.3701	144.6890
		21	R	1	175.2107	88.1093
					59.0755	

Report

Cell-Nonautonomous Regulation of *C. elegans* Germ Cell Death by *kri-1*

Shu Ito,^{1,2} Sebastian Greiss,³ Anton Gartner,³
and W. Brent Derry^{1,2,*}

¹Developmental & Stem Cell Biology, The Hospital for Sick Children, Toronto, ON M5G 1X8, Canada

²Department of Molecular Genetics, University of Toronto, Toronto, ON M5S 1A8, Canada

³Wellcome Trust Centre for Gene Regulation and Expression, University of Dundee, Dundee DD1 5EH, UK

Summary

Programmed cell death (or apoptosis) is an evolutionarily conserved, genetically controlled suicide mechanism for cells that, when deregulated, can lead to developmental defects, cancers, and degenerative diseases [1, 2]. In *C. elegans*, DNA damage induces germ cell death by signaling through *cep-1/p53*, ultimately leading to the activation of CED-3/caspase [3–13]. It has been hypothesized that the major regulatory events controlling cell death occur by cell-autonomous mechanisms, that is, within the dying cell. In support of this, genetic studies in *C. elegans* have shown that the core apoptosis pathway genes *ced-4/APAF-1* and *ced-3/caspase* are required in cells fated to die [9]. However, it is not known whether the upstream signals that activate apoptosis function in a cell-autonomous manner. Here we show that *kri-1*, an ortholog of *KRIT1/CCM1*, which is mutated in the human neurovascular disease cerebral cavernous malformation [14, 15], is required to activate DNA damage-dependent cell death independently of *cep-1/p53*. Interestingly, we find that *kri-1* regulates cell death in a cell-nonautonomous manner, revealing a novel regulatory role for nondying cells in eliciting cell death in response to DNA damage.

Results and Discussion

In an RNA interference (RNAi) screen unrelated to apoptosis, we serendipitously uncovered a *cep-1/p53*-interacting gene, *kri-1*, the ortholog of human *KRIT1/CCM1*, which is frequently mutated in the neurovascular disease cerebral cavernous malformation [14, 15]. Because this gene had been previously shown to integrate signals from reproductive tissues (germ cells) to elicit longevity effects in nonreproductive (somatic) tissues [16] and interacts with *cep-1*, an important mediator of germ cell death (Figure 1A) [7, 8], we asked whether *kri-1* is involved in a novel, cell-nonautonomous mechanism to regulate germ cell death. To test this, we first investigated whether *kri-1* regulates cell death like *cep-1*, by quantifying the number of germ cell corpses in wild-type animals fed bacteria producing double-stranded RNA against a control gene or *kri-1* exposed to ionizing radiation (IR) (Figure 1B). We found that knockdown of *kri-1* by RNAi significantly reduced the number of germ cell corpses after DNA damage (IR) compared to animals fed control RNAi ($p = 0.01$),

suggesting that *kri-1* is required for germ cell death. We verified this initial observation by performing a dose-response analysis of the *kri-1(ok1251)* deletion mutant. In contrast to wild-type animals, *kri-1(ok1251)* deletion mutants did not exhibit an increase in germ cell apoptosis after exposure to increasing doses of IR (Figure 1C; see also Figure S1 available online). This was reminiscent of *cep-1* loss-of-function (*lf*) mutants that are also resistant to IR-induced apoptosis. Therefore, we examined whether *kri-1* regulates germ cell death specifically, like *cep-1*, or whether it regulates cell death in all cells, like *ced-3*, by quantifying apoptosis in developing embryos of wild-type animals and *cep-1(lf)* and *kri-1(ok1251)* mutants. We found that developmental cell death was unaffected in *kri-1(ok1251)* mutants, suggesting that the regulation of cell death by *kri-1* is specific to germ cells, like *cep-1* (Figure 1D). Finally, to determine whether the *ok1251* allele is a null, we performed a deficiency analysis by crossing *ok1251* into a strain containing the *hDf9* deficiency that removes the *kri-1* locus and quantified the number of germ cell corpses after DNA damage (Figure 1E). Strains containing the *ok1251* allele in *trans* to *hDf9* were as resistant to damage-induced germ cell apoptosis as *ok1251* homozygotes, suggesting that *ok1251* is a null allele. Collectively, these and further observations (see below) indicate that *kri-1* is specifically required for germ cell death in response to DNA damage.

Given that *kri-1* is required to promote germ cell death in response to DNA damage, we were interested to know at which step in the pathway it might be functioning (Figure 1A). In the *C. elegans* germline, the DNA damage checkpoint genes (*hpr-9*, *mrt-2*, *hus-1*, and *clk-2*) are required to both transiently arrest mitotic proliferation and activate *cep-1*-dependent apoptosis of damaged germ cells [5, 6]. To ascertain whether *kri-1* is functioning in an analogous manner (i.e., upstream of *cep-1*), we tested whether *kri-1* null (*0*) mutants mimic the germline phenotypes of checkpoint gene mutants. In contrast to *clk-2* mutants that are defective in cell-cycle arrest, we found that *kri-1* was not required for IR-induced arrest of mitotically proliferating cells (Figure 2A; Figure S2A), implying that *kri-1* acts downstream or independently of the DNA damage checkpoint. To delineate whether *kri-1* is required to transduce signals to the *CEP-1* protein and therefore allow apoptosis to occur, we examined the activity of *CEP-1* by quantifying the transcript levels *egl-1*, a proapoptotic target gene of *CEP-1* [17, 18]. Consistent with previous work, *egl-1* transcript levels as assessed by real-time quantitative PCR (qPCR) increased in response to DNA damage in wild-type animals, but not in *cep-1(lf)* mutants (Figure 2B). Interestingly, *egl-1* induction in *kri-1(0)* mutants was similar to that seen in wild-type animals, indicating that the transcriptional activity of *CEP-1* is induced normally in the absence of *kri-1*. This is consistent with *kri-1* promoting damage-induced apoptosis downstream or independently of *cep-1*. Such a model raised the possibility that *cep-1* might regulate *kri-1* transcription or KRI-1 protein localization in response to DNA damage and that this was required to promote germ cell death. However, neither *kri-1* transcript levels nor GFP::KRI-1 localization was significantly affected by IR or *cep-1* status (Figures S2B–S2D).

*Correspondence: brent.derry@sickkids.ca

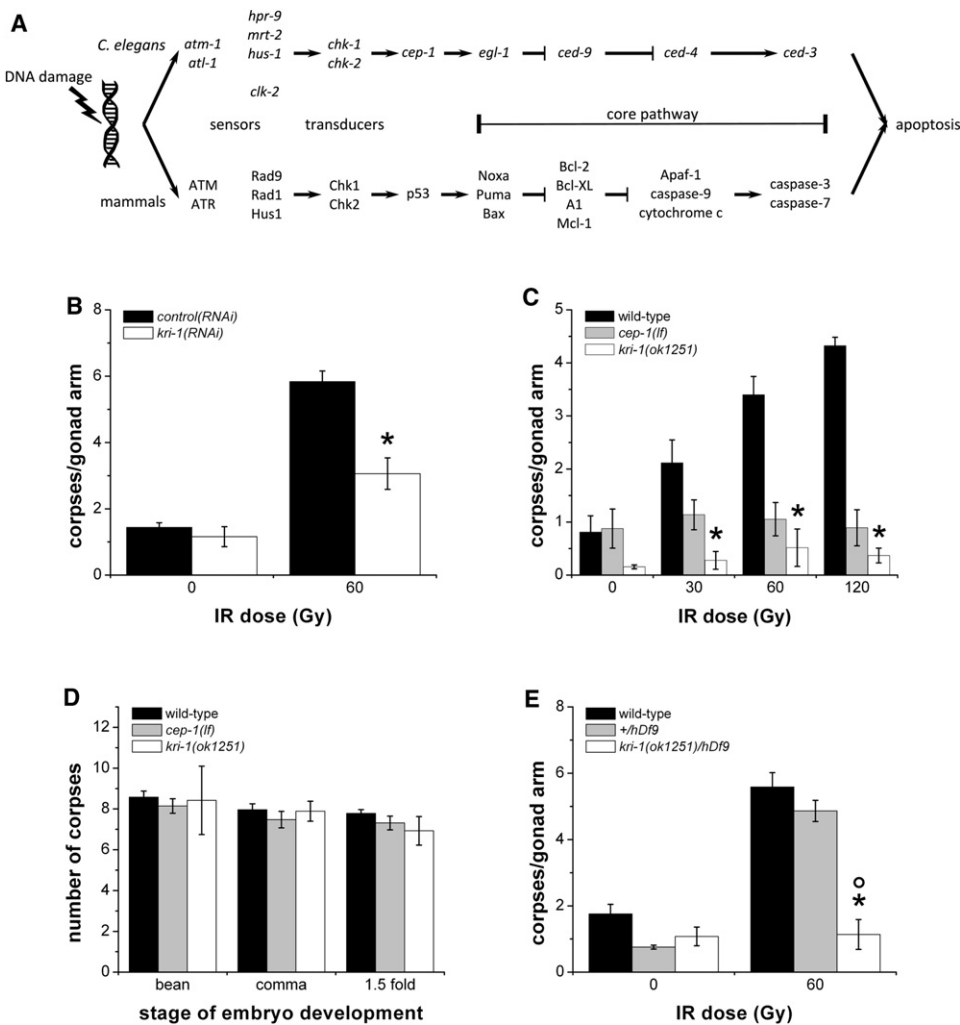
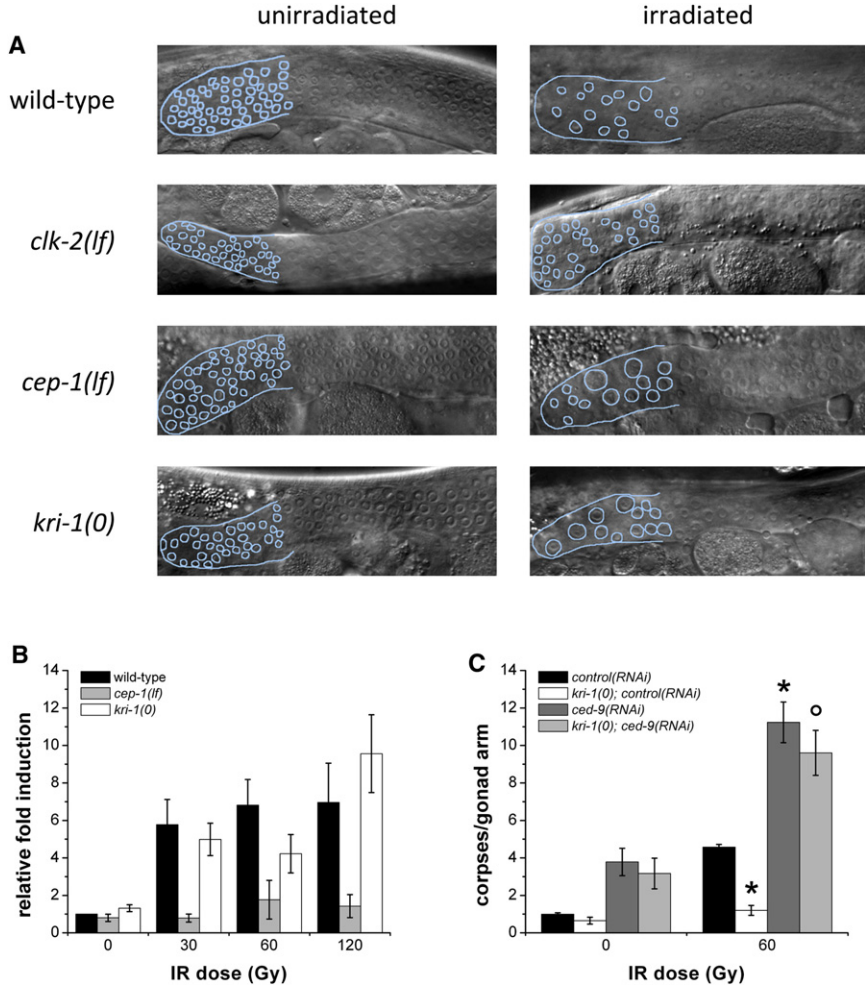


Figure 1. *kri-1* Is Required for DNA Damage-Induced Germ Cell Death Specifically

- (A) The conserved genetic pathway regulating cell death in mammals and *C. elegans*. Sensors and transducers relay DNA damage signals to CEP-1/p53, which transcriptionally activates one or more BH3-only genes to promote apoptosis.
- (B) Wild-type animals fed *control(RNAi)* (black) or *kri-1(RNAi)* (white) were subjected to ionizing radiation (IR) at 20°C, and germ cell apoptosis was quantified 24 hr later. Data represent mean ± standard error of the mean (SEM) of three independent experiments and at least 55 germlines in total per strain per condition. *p < 0.05 versus wild-type. See Table S1 for full list of p values.
- (C) Synchronized wild-type (black), *cep-1*(*lf*) (gray), and *kri-1(ok1251)* (white) young adult animals were treated with increasing doses of IR, and germ cell apoptosis was scored as above. Data represent mean ± SEM of at least three independent experiments and at least 50 germlines in total per strain per condition. *p < 0.05 versus wild-type.
- (D) Embryos at the indicated developmental stages were scored for apoptosis with Nomarski optics in wild-type (black), *cep-1*(*lf*) (gray bars), and *kri-1(ok1251)* (white) animals. Data represent mean ± SEM of three independent experiments and at least 45 embryos in total per strain per stage.
- (E) Apoptosis was scored in wild-type animals (black), a strain with a wild-type copy of *kri-1* in *trans* to the *hDf9* deficiency (gray), and *ok1251* in *trans* to *hDf9* (white) treated with IR as above. Data represent mean ± SEM of at least four independent experiments and at least 25 germlines in total per strain per condition. *p < 0.05 versus wild-type; °p < 0.01 between *kri-1(ok1251)/hDf9* and +/*hDf9*. See also Figure S1.

The data above suggest a model wherein *kri-1* functions downstream of or in parallel to the key decision-making step in the cell death pathway and likely regulates components of the core death pathway (i.e., *egl-1*, *ced-9*, *ced-4*, and *ced-3*). To investigate this further, we examined the epistatic relationship between *kri-1* and *ced-9*. Healthy cells require functional CED-9/BCL2 to prevent ectopic activation of CED-3/caspase by CED-4 (Figure 1A). We reasoned that if *kri-1* functions downstream of *ced-9*, ablation of *kri-1* would suppress the increased cell death caused by *ced-9*(*lf*); on the other hand, the converse would be true if *kri-1* acts upstream of *ced-9*. Knockdown of *ced-9* by RNAi (>50% knockdown; Figure S2E)

caused a significant increase in apoptosis both before and after DNA damage, but this was unaffected by loss of *kri-1* (Figure 2C), which we confirmed in *kri-1(0)*; *ced-9*(*lf*) double mutants (data not shown). This indicates that *kri-1* is not functioning strictly downstream of *ced-9* (i.e., in a manner similar to *ced-4* or *ced-3*). To be sure, we quantified the mRNA of both *ced-4* and *ced-3* by qPCR and found that their levels were not affected in *kri-1(0)* mutants in response to IR (Figures S2F-S2H); in addition, CED-4 protein expression and localization was not affected in *kri-1(0)* mutants (data not shown). Therefore, we infer from these results that *kri-1* acts upstream of, or parallel to, *ced-9*.



Because *kri-1* functions independently of *cep-1* and impinges on the core death pathway, we were interested to know whether *kri-1* is cooperating with other genes known to regulate germ cell death independently or downstream of *cep-1*. In particular, the histone deacetylase *sir-2.1* [19], the MAP kinase *pmk-3* [20], and the retinoblastoma (RB) ortholog *lin-35* [21] have all been shown to regulate germ cell death independently of *cep-1*. In addition to activating cell death independently of *cep-1* in a manner similar to *kri-1*, the SIR-2.1 protein exits the nuclei of germ cells after DNA damage [19]. To determine whether the relocalization of SIR-2.1 is required for *kri-1*-mediated germ cell death, we immunostained *kri-1(0)* animals with SIR-2.1 antibodies to ascertain whether SIR-2.1 protein levels or localization was altered. Although we found that *kri-1* did not affect the SIR-2.1 protein staining pattern (Figure 3A), it still remained possible that *kri-1* and *sir-2.1* function in the same pathway. To address this, we created a double heterozygous mutant containing both the *kri-1(0)* and *sir-2.1(lf)* mutations (*kri-1(0)/+; sir-2.1(lf)/+*), and we observed wild-type levels of germ cell apoptosis in response to DNA damage (data not shown), suggesting that these genes operate in different pathways. In contrast to *sir-2.1* and *kri-1*, which positively regulate germline apoptosis, the MAP kinase gene *pmk-3* inhibits germline apoptosis independently of *cep-1* [20]. Therefore, we tested whether *kri-1* was required for germ cell death caused by loss of function of *pmk-3*. We created *kri-1(0); pmk-3(lf)* double mutants and

Figure 2. *kri-1* Functions Downstream of the Checkpoint Genes but Upstream of *ced-9*

(A) Synchronized hermaphrodites at the fourth larval stage (L4) were treated with IR, and the number of nuclei per unit area in the mitotic region of the germline was quantified 24 hr later at 20°C. The mitotic region and nuclei have been outlined for clarity. Representative images from three independent experiments are shown.

(B) RNA was isolated by TRIzol from synchronized wild-type (black), *cep-1(lf)* (gray), and *kri-1(0)* (white) mutants, and *egl-1* transcript levels were measured by quantitative real-time PCR. Data represent mean ± SEM of three independent experiments.

(C) Synchronized wild-type and *kri-1(0)* L4 animals fed *control(RNAi)* (Y95B8A_84.g, a non-expressed gene) (black and white, respectively) or *ced-9(RNAi)* (dark gray and light gray, respectively) were subjected to IR, and germ cell death was quantified as described above. Data represent mean ± SEM of three independent experiments and at least 25 germlines in total per strain per condition. *p < 0.01 versus wild-type; °p < 0.05 versus *kri-1(0)*; *control(RNAi)*. See also Figure S2.

found that germ cell death was suppressed to the same degree as *kri-1(0)* single mutants (Figure 3B), suggesting that *kri-1* is epistatic to *pmk-3* and does not regulate cell death through *pmk-3*. We do not believe that *pmk-3* regulates *kri-1* because *kri-1* transcript levels and protein localization remained unchanged in *pmk-3(lf)* mutants (Figure S3). Finally, because *lin-35* positively regulates germ cell apoptosis by controlling the levels

of the CED-9 protein (i.e., loss of *lin-35* lead to an increase in CED-9 protein levels) [21], we tested whether *kri-1* functions through *lin-35/RB* by quantifying CED-9 protein levels in *kri-1(0)* animals by western blot. We found that CED-9 protein levels were unaffected in *kri-1(0)* (A. Ross, personal communication; data not shown), suggesting that *kri-1* does not regulate germline apoptosis through this pathway.

Additionally, it has been shown that *kri-1* influences the localization of the forkhead transcription factor DAF-16 in the intestine by responding to signals from the germline and regulating worm life span [16] and that DAF-16 may negatively regulate IR-induced germ cell apoptosis [17]. These two pieces of evidence suggested that *kri-1* might function through *daf-16* to regulate germ cell death. Animals fed *daf-16(RNAi)* exhibited wild-type levels of germ cell death in response to IR (Figure 3C), consistent with published results reporting that DAF-16 has a weak effect on germ cell death [17, 19]. We tested whether *kri-1(0)* could suppress apoptosis in animals fed *daf-16(RNAi)* and found that it did (Figure 3C), which we confirmed by creating *kri-1(0); daf-16(lf)* double mutants (data not shown). This suggests that *kri-1* does not require *daf-16* to mediate its apoptotic function. Alternatively, it was possible that *daf-16* regulates *kri-1* to mediate germ cell death; however, neither *kri-1* transcript nor protein levels were significantly affected in *daf-16(lf)* mutants (Figure S3). These observations reveal that *kri-1* is involved in a novel pathway that regulates germ cell death in response to DNA damage.

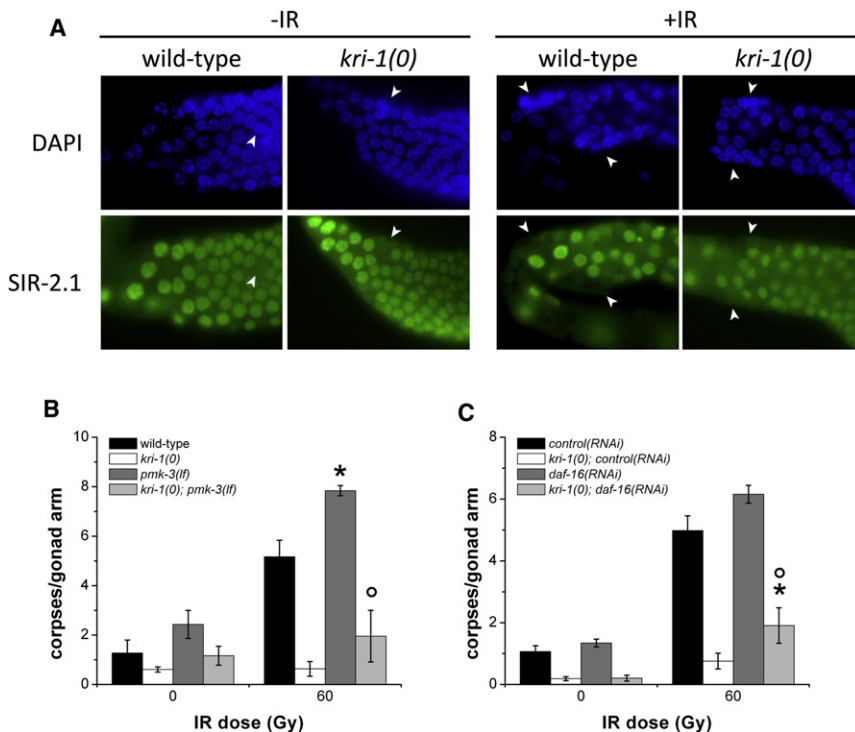


Figure 3. *kri-1* Functions Independently of Known *cep-1*-Independent Pathways

(A) Wild-type and *kri-1(0)* animals were immunostained with DAPI or SIR-2.1 antibodies before and after IR. The images show the pachytene region of the germline. Arrowheads indicate nuclei positive for DAPI staining but negative for SIR-2.1 protein expression. Representative images of at least three independent experiments are shown.

(B) Wild-type (black), *kri-1(0)* (white), *pmk-3(lf)* (dark gray), and *kri-1(0); pmk-3(lf)* (light gray) animals were synchronized and scored for apoptosis as described in Figure 1B. Data represent mean \pm SEM of three independent experiments and at least 50 germlines in total per strain per condition. * $p < 0.05$ versus wild-type; ° $p < 0.05$ versus *pmk-3(lf)*.

(C) Germline apoptosis was quantified in synchronized wild-type and *kri-1(0)* mutants fed *control(RNAi)* (black and white, respectively) or *daf-16(RNAi)* (dark and light gray, respectively) and treated with IR as described above. Data represent mean \pm SEM of four independent experiments and at least 25 germlines in total per strain per condition. * $p < 0.01$ versus wild-type; ° $p < 0.01$ versus *daf-16(RNAi)*. See also Figure S3.

There are two possible mechanisms by which *kri-1* may promote germ cell death. The first is a cell-autonomous mechanism, in which *kri-1* regulates the core death pathway (EGL-1 or CED-9) in germ cells to initiate cell death. Alternatively, it is possible that *kri-1* regulates cell death outside of germ cells (i.e., from somatic cells) via a novel pathway. In support of the latter hypothesis, *kri-1* is required to extend the life span of worms through its effects on DAF-16 in the intestine, possibly by receiving signals from germ cells [16]; in addition, microarray data suggest that *kri-1* is not expressed in the germline [22]. To distinguish between these possibilities, we took advantage of tissue-specific RNAi in *C. elegans* and selectively knocked down *kri-1* in germ cells and the soma in *rrf-1(lf)* [23] and *ppw-1(lf)* [24] mutants, respectively, and quantified IR-induced germ cell apoptosis [21] (Figure 4A). Wild-type, *rrf-1(lf)*, and *ppw-1(lf)* mutants fed bacteria producing *control(RNAi)* had similar numbers of germ cell corpses after DNA damage. Abolition of *kri-1* by RNAi in wild-type animals inhibited DNA damage-induced germ cell apoptosis to the same extent as *kri-1(0)* mutants. However, selective knockdown of *kri-1* in germ cells in *rrf-1(lf)* mutants caused an increase in IR-induced apoptosis, suggesting that *kri-1* expression in germ cells is not required to promote apoptosis. Conversely, specific knockdown of *kri-1* in the soma in *ppw-1(lf)* mutants prevented germ cell death, suggesting that *kri-1* is required in somatic tissue to regulate germ cell death. In support of this contention, we were able to rescue damage-induced germ cell apoptosis to wild-type levels by expressing GFP::KRI-1 from a somatic extrachromosomal array (Figures 4B and 4C). Although it is possible that low-level expression of GFP::KRI-1 in the germline may account for this observation, the fact that extrachromosomal arrays are generally silenced in the *C. elegans* germline [25] strongly supports a model in which *kri-1* is required in nondying somatic cells to promote germ cell death.

Collectively, these data imply a novel mechanism whereby somatic cells communicate with germ cells to promote their death in response to DNA damage (Figure 4D). Indeed, other genes have been shown to participate in germline-soma signaling during proliferation and differentiation of the germline [26, 27], dauer formation, and life-span control [28, 29], confirming that these two tissues can signal to each other in response to certain stimuli. The fact that *kri-1/KRIT1* regulates germ cell death from cells outside of the germline independently of *cep-1/p53* implies that cells not fated to die (somatic cells) in *C. elegans* can regulate the core death pathway in germ cells by novel, cell-nonautonomous mechanisms. In the case of *kri-1*, there are several ways in which it may be performing this function. First, we examined the possibility that *kri-1* may be acting through *daf-9* and *daf-12* to promote apoptosis, in a manner analogous to its proposed role in life-span control [16], by feeding *kri-1(RNAi)* to *daf-9(lf)* and *daf-12(lf)* mutants. We found that both mutants exhibited a resistance to apoptosis when fed *kri-1(RNAi)*, suggesting that *kri-1* does not act through these two genes (Figure S4). Second, although we have shown that *kri-1* does not affect the transcript levels of the BH3-only gene *egl-1*, it is possible that the *kri-1* is required to activate the EGL-1 protein. Similar to mammalian BH3-only proteins, EGL-1 may require other coactivating proteins or modifications in order to induce cell death in germ cells. For example, BID, BAD, and BIM/BMF are proapoptotic BH3-only proteins regulated at the post-translational level through cleavage, phosphorylation, and sequestration by interacting proteins, respectively [30]. Therefore, it is formally possible that KRI-1 may facilitate the activation of EGL-1 by similar transcription-independent mechanisms. Alternatively, KRI-1 may be involved in receiving signals from the germ cells, which results in the subsequent release of death-inducing factors. Although further studies are required to resolve the biochemical mechanism by which KRI-1 dictates germ cell death from the soma, our

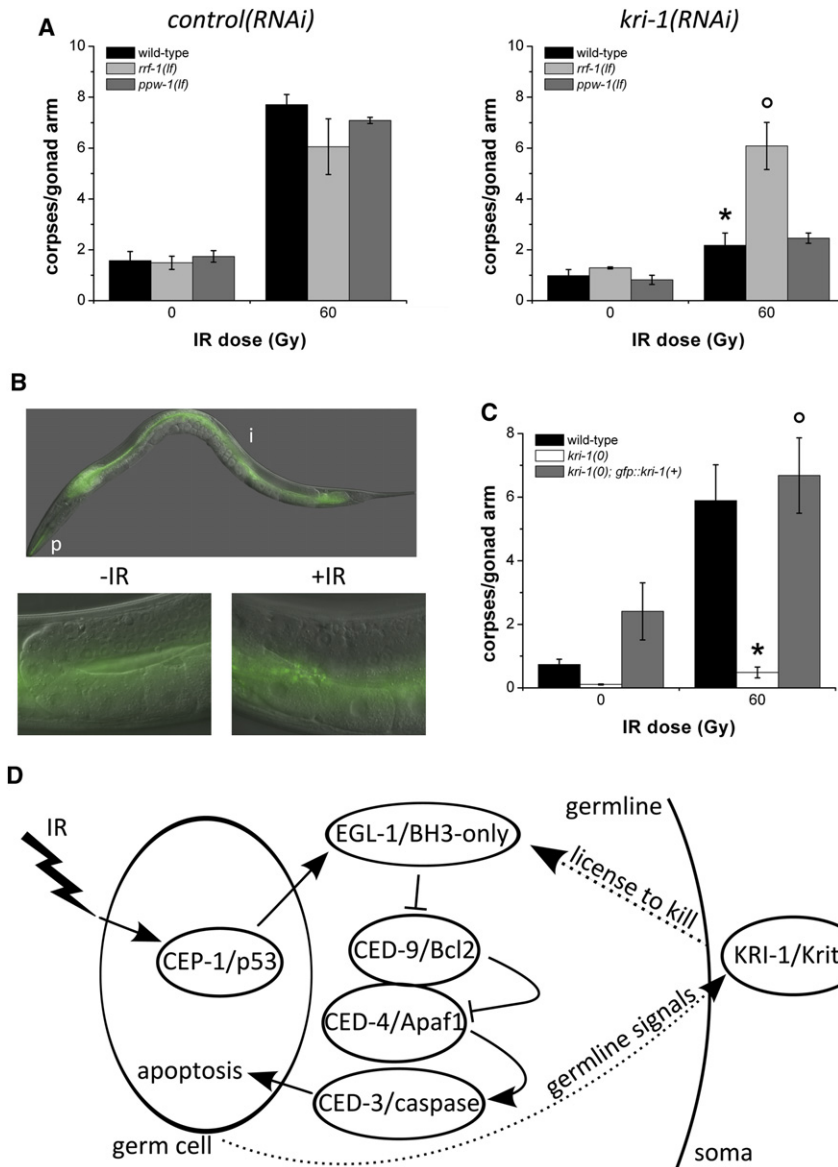


Figure 4. *kri-1* Regulates Germ Cell Death from Somatic Tissues by a Cell-Nonautonomous Mechanism

(A) Germ cell death was quantified after treatment with IR in wild-type (black), *rrf-1(lf)* (light gray), and *ppw-1(lf)* (dark gray) L4 worms fed bacteria producing double-stranded RNA against a control gene (left panel) or *kri-1* (right panel). Data represent mean \pm SEM of three independent experiments and at least 35 germlines in total per strain per condition. * $p < 0.01$ versus control(RNAi); $^{\circ}p < 0.01$ versus *kri-1*(RNAi).

(B) GFP::KRI-1 expressed under the control of the endogenous *kri-1* promoter is detectable in the pharynx (p) and intestine (i) of transgenic animals (top panel). GFP::KRI-1 is excluded from the germline in unirradiated animals (bottom left panel) and does not change localization after irradiation (bottom right panel). Representative images of at least three independent experiments are shown.

(C) Apoptotic germ cells were quantified in wild-type (black), *kri-1*(0) (white), and a *kri-1*(0) strain expressing a wild-type copy of GFP::KRI-1 in the soma (dark gray). Data represent mean \pm SEM of three independent experiments and at least 40 germlines in total per strain per condition. * $p < 0.01$ versus wild-type; $^{\circ}p < 0.01$ versus *kri-1*(0).

(D) Model depicting somatic requirement for *kri-1* in promoting germ cell death in response to DNA damage. We hypothesize that there are “license to kill” factors secreted from the soma into the germline to mediate cell death. Solid lines represent known regulatory interactions; dotted lines represent hypothetical interactions.

observations reveal a novel cross-tissue signaling mechanism whereby somatic tissue can promote germ cell death in response to DNA damage in *C. elegans*, which may have broader applicability to cell death in general.

Supplemental Information

Supplemental Information includes four figures, Supplemental Experimental Procedures, and one table and can be found with this article online at doi:10.1016/j.cub.2009.12.032.

Acknowledgments

We thank the Caenorhabditis Genetics Center, which is supported by the National Institutes of Health National Center for Research Resources, for worm strains. We are grateful to C. Kenyon (University of California, San Francisco) for providing the *muEx353* strain and B. Conradt (Dartmouth University) for CED-9 antibody. This work was supported by a Canadian Institutes of Health Research award to W.B.D.; a Research Training Competition (Rstraccomp) award from the SickKids Foundation to S.I.; and Wellcome Trust, Cancer Research UK, and American Institute for Cancer Research awards to A.G. We thank M. Irwin, M. Zhen, A. Perrin,

A. Ross, I. Watson, and J. Lau for critical input on the manuscript and fruitful discussions.

Received: July 28, 2009

Revised: December 9, 2009

Accepted: December 10, 2009

Published online: February 4, 2010

References

- Ellis, H.M., and Horvitz, H.R. (1986). Genetic control of programmed cell death in the nematode *C. elegans*. *Cell* 44, 817–829.
- Hipfner, D.R., and Cohen, S.M. (2004). Connecting proliferation and apoptosis in development and disease. *Nat. Rev. Mol. Cell Biol.* 5, 805–815.
- Ahmed, S., and Hodgkin, J. (2000). MRT-2 checkpoint protein is required for germline immortality and telomere replication in *C. elegans*. *Nature* 403, 159–164.
- Gartner, A., Milstein, S., Ahmed, S., Hodgkin, J., and Hengartner, M.O. (2000). A conserved checkpoint pathway mediates DNA damage-induced apoptosis and cell cycle arrest in *C. elegans*. *Mol. Cell* 5, 435–443.

5. Hofmann, E.R., Milstein, S., Boulton, S.J., Ye, M., Hofmann, J.J., Stergiou, L., Gartner, A., Vidal, M., and Hengartner, M.O. (2002). *Caenorhabditis elegans* HUS-1 is a DNA damage checkpoint protein required for genome stability and EGL-1-mediated apoptosis. *Curr. Biol.* 12, 1908–1918.
6. Ahmed, S., Alpi, A., Hengartner, M.O., and Gartner, A. (2001). *C. elegans* RAD-5/CLK-2 defines a new DNA damage checkpoint protein. *Curr. Biol.* 11, 1934–1944.
7. Derry, W.B., Putzke, A.P., and Rothman, J.H. (2001). *Caenorhabditis elegans* p53: Role in apoptosis, meiosis, and stress resistance. *Science* 294, 591–595.
8. Schumacher, B., Hofmann, K., Boulton, S., and Gartner, A. (2001). The *C. elegans* homolog of the p53 tumor suppressor is required for DNA damage-induced apoptosis. *Curr. Biol.* 11, 1722–1727.
9. Yuan, J.Y., and Horvitz, H.R. (1990). The *Caenorhabditis elegans* genes ced-3 and ced-4 act cell autonomously to cause programmed cell death. *Dev. Biol.* 138, 33–41.
10. Conradt, B., and Horvitz, H.R. (1998). The *C. elegans* protein EGL-1 is required for programmed cell death and interacts with the Bcl-2-like protein CED-9. *Cell* 93, 519–529.
11. del Peso, L., González, V.M., and Núñez, G. (1998). *Caenorhabditis elegans* EGL-1 disrupts the interaction of CED-9 with CED-4 and promotes CED-3 activation. *J. Biol. Chem.* 273, 33495–33500.
12. Chen, F., Hersh, B.M., Conradt, B., Zhou, Z., Riemer, D., Gruenbaum, Y., and Horvitz, H.R. (2000). Translocation of *C. elegans* CED-4 to nuclear membranes during programmed cell death. *Science* 287, 1485–1489.
13. Schumacher, B., Hanazawa, M., Lee, M.H., Nayak, S., Volkmann, K., Hofmann, E.R., Hengartner, M., Schedl, T., and Gartner, A. (2005). Translational repression of *C. elegans* p53 by GLD-1 regulates DNA damage-induced apoptosis. *Cell* 120, 357–368.
14. Sahoo, T., Johnson, E.W., Thomas, J.W., Kuehl, P.M., Jones, T.L., Dokken, C.G., Touchman, J.W., Gallione, C.J., Lee-Lin, S.Q., Kosofsky, B., et al. (1999). Mutations in the gene encoding KRIT1, a Krev-1/rap1a binding protein, cause cerebral cavernous malformations (CCM1). *Hum. Mol. Genet.* 8, 2325–2333.
15. Laberge-le Couteulx, S., Jung, H.H., Labauge, P., Houtteville, J.P., Lescoat, C., Cecillon, M., Marechal, E., Joutel, A., Bach, J.F., and Tournier-Lasserre, E. (1999). Truncating mutations in CCM1, encoding KRIT1, cause hereditary cavernous angiomas. *Nat. Genet.* 23, 189–193.
16. Berman, J.R., and Kenyon, C. (2006). Germ-cell loss extends *C. elegans* life span through regulation of DAF-16 by kri-1 and lipophilic-hormone signaling. *Cell* 124, 1055–1068.
17. Quevedo, C., Kaplan, D.R., and Derry, W.B. (2007). AKT-1 regulates DNA-damage-induced germline apoptosis in *C. elegans*. *Curr. Biol.* 17, 286–292.
18. Schumacher, B., Schertel, C., Wittenburg, N., Tuck, S., Mitani, S., Gartner, A., Conradt, B., and Shaham, S. (2005). *C. elegans* ced-13 can promote apoptosis and is induced in response to DNA damage. *Cell Death Differ.* 12, 153–161.
19. Greiss, S., Hall, J., Ahmed, S., and Gartner, A. (2008). *C. elegans* SIR-2.1 translocation is linked to a proapoptotic pathway parallel to cep-1/p53 during DNA damage-induced apoptosis. *Genes Dev.* 22, 2831–2842.
20. Lettre, G., Kritikou, E.A., Jaeggi, M., Calixto, A., Fraser, A.G., Kamath, R.S., Ahringer, J., and Hengartner, M.O. (2004). Genome-wide RNAi identifies p53-dependent and -independent regulators of germ cell apoptosis in *C. elegans*. *Cell Death Differ.* 11, 1198–1203.
21. Schertel, C., and Conradt, B. (2007). *C. elegans* orthologs of components of the RB tumor suppressor complex have distinct pro-apoptotic functions. *Development* 134, 3691–3701.
22. Reinke, V., Smith, H.E., Nance, J., Wang, J., Van Doren, C., Begley, R., Jones, S.J., Davis, E.B., Scherer, S., Ward, S., and Kim, S.K. (2000). A global profile of germline gene expression in *C. elegans*. *Mol. Cell* 6, 605–616.
23. Sijen, T., Fleenor, J., Simmer, F., Thijssen, K.L., Parrish, S., Timmons, L., Plasterk, R.H., and Fire, A. (2001). On the role of RNA amplification in dsRNA-triggered gene silencing. *Cell* 107, 465–476.
24. Tijsterman, M., Okihara, K.L., Thijssen, K., and Plasterk, R.H.A. (2002). PPW-1, a PAZ/PIWI protein required for efficient germline RNAi, is defective in a natural isolate of *C. elegans*. *Curr. Biol.* 12, 1535–1540.
25. Kelly, W.G., Xu, S., Montgomery, M.K., and Fire, A. (1997). Distinct requirements for somatic and germline expression of a generally expressed *Caenorhabditis elegans* gene. *Genetics* 146, 227–238.
26. Killian, D.J., and Hubbard, E.J.A. (2004). *C. elegans* pro-1 activity is required for soma/germline interactions that influence proliferation and differentiation in the germ line. *Development* 131, 1267–1278.
27. Kimble, J.E., and White, J.G. (1981). On the control of germ cell development in *Caenorhabditis elegans*. *Dev. Biol.* 81, 208–219.
28. Apfeld, J., and Kenyon, C. (1998). Cell nonautonomy of *C. elegans* daf-2 function in the regulation of diapause and life span. *Cell* 95, 199–210.
29. Wolkow, C.A., Kimura, K.D., Lee, M.S., and Ruvkun, G. (2000). Regulation of *C. elegans* life-span by insulinlike signaling in the nervous system. *Science* 290, 147–150.
30. Puthalakath, H., and Strasser, A. (2002). Keeping killers on a tight leash: Transcriptional and post-translational control of the pro-apoptotic activity of BH3-only proteins. *Cell Death Differ.* 9, 505–512.

CCM3/PDCD10 Heterodimerizes with Germinal Center Kinase III (GCKIII) Proteins Using a Mechanism Analogous to CCM3 Homodimerization*

Received for publication, December 17, 2010, and in revised form, April 26, 2011. Published, JBC Papers in Press, May 11, 2011, DOI 10.1074/jbc.M110.213777

Derek F. Ceccarelli^{‡†}, Rob C. Laister^{§†}, Vikram Khipple Mulligan[¶], Michelle J. Kean^{‡||‡}, Marilyn Goudreault[‡], Ian C. Scott^{||**}, W. Brent Derry^{||**}, Avijit Chakrabarty^{¶††}, Anne-Claude Gingras^{¶††‡}, and Frank Sicheri^{‡||‡}

From the [†]Centre for Systems Biology, Samuel Lunenfeld Research Institute at Mount Sinai Hospital, Toronto, Ontario M5G 1X5, the

[§]Division of Stem Cell and Developmental Biology, Ontario Cancer Institute, Toronto, Ontario M5G 1L7, the [¶]Campbell Family Institute for Cancer Research, Ontario Cancer Institute/University Health Network, Department of Biochemistry, University of

Toronto, Toronto, Ontario M5G 1L7, the ^{||}Department of Molecular Genetics, University of Toronto, Toronto, Ontario M5S 1A8, the

^{**}Program in Developmental and Stem Cell Biology, The Hospital for Sick Children, Toronto, Ontario M5G 1X8, and the

^{††}Department of Medical Biophysics, University of Toronto, Toronto, Ontario M5G 1L7, Canada

CCM3 mutations give rise to cerebral cavernous malformations (CCMs) of the vasculature through a mechanism that remains unclear. Interaction of CCM3 with the germinal center kinase III (GCKIII) subfamily of Sterile 20 protein kinases, MST4, STK24, and STK25, has been implicated in cardiovascular development in the zebrafish, raising the possibility that dysregulated GCKIII function may contribute to the etiology of CCM disease. Here, we show that the amino-terminal region of CCM3 is necessary and sufficient to bind directly to the C-terminal tail region of GCKIII proteins. This same region of CCM3 was shown previously to mediate homodimerization through the formation of an interdigitated α -helical domain. Sequence conservation and binding studies suggest that CCM3 may preferentially heterodimerize with GCKIII proteins through a manner structurally analogous to that employed for CCM3 homodimerization.

Cerebral cavernous malformations (CCMs)⁵ are vascular abnormalities in the brain characterized by focal dilations of cranial vasculature that can progress to hemorrhages and stroke (OMIM ID 116860). Mutations have been identified in

three distinct genes, denoted CCM1–3, that are causative for the formation of most familial CCM lesions (1, 2). CCM3, also named PDCD10, is a 212 amino acid protein conserved among metazoans (3, 4). Knockdown of CCM3 in zebrafish causes an enlarged heart phenotype (5), whereas targeted deletion of CCM3 in the mouse results in defects of early angiogenesis and early embryonic lethality, a phenotype also observed following tissue-specific deletion in the vascular endothelium (6). A non-cell autonomous role for CCM3 in neuroglia on the vasculature has also been uncovered in mouse recently, indicating that CCMs may arise in the central nervous system by the loss of CCM3 signaling in neural as well as endothelial populations (7).

CCM3 has been detected in complex with CCM1 and CCM2 proteins, suggesting that the three proteins may share a common biochemical function (8–10). Yeast two-hybrid, co-immunoprecipitation, and GST pulldown experiments from cell lysates demonstrated that CCM3 also readily interacts with MST4, STK24, and STK25, a grouping of protein kinases termed the germinal center kinase class III (GCKIII) family (10–13). CCM3 and the GCKIII proteins have also been detected as part of a large multiprotein complex termed STRIPAK (striatin-interacting phosphatase and kinase; see Refs. 14, 15). The knockdown of GCKIII proteins in zebrafish gives rise to the same cardiovascular defects as CCM3 knockdown, suggesting the CCM3-GCKIII protein interaction is important for proper CCM3 function (5).⁶

The GCKIII proteins (STK24, STK25, and MST4) are members of the larger Sterile 20 kinase family and are characterized by highly conserved catalytic domains and a 100–120 residue carboxyl-terminal tail, whose function is not currently known. The closely related GCKII proteins MST1 and MST2 possess completely distinct C-terminal tails that mediate homotypic and heterotypic interactions (16), raising the possibility that an analogous function might be served by the tail region of GCKIII proteins, albeit through an unrelated structural mechanism.

Crystal structures of the CCM3 protein revealed an architecture consisting of two distinct structural domains (17, 18). The N-terminal helical domain of CCM3 mediates homodimeriza-

* This work was supported in part by Canadian Institutes of Health Research Grants MOP-36399 (to F. S.) and MOP-84314 (to A.-C. G.).

♦ This article was selected as a Paper of the Week.

¹ Both authors contributed equally to this work.

² Supported by the Canadian Institutes of Health Research through a Banting and Best Canada graduate scholarship.

³ Canada Research chair in Functional Proteomics and the Lea Reichmann chair in Cancer Proteomics. To whom correspondence may be addressed: Samuel Lunenfeld Research Institute at Mount Sinai Hospital, 600 University Ave., Toronto, ON M5G1X5, Canada. Tel.: 416-586-5027; Fax: 416-586-8869; E-mail: gingras@lunenfeld.ca.

⁴ Canada Research chair in Structural Principles of Signal Transduction. To whom correspondence may be addressed: Samuel Lunenfeld Research Institute at Mount Sinai Hospital, 600 University Ave., Toronto, ON M5G1X5, Canada. Tel.: 416-586-8471; Fax: 416-586-8869; E-mail: sicheri@lunenfeld.ca.

⁵ The abbreviations used are: CCM, cerebral cavernous malformation; GCKIII, germinal center kinase group III; STRIPAK, striatin-interacting phosphatase and kinase; TEV, tobacco etch virus; SEC-MALS, size exclusion chromatography-multiangle light scattering; FAT, focal adhesion targeting; PP4C, catalytic subunit of the serine/threonine protein phosphatase 4; mAU, milli absorbance units.

⁶ B. Yoruk, B. S. Gillers, N. C. Chi, and Ian C. Scott, submitted for publication.

tion. The C-terminal four-helix bundle, termed the focal adhesion targeting (FAT) homology domain (17), functions as a linear peptide binding module that mediates direct interactions with CCM2, paxillin, and the striatin component of STRIPAK (17).⁷ Of note, the N-terminal region of CCM3 has also been implicated in the interaction with GCKIII proteins in cells and model organisms (5, 13, 19). Given the critical role for CCM3 and GCKIII proteins in maintaining vascular integrity, we have probed the basis for their interaction in close detail. The results presented here demonstrate that the amino terminus of CCM3 interacts directly with the C-terminal regions of GCKIII proteins. Based on sequence similarity between the interacting regions of CCM3 and GCKIII proteins, we propose that heterodimerization of the two proteins is achieved through an analogous structural mechanism to that reported for the homodimerization for CCM3 and present data indicating that heterodimerization may be favored over homodimerization.

EXPERIMENTAL PROCEDURES

Cloning of Expression Constructs—PDCD10/CCM3, STK25/SOK1, MST4, STK4/MST1, and STRN3 were amplified by PCR and cloned into the modified bacterial expression vectors pGEX-TEV and/or ProEX-TEV. CCM3 point mutations were generated by PCR using standard techniques, and all clones were sequence verified. The N-terminal mutant of CCM3 (LAIL-4D) comprises L44D, A47D, I66D, L67D and the C-terminal mutant (K4A) comprises K132A, K139A, K172A, K179A. CCM3 point mutants were subcloned into the pcDNA5-FRT-GFP vector (20) for expression in mammalian cells. pcDNA3-FLAG-MST4 was reported previously (14).

Protein Expression and Purification—BL21-Codon+ cells (Agilent Technologies) were transformed and grown to A_{600} of 0.8 and induced by addition of 0.25 mM isopropyl 1-thio- β -D-galactopyranoside for 12–18 h at 18 °C. Bacterial cell pellets were harvested and stored at –20 °C. Full-length STK25 and MST4 were also cloned into pFastBAC GST-TEV (Invitrogen), and recombinant baculoviruses were generated for expression in SF9 cells. Infection of SF9 monolayer cells with a multiplicity of infection of >5 were performed for 72 h, followed by harvesting of cell pellets and storage at –80 °C.

Bacterial or SF9 cell pellets of His-tagged proteins were thawed and resuspended in nickel-loading buffer containing 20 mM HEPES, pH 7.5, 400 mM NaCl, 5 mM imidazole, and 5 mM β -mercaptoethanol. Cells were lysed in the presence of 1 mM phenylmethylsulfonyl fluoride by passage through a cell homogenizer (Avestin, Inc.). Supernatant following centrifugation at 20,000 $\times g$ was applied to a nickel-chelating column (GE Healthcare) and eluted over a gradient to 300 mM imidazole. Fractions containing the protein of interest were incubated overnight with an aliquot of tobacco etch virus (TEV) protease and 1 mM DTT. Protein was dialyzed into nickel-loading buffer and flowed over a 1-ml nickel chelating column to remove uncleaved protein, concentrated, and injected onto a 120-ml

S-75 size exclusion column (GE Healthcare) in 20 mM HEPES, pH 7.5, 100 mM NaCl, and β -mercaptoethanol. Fractions containing purified protein were concentrated, flash frozen, and stored at –80 °C. Bacterial pellets of GST-tagged proteins were lysed in 20 mM HEPES, pH 7.5, 400 mM NaCl, and 5 mM β -mercaptoethanol, and the supernatant was applied to glutathione-Sepharose resin (GE Healthcare). The protein of interest was separated from the GST affinity tag following overnight incubation with TEV protease and further purified by size exclusion chromatography as described above. The heterodimeric CCM3 and MST4 complex was obtained by mixing bacterial lysates expressing GST-MST4 and His-CCM3 proteins. Protein eluted from a nickel-chelating column was applied directly to glutathione Sepharose resin and subsequently purified as described above for GST-tagged proteins.

In Vitro Binding Studies—Bacterial or SF9 cell lysates containing GST fusion proteins were prepared as above, however the supernatant was applied to glutathione-Sepharose resin (GE Healthcare) in GST-loading buffer containing 20 mM HEPES, pH 7.5, 400 mM NaCl, and 5 mM β -mercaptoethanol and washed extensively. The protein-bound affinity resin was equilibrated with interaction buffer (20 mM HEPES, pH 7.5, 150 mM NaCl, and 5 mM β -mercaptoethanol). Previously purified binding partner proteins were added to the protein-bound affinity resin and incubated on ice with gentle mixing for 20 min. The affinity resin was then washed three times with 500 μ l of interaction buffer and aliquots of the binding reactions were separated by SDS-PAGE with proteins visualized following Coomassie staining.

Light Scattering—Size exclusion chromatography-multi-angle light scattering (SEC-MALS) was performed with 200 μ M protein samples injected onto a 24-ml S200 Superdex column and measured using a three-angle (45, 90, and 135°) miniDawn light-scattering instrument equipped with a 690-nm laser and an Optilab rEX differential refractometer (Wyatt Technologies, Inc.) as described in Ref. 21. Molecular weights were calculated by using ASTRA software (Wyatt Technologies, Inc.) based on Zimm plot analysis and by using a protein refractive index increment, $dn/dc = 0.185 \text{ liters g}^{-1}$.

Analytical Ultracentrifugation—Sedimentation equilibrium experiments were carried out on samples containing CCM3 alone, MST4 alone, and a CCM3-MST4 complex obtained by dual affinity tag purification. Samples were loaded at concentrations yielding initial A_{280} values of 0.2, 0.4, and 0.8. Ultracentrifugation was performed at 25 °C in 20 mM sodium phosphate buffer, pH 7.0, with 100 mM NaCl and 5 mM β -mercaptoethanol using an Optima XL-I analytical ultracentrifuge (Beckman Instruments, Palo Alto, CA) with a AN50-Ti rotor, quartz windows, and standard six-sector charcoal-filled Epon centerpieces. Absorbance profiles at 280 nm were collected at spin speeds of 3,000, 10,000, 15,000, 20,000, and 25,000 rpm after 24 h of equilibration at each spin speed. Data were analyzed by nonlinear least-squares fitting using Origin software (version 7.0, OriginLab Corp., Northampton, MA). Global fits were obtained to Equation 1, representing a single-species model. Data from CCM3 and MST4 samples were also fit to Equation 2, representing a monomer-homodimer equilibrium model.

⁷ M. J. Kean, D. F. Ceccarelli, M. Goudreault, S. Tate, B. Larsen, M. Sanches, L. C. D. Gibson, W. B. Derry, I. C. Scott, L. Pelletier, G. S. Baillie, F. Sicheri, and A.-C. Gingras, submitted for publication.

CCM3 Interacts Directly with GCKIII Proteins

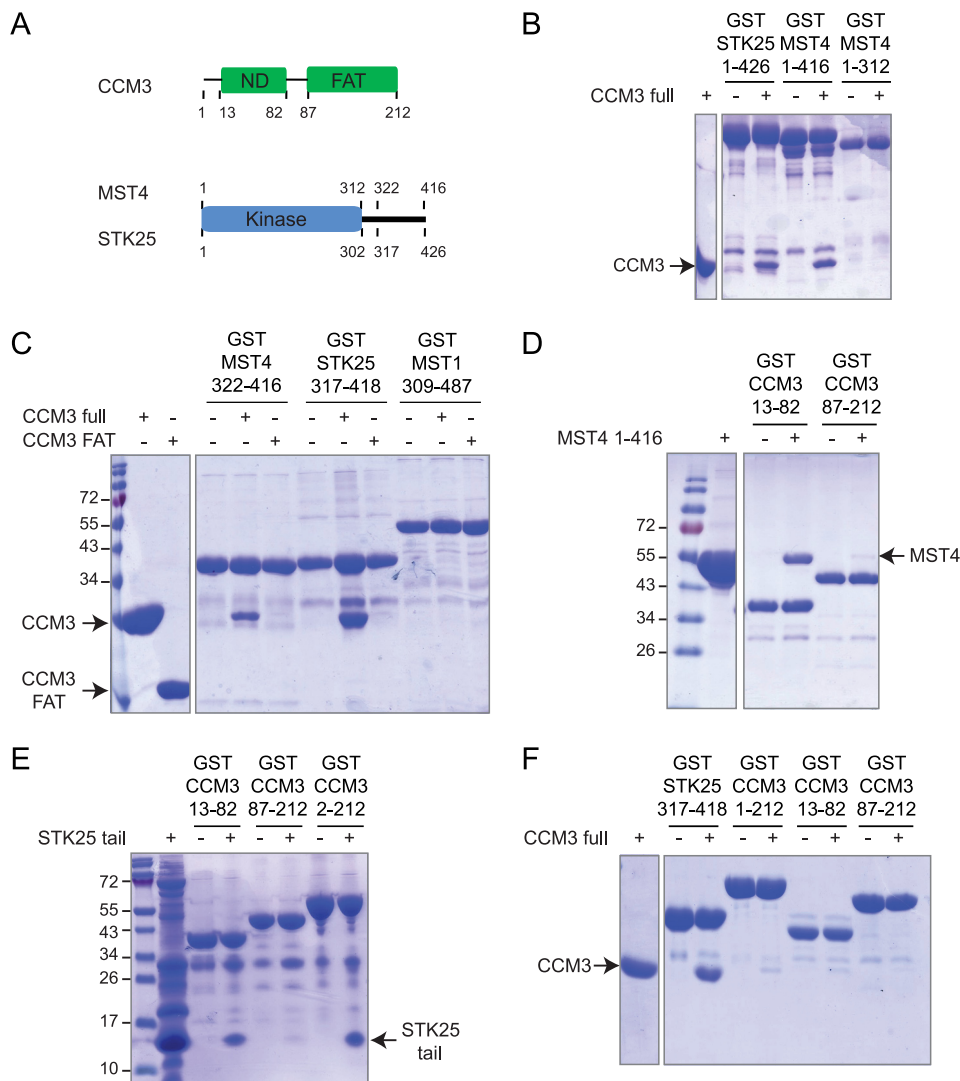


FIGURE 1. **Purified CCM3 and GCKIII proteins interact directly.** *A*, domain organization of CCM3 and GCKIII proteins. ND, N-terminal dimerization region of CCM3. *B*, *in vitro* interaction between GST fusions of STK25 and MST4 with CCM3. The minimal MST4 kinase domain does not bind CCM3. *C*, CCM3 interacts with the C-terminal tail regions of MST4 and STK25 but not MST1. The CCM3 C-terminal FAT domain does not interact with the kinases. *D*, the amino terminus of CCM3 (CCM3-ND) is sufficient for interaction with full length MST4. *E*, CCM3-ND is sufficient for interaction with the C-terminal tail region of STK25. *F*, CCM3 binds tightly to the GST-STK25 tail but not to GST-CCM3.

$$A_{280} = A_{280,F} e^{\frac{\omega^2}{2RT} M(1 - \bar{v}\rho)(r^2 - F^2)} + C \quad (\text{Eq. 1})$$

$$A_{280} = \left(\epsilon_{\text{mon}} C_{\text{mon},F} \frac{\omega^2}{2RT} M_{\text{mon}}(1 - \bar{v}\rho)(r^2 - F^2) + 2\epsilon_{\text{mon}} \frac{C_{\text{mon},F}^2}{K_D} e^{\frac{\omega^2}{RT} M_{\text{mon}}(1 - \bar{v}\rho)(r^2 - F^2)} \right) + C \quad (\text{Eq. 2})$$

In the equations shown above, ω is the spin speed, ϵ_{mon} is the 280-nm molar extinction coefficient of a monomer, $C_{\text{mon},F}$ is the concentration of monomers at the reference radius (F), r is the radius from the spin axis, \bar{v} is the partial specific volume of the protein, ρ is the density of the solvent, R is the gas constant, T is the temperature, l is the optical path length, C is a baseline correction constant, and M_{mon} is the sequence molecular mass of a protein monomer. Values of \bar{v} and ρ were predicted using SEDNTERP software (John Philo, Thousand Oaks, CA). Extinction coefficients of $10,430 \text{ M}^{-1} \text{ cm}^{-1}$ and

$39,670 \text{ M}^{-1} \text{ cm}^{-1}$ were used for CCM3 and MST4, respectively.

Mammalian Cell Culture and Immunoprecipitation—Transient transfection of HEK293T cells and immunoprecipitation followed by immunoblotting was performed essentially as described (14).

RESULTS

CCM3 N Terminus Interacts Directly with C Terminus of GCKIII Proteins—To examine whether binding between CCM3 and GCKIII proteins is direct and to localize the determinants for binding, we tested bacterial- or baculovirus-expressed and purified proteins for interaction *in vitro* (see Fig. 1A for schematic of constructs). In glutathione-Sepharose pull-down experiments visualized by Coomassie staining (Fig. 1B), GST fusions of full-length STK25 and MST4 interacted robustly with full-length CCM3, whereas the minimal kinase domain of MST4 lacking the C-terminal tail region did not.

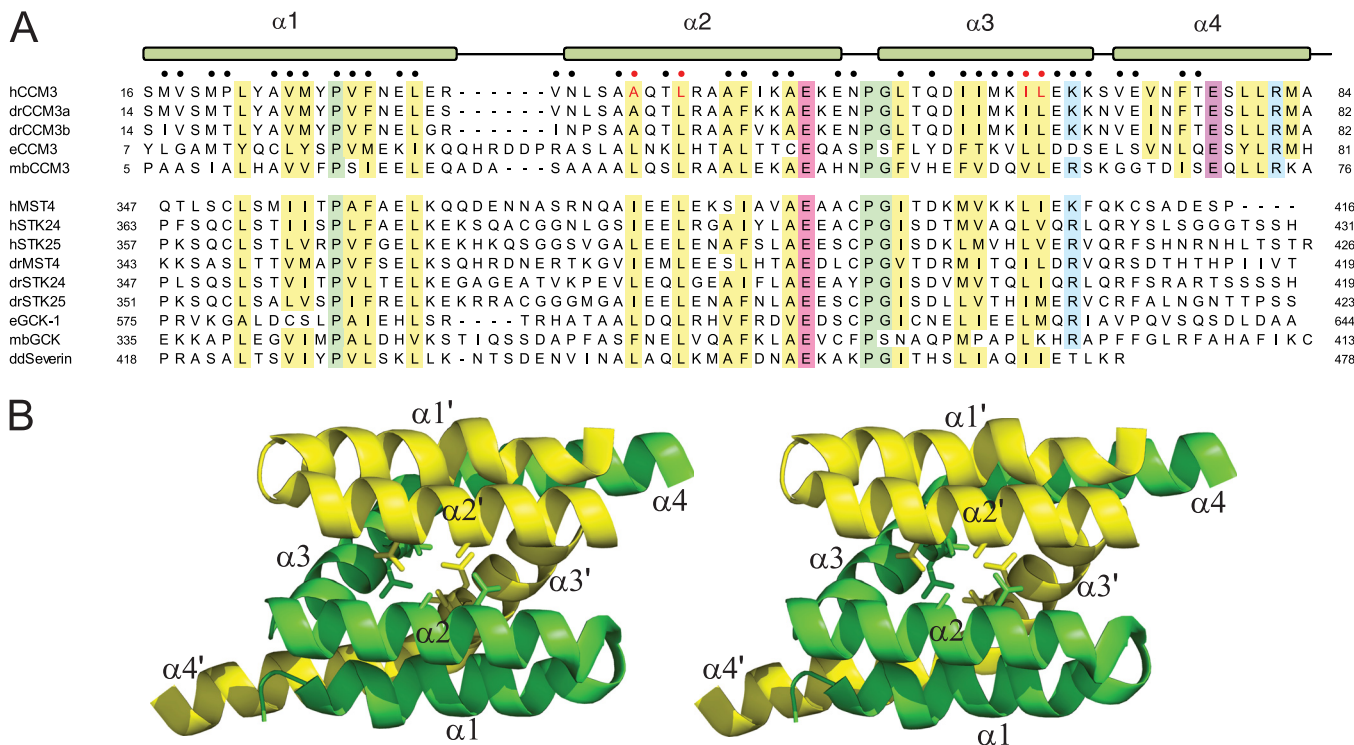


FIGURE 2. Sequence conservation between CCM3 and GCKIII proteins. *A*, sequence alignment of CCM3 N-terminal and GCKIII protein C-terminal tails regions. *h*, human; *dr*, *Danio rerio*; *e*, *C. elegans*; *mb*, *Monosiga brevicollis*; and *dd*, *Dictyostelium discoideum* sequences of CCM3 and GCKIII proteins (STK24, MST4, STK25, and severin) are shown. Conserved hydrophobic, acidic, basic, and proline/glycine residues are highlighted in yellow, red, blue, and green, respectively. Residues comprising the CCM3 homodimer interface are indicated by circles (●) at the top of the alignment. The CCM3 residues (Leu-44, Ala-047, Ile-66, and Leu-67) mutated in this study are highlighted with red circles. *B*, schematic of the N-terminal dimerization region of CCM3 (Protein Data Bank code 3L8I). Protomer chains are colored yellow and green with residues mutated in this study shown in stick representation. Secondary structure elements are labeled.

These results demonstrated that binding is direct and that the C-terminal region of the GCKIII proteins is a key determinant for CCM3 recognition.

The C-terminal tails of MST4 and STK25, when expressed as GST fusion proteins, were sufficient for robust binding to full length CCM3 (Fig. 1C). Interestingly, neither GST kinase tail fusion was able to bind to the isolated FAT domain of CCM3, suggesting that the N-terminal dimerization domain of CCM3 provides the determinant for GCKIII protein binding. We also demonstrated the interaction is specific to GCKIII protein tails because no interaction was detected between full-length CCM3 and the tail region of MST1, a GCKII protein possessing a divergent C-terminal tail (Fig. 1C).

We next tested whether the N terminus of CCM3 is sufficient for binding to GCKIII proteins. As shown in Fig. 1D, the N terminus of CCM3 but not the FAT domain displayed robust binding to full-length MST4. We reconstituted a robust interaction between the N-terminal tail of CCM3 fused to GST and the free C-terminal tail of STK25, demonstrating that the minimal delineated regions in CCM3 and the GCKIII proteins are fully sufficient for the interaction (Fig. 1E). Together, these results define a model in which the binding of GCKIII proteins with CCM3 is mediated entirely by their C- and N-terminal tail regions, respectively. Interestingly, although full-length CCM3 interacted robustly with the GST-STK25 kinase tail, binding of CCM3 full-length to GST-CCM3 full-length and to the GST-CCM3 N terminus was barely detectable (Fig. 1F). This result raised the question of how precisely the respective N- and

C-terminal tail regions of CCM3 and GCKIII proteins mediate complex formation and how this interaction is affected by the ability of the CCM3 N-terminal tail region to form homodimers.

The N-terminal tail region of CCM3 facilitates homodimerization through the formation of a six-helix cluster (17). We reasoned that CCM3 might employ this dimer structure to bind the GCKIII protein tail. Alternatively, CCM3 might bind to GCKIII proteins with a 1:1 stoichiometry that displaces the CCM3 dimer. Supporting the latter model, examination of the primary sequence of the CCM3 N terminus revealed striking similarity to the C-terminal tail region of the GCKIII proteins (Fig. 2A) (19). Of 39 total residues comprising the dimer contact surface of the CCM3 homodimer structure (Fig. 2B), 10 are identical, and an additional nine are similar in nature to residues in MST4 (Fig. 2A). This conservation suggested that CCM3 might form a heterodimeric complex with the C-terminal tail region of GCKIII proteins using the same interaction mode observed in the homodimeric CCM3 crystal structure (Fig. 2B) (17).

CCM3 and MST4 Form Heterodimers in Solution—To differentiate between the two possible models of CCM3-GCKIII protein interaction, we performed SEC-MALS analysis on purified CCM3 and MST4 proteins and their complexes. As demonstrated previously (22), full-length CCM3 eluted as a single 46-kDa species consistent with the expected size of a homodimer (Table 1 and Fig. 3A). Interestingly, full-length MST4 kinase also eluted as dimeric species with a molecular

CCM3 Interacts Directly with GCKIII Proteins

TABLE 1
Summary of SEC-MALS data

Figure panel	Proteins injected	Expected monomeric molecular mass	Expected dimeric molecular mass	MALS averaged molecular mass	Molecular state
3A	CCM3	24.7	49.4	45.8 ± 4.4	CCM3 dimer
3B	MST4	46.7	93.4	94.0 ± 8.2	MST4 dimer
3C	MST4 kinase domain	34.0	68.0	37.9 ± 1.6	MST4 monomer
3D	CCM3+MST4 (co-purified)	24.7, 46.7	49.4, 93.4 (heterodimer, 71.4)	61.7 ± 2.0	CCM3-MST4 heterodimer
4A	CCM3 LAIL-4D	24.7	49.4	25.2 ± 2.9	CCM3 monomer
4B	CCM3 LAIL-4D+MST4	24.7, 46.7	49.4, 93.4	20.4 ± 1.0, 104.6 ± 4.9	CCM3 monomer, MST4 dimer

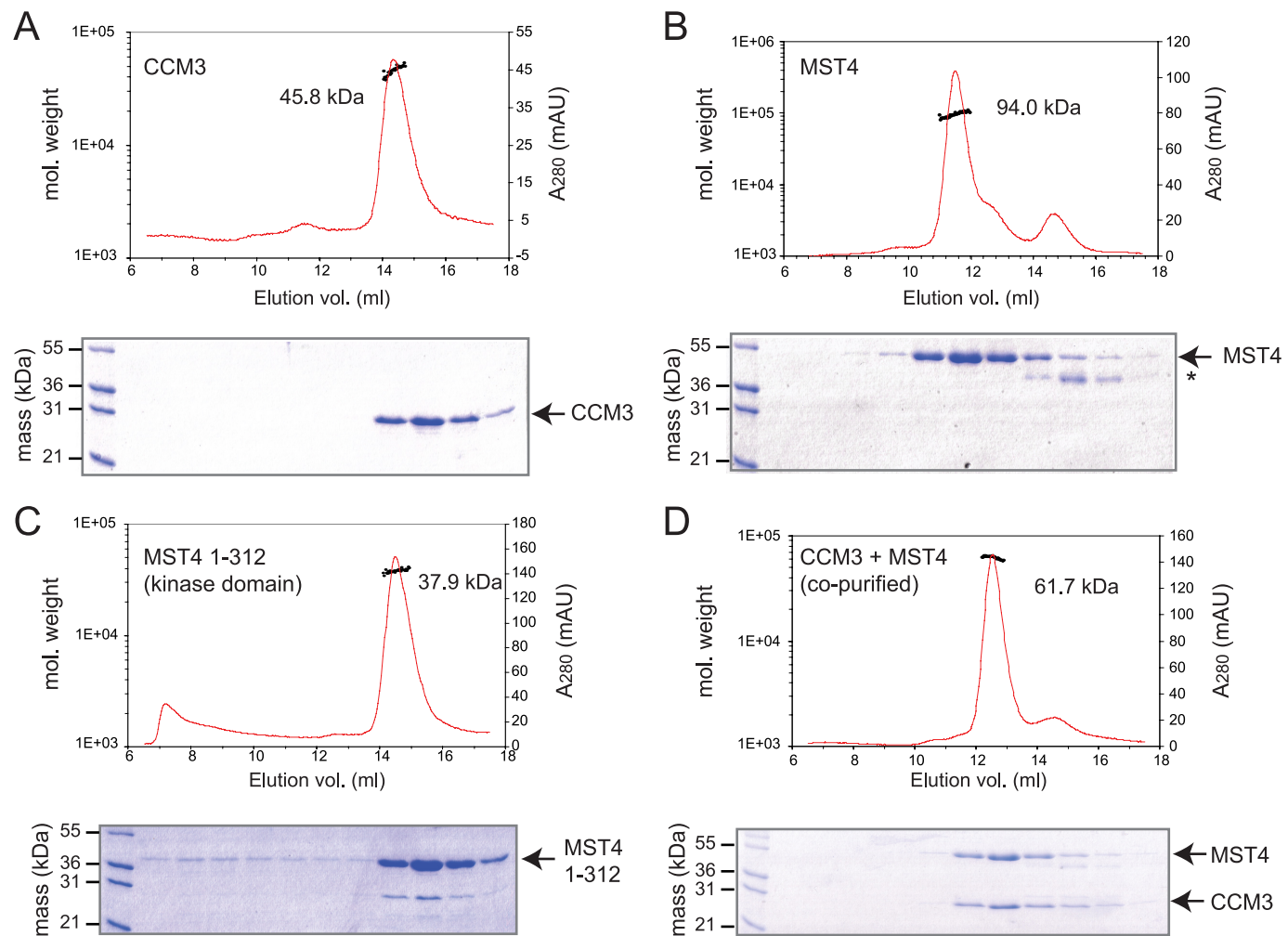


FIGURE 3. Size exclusion chromatography and multiangle light scattering of purified CCM3 and MST4 proteins. The left vertical axis denotes molecular weight of eluting species. The right vertical axis denotes absorbance measurement of eluent. The area of the peak integrated for analysis of molecular mass is indicated by a black line. An SDS-PAGE analysis of the corresponding eluted proteins is shown below each chromatogram. *A*, CCM3 alone. *B*, MST4 full-length alone (the asterisk indicates a likely MST4 degradation product). *C*, MST4 kinase domain (residues 1–312). *D*, co-purified CCM3-MST4 complex.

mass of 94 kDa (Fig. 3B). The ability of MST4 to form dimers was dependent on the C-terminal tail region as the isolated kinase domain eluted as a single monomeric species of 38 kDa (Fig. 3C). Thus, the C-terminal tail regions of GCKIII proteins, which are similar in sequence to the N-terminal tail region of CCM3, can also function as homodimerization domains.

SEC-MALS analysis of a CCM3-MST4 protein complex obtained by co-purification utilizing successive affinity tag purification steps yielded a single species with molecular mass of 62 kDa consistent with a 1:1 heterodimer (Fig. 3D). Under these conditions, no evidence of CCM3 or MST4 homodimers was observed. This result indicated that CCM3 and MST4 form

a stable heterodimer whose stability may exceed that of the CCM3 and MST4 homodimers.

CCM3 N-terminal Mutation Disrupts Heterodimer Formation with MST4—If the six-helix cluster observed in the crystal structure of the CCM3 homodimer also reflects the mode of CCM3-GCKIII protein heterodimerization, then we expected that mutations that disrupt homodimerization of CCM3 might similarly abolish heterodimerization with GCKIII proteins. Mutation of the four hydrophobic residues, Leu-44, Ala-47, Ile-66, and Leu-67 to aspartic acid residues (mutant denoted LAIL-4D) within the CCM3 dimerization interface abolished homodimerization, as reflected by the transition of CCM3 to a

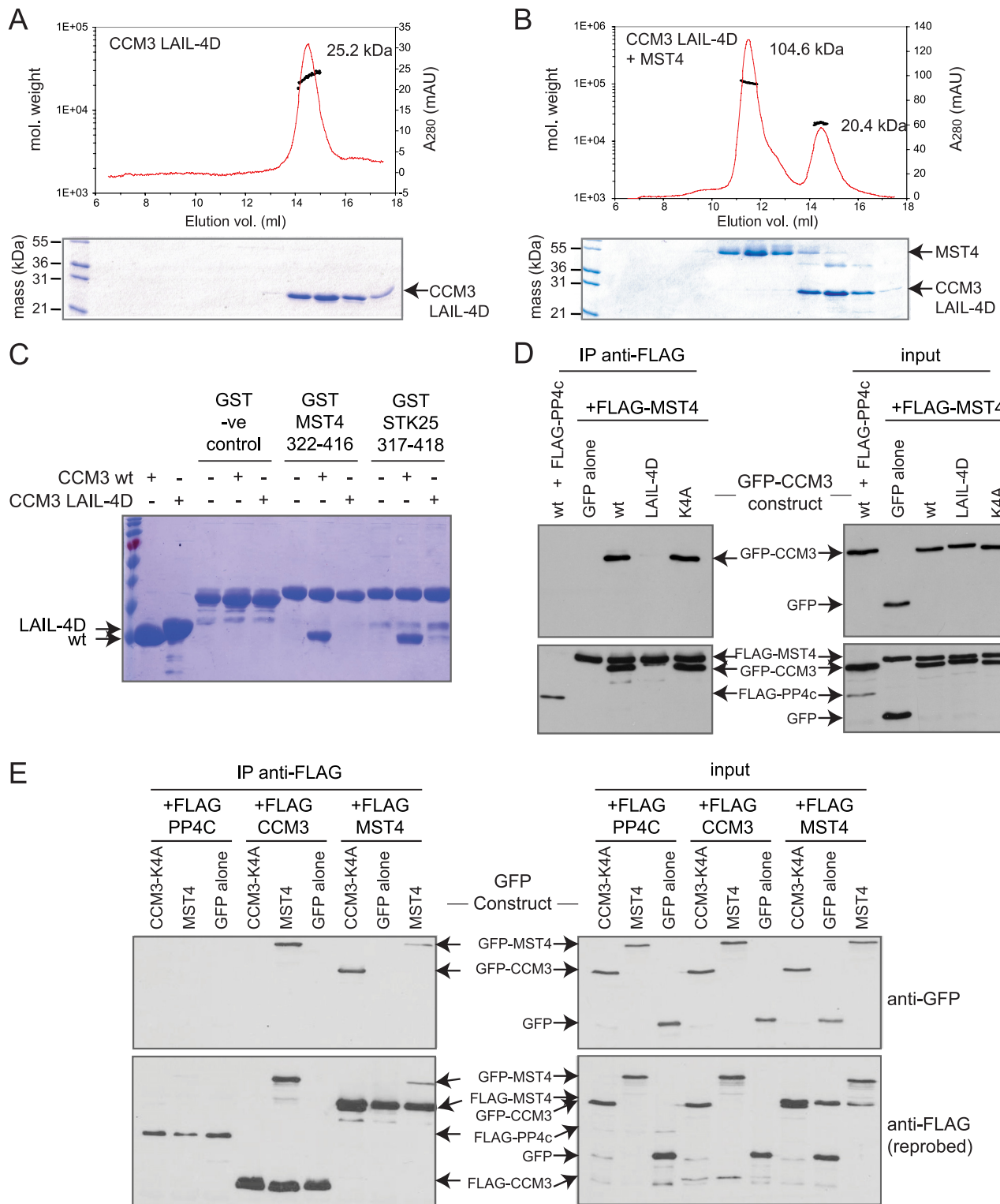


FIGURE 4. Mutations in the amino terminus of CCM3 disrupt the CCM3-GCKIII heterodimer interaction *in vitro* and *in vivo*. *A*, the N-terminal CCM3 mutant (LAIL-4D) elutes as a monomer, as assessed by SEC-MALS. *mAU*, milli absorbance units. *B*, the N-terminal CCM3 mutant (LAIL-4D) does not co-elute with full-length wild type MST4, as assessed by SEC-MALS. *C*, the N-terminal CCM3 mutant (LAIL-4D) does not interact with MST4 or STK25 tail regions in a GST pulldown assay. *D*, FLAG-MST4 interaction with GFP-CCM3 in transiently transfected HEK293T cells is disrupted by mutations in the N-terminal region of CCM3 (LAIL-4D) but not by mutations within the FAT domain (K4A) of CCM3. FLAG-tagged PP4C was used as a negative binding control. Right panels show expression in the cell lysate; left panels show immunoprecipitated proteins. Top panels are blotted with anti-GFP antibody; bottom panels have been reprobed with anti-FLAG. *E*, FLAG-CCM3 and FLAG-MST4 interact strongly with GFP-MST4 and GFP-CCM3, respectively, in HEK293T cells. A weaker interaction of GFP-MST4 with FLAG-MST4 was detected. (Note that this interaction may be mediated via dimerization of other STRIPAK components.) No interaction of FLAG-CCM3 with GFP-CCM3 was detected. To eliminate detection of indirect interactions between GFP-CCM3 and FLAG-CCM3 arising from bridging interactions with a dimeric STRIPAK complex, we employed a four site mutant within the FAT domain of CCM3 (in the context of the GFP-CCM3 construct) that abolishes interaction with STRIPAK. FLAG-tagged PP4C was used as a negative binding control. Right panels show expression in the cell lysate; left panels show immunoprecipitated proteins. Top panels are blotted with anti-GFP antibody; bottom panels have been reprobed with anti-FLAG. *vol.*, volume.

CCM3 Interacts Directly with GCKIII Proteins

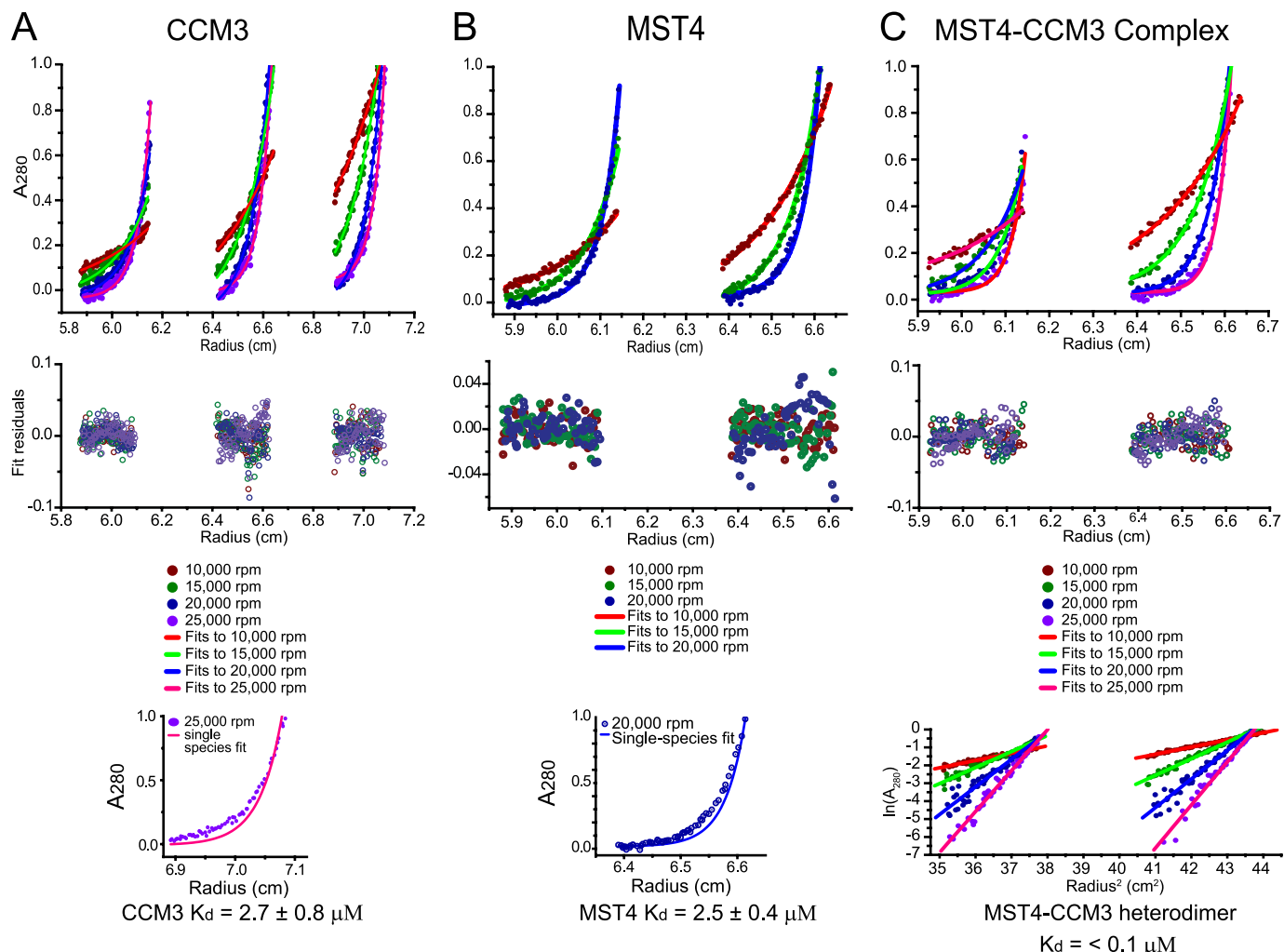


FIGURE 5. Analytical ultracentrifugation analysis of CCM3 and MST4 dimerization potential. *A*, sedimentation equilibrium analysis of CCM3. Sedimentation equilibrium ultracentrifugation was performed at 25 °C and spin speeds of 10,000, 15,000, 20,000, and 25,000 rpm. Global fits to a dimer-monomer equilibrium model performed on 12 data sets (*top panel*), which were acquired at four spin speeds and three spin radii. This model yielded a good fit and a measured K_d value of $2.7 \pm 0.8 \mu\text{M}$. Residuals to the monomer-dimer equilibrium fits are shown in the *middle panel*. Fit to a single-species dimer model (*lower panel*) yielded poor agreement. *B*, sedimentation equilibrium analysis of MST4. Sedimentation equilibrium ultracentrifugation was performed at 25 °C and spin speeds of 10,000, 15,000, and 20,000 rpm. Global fits to a dimer-monomer equilibrium model performed on six data sets (*top panel*), which were acquired at three spin speeds and two spin radii. This model yielded a good fit and a measured K_d value of $2.5 \pm 0.4 \mu\text{M}$. Residuals to the monomer-dimer equilibrium fits are shown in *middle panel*. Fit to a single-species dimer model (*lower panel*) yielded poor agreement. *C*, sedimentation equilibrium analysis of an equimolar CCM3-MST4 complex. Sedimentation equilibrium ultracentrifugation was performed at 25 °C and spin speeds of 10,000, 15,000, 20,000, and 25,000 rpm. Global fits to a single-species model performed on eight data sets (*top panel*) acquired at four spin speeds and two spin radii. With the mass of the heterodimer input as an initial parameter, this model yielded a good fit. Residuals to the monomer-dimer equilibrium fits are shown in *middle panel*. Plot of the natural logarithm of the A_{280} value versus the square of the spin radius (*lower panel*). All spin speeds yield straight lines, consistent with only one species present at detectable levels at equilibrium.

25-kDa monomeric species in SEC-MALS analysis (Fig. 4*A*). The four-site mutant, unlike wild type CCM3, was also compromised for its ability to interact with wild type MST4, as assessed by SEC-MALS (Fig. 4*B*), and to interact with the dimerization mediating tails of either MST4 or STK25 in pull-down experiments (Fig. 4*C*). These results were consistent with the notion that CCM3 and GCKIII proteins form heterodimers through a mechanism analogous to that employed in the CCM3 homodimer structure (17).

To investigate whether the CCM3-GCKIII protein heterodimers exist *in vivo* through the formation of a CCM3-like dimer structure, we tested wild type CCM3 and the four site CCM3 mutant for their ability to interact with GCKIII proteins by immunoprecipitation from HEK293T cells co-transfected

with GFP-tagged CCM3 and FLAG-tagged MST4 kinase. Wild type GFP-tagged CCM3 was readily recovered in immunoprecipitates of FLAG-MST4, but not in immunoprecipitations of FLAG-PP4C, used here as a negative control (Fig. 4*D*). This interaction was abolished by the four-site mutation within the CCM3 dimerization domain (Fig. 4*D*; proteins expressed at similar levels). In contrast, a CCM3 mutation within the C-terminal FAT domain of CCM3 (K4A), which prevents interaction with STRIPAK, CCM2, and paxillin (17),⁷ had no effect on the interaction with MST4 (Fig. 4*D*). This result confirmed the role of the N terminus of CCM3 in mediating GCKIII protein interactions *in vivo* and further supported the notion that heterodimerization is mediated by a mechanism analogous to the CCM3 homodimerization mechanism (17).

We also used the HEK293T cell system to further investigate the homo- and heterodimerization properties of MST4 and CCM3. FLAG-tagged CCM3, MST4, or PP4C (negative control) were co-transfected with GFP-tagged CCM3 (K4A), MST4, or GFP alone. CCM3 (K4A) was employed for this assay to prevent interactions which would be mediated by interaction with the striatin component of STRIPAK, which also homo- and heterodimerizes.⁷ As seen in Fig. 4D, strong heterodimerization of FLAG-MST4 and GFP-CCM3 (K4A) was observed; the reciprocal interaction between GFP-MST4 and FLAG-CCM3 was also readily detected (Fig. 4E). By contrast, the recovery of GFP-MST4 with FLAG-MST4 was much weaker (note that this could potentially be mediated by striatin dimerization), and no detectable homodimerization of CCM3 was observed (Fig. 4E). These results further hinted that the heterodimer state between CCM3 and MST4 might be a preferred dimer conformation. To test whether this was in fact the case, we sought to quantify the binding affinity for homo- versus heterodimerization by analytical ultracentrifugation.

We performed equilibrium analytical ultracentrifugation analysis on CCM3 and MST4 proteins in isolation and on a CCM3-MST4 complex obtained by co-purification using dual affinity tag purification. Under the protein concentrations tested (see "Experimental Procedures"), CCM3 and MST4 profiles were best fit using a monomer-dimer equilibrium model with an extracted K_d of 2.5 and 2.7 μM , respectively (Fig. 5, A and B). In contrast, the CCM3-MST4 complex profiles were best fit as a single species model corresponding to a tight heterodimer (Fig. 5C). Based on the linearity of $\ln(A_{280})$ versus radius² plots (Fig. 5C, bottom panel), which revealed no evidence of alternate monomeric or homodimeric species, we estimated a binding constant for heterodimerization of <0.1 μM , which is thus minimally 25-fold tighter than the CCM3 and MST4 homotypic interactions. From these data, we concluded that the heterodimer state between CCM3 and MST4 is greatly favored over either of the two homodimer states.

DISCUSSION

In this study, we mapped the determinants of a direct interaction between CCM3 and GCKIII proteins to the N-terminal region of CCM3 and the C-terminal tail region of GCKIII proteins. These elements of both protein families are highly related in amino acid sequence, suggesting a common folded structure and binding function (Fig. 2A). Our data lead us to propose that CCM3-MST4 complex formation is achieved through the adoption of a heterodimeric helical structure analogous to that revealed by the CCM3 homodimer crystal structure (17). We also confirmed the existence of CCM3 homodimers in solution and that mutations within the N-terminal region of CCM3 disrupt both homodimerization and heterodimerization with purified GCKIII proteins (Fig. 4). Dimerization of STE20 family kinases mediated by conserved auxiliary domains has now been observed for GCKIII proteins (this study), the GCKII proteins (16), and the p21 activated kinases (23, 24). We reason that conserved regions flanking the kinase domains of other STE20 family kinases might serve analogous interaction functions albeit through the adoption of distinct structures.

The uncovered binding mode between CCM3 and GCKIII proteins helps to explain the following biological observations. Depletion of CCM3 led to the destabilization of STK25/SOK1 in cells (13) demonstrating an interdependence of protein function. A mutant in exon 5 of CCM3 that results in deletion of residues 33–50 within the N-terminal region (3) failed to bind the GCKIII proteins MST4, STK24, and STK25 (5, 19). This observation is consistent with our finding that point mutations within the N-terminal region of CCM3 disrupt binding to GCKIII proteins both *in vitro* and in cells (Fig. 4). Exon 5-deleted CCM3 also failed to rescue the cardiac phenotype of zebrafish, further demonstrating the biological importance of the CCM3-GCKIII protein interaction (5, 19). Because these regions of CCM3 and GCKIII proteins mediate both hetero- and homotypic dimerization, the relative importance of each state in the etiology of CCM disease needs to be explored further.

The interacting tail regions of GCKIII proteins and CCM3 are similar in sequence across the three α -helices that mediate CCM3 homodimerization (Fig. 2) (19). Although highly similar, the observed differences (29 of 39 contact residues are not identical) likely account for the tendency of CCM3 and MST4 kinases to preferentially heterodimerize *versus* homodimerize. Because the dimerization-mediating tails of the two other GCKIII proteins, STK24 and STK25, are more similar to MST4 than to CCM3 (Fig. 2A), we predict that they too will preferentially heterodimerize with CCM3. This, however, remains to be tested experimentally.

The CCM3-interacting region of GCKIII proteins is unrelated in sequence to the C-terminal SARAH domain of GCKII kinase MST1, an element that does not interact with CCM3 (Fig. 1C). Further database searches with the dimerization sequences of CCM3 and GCKIII proteins did not reveal other proteins in the human genome that might interact with CCM3 or GCKIII through a related structural mechanism. Interestingly, the dimerization regions of CCM3 and GCKIII proteins are well conserved throughout evolution, even in more distantly-related species, such as *Caenorhabditis elegans* and *Monosiga brevicollis*, the latter being the most distantly related choanoflagellate of metazoan origin sequenced to date (Fig. 2A) (25). This conserved evolution of CCM3 (formerly called DUF1241) and GCKIII proteins further supports the functional relevance of their observed interaction. A GCKIII-related kinase called severin exists in the slime mold *Dictyostelium discoideum*; however, a CCM3 homologue has not been identified in this organism suggesting that GCKIII proteins may retain functions independent of a CCM3 protein.

Acknowledgments—We thank P. Stathopoulos, Le Zheng, and M. Ikura for useful discussions regarding SEC-MALS analysis.

REFERENCES

1. Labauge, P., Denier, C., Bergametti, F., and Tournier-Lasserve, E. (2007) *Lancet Neurol.* **6**, 237–244
2. Revencu, N., and Viikku, M. (2006) *J. Med. Genet.* **43**, 716–721
3. Bergametti, F., Denier, C., Labauge, P., Arnoult, M., Boetto, S., Clanet, M., Coubes, P., Echenne, B., Ibrahim, R., Irthum, B., Jacquet, G., Lonjon, M., Moreau, J. J., Neau, J. P., Parker, F., Tremoulet, M., and Tournier-Lasserve,

CCM3 Interacts Directly with GCKIII Proteins

- E. (2005) *Am. J. Hum. Genet.* **76**, 42–51
4. Guclu, B., Ozturk, A. K., Pricola, K. L., Bilguvar, K., Shin, D., O’Roak, B. J., and Gunel, M. (2005) *Neurosurgery* **57**, 1008–1013
 5. Zheng, X., Xu, C., Di Lorenzo, A., Kleaveland, B., Zou, Z., Seiler, C., Chen, M., Cheng, L., Xiao, J., He, J., Pack, M. A., Sessa, W. C., and Kahn, M. L. (2010) *J. Clin. Invest.* **120**, 2795–2804
 6. He, Y., Zhang, H., Yu, L., Gunel, M., Boggon, T. J., Chen, H., and Min, W. (2010) *Sci. Signal* **3**, ra26
 7. Louvi, A., Chen, L., Two, A. M., Zhang, H., Min, W., and Gunel, M. (2011) *Proc. Natl. Acad. Sci. U.S.A.* **108**, 3737–3742
 8. Hilder, T. L., Malone, M. H., Benchari, S., Colicelli, J., Haystead, T. A., Johnson, G. L., and Wu, C. C. (2007) *J. Proteome Res.* **6**, 4343–4355
 9. Voss, K., Stahl, S., Schleider, E., Ullrich, S., Nickel, J., Mueller, T. D., and Felbor, U. (2007) *Neurogenetics* **8**, 249–256
 10. Stahl, S., Gaetzner, S., Voss, K., Brackertz, B., Schleider, E., Sürückü, O., Kunze, E., Netzer, C., Korenke, C., Finckh, U., Habek, M., Poljakovic, Z., Elbracht, M., Rudnik-Schöneborn, S., Bertalanffy, H., Sure, U., and Felbor, U. (2008) *Hum. Mut.* **29**, 709–717
 11. Rual, J. F., Venkatesan, K., Hao, T., Hirozane-Kishikawa, T., Dricot, A., Li, N., Berriz, G. F., Gibbons, F. D., Dreze, M., Ayivi-Guedehousou, N., Klitgord, N., Simon, C., Boxem, M., Milstein, S., Rosenberg, J., Goldberg, D. S., Zhang, L. V., Wong, S. L., Franklin, G., Li, S., Albala, J. S., Lim, J., Fraughton, C., Llamasas, E., Cevik, S., Bex, C., Lamesch, P., Sikorski, R. S., Vandenhoute, J., Zoghbi, H. Y., Smolyar, A., Bosak, S., Sequerra, R., Doucette-Stamm, L., Cusick, M. E., Hill, D. E., Roth, F. P., and Vidal, M. (2005) *Nature* **437**, 1173–1178
 12. Ma, X., Zhao, H., Shan, J., Long, F., Chen, Y., Chen, Y., Zhang, Y., Han, X., and Ma, D. (2007) *Mol. Biol. Cell* **18**, 1965–1978
 13. Fidalgo, M., Fraile, M., Pires, A., Force, T., Pombo, C., and Zalvide, J. (2010) *J. Cell Sci.* **123**, 1274–1284
 14. Goudreault, M., D’Ambrosio, L. M., Kean, M. J., Mullin, M. J., Larsen, B. G., Sanchez, A., Chaudhry, S., Chen, G. I., Sicheri, F., Nesvizhskii, A. I., Aebersold, R., Raught, B., and Gingras, A. C. (2009) *Mol. Cell Proteomics* **8**, 157–171
 15. Glatter, T., Wepf, A., Aebersold, R., and Gstaiger, M. (2009) *Mol. Syst. Biol.* **5**, 237
 16. Hwang, E., Ryu, K. S., Pääkkönen, K., Güntert, P., Cheong, H. K., Lim, D. S., Lee, J. O., Jeon, Y. H., and Cheong, C. (2007) *Proc. Natl. Acad. Sci. U.S.A.* **104**, 9236–9241
 17. Li, X., Zhang, R., Zhang, H., He, Y., Ji, W., Min, W., and Boggon, T. J. (2010) *J. Biol. Chem.* **285**, 24099–24107
 18. Ding, J., Wang, X., Li, D. F., Hu, Y., Zhang, Y., and Wang, D. C. (2010) *Biochem. Biophys. Res. Commun.* **399**, 587–592
 19. Voss, K., Stahl, S., Hogan, B. M., Reinders, J., Schleider, E., Schulte-Merker, S., and Felbor, U. (2009) *Hum. Mut.* **30**, 1003–1011
 20. Skarra, D. V., Goudreault, M., Choi, H., Mullin, M., Nesvizhskii, A. I., Gingras, A. C., and Honkanen, R. E. (2011) *Proteomics* **11**, 1508–1516
 21. Stathopoulos, P. B., Zheng, L., Li, G. Y., Plevin, M. J., and Ikura, M. (2008) *Cell* **135**, 110–122
 22. Dibble, C. F., Horst, J. A., Malone, M. H., Park, K., Temple, B., Cheeseman, H., Barbaro, J. R., Johnson, G. L., and Benchari, S. (2010) *PLoS One* **5**, e11740
 23. Lei, M., Lu, W., Meng, W., Parrini, M. C., Eck, M. J., Mayer, B. J., and Harrison, S. C. (2000) *Cell* **102**, 387–397
 24. Parrini, M. C., Lei, M., Harrison, S. C., and Mayer, B. J. (2002) *Molecular cell* **9**, 73–83
 25. King, N., Westbrook, M. J., Young, S. L., Kuo, A., Abedin, M., Chapman, J., Fairclough, S., Hellsten, U., Isogai, Y., Letunic, I., Marr, M., Pincus, D., Putnam, N., Rokas, A., Wright, K. J., Zuzow, R., Dirks, W., Good, M., Goodstein, D., Lemons, D., Li, W., Lyons, J. B., Morris, A., Nichols, S., Richter, D. J., Salamov, A., Sequencing, J. G., Bork, P., Lim, W. A., Manning, G., Miller, W. T., McGinnis, W., Shapiro, H., Tjian, R., Grigoriev, I. V., and Rokhsar, D. (2008) *Nature* **451**, 783–788

Structure-Function Analysis of Core STRIPAK Proteins

A SIGNALING COMPLEX IMPLICATED IN GOLGI POLARIZATION*

Received for publication, December 23, 2010, and in revised form, April 25, 2011. Published, JBC Papers in Press, May 11, 2011, DOI 10.1074/jbc.M110.214486

Michelle J. Kean^{†§1}, Derek F. Ceccarelli[‡], Marilyn Goudreault[‡], Mario Sanches[‡], Stephen Tate[¶], Brett Larsen[‡], Lucien C. D. Gibson^{||}, W. Brent Derry^{§**}, Ian C. Scott^{§**}, Laurence Pelletier^{‡§2}, George S. Baillie^{**}, Frank Sicheri^{‡§2}, and Anne-Claude Gingras^{†§2,3}

From the [‡]Samuel Lunenfeld Research Institute at Mount Sinai Hospital, Toronto, Ontario M5G 1X5, Canada, the [§]Department of Molecular Genetics, University of Toronto, Toronto, Ontario M5S 1A8, Canada, [¶]AB-SCIEX, Concord, Ontario L4K 4V8, Canada, the ^{||}Molecular Pharmacology Group, Institute of Psychology and Neuroscience, University of Glasgow, Glasgow G12 8QQ, Scotland, United Kingdom, and the ^{**}Program in Developmental and Stem Cell Biology, Hospital for Sick Children, Toronto, Ontario M5G 1L7, Canada

Cerebral cavernous malformations (CCMs) are alterations in brain capillary architecture that can result in neurological deficits, seizures, or stroke. We recently demonstrated that CCM3, a protein mutated in familial CCMs, resides predominantly within the STRIPAK complex (striatin interacting phosphatase and kinase). Along with CCM3, STRIPAK contains the Ser/Thr phosphatase PP2A. The PP2A holoenzyme consists of a core catalytic subunit along with variable scaffolding and regulatory subunits. Within STRIPAK, striatin family members act as PP2A regulatory subunits. STRIPAK also contains all three members of a subfamily of Sterile 20 kinases called the GCKIII proteins (MST4, STK24, and STK25). Here, we report that striatins and CCM3 bridge the phosphatase and kinase components of STRIPAK and map the interacting regions on each protein. We show that striatins and CCM3 regulate the Golgi localization of MST4 in an opposite manner. Consistent with a previously described function for MST4 and CCM3 in Golgi positioning, depletion of CCM3 or striatins affects Golgi polarization, also in an opposite manner. We propose that STRIPAK regulates the balance between MST4 localization at the Golgi and in the cytosol to control Golgi positioning.

PP2A⁴ is an essential serine threonine phosphatase involved in many aspects of cell function (1, 2). PP2A acquires substrate and subcellular localization specificity via association with various scaffolding and regulatory subunits to form a number of different holoenzymes, most of which are trimers. In previous

studies using affinity purification coupled to mass spectrometry, a portion of PP2A was also found in a higher order complex that we termed STRIPAK (striatin interacting phosphatase and kinase) (3, 4). In addition to the catalytic subunit PP2A_{cat}, its scaffolding subunit PP2A_A and members of the striatin family of regulatory subunits (5), the core STRIPAK complex contains the striatin interactor Mob3 (6), the uncharacterized protein STRIP1, members of the germinal center kinase III (GCKIII) group (STK24, STK25, and MST4; Ref. 7), and the small molecular weight protein CCM3 (Fig. 1A). Additional proteins can associate with this core STRIPAK complex in a mutually exclusive manner (4).

CCM3 is encoded by one of the three genes mutated in familial cerebral cavernous malformations (CCMs; Ref. 8) and was identified previously as an interactor for the GCKIII proteins (9, 10). CCMs are vascular lesions of the brain characterized by enlarged capillaries that lack structural integrity and that form caverns that tend to bleed, leading to symptoms ranging from headaches and dizziness to severe strokes and death (reviewed in Ref. 11). Recent studies have implicated defective Rho signaling as one of the consequences of depletion (or overexpression) of the CCM1, CCM2, and CCM3 proteins (12–14). Further links between CCM3 and its kinase partners and cytoskeletal dynamics via the Golgi were also uncovered. The Ser/Thr kinases STK25 and MST4 were found to localize to the Golgi apparatus via an association with the Golgi resident protein GM130 (15). Mislocalization of these kinases results in defects in Golgi positioning and cell migration (15). Recently, CCM3 was shown to participate in this effect by stabilizing the GCKIII proteins to promote Golgi orientation and assembly and proper cell orientation (16).

Here, we define the structural organization of the STRIPAK complex, identifying direct interactions and interacting regions within the complex. Specifically, we demonstrate that the striatins and CCM3 act as adapter molecules to bridge the kinase and phosphatase catalytic activities (an accompanying publication by Ceccarelli *et al.* characterizes interactions between the GCKIII proteins and CCM3; 49). We also report the surprising finding that CCM3 and striatins exhibit opposing functions on the targeting of MST4 to the Golgi and Golgi positioning.

* This work was supported in part by Canadian Institutes of Health Research Grants MOP-36399 (to F. S.) and MOP-84314 (to A.-C. G.).

† The on-line version of this article (available at <http://www.jbc.org>) contains supplemental Tables I–V, Figs. 1–7, and additional references.

‡ Supported by Canadian Institutes of Health Research through a Banting and Best Canada graduate scholarship.

² Canada Research chairs.

³ A Lea Reichmann chair. To whom correspondence should be addressed: Samuel Lunenfeld Research Institute at Mount Sinai Hospital, 600 University Ave., Rm. 992, Toronto, ON M5G 1X5, Canada. Tel.: 416-586-5027; Fax: 416-586-8869; E-mail: gingras@lunenfeld.ca.

⁴The abbreviations used are: PP2A, phosphoprotein phosphatase 2A; CCM, cerebral cavernous malformation; FAT, focal adhesion targeting; eGFP, enhanced GFP; STRIPAK, striatin-interacting phosphatase and kinase; AP-MS, affinity purification coupled to mass spectrometry; GCKIII, germinal center kinase III; esiRNA, endoribonuclease-prepared siRNA; N-mut, L44D,A47D,I66D,L67D; C-mut(4A), K132A,K139A,K172A,K179A.

EXPERIMENTAL PROCEDURES

Plasmids—pcDNA5-FRT-FLAG was engineered to inducibly express fusion proteins with a single N-terminal FLAG epitope and was constructed from the parent vector pcDNA5-FRT-TO (Invitrogen) and the vector pcDNA3-FLAG (17) as follows. A HindIII/XhoI cassette from pcDNA3-FLAG (containing the FLAG and the multiple cloning site) was subcloned into the pcDNA5-FRT-TO vector also digested with HindIII/XhoI. An internal EcoRI site was subsequently destroyed by mutagenesis. pcDNA5-FRT-eGFP was constructed by subcloning the HindIII/AscI cassette from pcDNA3-eGFP into pcDNA5-FRT-TO. The complete sequences of the cloning vectors are available at the Gingras Laboratory website (Samuel Lunenfeld Research Institute). FLAG-tagged mammalian expression constructs for full-length STRIPAK proteins are described in Ref. 4. Truncations of STRN3 (amino acids 1–169, 1–338, and 220–338) and mouse Strn (amino acids 46–781 and 91–781) were cloned into pcDNA3-FLAG for mammalian expression (*supplemental Fig. 1*). All point mutations were generated by overlap extension PCR; CCM3 point mutants were subcloned into the pcDNA5-FRT-GFP vector. N-mut is L44D,A47D,I66D,L67D; C-mut (4A) is K132A,K139A, K172A,K179A, and the N-mut/C-mut construct contains both sets of mutations. Inserts were fully sequenced. The full-length and several truncations in human STRN3 (amino acids 1–57, 1–169, 220–713, 58–713, 58–169, and 220–338; *supplemental Fig. 1*) as well as full-length mouse Strn, mouse Mst4 D162A, and MOB3 were cloned into the GST-tagged expression vector pGEX-2T-TEV HTa for bacterial expression and purification. pGEX-2T-TEV HTa (which expresses a tobacco etch virus-cleavable GST protein was described previously (18). Wild-type CCM3, CCM3 C-mut (4A) (generated by overlap extension PCR), and PP2A_A were inserted into the His-tagged expression vector pProEx-HTa for bacterial expression and purification. The coding sequence of GOLGA2 (encoding protein GM130) was amplified by PCR from the cDNA clone from the mammalian gene collection BC069268. The full-length and minimal kinase interaction region at amino acids 72–271 (15) were cloned into pcDNA5-FRT-FLAG.

Antibodies—Commercial antibodies were as follows (catalogue numbers are in parentheses): anti-PP2A_{cat} (610555), anti-striatin (610838), anti-GM130 (610822), and anti-MST4 (612684) were from BD Transduction Laboratories; anti-PP2A_A was from Upstate Biotechnology (07-250); anti-STRN3 was from Cell Signaling Technology (S68); anti-giantin was as described (19); anti-FLAG was from Sigma (F3165); and anti-HA was from Covance Research Products (MMS-101R). Anti-CCM3 antibody was raised in rabbit (Covance) using GST-CCM3 (amino acids 2–212) as an antigen. This antibody was tested for specificity in immunoblots against the GST-CCM3 antigen, FLAG-CCM3 transiently transfected in HEK293T cells and endogenous CCM3 (after silencing by RNAi) (data not shown). Secondary antibodies for immunoblotting were sheep anti-mouse IgG and donkey anti-rabbit IgG, both conjugated to horseradish peroxidase from GE Healthcare (NA931 and NA934). Alexa Fluor-labeled secondary antibodies for immunofluorescence were from Invitrogen

Molecular Probes: goat anti-mouse 594 (A11005), goat anti-rabbit 594 (A11012), goat anti-mouse 488 (A11001), and goat anti-rabbit 488 (A11034).

Recombinant Protein Purification, Gel Filtration, and *In Vitro* Binding Assays—His- or GST-tagged fusion proteins were purified as described (20), using lysis buffer with 20 mM Hepes, pH 7.5, 500 mM NaCl, and 5 mM β-mercaptoethanol at 4 °C. Gel filtration was performed to purify proteins and complexes based on size, in buffer containing 100 or 150 mM NaCl. For the PP2A_A:STRN3(58–169) complex, a 1:2 ratio of proteins (purified by gel filtration) was mixed before loading onto a Superdex 200 column. For the PP2A_A:STRN3(1–338):CCM3 complex, a 1:2:2 ratio of proteins was mixed before loading onto a Superdex 200 column. Fractions encompassing the elution of these protein complexes (as detected by UV) were run on a SDS-PAGE gel and Coomassie stained. *In vitro* binding assays (GST pulldowns) were performed essentially as described (18), with the following modifications: GST-tagged proteins were purified as described above, without cleavage of proteins from GST resin. Untagged or His-tagged proteins were incubated with GST-tagged proteins on resin in 150 μl of binding buffer (20 mM Hepes, pH 7.5, 100 mM NaCl, and 5 mM β-mercaptoethanol). Glutathione resin was washed rapidly three times in 500 μl of binding buffer, and elution was performed by boiling in Laemmli sample buffer.

Peptide Overlay Assay—Peptide libraries were produced by automatic SPOT synthesis and probed as described previously (21). They were synthesized on continuous cellulose membrane supports on Whatman 50 cellulose membranes using Fmoc (*N*-(9-fluorenyl)methoxycarbonyl) chemistry with the Auto-Spot-Robot ASS 222 (Intavis Bioanalytical Instruments AG, Köln, Germany). The interaction of spotted peptides with purified, recombinant GST and GST-CCM3 fusion proteins was determined by overlaying the cellulose membranes with 10 μg/ml recombinant protein. Bound recombinant proteins were then detected following wash steps with rabbit anti-GST, and detection was performed with a secondary anti-rabbit horseradish peroxidase-coupled antibody.

Fluorescence Polarization Peptide Binding Assay—A 25-mer peptide (²⁸⁶EGLAADLTDDPDTEEALKEFDLVT³¹⁰) from human STRN3 was synthesized by Biomatik Corporation (Wilmington, DE) and used for fluorescence polarization binding studies with purified CCM3 proteins as described (22). Equilibrium binding constant determination was carried out on a Beacon fluorescence polarization system (Pan Vera, WI) and data were analyzed using the GraphPad Prism software (GraphPad Software, Inc.)

Mammalian Cell Culture, Immunoprecipitation, and Mass Spectrometry—Transient transfection and immunoprecipitation followed by immunoblotting and/or mass spectrometry were performed essentially as described (4), using either pools of stable cells (FLAG-Strn, FLAG-STRN3, FLAG-Mst4, and their deletion constructs) or a stable inducible clone (FLAG-GM130). Samples were analyzed on a ThermoFinnigan LTQ or an AB-SCIEX 5600 TripleTOF instrument, as described below.

esiRNA and siRNA-mediated Knockdown—All siRNAs were purchased from Dharmacon: CCM3 (L-004436-00), STRN (D-019572-02, -04, -19, -20), STRN3 (D-019145-01, -03, 04,

-17) and STRN4 (D-020389-01, -02, -03, -04), as well as the siGENOME non-targeting RNA (D-001210-0X). For endoribonuclease-prepared siRNA (esiRNA), primers were as follows: CCM3 (TCACTATAGGGAGAGTCTCGTATGGCAGCT-GATG; TCACTATAGGGAGACTAGTCGGTTGGCACTT-ACGA); STRN (TCACTATAGGGAGAGCTTCGATCAG-CATCACTGC; TCACTATAGGGAGACTCTCTGTGCTC-CTTCAGCA); STRN3 (TCACTATAGGGAGAGAAGTCA-TCCCCACACTTCCTGTT; TCACTATAGGGAGACCTTTC-TGATGGCAGTGATGC); and STRN4 (TCACTATAGGGAGAGCAGATCTCACCGTCACCAAC; TCACTATAGGGAGACTAGGGATCCATGCTGAGGTC), as well as esiRNA directed against luciferase as described (23).

esiRNAs were prepared as described (23) and diluted to 100 ng/ μ l; siRNAs (Dharmacon) were diluted to 20 μ M. HeLa or HEK293 cells were transfected with esiRNAs using RNAiMAX (Invitrogen; 100 ng per 1 well in a 24-well dish). For striatins, esiRNAs against all three paralogs were pooled and used at 70 ng each. HeLa cells were transfected with siRNAs using RNAiMAX (Invitrogen; 20 pmol per 1 well in a 24-well dish). (siRNAs for all striatin paralogs were pooled, and 40 pmol total was used.) RNA silencing experiments were performed for 72 h before harvesting or imaging cells. Knockdown was assessed using immunoblotting and/or RT-PCR.

RT-PCR Procedure and Primers—RT-PCR was performed as follows: RNA was purified from cells using the RNeasy kit (Qiagen 74104). Cells were lysed in 600 μ l using a 20-gauge needle for homogenization. The final product was eluted in 30 μ l of water. 200 ng of RNA was run on an agarose gel to check quality. Reverse transcription of RNA into cDNA was performed following the instructions from the Invitrogen SuperScript III reverse transcriptase guide (Invitrogen 18080-093). cDNA was amplified by PCR and analyzed on an agarose gel. Primers were GGATGACAATGGAAGAGATGAAG and GAC-AGATTCTACTCGTTCTAGCTC for *PDCD10* (encoding CCM3) and TGAATGACACGAGACTTACC and TGAA-GAGGGAAAGGTGGAAC for *TIPRL* (encoding an unrelated protein used as a loading control).

Immunofluorescence—Immunofluorescence was performed on HeLa cells as described previously (24) with the following modifications: cells were permeabilized with 0.1% Triton X-100, incubated with primary antibodies for 2 h at room temperature, and mounted with ProLong Gold (Invitrogen, P36930). Images were acquired on a DeltaVision at 60 \times magnification (with a 2 \times digital zoom for Fig. 5A, essentially as described (25)). Fig. 5E and supplemental Figs. 5, 6 (C and D), and 7 were acquired on an Olympus epifluorescence microscope at 40 \times magnification. Fig. 6A was acquired on an Olympus epifluorescence microscope at 20 \times magnification.

Wound Healing and Quantification of Golgi Polarization—Assays were performed as described previously (16) with the following modifications: Cells were plated to confluence on fibronectin-coated coverslips. After 6–8 h, cells were serum-starved in DMEM with 0.1% FBS overnight, and the monolayer was wounded. Cells were incubated in DMEM with 10% FBS for 90 min and fixed with ice-cold 4% paraformaldehyde. Golgi staining was performed using anti-GM130 or anti-giantin, and the first row of cells was counted. A minimum of 150 cells were

counted per treatment per experiment; experiments were performed in quadruplicates. Treatments were labeled in code, and polarization was assessed independently by two people. The Golgi of cells on the wound edge were counted as polarized when the majority of the stained Golgi was located within a 90° angle facing the wound (26).

Mass Spectrometric Analysis—Acquired RAW files were converted to mgf format, which were searched with the Mascot search engine (Matrix Sciences, London, UK) against the human RefSeq database (release 37) with a precursor ion mass tolerance of 3.0 and a fragment ion mass tolerance of 0.6. Methionine oxidation and asparagine deamidation were allowed as variable modifications, and trypsin specificity (with one missed cleavage allowed) was selected. The data were analyzed in the “Analyst” module of ProHits (27) and exported into Excel files for spectral normalization and manual curation. For the STRIPAK pulldowns, only interaction partners previously reported and confirmed (4) are reported (supplemental Table 1). For GM130 pulldowns, database searches were performed as above, and the results were analyzed using SAINT (version 2.0) (28, 29), using eight negative control runs as part of the modeling. Hits detected with SAINT AvgP \geq 0.7 and with a minimum of 10 spectra in at least one of the replicates are reported (supplemental Table 3; detailed mass spectrometry data are presented in supplemental Table 4); interactions with the wild-type protein were deposited to the BioGRID database.

For quantitative analysis (Fig. 5C), immunoprecipitation of FLAG-Mst4 was performed after depletion of CCM3 or all striatins by esiRNA from HEK293 cells stably expressing FLAG-Mst4. Data were acquired on an ABSciEX 5600 TripleTOF instrument using an Eksigent Ultra nanoLC with NanoFlex cHiPLC columns. The samples were loaded onto a C18 Trap chip at 500 nl/min and separated over a C18 column chip at 250 nl/min (120 min gradient). Data acquisition was done with 1 high resolution MS scan followed by 20 high resolution MS/MS scans. Resulting data were searched using ProteinPilot (version 4.0) against human proteins in Uniprot (release 8.8) (spectral counts are presented in supplemental Table 5). PeakView was used to extract peak areas for all peptides identified for target proteins (STRIPAK core components and GM130). The total number of peptides used for the quantification of each protein is shown in supplemental Table 5 (each of them was manually inspected). Total sum areas for proteins were determined and exported to Markerview where values were normalized to Mst4 across all samples. Further normalization for each protein in the esiCCM3 or esiSTRNs sample to the esiLuc control was performed.

Structure Modeling—The crystal structure of human CCM3 (Protein Data Bank 3L8I (30)) was superimposed on the focal adhesion targeting (FAT) domain of focal adhesion kinase in complex with a peptide derived from paxillin (PDB 1OW7 (31)). Residues of CCM3 FAT domain (Lys-132, Lys-139, Lys-172, and Lys-179) analogous to focal adhesion kinase residues lining the paxillin binding groove were mutated to alanines for the purpose of interaction studies (see Fig. 3).

RESULTS

Striatins Act as Molecular Scaffolds within STRIPAK—The STRIPAK complex contains members of the evolutionarily

Structure-Function Analysis of Core STRIPAK

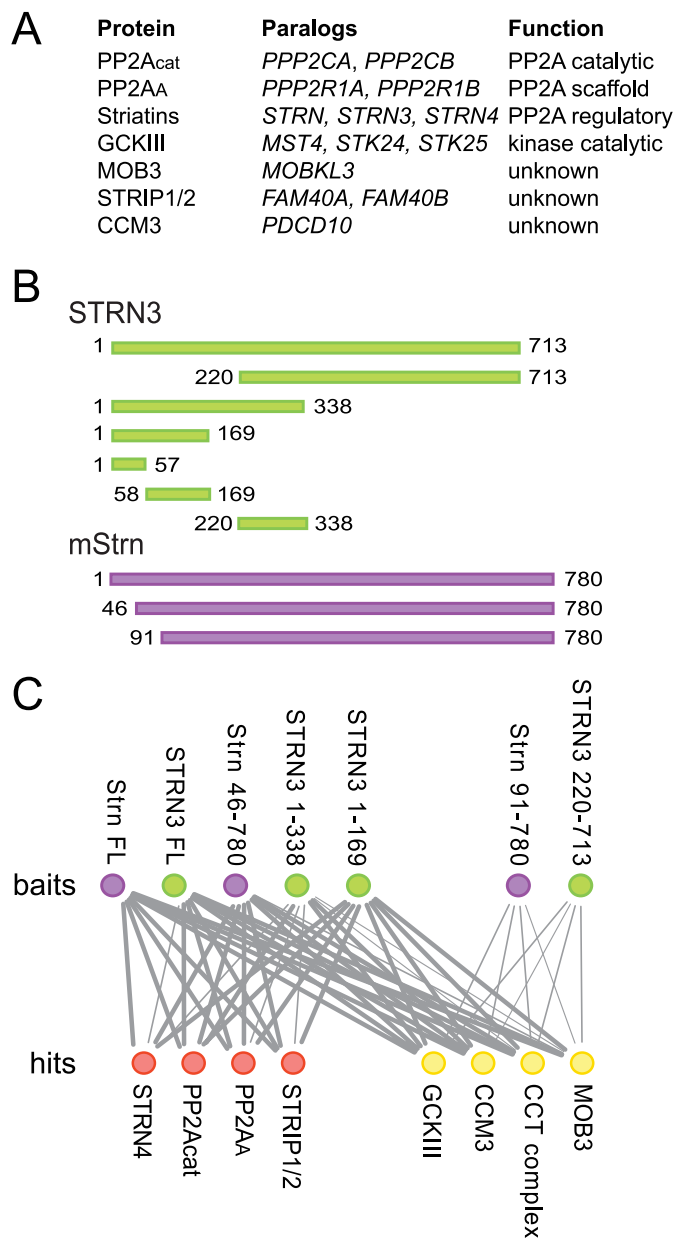


FIGURE 1. Striatin is a scaffolding subunit within STRIPAK. *A*, composition of core STRIPAK. Proteins, paralogous genes (human nomenclature), and function of proteins are listed. *B*, schematic of the constructs used in this study. Human STRN3 constructs are in green, mouse Strn constructs are in purple. The first and last amino acid in each construct are indicated. *C*, summary of AP-MS results for the association of core STRIPAK components with the STRN3 (green) and Strn (purple) deletion mutants (top row). Identified proteins (hits; bottom row) in red do not interact with Strn(91–780) or STRN3(220–713), whereas hits in yellow do. The thickness of each line is proportional to the number of spectral counts (total number of peptides) recovered for each of the proteins in the analysis of the striatin mutants, relative to the spectral counts for the same protein in the AP-MS of full-length Strn. Note that each node (and its associated edges) represents paralogous families, as defined in *A*. The complete mass spectrometry data used to make this figure are presented in [supplemental Table 1](#).

conserved striatin family of PP2A regulatory subunits. To investigate the binding topology of the STRIPAK complex with respect to striatin, full-length and truncation mutants of striatin molecules (Fig. 1*B*) were stably expressed in HEK293 cells and subjected to affinity purification coupled to mass spectrometry (as described in Ref. 4). As expected (Fig. 1*C*; [supplemental Table 1](#)), full-length striatins recovered all core STRIPAK components, as well as members of the Chaperone containing TCP complex. Although deletion of the first 45 amino acids of Strn did not affect any of the interactions, truncation of the amino-terminal 90 amino acids completely abolished the interactions with most STRIPAK components, including PP2A_{cat} and PP2A_A (shown as red circles in Fig. 1*C*). (Note that only “core” STRIPAK components as defined in Fig. 1*A* are shown on this figure; alternative STRIPAK components, including SLMAP, SIKE, and CTTNBP2NL are also unable to associate with this truncated striatin molecule, see [supplemental Table 1](#)). Importantly, however, interactions with components of the Chaperone containing TCP complex, Mob3, CCM3, and the GCKIII proteins were not abrogated by this truncation. Further mapping with STRN3 deletion mutants extended these observations (Fig. 1*C*), indicating that the N-terminal portion of the molecule is essential for mediating interactions with PP2A and various STRIPAK components, whereas the C-terminal region (amino acids 220–713 in STRN3) is sufficient for interactions with Mob3, CCM3, GCKIII, and the Chaperone containing TCP complex. Interestingly, STRN3 fragments encompassing amino acids 1–169 and 1–338 interacted with all of the STRIPAK proteins (Fig. 1*C*). We attributed these observations to the fact that a coiled-coil element (amino acids 85–130; Ref. 32) is located within this region and likely mediates homo- and hetero-oligomerization (33) of these deletants with endogenous full-length striatin molecules.

STRN3 Binds Directly to PP2A_A and CCM3—Yeast two-hybrid interactions between PP2A_A and striatins were detected previously in a high-throughput experiment, suggesting a direct association between these molecules (AfCS yeast two-hybrid screen). To demonstrate that PP2A_A and striatin did interact directly in the absence of bridging proteins, an *in vitro* binding assay was performed using bacterially expressed and purified proteins. Soluble His-PP2A_A was incubated with immobilized GST-STRN3 in a pulldown experiment followed by an SDS-PAGE gel and Coomassie staining. His-PP2A_A was efficiently captured by full-length GST-STRN3 (Fig. 2*A*, *top panel*, compare lanes 1 and 2). To delimit the STRN3 region responsible for interacting with PP2A_A, a series of STRN3 truncation mutants was assayed. This analysis revealed that amino acids 1–57 and 169–713 were dispensable for PP2A_A binding activity, whereas further truncations inside this region prevented interaction (Fig. 2*A*). To test whether residues 58–169 were sufficient to mediate the interaction, GST-STRN3(58–169) and a negative control, GST-STRN3(1–57), were incubated with His-PP2A_A. Only the GST-STRN3(58–169) protein efficiently pulled down PP2A_A (Fig. 2*B*, *left panel*).

Our mass spectrometry results indicated that Mob3, CCM3, and the GCKIII proteins interact with a portion of the C terminus of both Strn and STRN3 (from amino acids 220–713 in STRN3). GST pulldown assays were conducted to uncover possible direct interactions. Full-length GST-STRN3 efficiently pulled down CCM3 *in vitro* (Fig. 2*A*, *bottom panel*). To map the interaction region(s), truncation mutants of STRN3 were tested for CCM3 binding, as above. Deletion of the first 219 amino acids or residues 338–713 of STRN3 did not prevent associ-

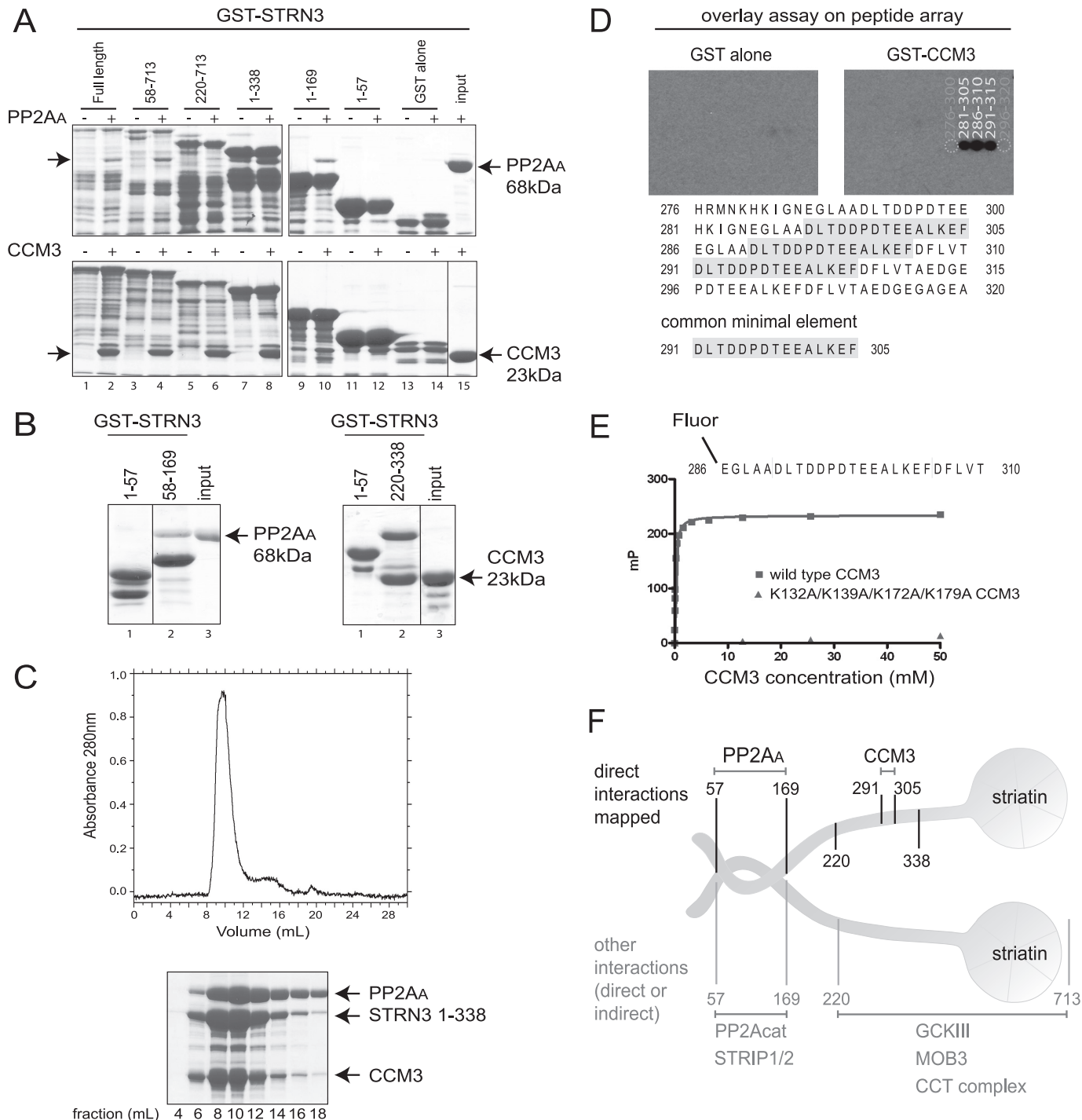


FIGURE 2. Striatin binds directly to PP2A_A and CCM3. *A*, mapping of the direct *in vitro* association between GST-STRN3 truncation mutants and PP2A_A (top) or CCM3 (bottom). Bacterially expressed and purified GST-STRN3 deletion proteins were used for GST pulldown assays with soluble PP2A_A or CCM3; GST alone was used as a negative control. Proteins were visualized by SDS-PAGE and Coomassie staining. The soluble proteins were added to even numbered lanes only. The position of the soluble proteins are indicated by arrows. *B*, amino acids 58–169 of GST-STRN3 are sufficient to mediate an interaction with PP2A_A (left) and amino acids 220–338 are sufficient to mediate the interaction with CCM3 (right) in a GST pulldown assay. GST-STRN3(1–57) was used as a negative control. *C*, PP2A_A, STRN3(1–338), and CCM3 form a complex that is stable throughout the course of gel filtration. Bacterially expressed recombinant proteins were purified and loaded onto a Superdex 200 gel filtration column. The proteins elute as one major peak, ~8–12 ml, as detected by $A_{280\text{ nm}}$ (top) and SDS-PAGE followed by Coomassie staining (bottom). *D*, peptide array identifies the core STRN3 residues (amino acids 291–305) responsible for binding to GST-CCM3 in an overlay assay. 25-mer peptides derived from STRN3(220–338) were spotted on a membrane (see supplemental Fig. 3 for Coomassie staining of the membrane) and subjected to an overlay assay with GST-CCM3 (or GST alone) followed by detection with anti-GST and horseradish peroxidase-coupled secondary antibodies. The sequence of the common minimal element from the peptides that display association is highlighted. *E*, fluorescence polarization indicates that a fluorescent 25-mer STRN3 peptide (amino acids 286–310) interacts with wild-type CCM3. The minimal sequence of STRN3 determined in *D*, plus five flanking residues on either side, was synthesized as a fluorescent peptide and used in a fluorescence polarization assay. This peptide readily interacts with wild-type CCM3 (blue curve). However, substitution of Lys-132, Lys-139, Lys-172, and Lys-179 in CCM3 for alanines completely abrogated association with the STRN3 peptide (see Fig. 3 for description of this mutant). *F*, summary of the binding surfaces mapped on striatin (results from Figs. 1 and 2).

Structure-Function Analysis of Core STRIPAK

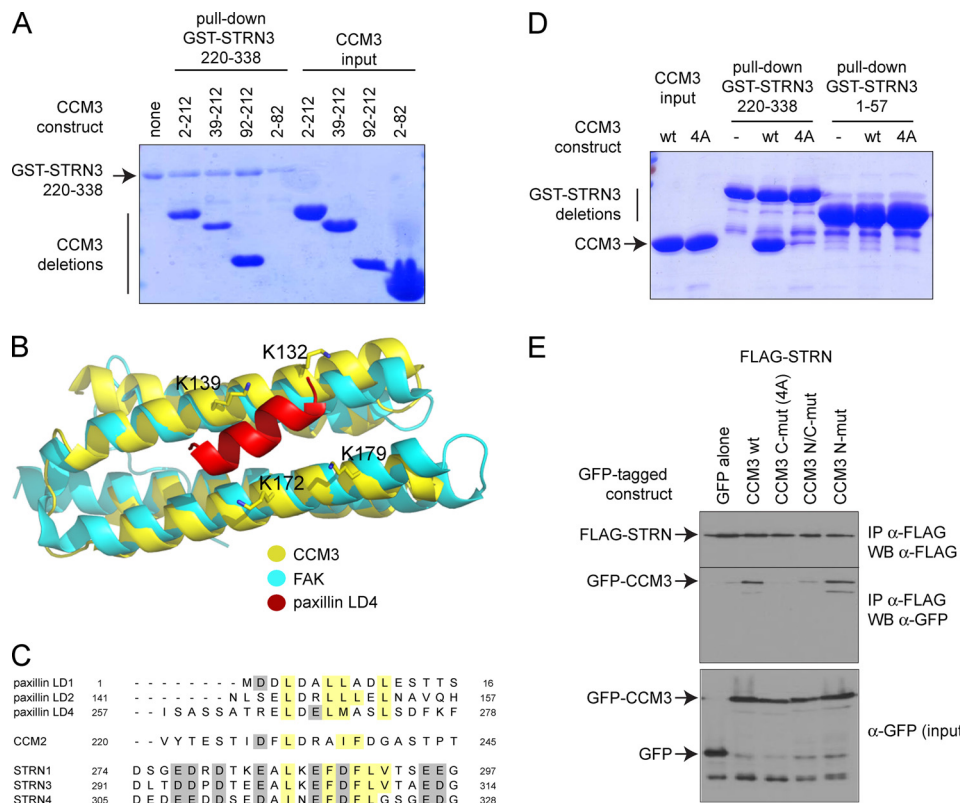


FIGURE 3. CCM3 interacts with STRN3 via its FAT domain. *A*, STRN3 interacts with the C-terminal portion of CCM3. A GST pulldown assay was performed with GST-STRN3 220–338 and bacterially expressed and purified CCM3 deletions to map the region on CCM3 responsible for binding to GST-STRN3. Deletion of the first 92 amino acids of CCM3 did not affect the interaction, and a region encompassing amino acids 2–82 was unable to associate to GST-STRN3(220–338). *B*, structural modeling of the CCM3 FAT domain with a peptide derived from paxillin. The CCM3 crystal structure (30) revealed that the region that we have mapped as interacting with STRN3 also folds as a focal adhesion targeting domain (yellow) similar to focal adhesion kinase (FAK, cyan). Interaction with peptides derived from paxillin (shown in red) are mediated via four lysine residues (highlighted). *C*, alignment of the peptide derived from STRN3 (and corresponding peptides in the STRN and STRN4 paralogs) with the CCM3 binding regions of CCM2 and paxillin suggests a common mode of association. *D*, mutation to alanines of the four conserved lysines (Lys-132, Lys-139, Lys-172, and Lys-179) in CCM3 C-mut (4A) abrogates interaction with GST-STRN3(220–338) *in vitro*. GST pulldown assays were performed with GST-STRN3(220–338) to monitor binding of wild-type CCM3 or CCM3 C-mut (4A). Only wild-type CCM3 is pulled down by GST-STRN3. GST-STRN3(1–57) was used as a negative control. *E*, mutation to alanines of the four conserved lysines in CCM3 abrogates the interaction with full-length Strn in HEK293T cells. Co-transfection of FLAG-tagged full-length Strn with GFP-tagged CCM3 constructs WT, C-mut (4A), N-mut, and N/C-mut was performed. Immunoprecipitation of FLAG-Strn was followed by immunoblotting with anti-GFP to detect CCM3 association. CCM3 C-mut, 4A is unable to interact with FLAG-Strn, whereas CCM3 N-mut has no effect on the interaction. A combination of both mutations also prevented the interaction, as expected.

ation of CCM3 (Fig. 2A). We next demonstrated that STRN3(220–338) was sufficient to mediate the interaction with CCM3 (Fig. 2B, right panel). To further examine the interactions between PP2A_A, STRN3, and CCM3, the recombinant proteins were mixed and analyzed by gel filtration chromatography followed by Coomassie staining. PP2A_A and STRN3(58–169) form a complex that is stable throughout chromatographic fractionation (supplemental Fig. 4). Similarly, a trimeric complex formed of PP2A_A, STRN3(1–338), and CCM3(2–212) also eluted as a stable complex from gel filtration experiments (Fig. 2C).

To further refine the location of the CCM3 binding site on STRN3, overlay assays of peptides derived from STRN3(220–338), using full-length GST-CCM3 as a probe, were performed. STRN3 peptides containing amino acids 291–305 were able to interact with CCM3 on a membrane (Fig. 2D). Furthermore, a peptide encompassing amino acids 286–310 was sufficient for interaction in solution (as detected by fluorescence polarization) and had an apparent K_d of 132 ± 0.003 nm when modeled as one site binding (Fig. 2E and supplemental Table 2). Taken together, our mapping studies identified striatin as a scaffolding

molecule within the STRIPAK complex and revealed direct interactions with both PP2A_A (amino acids 58–169 of STRN3) and CCM3 (amino acids 291–305 of STRN3; Fig. 2F).

CCM3 Associates with Striatin via Its FAT Domain—Deletion mutants of CCM3 were next analyzed for their ability to bind to GST-STRN3(220–338) *in vitro*. Although deletion of CCM3 amino acids 82–212 precluded interaction with STRN3, a construct expressing only amino acids 92–212 was sufficient to bind to STRN3 (Fig. 3A). This region of CCM3 forms a globular domain consisting of four α -helices exhibiting structural resemblance to the FAT domain, which mediates the interaction between focal adhesion kinase and paxillin. On this basis, an interaction of CCM3 with paxillin was validated previously (30) and shown to require four lysine residues that establish interactions with paxillin (Fig. 3B); the same residues were also implicated in mediating the interaction between CCM3 and CCM2, as CCM2 shares a stretch of homology to paxillin (30). The striatin peptide responsible for association with CCM3 exhibits an amino acid composition similar to the paxillin and CCM2-derived peptide (Fig. 3C), suggesting that the same mode of binding may be employed for striatin-CCM3 interac-

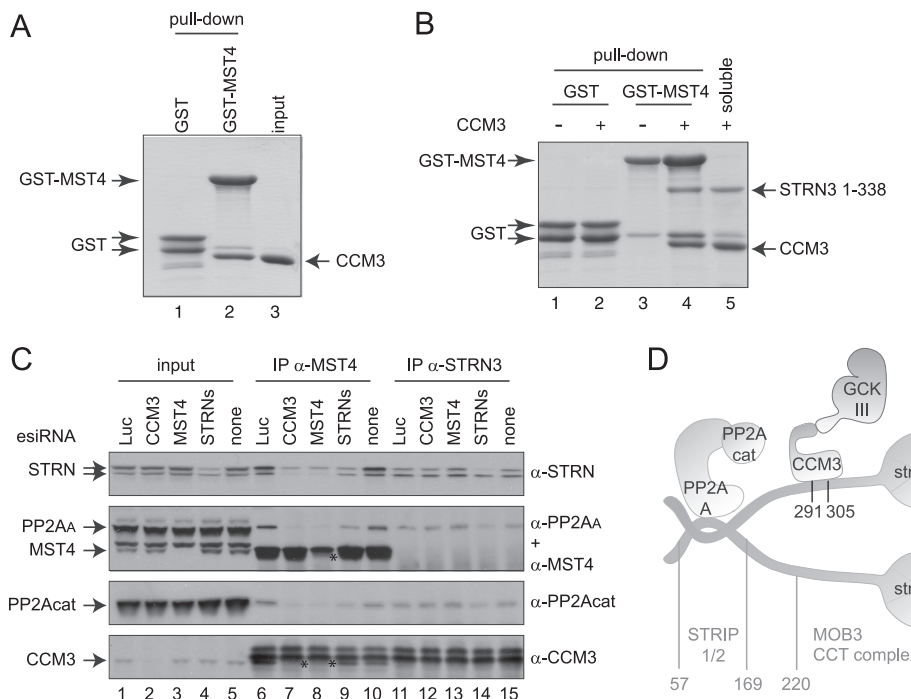


FIGURE 4. Striatin and CCM3 bridge the kinase and phosphatase components of STRIPAK. *A*, direct *in vitro* interaction between GST-Mst4 and CCM3. GST-Mst4 kinase or GST alone were incubated with soluble CCM3, and a GST pulldown followed by SDS-PAGE and Coomassie staining was performed. *B*, CCM3 bridges Mst4 to STRN3 *in vitro*. GST-Mst4 was incubated with soluble STRN3(1–338) in the absence or presence of soluble CCM3. GST pulldown was followed by SDS-PAGE and Coomassie staining. STRN3(1–338) could be precipitated with GST-Mst4 only when incubated with free CCM3. The *soluble* lane shows amount of CCM3 and/or STRN3(1–338) in the binding assay. *C*, depletion of CCM3 or striatins by esiRNA prevents association of the PP2A phosphatase and MST4 kinase. HeLa cells were transfected with the indicated esiRNAs. (Note that the esiRNA mixture for striatins targets all three paralogs.) *Luc* indicates that a non-targeting esiRNA directed against luciferase was employed; *none* indicates a mock transfection. After cell lysis (total cell lysate input shown on the left), immunoprecipitation of MST4 (*center*) or STRN3 (*right*) was performed using antibodies against the endogenous proteins. SDS-PAGE was followed by immunoblotting using antibodies against the indicated endogenous proteins. Arrows indicate the position of each protein; stars indicate the decrease in intensities of the MST4 and CCM3 bands in the immunoprecipitates, as these proteins migrate close to cross-reacting species in the immunoprecipitates. Depletion of striatins, CCM3, or MST4 all prevent recruitment of PP2A_{cat} and PP2A_A to MST4, indicating that CCM3 and striatins are responsible for the interaction between the kinase and the phosphatase components of STRIPAK. STRN association with MST4 is prevented by the depletion of MST4 and CCM3, consistent with the bridge model described in *B*. Depletion of striatins has no effect on the recruitment of CCM3 to MST4. Although depletion of the striatins alters the recovery of PP2A_{cat} and PP2A_A to STRN3, as expected, depletion of CCM3 or MST4 has no effect on these interactions. *D*, model for the structural organization of core STRIPAK.

tions. These four surface lysine residues at the interface of the paxillin-CCM3 model (Lys-132, Lys-139, Lys-172, Lys-179) were mutated to alanines (called CCM3 C-mut 4A). As measured by fluorescence polarization, these mutations abrogated the interaction with the STRN3 peptide (Fig. 2E). These mutations also abrogated the interaction with a STRN3(220–338) protein in a GST pulldown assay (Fig. 3D). (WT CCM3 is pulled down but not CCM3 C-mut 4A.) Lastly, we tested the recovery with endogenous striatin of transiently transfected GFP-tagged versions of CCM3 WT, C-mut 4A, N-mut (which should not abrogate the interaction) as well as N/C-mut (a combination of both the N and C mutations). Only those constructs with the C-mut 4A lost the interaction (Fig. 3E). Taken together, these data indicate a similar mode of association for CCM3-paxillin, CCM3-CCM2, and CCM3-striatin, suggesting mutually exclusive interactions between these proteins. (The CCM3-striatin interaction is more readily detected by AP-MS in our cells.) Consistent with this, an interaction between CCM2 and striatin was never detected by AP-MS (data not shown).

CCM3 Bridges GCKIII Proteins to STRIPAK via Striatin— It was reported previously that CCM3 interacts with members of the GCKIII protein family (9, 10), and direct associations between this kinase family and CCM3 were mapped to

a CCM3 region (amino acids 2–82) different from that implicated in striatin binding (49). Motivated by the finding that CCM3 binds directly to striatins, we sought to determine whether CCM3 could bridge GCKIII proteins to striatin. A direct interaction between the GCKIII protein Mst4 and CCM3 was first recapitulated *in vitro* (Fig. 4A). To test whether CCM3 acts as a bridge between the kinases and striatins, pulldown assays using GST-Mst4 and untagged STRN3(1–338) were performed in the presence or absence of untagged CCM3. STRN3 alone did not associate with GST-Mst4 (Fig. 4B, lane 3). However, in the presence of CCM3, GST-Mst4 efficiently pulls down STRN3 (in addition to CCM3; lane 4). CCM3 is therefore able to bridge interactions between the GCKIII protein Mst4 and STRN3.

To determine whether CCM3 and the striatin proteins were responsible for bridging Mst4 to PP2A *in vivo*, endogenous Mst4 or STRN3 were immunoprecipitated from cells in which CCM3, Mst4, or the three striatin family members were depleted by esiRNA (Fig. 4C). Recovery of PP2A was monitored using antibodies directed against either PP2A_{cat} or PP2A_A. Depletion of CCM3 or striatins largely abrogated the interaction between Mst4 and both phosphatase subunits (Fig. 4C, lanes 7–9). Note, however, that depletion of CCM3 or Mst4

Structure-Function Analysis of Core STRIPAK

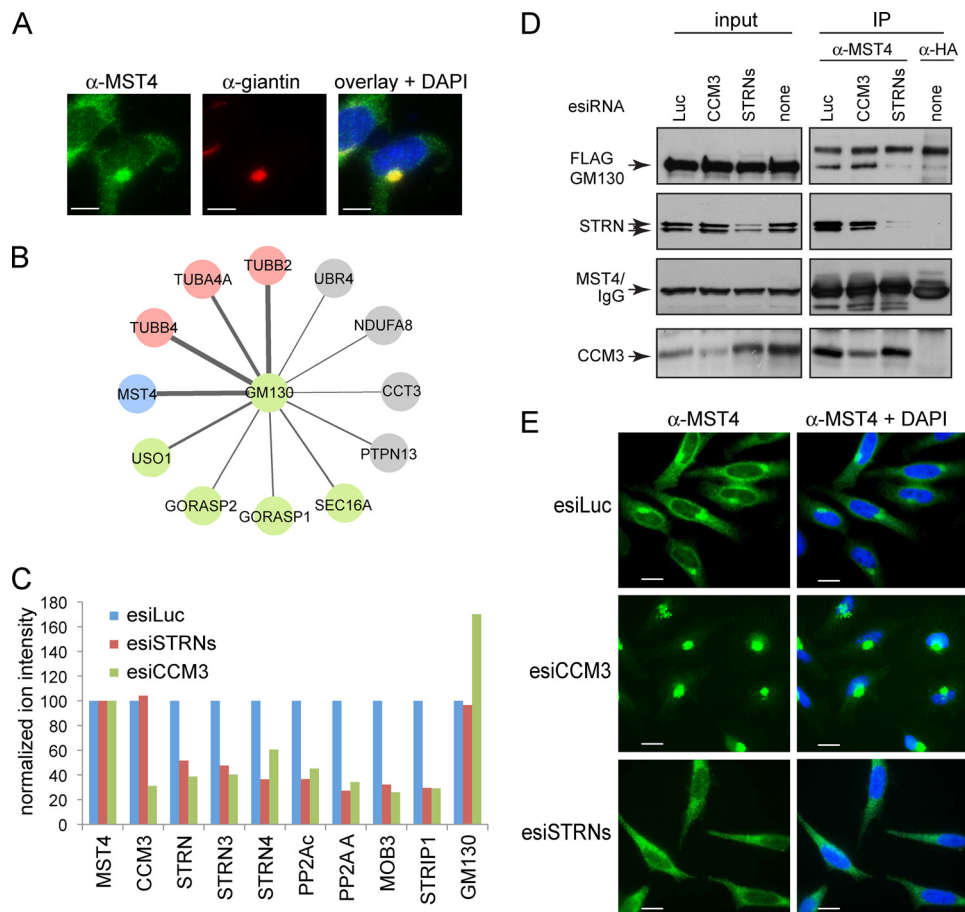


FIGURE 5. CCM3 and striatins exert opposite effects on MST4 localization. *A*, co-localization of endogenous MST4 (green) with the Golgi protein giantin (red). In the overlay (right), co-localization to the Golgi is shown in yellow; note that a fraction of MST4 does not localize to the Golgi but is instead detected as green punctae in the cytosol. Scale bar, 7.5 μ m. *B*, GM130 interactors identified by mass spectrometry. AP-MS was performed as described under “Experimental Procedures.” Statistical analysis of the interactions using SAINT was performed; see supplemental Tables 3 and 4 for complete mass spectrometric data. The thickness of the edges is proportional to spectral counts (total number of peptides) for the prey, whereas the color indicates MST4 (blue), known Golgi proteins (green), tubulins (pink), or proteins other than MST4, Golgi proteins, or tubulins (gray). Note that MST4 is a major interaction partner for GM130. *C*, depletion of CCM3 decreases association of MST4 with STRIPAK but not the interaction with GM130. Stable HEK293 cells expressing FLAG-Mst4 were transfected with the indicated esiRNAs (see Fig. 4C for details). FLAG-Mst4 was immunoprecipitated using anti-FLAG antibodies, and the sample was processed for quantitative mass spectrometry. Relative quantification by mass spectrometry was performed using a TripleTOF 5600 with cells depleted of STRN proteins or CCM3; normalization to Mst4 (bait) levels and to the expression levels in the luciferase samples is shown. See supplemental Table 5 for mass spectrometric results. As shown in Fig. 4C, depletion of CCM3 affects recovery of all STRIPAK components with Mst4; depletion of the striatins affects recovery of all STRIPAK components with the exception of CCM3. By contrast, depletion of CCM3 appeared to increase the GM130 interaction with FLAG-Mst4, indicating that this interaction is not mediated via STRIPAK. *D*, GM130 interaction with endogenous MST4 is reduced by depletion of striatins in HEK293 cells stably expressing FLAG-GM130. Transfection of esiRNAs was followed by immunoprecipitation of endogenous MST4 and immunoblotting for FLAG-GM130 and STRIPAK proteins. To control for the amount of FLAG-GM130 non-specifically binding to the beads, we performed immunoprecipitation in parallel with an isotype-matched antibody (anti-HA). (There is no HA protein transfected in these cells.) *E*, esiRNA-mediated depletion of CCM3 in HeLa cells induces near complete localization of MST4 to the Golgi, whereas depletion of striatins prevents Golgi localization. Transfection of indicated esiRNAs was followed by immunofluorescence staining of MST4 and DAPI. Scale bar, 10 μ m.

does not affect the interaction between STRN3 and PP2A (*lanes 12 and 13*).

On the basis of the data presented above, we propose the following architectural model for the STRIPAK complex (Fig. 4*D*). Striatin functions as a core scaffold within STRIPAK, mediating homo- and hetero-oligomerization, as well as (minimally) direct interactions with PP2A_A and CCM3, via two separate regions. Through direct interactions, CCM3 docks onto striatin and recruits the GCKIII proteins to the phosphatase component of STRIPAK.

Localization of MST4 to Golgi and Interaction with GM130 Is Regulated by CCM3 and Striatin in Opposite Manner—The kinase MST4 had been shown previously to localize to the Golgi and had been implicated in Golgi positioning and integrity (15,

16). To begin to understand the functional consequences of the interaction between the kinase and phosphatase components of STRIPAK, the localization of MST4 to the Golgi was monitored in HeLa cells. Consistent with previous studies, we observed strong co-localization between MST4 and the Golgi protein giantin, although localization of MST4 in punctate structures in the cytoplasm (that are not stained with giantin) was also readily apparent (Fig. 5*A*; supplemental Fig. 4). MST4 was reported to be targeted to the Golgi at least partially due to its interaction with the protein GM130 (15). In agreement with these data, when we conducted an AP-MS analysis on FLAG-Mst4, GM130 was also recovered (data not shown), and the reciprocal AP-MS analysis of FLAG-GM130 recovered MST4 (but not the additional components of STRIPAK) as a major interactor (Fig.

5B; supplemental Tables 3 and 4). These results suggested that MST4 can be found in at least two separate complexes, one with STRIPAK and one with GM130.

To test the effect of CCM3 depletion on the interactions established by MST4, AP-MS was performed in HEK293 cells expressing FLAG-Mst4 after CCM3 knockdown, using a quantitative mass spectrometric approach. CCM3 knockdown resulted in decreased interactions between FLAG-Mst4 and the remaining STRIPAK components (*green bars*), but not between FLAG-Mst4 and GM130. (In fact, the interaction with GM130 appeared to increase in some experiments (Fig. 5C and supplemental Table 5).) Similarly, depletion of CCM3 in FLAG-GM130 expressing HEK293 cells did not disrupt the interaction between immunoprecipitated endogenous MST4 and FLAG-GM130, when evaluated by immunoblot. This confirms that MST4 is not recruited to GM130 via CCM3.

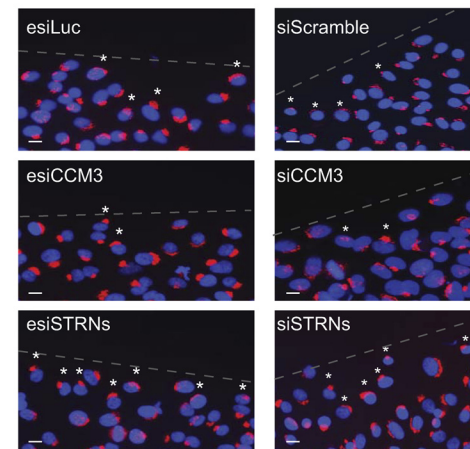
We next evaluated the effect of CCM3 knockdown on the MST4 localization pattern in HeLa cells. Interestingly, in cells in which CCM3 was silenced, the localization of MST4 is shifted almost completely to the Golgi region (Fig. 5E). Similar results were obtained using independent silencing reagents (supplemental Fig. 7), demonstrating that the observed effects are caused by the depletion of CCM3, and very little of the protein remains localized to the cytosol. These data suggest that CCM3 may favor the cytosolic (and perhaps punctate) localization of MST4 over Golgi localization.

Because CCM3 and striatin bridge MST4 to other STRIPAK components, we expected that silencing striatins would have the same effect on MST4 Golgi localization as silencing CCM3. However, when striatins were depleted, MST4 Golgi localization was strikingly perturbed, leading to a more prominent cytosolic localization (Fig. 5E). This was accompanied by a reduction in the amount of FLAG-GM130 precipitated with endogenous MST4 (Fig. 5D). (Note that this reduction was not significantly detected in the quantitative mass spectrometry experiment with FLAG-Mst4 cells shown in Fig. 5C.) Taken together, these results suggest that CCM3 and striatin exhibit opposing roles on the localization of the kinase MST4 to the Golgi, with striatins favoring a Golgi localization and CCM3 promoting cytosolic location.

CCM3 and Striatin Oppose Each Other in Golgi Positioning—Depletion of MST4, and more recently CCM3, was shown to affect the positioning of the Golgi toward the leading edge of a wound (15, 16). Prompted by the surprising results that CCM3 and striatin knockdowns have opposing effects on MST4 localization (and in some cases, on the interaction with GM130), the effects of depletion of each of these proteins on Golgi orientation was assessed. Golgi orientation was determined by a well established criterion: the Golgi of cells on the wound edge were considered to be oriented toward the leading edge when the majority of the stained Golgi was located within the quadrant facing the wound (26).

In cells transfected with control esiRNA, ~40% ($\pm 2\%$, $n = 4$) of the cells displayed Golgi positioned toward the leading edge 1.5 h after wounding (Fig. 6, A and B). As reported previously, depletion of CCM3, using either esiRNA or siRNA, reduced the percentage of properly positioned Golgi to roughly 25% (the

A GM130 and DAPI at wound edge



B

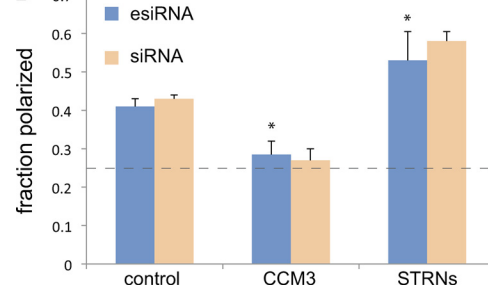


FIGURE 6. CCM3 and striatins exert opposite effects on Golgi polarization. A, GM130 and DAPI staining at the wound edge in cells depleted of indicated proteins by esiRNA (left) and chemical siRNA (right). esiLuc and siScramble are negative controls. The position of the wound is indicated by a dashed line. A 90° quadrant scoring of the Golgi positioning relative to the wound was performed (see “Experimental Procedures”). Small white asterisks indicate Golgi that are polarized toward the wound within the first cell layer. Scale bar, 10 μ m. B, quantification of Golgi polarization from A indicated that ~40% of control cells had Golgi polarized toward the wound. In cells depleted of CCM3, this value was decreased to ~25–30%, whereas in cells depleted of striatins, this value increased to ~54–60% (esiRNA, $n = 4$, $p < 0.05$; siRNA, $n = 2$). The dashed line indicates the number of cells expected to randomly orient their Golgi toward the wound in our scoring system (25%).

number of cells expected to randomly orient their Golgi toward the wound). By contrast, but consistent with the data presented above, depletion of striatin using esiRNA markedly enhanced Golgi orientation toward the wound, from ~40% in controls to >54%. Similar results were observed following striatin knockdown with siRNA ($n = 2$). These data indicate that depletion of CCM3 and striatin not only have opposite effects on MST4 localization but also have opposing effects on Golgi repositioning during wound healing.

DISCUSSION

We have described the molecular organization of the STRIPAK complex and assigned a role to the disease-related CCM3 protein as an adaptor that links the kinase and phosphatase subunits of STRIPAK. We have also described a means by which the functions of striatin and CCM3 oppose each other, through the regulation of MST4 interactions and localization as well as their effect on Golgi positioning after stimulation by wounding the cell monolayer. These data suggest that the interaction between CCM3 and STRIPAK via direct association with striatin may serve as a regulatory mechanism to control

the function of the MST4 kinase. Importantly, these results also suggest that Golgi localization of MST4 may be detrimental to polarization. The Golgi apparatus has emerged as a critical hub for intracellular signaling (34), and signaling is essential for Golgi polarization. For example, phosphorylation of the Golgi protein, GORASP1 (also known as GRASP65, a GM130 interaction partner), by the kinase ERK is required for Golgi reorientation (35). Interestingly, ERK activity has been shown to be modulated by CCM3 and MST4 (9); whether or not GORASP1 phosphorylation is modulated in our system remains to be tested.

A large body of evidence suggests important roles for polarized localization of the Golgi (36). Cell migration requires polarized secretion at the leading edge for the regulated transport of vesicles, the delivery of adhesion molecules and cytoskeletal components, as well as the addition of new membranes. The polarized localization of the Golgi has also been intimately linked to the small proteins of the Rho-GTPase family (26, 37). In light of the defects in Rho signaling following modulation of CCM1, CCM2, or CCM3 expression (12–14), it is tempting to postulate that CCM3, MST4, and perhaps STRIPAK may regulate Golgi polarization via regulation of Rho-GTPases. Whether striatins, CCM3, and MST4 play a role in all aspects of Golgi polarization, including cell migration, remains to be answered.

Given that STRIPAK contains both kinase and phosphatase activities, our results suggest the existence of a molecular switch defined by the balance of phosphorylation and dephosphorylation at the Golgi. At this point, the target(s) for the MST4 kinase (or the PP2A phosphatase) in the Golgi polarization process are still unknown. Additionally, whether and how Golgi polarization may contribute to the vascular defects observed in CCM patients remains to be investigated.

New roles for STRIPAK complex components are beginning to emerge, in large part through analysis of STRIPAK paralogs across species. It is noteworthy that a portion of the STRIPAK complex (lacking CCM3 and the GCKIII protein component) has been conserved throughout eukaryotic evolution. Ancestral roles for STRIPAK point to cytoskeletal and membrane dynamics functions. In *Saccharomyces cerevisiae*, Far8 (striatin), Far11 (STRIP1/2), Vps64/Far10 (orthologous to the alternate STRIPAK component SLMAP), along with Far3 and Far7 (for which no human orthologs are known) form a protein complex implicated in cell cycle arrest following pheromone treatment (38). Orthologs of these ancestral STRIPAK genes are required for proper vegetative membrane fusion in filamentous fungi (39, 40). The function of STRIPAK in mediating membrane fusion appears to have been conserved in mammals, as deregulation of SLMAP prevents myoblast fusion to myotubes (41). More recently, deletion of the orthologs of striatin (*FAR8*), STRIP1/2 (*FAR11*), or one of the PP2A catalytic subunits (*PPG1*) was demonstrated to suppress lethality and actin cytoskeleton disorganization caused by mutations of TORC2 (target of rapamycin complex 2) (42). Interestingly, TORC2 controls actin cytoskeleton assembly across multiple species, in part via regulation of the Rho1 GTPases (43–45). CCM disease, CCM3, and MST4 are intimately linked to Rho signaling in human cells (12–14, 46), suggesting that this function of STRIPAK has been evolu-

tionarily conserved. In addition to these roles in cytoskeleton and membrane dynamics, a surprising recent report implicated the *Drosophila* STRIPAK complex (including CCM3) in Hippo signaling (47), indicating that STRIPAK may control multiple signaling pathways. The elucidation of the substrates of the kinase and phosphatase components of STRIPAK will be required for a full molecular understanding of STRIPAK function.

Finally, although our data point to the STRIPAK complex as the major interactor for epitope-tagged or endogenous CCM3 protein in HEK293 cells (4), HeLa cells, C2C12 myoblasts, and myotubes and in bovine endothelial aortic cells (data not shown) CCM3 is also capable of interacting with CCM2 (48) and paxillin (30). Because these interactions are apparently mediated via the same surface as the striatin binding site on CCM3, we propose here that they may be mutually exclusive. Further studies on CCM3 function in vascular disease and elsewhere will need to take these alternative protein assemblies into consideration.

Acknowledgments—We thank A. Fernandes and members of the Gingras, Pelletier, and Sicheri laboratories for discussion and technical help and J.-P. Lambert for comments on the manuscript.

REFERENCES

- Virshup, D. M., and Shenolikar, S. (2009) *Mol. Cell.* **33**, 537–545
- Shi, Y. (2009) *Cell* **139**, 468–484
- Glatter, T., Wepf, A., Aebersold, R., and Gstaiger, M. (2009) *Mol. Syst. Biol.* **5**, 237
- Goudreault, M., D'Ambrosio, L. M., Kean, M. J., Mullin, M. J., Larsen, B. G., Sanchez, A., Chaudhry, S., Chen, G. I., Sicheri, F., Nesvizhskii, A. I., Aebersold, R., Raught, B., and Gingras, A. C. (2009) *Mol. Cell Proteomics* **8**, 157–171
- Moreno, C. S., Park, S., Nelson, K., Ashby, D., Hubalek, F., Lane, W. S., and Pallas, D. C. (2000) *J. Biol. Chem.* **275**, 5257–5263
- Moreno, C. S., Lane, W. S., and Pallas, D. C. (2001) *J. Biol. Chem.* **276**, 24253–24260
- Dan, I., Ong, S. E., Watanabe, N. M., Blagoev, B., Nielsen, M. M., Kajikawa, E., Kristiansen, T. Z., Mann, M., and Pandey, A. (2002) *J. Biol. Chem.* **277**, 5929–5939
- Guclu, B., Ozturk, A. K., Pricola, K. L., Bilguvar, K., Shin, D., O'Roak, B. J., and Gunel, M. (2005) *Neurosurgeon* **57**, 1008–1013
- Ma, X., Zhao, H., Shan, J., Long, F., Chen, Y., Chen, Y., Zhang, Y., Han, X., and Ma, D. (2007) *Mol. Biol. Cell* **18**, 1965–1978
- Rual, J. F., Venkatesan, K., Hao, T., Hirozane-Kishikawa, T., Dricot, A., Li, N., Berriz, G. F., Gibbons, F. D., Dreze, M., Ayivi-Guedehoussou, N., Klitgord, N., Simon, C., Boxem, M., Milstein, S., Rosenberg, J., Goldberg, D. S., Zhang, L. V., Wong, S. L., Franklin, G., Li, S., Albala, J. S., Lim, J., Fraughton, C., Llamas, E., Cevik, S., Bex, C., Lamesch, P., Sikorski, R. S., Vandenhoute, J., Zoghbi, H. Y., Smolyar, A., Bosak, S., Sequerra, R., Doucette-Stamm, L., Cusick, M. E., Hill, D. E., Roth, F. P., and Vidal, M. (2005) *Nature* **437**, 1173–1178
- Riant, F., Bergametti, F., Ayrignac, X., Boulay, G., and Tournier-Lasserve, E. (2010) *FEBS. J.* **277**, 1070–1075
- Borikova, A. L., Dibble, C. F., Sciaky, N., Welch, C. M., Abell, A. N., Bencharit, S., and Johnson, G. L. (2010) *J. Biol. Chem.* **285**, 11760–11764
- Whitehead, K. J., Chan, A. C., Navankasattusas, S., Koh, W., London, N. R., Ling, J., Mayo, A. H., Drakos, S. G., Jones, C. A., Zhu, W., Marchuk, D. A., Davis, G. E., and Li, D. Y. (2009) *Nat. Med.* **15**, 177–184
- Stockton, R. A., Shenkar, R., Awad, I. A., and Ginsberg, M. H. (2010) *J. Exp. Med.* **207**, 881–896
- Preisinger, C., Short, B., De Corte, V., Bruyneel, E., Haas, A., Kopajtich, R., Gettemans, J., and Barr, F. A. (2004) *J. Cell Biol.* **164**, 1009–1020

16. Fidalgo, M., Fraile, M., Pires, A., Force, T., Pombo, C., and Zalvide, J. (2010) *J. Cell Sci.* **123**, 1274–1284
17. Gingras, A. C., Caballero, M., Zarske, M., Sanchez, A., Hazbun, T. R., Fields, S., Sonnenberg, N., Hafen, E., Raught, B., and Aebersold, R. (2005) *Mol. Cell Proteomics* **4**, 1725–1740
18. Mao, D. Y., Neculai, D., Downey, M., Orlicky, S., Haffani, Y. Z., Ceccarelli, D. F., Ho, J. S., Szilard, R. K., Zhang, W., Ho, C. S., Wan, L., Fares, C., Rumpel, S., Kurinov, I., Arrowsmith, C. H., Durocher, D., and Sicheri, F. (2008) *Mol. Cell.* **32**, 259–275
19. Pelletier, L., Jokitalo, E., and Warren, G. (2000) *Nat. Cell Biol.* **2**, 840–846
20. Lee, K. P., Dey, M., Neculai, D., Cao, C., Dever, T. E., and Sicheri, F. (2008) *Cell* **132**, 89–100
21. Li, X., Baillie, G. S., and Houslay, M. D. (2009) *J. Biol. Chem.* **284**, 16170–16182
22. Smith, M. J., Hardy, W. R., Murphy, J. M., Jones, N., and Pawson, T. (2006) *Mol. Cell. Biol.* **26**, 8461–8474
23. Kittler, R., Pelletier, L., Heninger, A. K., Slabicki, M., Theis, M., Miroslaw, L., Poser, I., Lawo, S., Grabner, H., Kozak, K., Wagner, J., Surendranath, V., Richter, C., Bowen, W., Jackson, A. L., Habermann, B., Hyman, A. A., and Buchholz, F. (2007) *Nat. Cell Biol.* **9**, 1401–1412
24. Gonon, E. M., Skalski, M., Kean, M., and Coppolino, M. G. (2005) *FEBS Lett.* **579**, 6169–6178
25. Lawo, S., Bashkurov, M., Mullin, M., Ferreria, M. G., Kittler, R., Habermann, B., Tagliaferro, A., Poser, I., Hutchins, J. R., Hegemann, B., Pinchev, D., Buchholz, F., Peters, J. M., Hyman, A. A., Gingras, A. C., and Pelletier, L. (2009) *Curr. Biol.* **19**, 816–826
26. Etienne-Manneville, S., and Hall, A. (2001) *Cell* **106**, 489–498
27. Liu, G., Zhang, J., Larsen, B., Stark, C., Breitkreutz, A., Lin, Z. Y., Breitkreutz, B. J., Ding, Y., Colwill, K., Pascalescu, A., Pawson, T., Wrana, J. L., Nesvizhskii, A. I., Raught, B., Tyers, M., and Gingras, A. C. (2010) *Nat. Biotechnol.* **28**, 1015–1017
28. Skarra, D. V., Goudreault, M., Choi, H., Mullin, M., Nesvizhskii, A. I., Gingras, A. C., and Honkanen, R. E. (2011) *Proteomics* **11**, 1508–1516
29. Choi, H., Larsen, B., Lin, Z. Y., Breitkreutz, A., Mellacheruvu, D., Fermin, D., Qin, Z. S., Tyers, M., Gingras, A. C., and Nesvizhskii, A. I. (2011) *Nat. Methods* **8**, 70–73
30. Li, X., Zhang, R., Zhang, H., He, Y., Ji, W., Min, W., and Boggon, T. J. (2010) *J. Biol. Chem.* **285**, 24099–24107
31. Hoellerer, M. K., Noble, M. E., Labesse, G., Campbell, I. D., Werner, J. M., and Arold, S. T. (2003) *Structure* **11**, 1207–1217
32. Lupas, A., Van Dyke, M., and Stock, J. (1991) *Science* **252**, 1162–1164
33. Gaillard, S., Bailly, Y., Benoist, M., Rakitina, T., Kessler, J. P., Fronzaroli-Molinieres, L., Dargent, B., and Castets, F. (2006) *Traffic* **7**, 74–84
34. Farhan, H., and Rabouille, C. (2011) *J. Cell Sci.* **124**, 171–180
35. Bisel, B., Wang, Y., Wei, J. H., Xiang, Y., Tang, D., Miron-Mendoza, M., Yoshimura, S., Nakamura, N., and Seemann, J. (2008) *J. Cell Biol.* **182**, 837–843
36. Yadav, S., Puri, S., and Linstedt, A. D. (2009) *Mol. Biol. Cell* **20**, 1728–1736
37. Jaffe, A. B., and Hall, A. (2005) *Annu. Rev. Cell Dev. Biol.* **21**, 247–269
38. Kemp, H. A., and Sprague, G. F., Jr. (2003) *Mol. Cell. Biol.* **23**, 1750–1763
39. Simonin, A. R., Rasmussen, C. G., Yang, M., and Glass, N. L. (2010) *Fungal Genet Biol.* **47**, 855–868
40. Xiang, Q., Rasmussen, C., and Glass, N. L. (2002) *Genetics* **160**, 169–180
41. Guzzo, R. M., Wigle, J., Salih, M., Moore, E. D., and Tuana, B. S. (2004) *Biochem. J.* **381**, 599–608
42. Baryshnikova, A., Costanzo, M., Kim, Y., Ding, H., Koh, J., Toufighi, K., Youn, J. Y., Ou, J., San Luis, B. J., Bandyopadhyay, S., Hibbs, M., Hess, D., Gingras, A. C., Bader, G. D., Troyanskaya, O. G., Brown, G. W., Andrews, B., Boone, C., and Myers, C. L. (2010) *Nat. Methods* **7**, 1017–1024
43. Jacinto, E., Loewith, R., Schmidt, A., Lin, S., Rueegg, M. A., Hall, A., and Hall, M. N. (2004) *Nat. Cell Biol.* **6**, 1122–1128
44. Loewith, R., Jacinto, E., Wullschleger, S., Lorberg, A., Crespo, J. L., Bonenfant, D., Oppliger, W., Jenoe, P., and Hall, M. N. (2002) *Mol. Cell.* **10**, 457–468
45. Helliwell, S. B., Howald, I., Barbet, N., and Hall, M. N. (1998) *Genetics* **148**, 99–112
46. Zheng, X., Xu, C., Di Lorenzo, A., Kleaveland, B., Zou, Z., Seiler, C., Chen, M., Cheng, L., Xiao, J., He, J., Pack, M. A., Sessa, W. C., and Kahn, M. L. (2010) *J. Clin. Invest.* **120**, 2795–2804
47. Ribeiro, P. S., Josue, F., Wepf, A., Wehr, M. C., Rinner, O., Kelly, G., Tapon, N., and Gstaiger, M. (2010) *Mol. Cell.* **39**, 521–534
48. Hilder, T. L., Malone, M. H., Bencharit, S., Colicelli, J., Haystead, T. A., Johnson, G. L., and Wu, C. C. (2007) *J. Proteome Res.* **6**, 4343–4355
49. Ceccarelli, D. F., Laister, R. C., Mulligan, V. K., Kean, M. J., Goudreault, M., Scott, I., Derry, W. B., Chakrabarty, A., Gingras, A. C., and Sicheri, F. (2011) *J. Biol. Chem.* **286**, 25056–25064

SAINT: probabilistic scoring of affinity purification–mass spectrometry data

Hyungwon Choi¹, Brett Larsen², Zhen-Yuan Lin², Ashton Breitkreutz², Dattatreya Mellacheruvu¹, Damian Fermin¹, Zhaojun S Qin^{3,8}, Mike Tyers^{2,4–6}, Anne-Claude Gingras^{2,4} & Alexey I Nesvizhskii^{1,7}

We present ‘significance analysis of interactome’ (SAINT), a computational tool that assigns confidence scores to protein-protein interaction data generated using affinity purification–mass spectrometry (AP-MS). The method uses label-free quantitative data and constructs separate distributions for true and false interactions to derive the probability of a bona fide protein-protein interaction. We show that SAINT is applicable to data of different scales and protein connectivity and allows transparent analysis of AP-MS data.

The analysis of protein complexes and protein interaction networks is very important for biological research. A combination of affinity purification and mass spectrometry (AP-MS) has been increasingly used for both small-scale and large-scale analysis of protein complexes and interaction networks^{1–4}. However, the development of computational tools for the processing of AP-MS data has not kept pace with improvements in experimental approaches. In addition to the general challenge of false positive protein identifications in mass spectrometry-based proteomic data⁵, unfiltered AP-MS datasets contain many nonspecifically binding proteins; filtering these contaminants is the foremost computational challenge.

Whereas early methods filtered the noise using binary data (presence or absence of a protein), newer methods take into account quantitative information embedded in the mass spectrometric data (for example, label-free quantification, such as spectral counts). One such method converts the normalized spectral abundance factor (NSAF) into the posterior probability of a true interaction between a bait-prey pair using simple heuristics, which we term PP-NSAF hereafter⁶. Another method, named

CompPASS, computes scores that adjust observed spectral counts relative to the reproducibility of detection across biological replicates and to the frequency of observing prey proteins in purifications of different baits⁷. Although both approaches can effectively analyze the datasets for which they had been developed, these scores are an empirical transformation of spectral counts without a probability model that can be used to estimate the measurement errors in the data in a transparent manner.

We have recently introduced an advanced approach for statistical analysis of interaction data from AP-MS experiments using label-free quantification, which we termed significance analysis of interactome (SAINT)⁸. As PP-NSAF and CompPASS, we had designed our original SAINT approach to analyze a specific dataset, the yeast kinase and phosphatase interactome. Expanding on this method, here we present a generalized SAINT framework that can be used to compute interaction probabilities in a variety of datasets. The method incorporates negative controls that are commonly generated as a part of the experimental study but can also be applied to large datasets in the absence of such data. We illustrate the methodology and its advantages through the analysis of datasets of different sizes and network density: from a large, sparsely connected network involving human deubiquitinating enzymes to a smaller, highly interconnected network for chromatin remodeling proteins and even to the analysis of a single bait, the protein CDC23.

The aim of SAINT is to convert the label-free quantification (spectral count X_{ij}) for a prey protein i identified in a purification of bait j into the probability of a true interaction between the two proteins, $P(\text{true} | X_{ij})$. The spectral counts for each prey-bait pair are modeled with a mixture distribution of two components representing true and false interactions. Note that these distributions are specific to each bait-prey pair. The parameters for true and false distributions, $P(X_{ij} | \text{true})$ and $P(X_{ij} | \text{false})$, and the prior probability π_T of true interactions in the dataset, are inferred from the spectral counts for all interactions that involve prey i and bait j . SAINT normalizes spectral counts to the length of the proteins and to the total number of spectra in the purification.

In addition to the experimental data for bait proteins, AP-MS data often contain negative controls (Fig. 1a). When these are available, SAINT estimates the spectral count distribution for false interactions directly from the negative controls, which makes the modeling approach semisupervised (Online Methods). SAINT modeling can also be performed without negative control data, so long as a sufficient number of independent baits are profiled and provided that these baits are not densely interconnected. In this case (Fig. 1b), a prey detected in the purification of a bait is

¹Department of Pathology, University of Michigan, Ann Arbor, Michigan, USA. ²Centre for Systems Biology, Samuel Lunenfeld Research Institute, Toronto, Ontario, Canada. ³Department of Biostatistics and Center for Statistical Genetics, University of Michigan, Ann Arbor, Michigan, USA. ⁴Department of Molecular Genetics, University of Toronto, Toronto, Ontario, Canada. ⁵Wellcome Trust Centre for Cell Biology, University of Edinburgh, Edinburgh, UK. ⁶Centre for Systems Biology, School of Biological Sciences, University of Edinburgh, Edinburgh, UK. ⁷Center for Computational Medicine and Bioinformatics, University of Michigan, Ann Arbor, Michigan, USA. ⁸Present address: Department of Biostatistics and Bioinformatics, Emory University, Atlanta, Georgia, USA. Correspondence should be addressed to A.C.G. (gingras@lunenfeld.ca) or A.I.N. (nesvi@med.umich.edu).

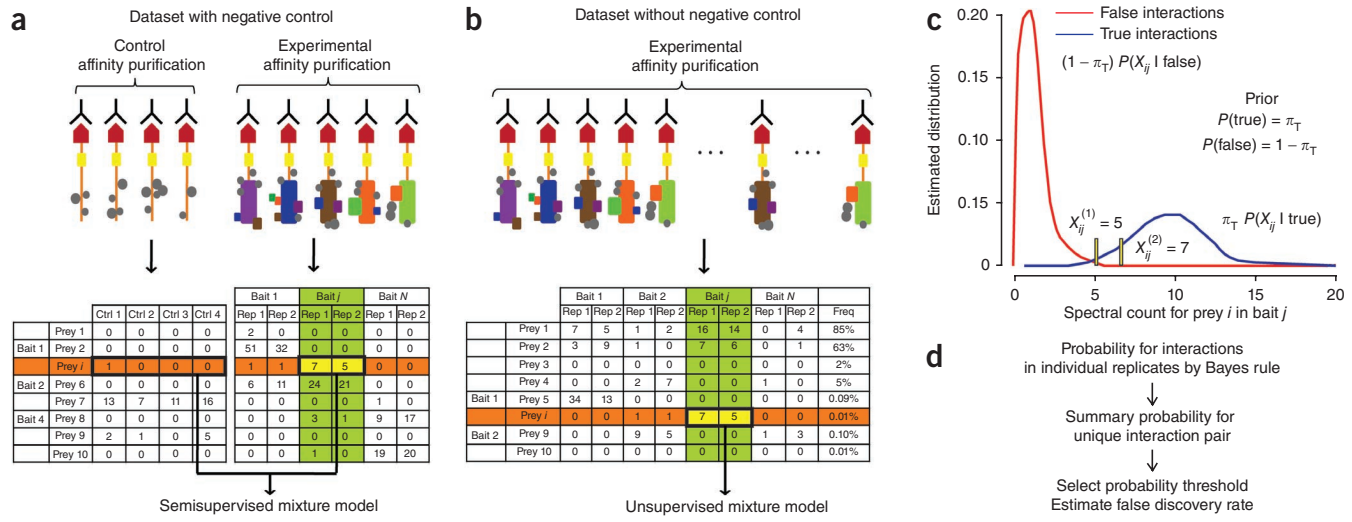


Figure 1 | Probability model in SAINT. **(a,b)** Interaction data in the presence (**a**) and absence (**b**) of control purifications. Schematic of the experimental AP-MS procedure is shown at the top and a spectral count interaction table is illustrated at the bottom. Ctrl, control; rep, replicate; freq, frequency. **(c)** Modeling spectral count distributions for true and false interactions. For the interaction between prey i and bait j , SAINT uses all relevant data for the two proteins, as shown in the column of the bait (green) and the data in the row of the prey (orange) in **a** and **b**. **(d)** Probability is calculated for each replicate by application of Bayes rule, and a summary probability is calculated for the interaction pair (i,j) .

scored in reference to the quantitative information for the same prey across purifications of all other baits in the dataset. Although this is possible for large datasets such as the yeast kinase and phosphatase network⁸, and the human deubiquitinating (DUB) enzyme interaction network⁷ (which each contain more than 75 baits), this unsupervised approach involves additional assumptions and separate treatment of high- and low-frequency prey proteins (Online Methods).

One challenge in modeling AP-MS data is the limited number of replicates that are typically available for each bait. SAINT addresses this problem by inferring individual bait-prey interaction parameters through joint modeling of the entire bait-prey data. To this end, SAINT defines a protein-specific abundance parameter and establishes a multiplicative model in the mixture component distributions. In other words, if prey i and bait j interact, then the ‘interaction abundance’ (the spectral count of the prey i in purification with bait j) is assumed to be proportional to $\alpha_i \times \alpha_j$. Under this assumption, the protein-specific abundance parameters α_i and α_j can be learned not only from the interaction between the two proteins themselves but also from other bona fide interactions that involve either one of them. The same principle applies to false interactions. Hence, SAINT builds a large number of mixture distributions by pooling data (separate mixture distributions for individual prey-bait pairs), but all models are interconnected through the shared abundance parameters.

The probability distributions $P(X_{ij} | \text{true})$ and $P(X_{ij} | \text{false})$ are then used to calculate the posterior probability of true interaction $P(\text{true} | X_{ij})$ (Fig. 1c,d and Online Methods). For baits profiled in replicates, the next step involves the computation of a combined probability score from independent scoring of each replicate (Online Methods). Finally, SAINT probabilities can be used to estimate the false discovery rate (FDR). By ordering interactions in decreasing order of probability, a threshold can be selected that considers the average of the complement probabilities as the Bayesian FDR⁹. Although the accuracy of FDR estimates remains

to be validated, the availability of an objective reliability measure that has been widely used is an advantage over other methods.

We first tested performance of the generalized SAINT model using a human dataset⁶ centered around four key protein complexes that are involved in chromatin remodeling: prefoldin, hINO80, SRCAP and TRRAP or TIP60 (referred to as the TIP49 dataset). Although the original work focused the analysis on the interaction network between a core set of 65 proteins, here we analyzed the entire dataset provided by the authors of that study. The dataset consists of 27 baits (35 purifications) and 1,207 preys, and yielded 5,521 unfiltered interactions. The dataset also included 35 negative controls, which allows semisupervised modeling (Fig. 1a and Supplementary Table 1).

We applied SAINT to these data and compared the results to PP-NSAF⁶ and CompPASS Z and D^N scores^{7,10}, which we reimplemented in-house (Online Methods). We note that PP-NSAF⁶ removes all interactions involving prey proteins for which the sum of squared NSAF values across the negative control purifications is higher than that in the experiments that contain bait proteins. CompPASS is the only method that does not incorporate negative controls in scoring.

SAINT selected 1,375 interactions at the probability threshold 0.9, which was approximately equivalent to an estimated FDR of 2%. In PP-NSAF, as arbitrary cutoffs were set to define high, moderate and low probability interaction sets, the same number of top-scoring interactions was selected (corresponding to a PP-NSAF probability 0.2 or higher). In CompPASS, the same number of interactions corresponded to a D^N -score threshold of 1.48 (Supplementary Table 1).

We evaluated the performance of each algorithm first by benchmarking the selected interactions against two interaction databases named BioGRID¹¹ and iRefWeb¹² (Fig. 2a), and second by assessing the co-annotation rate of interaction partners to common Gene Ontology (GO) terms in ‘biological processes’ (Fig. 2b and Supplementary Table 1). SAINT-filtered interactions (with

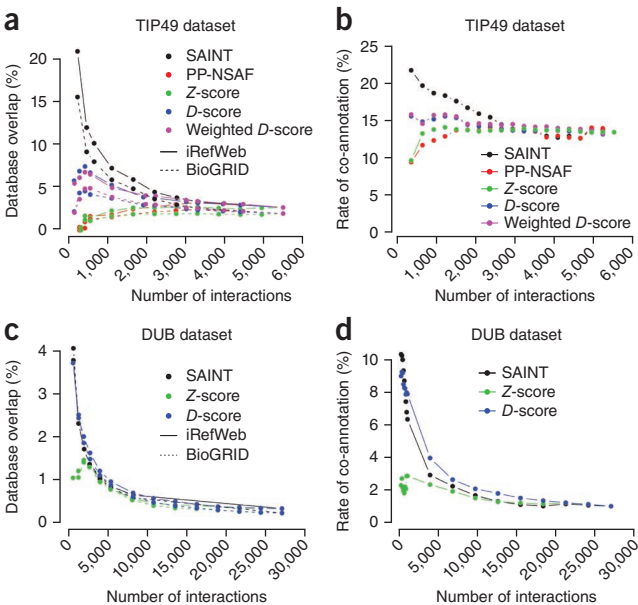


Figure 2 | Analysis of TIP49 and DUB datasets. **(a)** Benchmarking of filtered interactions in the TIP49 dataset by the overlap with interactions previously reported in BioGRID and iRefWeb databases. **(b)** Co-annotation of interaction partners to common GO terms in ‘biological processes’ in the TIP49 dataset. **(c)** Benchmarking against BioGRID and iRefWeb in the DUB dataset. **(d)** Co-annotation to GO terms in the DUB dataset.

controls) consistently showed the highest overlap with previously reported interactions and co-annotation rates to terms relevant to chromatin remodeling, including histone acetylation, protein amino acid acetylation, chromatin organization and modification, and cellular macromolecular complex assembly. Variation of the SAINT probability thresholds ($\sim 0.8\text{--}0.95$) did not qualitatively change this conclusion (data not shown). Note that omission of negative controls from SAINT modeling decreased the overlap with the interactions reported in BioGRID and iRefWeb (Supplementary Fig. 1). Explicit incorporation of the negative control data improved the robustness of modeling, especially in small or medium datasets.

We then tested the performance of SAINT for large-scale datasets without negative controls (Fig. 1b) on the human deubiquitinating enzymes (DUB) dataset⁷ (this dataset was used in the development of CompPASS). High confidence interactions from SAINT were compared to the high confidence set from CompPASS (Supplementary Table 2). Owing to the absence of negative controls, it was not possible to apply PP-NSAF to this dataset. SAINT probabilities and D^N scores were notably correlated (Pearson correlation, $r = 0.79$). At a probability threshold of 0.8, SAINT selected 1,300 interactions, whereas a threshold of CompPASS $D^N \geq 1$ (as used in ref. 7) reported 1,377 interactions. Of these, 1,051 interactions were identified by both methods. Reflecting the similarity of selected interactions, SAINT and CompPASS recovered previously reported interactions at comparable rates (Fig. 2c). In the top 1,000 interactions, SAINT showed higher overlap with published data. The co-annotation of interaction partners to the common GO terms also showed similar results between the two methods (Fig. 2d), including relevant terms such as positive and negative regulation of ubiquitin-protein ligase activity during mitotic cell cycle, proteasome, and

so on (Supplementary Table 2). Although SAINT and CompPASS recovered largely overlapping interactions, SAINT removed the interactions identified with 1–2 spectral counts, which were still scored by CompPASS if they were specific to a single bait protein and detected in duplicates.

Another advantage of SAINT over other methods is that it is applicable to the analysis of small-scale datasets for which control purifications are available; this extends to the case of a single bait. We illustrate this by using a recent dataset¹³ that contains three experimental purifications of the bait CDC23 and three control purifications. In the original analysis, the authors of the study identified true interactions using ion intensity-based quantification followed by a simple *t*-test. We applied the SAINT approach to the same dataset by using spectral counts (the data were re-searched in-house; Online Methods). The results obtained by SAINT were nearly identical to those in the initial report (Supplementary Table 3), the sole exception being the single peptide hit C11orf51, which was reported as a new interactor in the original analysis¹³ but which was removed by SAINT.

The SAINT model presented here is based on label-free quantification using spectral counts, a parameter that is easily extracted from most AP-MS datasets. SAINT can also be extended to model other types of quantitative parameters such as peptide ion intensity¹⁴ or other continuous variables¹⁵, which can be accommodated by simply substituting the likelihood with an appropriate continuous distribution. SAINT is available as Supplementary Software.

METHODS

Methods and any associated references are available in the online version of the paper at <http://www.nature.com/naturemethods/>.

Note: Supplementary information is available on the *Nature Methods* website.

ACKNOWLEDGMENTS

Supported by grants from the Canadian Institute of Health Research to A.-C.G. (MOP-84314) and M.T. (MOP-12246); the US National Institutes of Health to M.T. (5R01RR024031), A.I.N. and A.-C.G. (R01-GM094231), and A.I.N. (R01-CA126239); a Royal Society Wolfson Research Merit Award and a Scottish Universities Life Sciences Alliance Research Chair to M.T.; a Canada Research Chair in Functional Proteomics to A.-C.G.; and the Lea Reichmann Chair in Cancer Proteomics to A.-C.G. We thank M. Sardiu, M. Washburn and M. Sowa for providing additional information regarding the datasets used in this work, G. Bader for discussions and W. Dunham for reading the manuscript.

AUTHOR CONTRIBUTIONS

H.C. and A.I.N. developed, implemented and tested the SAINT method; H.C. wrote the software; B.L., A.B., Z.-Y.L., A.-C.G. and M.T. generated data for the initial SAINT modeling and provided feedback on the model performance; D.M. and D.F. assisted with data analysis and processing; Z.S.Q. contributed to statistical model development; H.C., A.-C.G. and A.I.N. wrote the manuscript; A.I.N. and A.-C.G. conceived the study; A.I.N. directed the project with input from A.-C.G.

COMPETING FINANCIAL INTERESTS

The authors declare no competing financial interests.

Published online at <http://www.nature.com/naturemethods/>. Reprints and permissions information is available online at <http://npg.nature.com/reprintsandpermissions/>.

1. Ewing, R.M. et al. *Mol. Syst. Biol.* **3**, 89 (2007).
2. Gavin, A.C. et al. *Nature* **440**, 631–636 (2006).
3. Jeronimo, C. et al. *Mol. Cell* **27**, 262–274 (2007).
4. Krogan, N.J. et al. *Nature* **440**, 637–643 (2006).
5. Nesvizhskii, A.I., Vitek, O. & Aebersold, R. *Nat. Methods* **4**, 787–797 (2007).
6. Sardiu, M.E. et al. *Proc. Natl. Acad. Sci. USA* **105**, 1454–1459 (2008).

7. Sowa, M.E., Bennett, E.J., Gygi, S.P. & Harper, J.W. *Cell* **138**, 389–403 (2009).
8. Breitkreutz, A. et al. *Science* **328**, 1043–1046 (2010).
9. Müller, P., Parmigiani, G & Rice, K. in *Bayesian Statistics Vol. 8* (eds., Bernardo, J.M. et al.) 349–370 (Oxford University Press, 2007).
10. Behrends, C., Sowa, M.E., Gygi, S.P. & Harper, J.W. *Nature* **466**, 68–76 (2010).
11. Breitkreutz, B.J. et al. *Nucleic Acids Res.* **36**, D637–D640 (2008).
12. Turner, B. et al. *Database (Oxford)* **2010**, baq023 (2010).
13. Hubner, N.C. et al. *J. Cell Biol.* **189**, 739–754 (2010).
14. Rinner, O. et al. *Nat. Biotechnol.* **25**, 345–352 (2007).
15. Griffin, N.M. et al. *Nat. Biotechnol.* **28**, 83–89 (2010).

ONLINE METHODS

Label-free quantification by spectral counting. Label-free quantification in this work was based on spectral counting. Spectral counts are the sum of every successful instance of sequencing a peptide from a particular protein by mass spectrometry, including redundant spectra. With proper normalization, spectral counts can be used as a quantitative measure of protein abundance in the sample. This method is conceptually similar to the approach of measuring gene expression using SAGE, EST or RNA-Seq fragment count data. For both DUB and TIP49 datasets, spectral count data were taken exactly as provided by the authors^{6,7}. Briefly, the DUB dataset and the TIP49 dataset were searched using SEQUEST¹⁶ using target-decoy database strategies against human databases; selected parameter sets were defined by the authors for filtering. The DUB dataset accepted peptides based on the following criteria. (i) High-stringency set: XCorr 2+ ≥ 2.5; 3+ ≥ 3.2; 4+ ≥ 3.5; +1 charge states were not collected. (ii) Complementary peptide set for proteins identified with high confidence: XCorr thresholds ≥ 1.0; ΔCn ≥ 0.05. The parameters selected by the authors of the TIP49 dataset were: XCorr 1+ ≥ 1.8 for 2+ ≥ 2.5, and 3+ ≥ 3.5 (fully tryptic peptides of at least seven amino acids long with max Sp score of 10). The reported spectral FDR for the entire TIP49 dataset was 0.065%; for the DUB data, a set FDR of 2% was selected to populate the interaction tables. No control data were used for the DUB dataset. In the case of the TIP49 dataset, 35 controls were provided alongside the experimental samples. These controls were generated from HeLa and HEK293 cell lines under nine different conditions. We merged the 35 measurements to 9 by taking the largest spectral count for each prey in each condition (**Supplementary Table 1**). For the analysis of the CDC23 data, the data were downloaded from Tranche (trancheproject.org), and re-searched in-house using X!Tandem/k-score against the RefSeq database using search parameters similar to those used in ref. 13. The search results were processed using PeptideProphet and ProteinProphet⁵, and filtered to achieve a protein-level FDR of less than 0.5%. The spectral counts were extracted using the in-house software Abacus (D.F. and A.I.N., unpublished data).

SAINT model. This section describes the generalized statistical modeling framework for the datasets with and without control purifications (**Fig. 1a,b**). In both cases, the spectral counts for prey *i* in purification with bait *j* are considered to be either from a Poisson distribution representing true interaction (with mean count λ_{ij}) or from a Poisson distribution representing false interaction (with mean count κ_{ij}). In the form of probability distribution, we write

$$P(X_{ij} | \bullet) = \pi_T P(X_{ij} | \lambda_{ij}) + (1 - \pi_T) P(X_{ij} | \kappa_{ij}) \quad (1)$$

where π_T is the proportion of true interactions in the data, and dot notation represents all relevant model parameters estimated from the data (here, specifically for the pair of prey *i* and bait *j*). The individual bait-prey interaction parameters λ_{ij} and κ_{ij} are estimated from joint modeling of the entire bait-prey association matrix, with the probability distribution (likelihood) of the form $P(X | \bullet) = \prod_{i,j} P(X_{ij} | \bullet)$. The proportion π_T is also estimated from the model, which relies on latent variables in the sampling algorithm (see below).

When at least three control purifications are available, and assuming that the control purifications provide a robust

representation of nonspecific interactors, the parameter κ_{ij} can be estimated from spectral counts for prey *i* observed in the negative controls. This is equivalent to assuming

$$\begin{aligned} P(X_{ij} | \bullet) &= \prod_{i,j: j \in E} (\pi_T P(X_{ij} | \lambda_{ij}) + (1 - \pi_T) P(X_{ij} | \kappa_{ij})) \times \\ &\quad \prod_{i,j: j \in C} (P(X_{ij} | \kappa_{ij})) \end{aligned} \quad (2)$$

where *E* and *C* denote the group of experimental purifications and the group of negative controls, respectively. This leads to a semisupervised mixture model in the sense that there is a fixed assignment to false interaction distribution for negative controls. As negative controls guarantee sufficient information for inferring model parameters for false interaction distributions, Bayesian nonparametric inference using Dirichlet process mixture priors can be used to derive the posterior distribution of protein-specific abundance parameters in the model. As a result, the mean parameters in the Poisson likelihood functions follow a nonparametric posterior distribution, allowing more flexible modeling at the proteome level. Under this setting, all model parameters are estimated from an efficient Markov chain Monte Carlo algorithm¹⁷.

To elaborate on the two distributions, the mean parameter for each distribution is assumed to have the following form. For false interactions, it is assumed that spectral counts follow a Poisson distribution with mean count

$$\log(\kappa_{ij}) = \log(l_i) + \log(c_j) + \gamma_0 + \mu_i \quad (3)$$

where l_i is the sequence length of prey *i*, and c_j is the bait coverage, the spectral count of the bait in its own purification experiment, γ_0 is the average abundance of all contaminants and μ_i is prey *i* specific mean difference from γ_0 . For true interactions, it is assumed that spectral counts follow a Poisson distribution with mean count

$$\log(\lambda_{ij}) = \log(l_i) + \log(c_j) + \beta_0 + \alpha_{bj} + \alpha_{pi} \quad (4)$$

where β_0 is the average abundance of prey proteins in those cases where they are true interactors of the bait, α_{bj} is bait *j* specific abundance factor and α_{pi} is prey *i* specific abundance factor. In other words, the mean spectral count for a prey protein in a true interaction is calculated using a multiplicative model combining bait- and prey-specific abundance parameters. This formulation substantially reduces the number of parameters in the model, avoiding the need to estimate every λ_{ij} separately.

For datasets without negative control purifications, the mixture component distributions for true and false interactions have to be identified solely from experimental (noncontrol) purifications. In this case, a user-specified threshold is applied to divide preys into high-frequency and low-frequency groups, denoted as $Y_i = 1$ or 0 if prey *i* belongs to the high- or low-frequency group, respectively. An arbitrary 20% threshold was applied in the case of the DUB dataset; however, the results were not very sensitive to the choice of the threshold. For preys in the high frequency group, the model considers spectral counts for the observed prey proteins (ignoring zero count data, which represent the absence of protein identification), as there are sufficient data to estimate distribution parameters. In the low-frequency group, nondetection of a prey is included to help the separation of high-count from low-count hits. The entire mixture model can then be expressed as

$$P(X_{ij} | \bullet) = \prod_{i,j} (\pi_T P(X_{ij} | \lambda_{ij}) + (1 - \pi_T) P(X_{ij} | \kappa_{ij}))^{Z_{ij}} \quad (5)$$

where $Z_{ij} = 1(Y_i=0) + 1(Y_i=1, X_{ij}>0)$ and the false and true interaction distributions are modeled by equations (3) and (4), respectively.

The posterior probability of a true interaction given the data is computed using Bayes rule

$$P(\text{true}|X_{ij}) = T_{ij} / (T_{ij} + F_{ij}) \quad (6)$$

where $T_{ij} = \pi_T P(X_{ij} | \lambda_{ij})$ and $F_{ij} = (1 - \pi_T) P(X_{ij} | \kappa_{ij})$. If there are replicate purifications for bait j , the final probability is computed as an average of individual probabilities over replicates. Note that one alternative approach is to compute the probability assuming conditional independence over replicates, that is, $\prod_{k \in j} P(X_{ijk} | \lambda_{ijk})$ and $\prod_{k \in j} P(X_{ijk} | \kappa_{ijk})$ for true and false interactions, with additional index k denoting replicates for bait j . Unlike average probability, this probability puts less emphasis on the degree of reproducibility, and thus may be more appropriate in datasets where replicate analysis of the same bait is performed using different experimental conditions (for example, purifications using different affinity tags) to increase the coverage of the interactome.

When probabilities have been calculated for all interaction partners, the Bayesian false discovery rate (FDR) can be estimated from the posterior probabilities as follows. For each probability threshold p^* , the Bayesian FDR is approximated by

$$\text{FDR}(p^*) = (\sum_k 1(p_k \geq p^*)(1 - p_k)) / (\sum_k 1(p_k \geq p^*)) \quad (7)$$

where p_k is the posterior probability of true interaction of protein pair k . The output from SAINT allows the user to select a probability threshold to filter the data to achieve the desired FDR.

Implementation of other scores. CompPASS^{7,10} calculates two different scores. First, Z score is constructed by mean centering and scale normalization in the conventional Z statistic, where

mean and s.d. are estimated from the data for each prey. D score is based on the spectral count adjusted by a scaling factor that reflects the reproducibility of prey detection over replicate purifications of the same bait. If X_{ij} denotes the spectral count between prey i and bait j , then $D_{ij} = ((k / f_i)^{p_{ij}} \cdot X_{ij})^{1/2}$, where k is the total number of baits profiled in the experiment, f_i is the number of experiments in which prey i was detected and p_{ij} is the number of replicate experiments of bait j in which prey i was detected. After computing the scores, a threshold D^T is selected from simulation data so that 95% of the simulated data falls below the chosen threshold. Note that CompPASS merges replicate data for bait j to produce a unique spectral count X_{ij} for a given pair. In doing so, it takes nonzero counts only when the prey is identified in a single replicate or otherwise averages counts over multiple replicates. In the analysis of TIP49 dataset, we used both the original D score and the more recently implemented ‘weighted D score’, which is designed for datasets with large protein complexes¹⁰. The weighted D scores are shown in **Figure 2** for the TIP49 dataset.

To replicate PP-NSAF⁶, we removed 330 contaminants from the dataset using the vector magnitude approach. After filtering, probabilities were computed using an in-house script following the method presented in ref. 6. Although our implementation did not reproduce exactly the same scores for the interactions reported in ref. 6, the scores computed by the in-house implementation showed a clear linear correspondence to the reported scores (Pearson correlation 0.89).

Software. The source C code and a user manual for the generalized SAINT model described in this work (SAINT 2.0) can be downloaded from <http://saint-apms.sourceforge.net/>, where updates will be distributed. The published version is also available as **Supplementary Software**.

16. Eng, J.K., McCormack, A.L. & Yates, J.R.I. *J. Am. Soc. Mass Spectrom.* **5**, 976–989 (1994).
17. Ishwaran, H. & James, L.F. *J. Am. Stat. Assoc.* **96**, 161–173 (2001).



THE UNIVERSITY OF CHICAGO Division of Biological Sciences

Issam A. Awad, MD, MSc, FACS, MA (Hon)

Professor and Director

NEUROVASCULAR SURGERY PROGRAM

SECTION OF NEUROSURGERY

5841 South Maryland Avenue, MC3026, Room J341, Chicago, Illinois 60637

Phone (773) 702-2123 Fax (773) 702-3518 iawad@uchicago.edu

February 24, 2012

Anne-Claude Gingras

Senior Investigator, Samuel Lunenfeld Research Institute

Associate Professor, Dept Molecular Genetics, University of Toronto

W. Brent Derry

Senior Scientist, Hospital for Sick Children

Associate Professor, Dept Molecular Genetics, University of Toronto

Dear Anne-Claude and Brent:

It is my pleasure to express my strong support for your CIHR application entitled "**Molecular Mechanisms of Cerebral Cavernous Malformations**". Your collaborative work on delineating the CCM regulatory network is very exciting and holds great potential for identifying new therapeutic targets for this potentially devastating, and heretofore untreated disease.

As you know, the CCM affects about 0.5% of the population, predisposing patients to a lifetime risk of stroke and epilepsy. Unfortunately, the only current treatment option for CCM patients is neurosurgery, which is costly and risky, and there is no guarantee that patients who undergo resection or radiosurgery are in fact cured or would become symptom free. Thus, there is a great need for developing targeted pharmacological strategies to prevent CCM lesion genesis and maturation. As you know, we have identified RhoA kinase (ROCK) activation as a signaling mechanism triggered by the loss of CCM1 and CCM2 gene activity, and potentially mediating CCM lesion development. We are testing specific ROCK inhibitor fasudil and statins (which also confer RhoA inhibition through their pleiomorphic effects, in addition to their cholesterol lowering properties) as potential therapies for reducing CCM lesion burden and bleeds in our mouse CCM models. Our preliminary results (published in *Stroke* 2012) are promising, but there is still a pressing need to consider alternative drug targets, particularly in the case of CCM3 patients for whom the mutation may have effects outside of the Rho pathway. CCM3, as you know, is the most devastating CCM genotype, and its unique genetic variants and signaling complex remain unknown.

Already the two of you have contributed important insights into the molecular basis of CCM and your collaborative efforts have resulted in two excellent papers. The association of the STRIPAK complex that Anne-Claude's lab discovered with CCM3 and the GCKII kinases provides a new framework for understanding the signaling partners of CCM3, and the structural resolution of the CCM3/GCKIII binding surfaces provides important insights into the molecular mechanism by which CCM3 regulates the kinase. Using the excretory cell of *C. elegans* as an in vivo model of vascular development and Brent's demonstration that the worm CCM3 gene is critical for its

development places you in a very good position to exploit the powerful genetics of this organism to identify CCM modifier genes and to define new therapeutic targets.

Indeed, my own team would be more than delighted to work with your group to test candidates you identify by proteomics and genetics using our pre-clinical murine CCM models which recapitulate the human disease in the heterozygous state. We are also able to validate your results through differential genomics of CCM vasculature from human and murine lesions, which are being studied in ongoing experiments our laboratory.

Clearly, the powerful synergy between your two groups has been recognized by the CIHR by bridge funding you received in the previous competition. The importance of your work to the CCM field and the potential for helping patients is certainly worthy of full funding, so I wish you the best of luck in the March competition.

Sincerely,



Issam A. Awad, MD, MSc, FACS
Professor of Surgery (Neurosurgery), Neurology and the Cancer Center
Biological Sciences Division
Director, Neurovascular Surgery Program
University of Chicago

Founding Chairman, Scientific Advisory Board, Angioma Alliance
Past President, Congress of Neurological Surgeons
Past Chairman, AANS/CNS Section on Cerebrovascular Surgery
Past Governor, American College of Surgeons
Past Member, Executive Council of the American Stroke Association
Founding Past President, World Association of Lebanese Neurosurgeons

Best Doctors in America



Yale University

*Murat Gunel MD
Nixdorff German Professor
Chief, Neurovascular Surgery
Co-director, Yale Program on Neurogenetics
Director, Yale Program on Brain Tumor Research
Depts. of Neurosurgery, Neurobiology and Genetics*

Anne-Claude Gingras

Senior Investigator, Samuel Lunenfeld Research Institute
Associate Professor, Dept Molecular Genetics, University of Toronto

W. Brent Derry

Senior Scientist, Hospital for Sick Children
Associate Professor, Dept Molecular Genetics, University of Toronto

Dear Anne-Claude and Brent,

It is my pleasure to offer this letter of collaboration for your CIHR grant application to define the cerebral cavernous malformation (CCM) regulatory network. Your work in establishing the network of genes and proteins associated with CCM1, CCM2 and CCM3 is really helping to resolve some hotly debated topics in the field, such as the composition of CCM protein complexes, the mechanisms by which these proteins signal between cells to regulate tube morphogenesis, etc. I am confident that your work will not only help us understand the molecular mechanisms by which these proteins function but also uncover novel therapeutic targets that may be exploited in the clinical management of CCM in humans. At present the only option for these patients is invasive brain surgery, and it would make my life much easier if this disease could be managed with pharmacological therapeutics.

The combined power of *C. elegans* genetics and proteomic analysis has enormous potential for breaking open the biological mechanisms that lead to this disease in humans and discovering potential therapeutic targets. In fact, both of your groups have already made substantial contributions with your identification of the STRIPAK complex, elucidation of *kri-1*/CCM1 in apoptosis, and your recent papers showing how CCM3 associates with the Ste20 kinase and how they function with the STRIPAK complex in Golgi polarization. Your preliminary data showing that worm CCM3 is required for morphogenesis of the excretory canal is very exciting and illustrates the power of this system for understanding the role of CCM3 and its associated proteins in tubulogenesis. Collectively, this work has provided new and important insights about the biological function of CCM3 that distinguishes it from CCM1/CCM2. This parallels nicely clinical studies that indicate that patients with CCM3 mutations are more severely affected than patients with a CCM1 or CCM2 deletion.

My research interests intersect very well with your groups and it would be my pleasure to help analyze expression of the STRIPAK proteins in our CCM mouse models, as well as the high ranking candidates discovered in your proposed genetics and proteomics studies. We have an extensive collection of patient samples in our tissue banks and expertise in histochemistry to analyze expression of these proteins in patient samples. In addition, I would be happy to send you tissue from our CCM mouse strains and/or patient database for proteomic analysis. I am also very excited to help you characterize the phenotypes of the mouse CCM3 knock-in, which I believe is the ideal mouse model to directly assess whether all of the physiological roles of CCM3 are mediated through these still ill-characterized kinases. If this turns out to be the case, it could be a game-changer with regards to therapeutic design. Therefore, I am making available to you my conditional CCM3 mouse and any advise to help guide you in selecting the appropriate Cre lines to analyze CCM-like microvasculature defects. Alternatively, I would be happy to help analyze microvasculature defects in the knock-in mice, as this is something that my laboratory has abundant expertise.

You also know that I have embarked into an exome sequencing project from CCM patient tissues as well as sporadic CCM patients. While the type of data we normally get from these analysis is complicated, I believe that having the list of your hits from the *C. elegans* and phosphoproteomics screens will help my group prioritize those sequence variants which are more likely linked to CCMs. I should also emphasize how important this work is for the future development of therapeutics. I know of a few groups that are in the early stages of developing Rho kinase inhibitors as potential therapeutics, but as you know, inhibiting this kinase can have many undesirable effects on the cell. Thus, delineating the network of proteins that function with CCM1/2 and 3, as well as modifiers identified by genetic screens in *C. elegans*, should have more specific effects on treating patients. Indeed, the potential for developing drugs tailored to CCM patients is vast and I would be delighted to collaborate with your groups to eventually bring these therapies to the clinic.

Once again Anne-Claude and Brent, I am delighted to collaborate with you on this novel and exciting project. Congratulations on obtaining bridge funding on your first submission and I wish you the best of luck in securing complete funding from the CIHR for this exciting and medically important work.

Sincerely,



Murat Gunel, MD.



Weizmann Institute of Science
Department of Biological Chemistry
76100 Rehovot, Israel

Michael Fainzilber, Ph.D.
The Chaya Professor in Molecular Neuroscience

Tel: 972-8-9344266
Fax: 972-8-9344112
E-mail: mike.fainzilber@weizmann.ac.il

http://www.weizmann.ac.il/Biological_Chemistry/scientist/Fainzilber/Fainzilber.html

Anne-Claude Gingras
Senior Investigator, Samuel Lunenfeld Research Institute
Associate Professor, Dept Molecular Genetics, University of Toronto

February 27, 2012

Re: CIHR Grant Application

Dear Anne-Claude,

This letter is to reconfirm my interest and strong enthusiasm in pursuing our collaboration on the analysis of the CCM2 interaction partners. In particular, within the context of your CIHR grant application with Toronto colleague Brent Derry, entitled "Molecular mechanisms of cerebral cavernous malformations", we will pursue our analysis of the interactors you identify for human CCM2 within the context of TrkA signalling. As you know, my group has a long standing interest in understanding the role of TrkA signaling in apoptosis in cancer cells.

We are very interested in the interaction partners that you have identified so far using our CCM2 wt and deletion mutant proteins. As you know, we are keenly interested in how the Karet domain of CCM2, which we have demonstrated to be important in mediating the role of CCM2 in cell death, performs its functions. The identification of the CCM3 protein and its associated kinases as interaction partners for this domain is very intriguing in this respect. My postdoctoral fellow Barbara Costa is currently studying the interactions of these proteins within the context of TrkA signaling. She has identified that CCM2 is phosphorylated in vitro by at least one of the kinases, and that this phosphorylation event is linked to the function of CCM2 in cell death. I am looking forward to further studies of this phosphorylation event together with your postdoctoral fellow James Knight.

I am very interested by your hypothesis that, by mediating the recruitment of the GCKIII kinases to CCM2, CCM3 may act as a substrate adaptor. In fact, I would suggest that we should continue to collaborate on this and assess whether, in addition to CCM2 (or, as you propose, its major interaction partners CCM1 and ICAP1), TrkA may itself be a substrate for the GCKIII kinases. We also are very much interested by any additional CCM2 interaction partners which you may uncover when you analyze CCM2 interactomes across different cell types. For example, the mesoderm development candidate (MESDC1) which you have identified as a CCM2 interaction partner and structurally resembles the FAT domain of CCM3 would warrant further exploration.

As we are already generating data together, I can assure you that I am looking forward with great interest to pursuing this excellent collaboration. Congratulations again on receiving bridge funding for this exciting project and best of luck with the application.

With best wishes,

A handwritten signature in blue ink that reads "m. fainzilber".

Mike Fainzilber

February 24th, 2012

Ian Scott, Ph.D.
ian.scott@sickkids.ca

Scientist

Program in Developmental
and Stem Cell Biology

The Hospital for Sick
Children

Assistant Professor

Department of
Molecular Genetics

University of Toronto

Address:
The Hospital for Sick
Children
101 College St.
TMDT, Rm 11-307
Toronto, ON M5G 1L7
CANADA

(416) 813-7654 ext1572

Dear Anne-Claude and Brent,

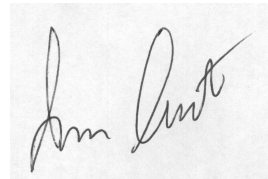
I am writing this letter in support of your Operating Grant application to the CIHR entitled "Molecular mechanisms of cerebral cavernous malformations". You work on the biology of CCM proteins through proteomics and genetics is poised to make some important contributions to the field. I would like to reiterate my enthusiasm to continue collaborating with our groups to study the roles of the CCM proteins and their associated components in vascular development. As you are aware, my laboratory has extensive experience and reagents for studying genes and proteins that control cardiovascular biology in zebrafish. Our first paper demonstrating a distinct role of Ccm3 in vascular development was (Yoruk, 2012, *Developmental Biology*) correlates well with your findings on Ccm3/Stk25 function. This is the first zebrafish model of *ccm3* function in the cranial vasculature, and as CCMs are of course a disease of the cranial vasculature this model will be highly relevant in studying disease-specific mechanism and pathways.

Our findings are in agreement with your proteomics data in cells and genetic analysis in *C. elegans*; namely that CCM3 and its associated kinase control vascular development by a mechanism that is independent of Ccm1/Ccm2. I believe that the collaborative efforts you have described in your CIHR application not only settle a major debate in the field, but also provide new and important insights into how the CCM regulatory network functions *in vivo* and *in vitro*. This is particularly evident by your discovery of the STRIPAK complex and the demonstration that it has conserved functions similar to Ccm3 in regulating vascular development. We have confirmed some of these observations in zebrafish, demonstrating that the Ccm3/STRIPAK pathway appears to be well-conserved from *C. elegans* to human. Indeed, we have recently found that knockdown of the Striatin component of the STRIPAK complex results in cranial hemorrhages in zebrafish.

I am therefore highly enthusiastic to continue working with the both of you to understand the function of Ccm1-3 and related proteins in our zebrafish models. We have the infrastructure in place at SickKids and experience on my team to image cranial vasculature development following knockdown of candidate CCM/STRIPAK pathway genes via morpholino injection. As our previous work on heart development has shown (*Nature Communications* 2011, *Development* 2011, *Developmental Biology* 2011), we can carry out these experiments with ease, and are well-versed in using proper controls to interpret morpholino experiments. Gene discovery via proteomics and *C. elegans* genetics, followed by *in vivo* analysis of vascular development in zebrafish, should yield many novel insights into both CCM pathogenesis and the regulation of vascular integrity.

Good luck with your CIHR application!

Best regards,



Ian Scott, Ph.D.
Scientist
The Hospital for Sick Children



February 27, 2012

Anne-Claude Gingras
Senior Investigator, Samuel Lunenfeld Research Institute
Associate Professor, Dept Molecular Genetics, U Toronto

W. Brent Derry
Senior Scientist, Hospital for Sick Children
Associate Professor, Dept Molecular Genetics, University of Toronto

Dear Anne-Claude and Brent,

It is my pleasure to provide you with this letter for your CIHR application entitled "Molecular Mechanisms of Cerebral Cavernous Malformations". I want to reiterate my full support to your application, and to our joint project on CCMs. Our continued collaboration on this project has been very fruitful so far, as exemplified by the three joint publications between our three groups on this topic.

In particular, I will be happy to continue working with you towards the generation of the detailed structural organization of CCM proteins and the interaction partners you will be identifying. The committee should know that my laboratory is very well equipped for protein expression (including in insect cells), purification using FPLC, and physico-chemical characterization of proteins. You have full access to these resources, and we will continue working with you towards the characterization of the structural organization of CCM signaling complexes.

I am very excited by the proposal you have put forward. I would be most interested to pursue atomic-resolution structural determination of new complexes that you find by your proteomics and genomics means. The CCM field has been evolving rapidly over the past few years, but is still lacking systematic approaches such as the one you are proposing in this application.

I also want to point out that my Research Associate, Derek Ceccarelli, has generated active GCKIII kinases that are appropriate for your substrate determination assays, and that we are gladly making available for your studies. As you well know, my laboratory is dedicated to structural characterization of signaling molecules, and kinases in particular, and you can be ensured that we are committed to help you on this project.

I wish you all the best with your CIHR application.

Sincerely,

Frank Sicheri, PhD.
Senior Investigator
Program in Systems Biology
Samuel Lunenfeld Research Institute
Mount Sinai Hospital

Professor
Depts. of Molecular Genetics and Biochemistry
University of Toronto

Manitoba Institute of Cell Biology

an Institute of CancerCare Manitoba and the University of Manitoba

The Centre for Mammalian Functional Genomics

Director: Dr. Geoff Hicks

Feb 24, 2012

675 McDermot Avenue
Winnipeg, Manitoba, Canada
R3E 0V9
Tel: 204.787.2133
Fax: 204.787.2190
Email: hicks@cc.umanitoba.ca
Website: www.EScells.ca

Dr. Anne-Claude Gingras
Samuel Lunenfeld Research Institute
Mount Sinai Hospital

RE: Letter of Collaboration

Dear Anne-Claude,

I am delighted to confirm that we have started generating targeted mutations in *Pdcd10* (*Ccm3*), *Mst4*, *Stk24* and *Stk25* for your CIHR grant, “*Molecular Mechanisms of Cerebral Cavernous Malformations*.”

As you know, we have established a high-throughput gene targeting pipeline as part of our NorCOMM project. Last year alone, we validated the successful targeting of knockout-first conditional ready mutations in over 600 genes. To create the targeted kinase-dead mutations in *Pdcd10*, we will use a parallel strategy we developed for creating knockin mutations of snp's and indels to model human disease alleles. Briefly, using our BAC recombineering technology, we'll pull out a short genomic region containing *Pdcd10* exons 3 and 4 into a plasmid vector (Fig 2). In that format, mutating the specific amino acid codons to create a kinase dead protein is straightforward (see Fig 1). Because our platform is highly modular, we simply take this cassette and plug it back into our gene targeting pipeline to create a knockin targeting cassette (Fig 4).

ES cells harboring Knockout-first Conditional-ready mutations for *Mst4*, *Stk24* and *Stk25* are already available from our International Knockout Mouse Consortium (IKMC, Fig 5). Briefly, our Mammalian Functional Genomics Centre (MFGC) is one of the lead centres for the IKMC Project – an international effort to establish a public resource of conditional-ready mutations for all 20,000 coding genes (www.NorCOMM.org, www.knockoutmouse.org). As part of our collaboration, we will select and fully validate at least three ES cell clones for each of the targeted *Mst4*, *Stk24* and *Stk25* genes. Validated ES cell clones can be converted to mice in either our or your transgenic centres, which ever is most expedient for you. Typically, one would mate germline mice derived from these ES cells with a *Cre*-deleter mouse to remove the neo-expression cassette.

Within our high-throughput NorCOMM gene targeting pipeline, germline transmission rates for any individual targeted ES cell clone is very high, 90.9%; and successful germline transmission rates for any single gene is 94.7%. Hence, with at least two independent knockout mouse ES clones I am very confident we will successfully derive these mice for you.



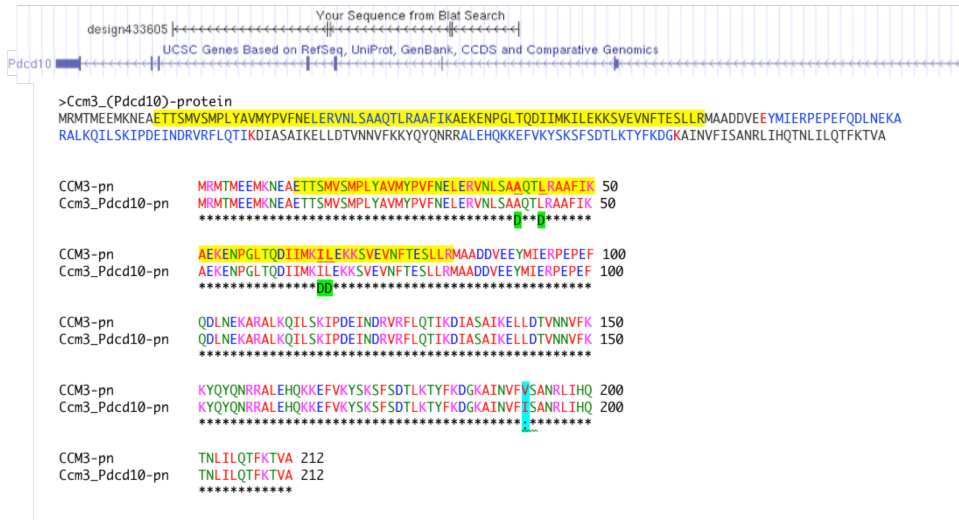
As you know from my groups' involvement with the International Mouse Knockout Project, we have extensive in-house expertise and transgenic facilities available for this collaboration, and I foresee no problems in generating the mice and MEFs in a relatively short period of time. We can also offer you any assistance you may require for the phenotypic or functional analysis of the mice, in addition to ensuring that the mice are archived in a public repository following first publication.



Geoff Hicks, PhD
Director, Regenerative Medicine
Associate Professor of Biochemistry & Medical Genetics
Senior Investigator of the Manitoba Institute of Cell Biology

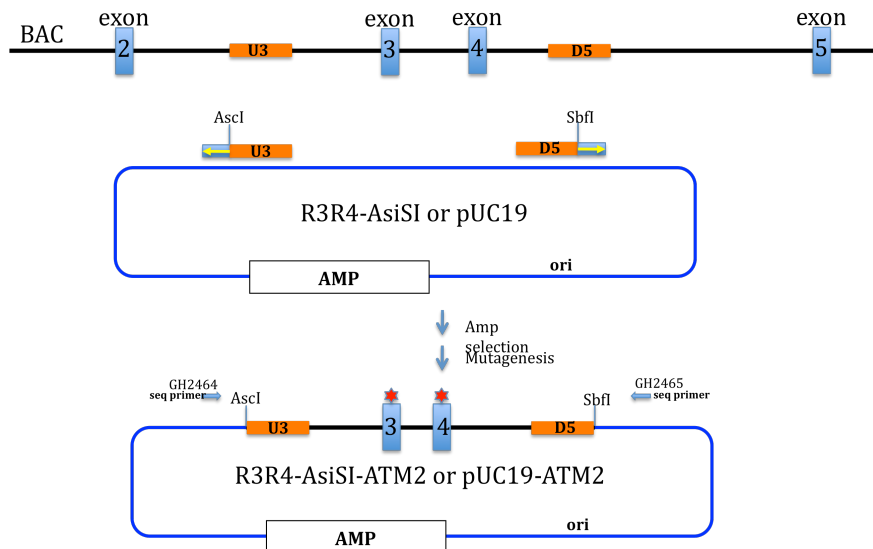
Gingras; Figure 1:

Pdcd10 (Ccm3): ENSMUSG00000027835; Sanger design ID 433605



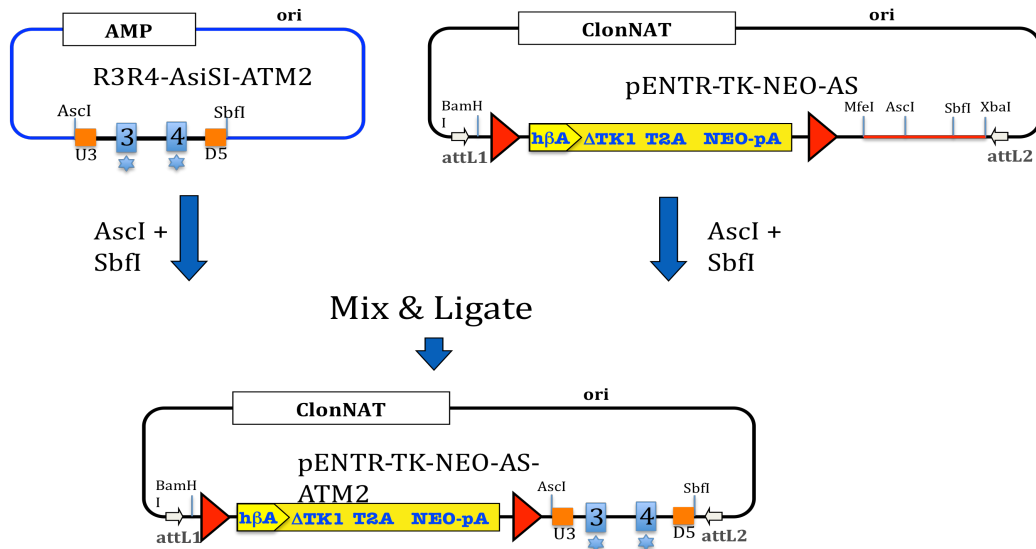
Gingras; Figure 2:

Generate a Plasmid Containing a Mutant Copy of Exon 3-4 of Pdcd10 by Recombineering



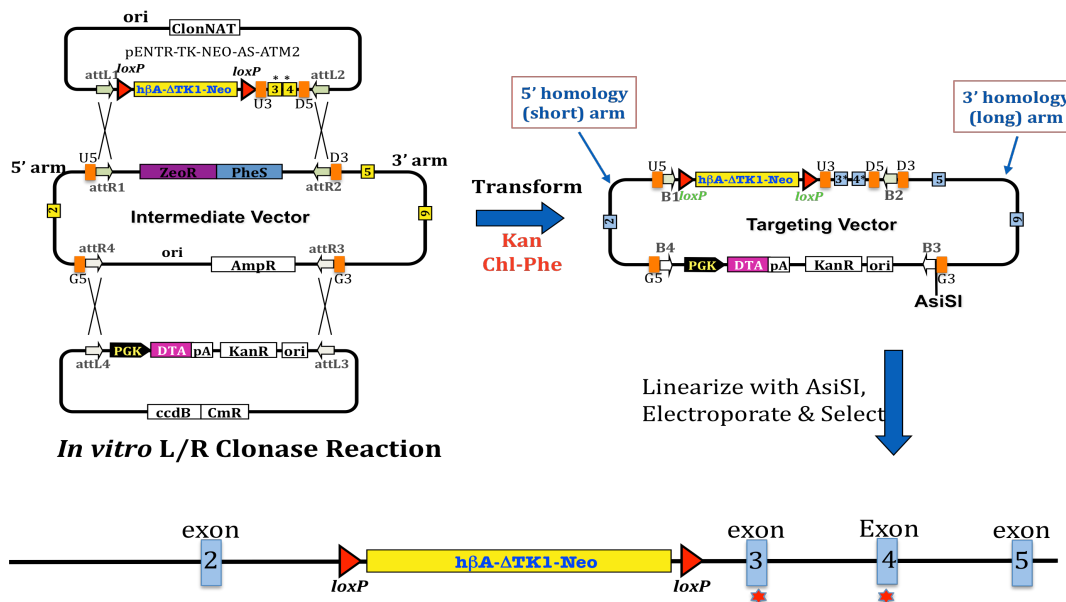
Gingras; Figure 3:

CLONE THE MUTATED EXON 3-4 INTO PENTR-TK-NEO-AS



Gingras; Figure 4:

Gateway Reaction to Generate Targeting Vector



Canadian Institutes of Health Research/Instituts de recherche en santé du Canada
Notice of Recommendation/Avis de recommandation

Application Number/Numéro de la demande: 260322

Committee Code/Code du comité: CP

Applicants/Candidats: Dr. Anne-Claude GINGRAS**With/Avec:** Dr. B. DERRY**Institution paid/
Établissement payé:** Mount Sinai Hospital (Toronto)**Title/Titre:** Molecular mechanisms of cerebral cavernous malformations**Primary Inst./Inst. principal:** Genetics**Other Related Inst./** Circulatory and Respiratory Health**Autres inst. connexes:**

Competition /Concours:	Operating Grant
	September/Septembre 15, 2011

Number in competition/Nbre de demandes dans le concours: 2294

**Peer Review Committee Recommendation, for your information and use/
Recommandation du comité d'examen par les pairs, pour fins d'information et d'utilisation:**

Committee/Comité:	Cell Physiology
--------------------------	-----------------

Number reviewed/ Demandes examinées:	41
---	----

Application rank within the committee/ Rang de la demande dans le comité:	8
--	---

Percent Rank within the committee / Rang en pourcentage au sein du comité:	19.51%
---	--------

Rated / Cote:	4.47
--------------------------	------

Recommended Term/ Durée recommandée:	5 years/ans 0 months/mois
---	--------------------------------

Recommended average annual operating amount/ Montant annuel moyen recommandé pour le fonctionnement:	\$245,196
---	-----------

Recommended equipment amount/ Montant recommandé pour les appareils:	\$0
---	-----

This document is for information only.

An application rated below 3.50 is ineligible for CIHR funding. For applications rated 3.50 and above, please note that it is the application's rank within the peer review committee that determines whether it is funded, rather than its absolute rating. The final funding decision will be communicated in the Notice of Decision.

Document à titre d'information seulement.

Une demande cotée en dessous de 3,5 n'est pas admissible au financement des IRSC. En ce qui a trait aux demandes cotées 3,50 ou plus, veuillez noter que l'on détermine l'attribution des fonds en fonction du classement obtenu au sein du comité d'examen par les pairs plutôt qu'en fonction du classement absolu. La décision finale relative au financement sera communiquée dans l'Avis de décision.

Canadian Institutes of Health Research / Instituts de recherche en santé du Canada**Notice of Decision / Avis de décision**

Application Number/Numéro de la demande: 260322

Committee Code/Code du comité: CP

Applicants/Candidats: Dr. Anne-Claude GINGRAS

With/Avec: Dr. B. DERRY

Institution paid/
Établissement payé: Mount Sinai Hospital (Toronto)

Title/Titre: Molecular mechanisms of cerebral cavernous malformations

Primary Inst./
Inst. principal: GeneticsOther Related Inst./
Autres inst. connexes: Circulatory and Respiratory Health

Competition Outcome/Résultats du concours: Operating Grant
 September/Septembre 15, 2011

Number in competition/Nbre de demandes dans le concours: 2294

Number approved/Nbre de demandes approuvées: 401

**Decision on your application/
Décision sur votre demande:** Not Approved

**Average annual amount/
Montant annuel moyen:** \$0

**Equipment amount/
Montant pour les appareils:** \$0

**Peer Review Committee Recommendation, for your information and use/
Recommandation du comité d'examen par les pairs, pour fins d'information et d'utilisation:**

Committee/Comité: Cell Physiology

**Number reviewed/
Nbre de demandes examinées:** 41

**Number approved in that committee/
Nbre de demandes approuvées dans ce comité:** 7

**Application rank within the committee/
Rang de la demande dans ce comité:** 8

**Percent Rank Within the Committee/
Rang en pourcentage au sein du comité:** 19.51%

**Rating/
Cote:** 4.47

**Recommended average annual amount/
Montant annuel moyen recommandé:** \$245,196

**Recommended equipment amount/
Montant recommandé pour les appareils:** \$0

Additional Funding Opportunities/ Opportunités de financement additionnelles	Decision/ Décision	Competition Code/ Cote de concours	Application Number/ Numéro de la demande
Operating Grant - PA: Institute of Genetics Bridge Funding	Approved	201109IG1	269527

*** Applications receiving a score of less than 3.5 on any evaluation criteria will not be considered for Funding. / Les demandes qui ont reçu une note inférieure à 3.5 pour n'importe quel des critères d'évaluation ne sont pas admissibles.

January 18, 2012

Institute of Aboriginal Peoples' Health
 Institute of Aging
 Institute of Cancer Research
 Institute of Circulatory and Respiratory Health
 Institute of Gender and Health
 Institute of Genetics
 Institute of Health Services and Policy Research
 Institute of Human Development and Child and Youth Health
 Institute of Infection and Immunity
 Institute of Musculoskeletal Health and Arthritis
 Institute of Neurosciences, Mental Health and Addiction
 Institute of Nutrition, Metabolism and Diabetes
 Institute of Population and Public Health
 Institut de la santé des Autochtones
 Institut du vieillissement
 Institut du cancer
 Institut de la santé circulatoire et respiratoire
 Institut de la santé des femmes et des hommes
 Institut de génétique
 Institut des services et des politiques de la santé
 Institut du développement et de la santé des enfants et des adolescents
 Institut des maladies infectieuses et immunitaires
 Institut de l'appareil locomoteur et de l'arthrite
 Institut des neurosciences, de la santé mentale et des toxicomanies
 Institut de la nutrition, du métabolisme et du diabète
 Institut de la santé publique et des populations

Dr. Anne-Claude GINGRAS
 Samuel Lunenfeld Research Institute
 Mt. Sinai Hospital
 Joseph and Wolf Lebovic Health Complex
 Samuel Lunenfeld Research Institute
 600 University Avenue, Room 992A
 Toronto, Ontario M5G 1X5

Dear Dr. GINGRAS:

Your recent application for support entitled "Molecular mechanisms of cerebral cavernous malformations" has been considered by the Canadian Institutes of Health Research (CIHR). Unfortunately, your application was not approved for funding in the Open Operating Grant competition. However, your application was deemed relevant to the "Operating Grant - PA: Institute of Genetics Bridge Funding" priority funding opportunity, and I am pleased to tell you that your application has been approved for funding.

Based on funds currently available to the Institute of Genetics (IG), your grant will be funded for one year for a total amount of \$100,000. This one year grant is paid out in the 2012-13 fiscal year and is effective from April 1, 2012 until March 31, 2013.

Please note that you are required to acknowledge the support of the Institute of Genetics (IG) in all communications and publications related to this project.

Should you have any questions about the peer review process, please address them directly to CIHR staff. As CIHR does not notify co-applicants of the decision, we ask that you inform those individuals involved, along with their research institutions (if different from your own), of the outcome of this application.

Should you have any questions or concerns, please do not hesitate to contact Janet Lemoine at 613-941-4394 or by email at janet.lemoine@cihr-irsc.gc.ca.

Congratulations on your success in this competition!

Sincerely,



Mary Fraser Valiquette, M.Sc.
 Deputy Director, Program Delivery
 Targeted Initiatives Branch
 Canadian Institutes of Health Research

292279-201109IG1-CP-269527-I005-145818-INST1

Review Type/Type dévaluation:	Committee Member 1/Membre de comité 1
Name of Applicant/Nom du chercheur:	GINGRAS, Anne-Claude
Application No./Numéro de demande:	260322
Agency/Agence:	CIHR/IRSC
Competition/Concours:	2011-09-15 Operating Grant/Subvention de fonctionnement
Committee/Comité:	Cell Physiology/Physiologie cellulaire
Title/Titre:	Molecular mechanisms of cerebral cavernous malformations

Assessment/Évaluation:
SYNOPSIS OF PROPOSAL

The overall objective of this proposal is to combine the use of proteomic and genomic approaches to elucidate the underlying basis of Cerebral Cavernous Malformations (CCM). A significant proportion of CCMs are associated with a network of genes designated CCM1, CCM2 and CCM3 that encode proteins that form complexes together and with other regulatory cellular components such as protein kinase/phosphatase networks. To elucidate functions of CCM proteins, the applicants propose to establish a physical interaction map for these proteins in mammals and in worms. Complementary studies, primarily performed in worms, will be directed towards the establishment of genetic interaction maps for CCM1 and CCM3 (to this point, a CCM2 homolog has not been identified in worms on the basis of similarity but the proposed studies are expected to identify this protein based on genetic interactions). The third aim of the proposal is focused on the use of proteomic strategies to identify substrates for the GCKIII kinases that associate with the CCM protein complexes.

ASSESSMENT

On the whole, this is an ambitious proposal in an important area of investigation. The proposal itself is very well written with extensive preliminary data and clear illustrations outlining the experimental strategies to be employed. The proposed studies build logically on previous work in both the Gingras and Derry laboratories and will capitalize on the expertise and facilities that reside within this team – or are available through a number of collaborations that have been documented. There are a number of obvious strengths related to this collaboration. For example, the combined use of proteomics and genetic strategies provides the opportunity to both reinforce specific aspects of the CCM networks that are elucidated and to fill in gaps that could only be identified by one of the approaches. Similarly, the complementary use of a genetically tractable organism such as worms as well as mammalian cells that have more direct relevance to human disease will both accelerate the pace of discovery as compared to studies exclusively performed in mammalian cells and enhance the impact of the studies if they were to be performed exclusively in worms. Based on the accomplishments and documented expertise of the applicants – and the fact that have an established working relationship – there is little doubt that this project will successfully yield comprehensive data sets that will enable elaboration of networks involving the CCM proteins. In this respect, the feasibility of achieving the first two stated aims is very high. Overall, there are many strengths and no major technical concerns. There are however a number of issues for consideration and discussion. While it can be argued that a comprehensive elaboration of the networks that are engaged by the CCM proteins will instruct the design of novel diagnostic or therapeutic approaches for CCM conditions, these possible applications are still not immediate. The applicants' do show some awareness of this issue through the establishment of a collaboration with Dr. Muret Genel at Yale. However, the impact of this proposal – especially given the 5 year time frame – may have been strengthened if the applicants applied more concrete consideration to the

Review Type/Type dévaluation: Committee Member 1/Membre de comité 1
Name of Applicant/Nom du chercheur: GINGRAS, Anne-Claude
Application No./Numéro de demande: 260322
Agency/Agence: CIHR/IRSC
Competition/Concours: 2011-09-15 Operating Grant/Subvention de fonctionnement
Committee/Comité: Cell Physiology/Physiologie cellulaire
Title/Titre: Molecular mechanisms of cerebral cavernous malformations

Assessment/Évaluation:

outcomes of their proteomic and genomic screens. The fact that the final aim of the proposal is focused on the identification of substrates for GCKIII suggests that the next step for this group might be to perform additional screens or systems analyses. This trajectory is certainly well suited to the background of the applicants – but at what stage does this work begin to more directly intersect the clinical realm? As an illustration of this issue, it is also not entirely clear what will be derived from the identification of GCKIII substrates beyond extending the depth of understanding of networks. What will be the practical applications of identifying GCKIII substrates? Since CCM is an important clinical problem with devastating consequences for patients, how will this project improve outcomes? This issue is raised as a point of discussion and is intended to be a constructive comment that does not in any way challenge the innovation and expertise of the research team. Overall, while the application begins by emphasizing the importance of understanding CCM signaling networks, as the proposal proceeds, the emphasis is more on the technology and approaches than on the problems/questions being addressed.

Applicants

One of the major strengths of this proposal is the complementary expertise of the applicants. Dr. Gingras is currently a Canada Research Chair in Functional Genomics as well as Associate Professor in the Department of Molecular Genetics at the University of Toronto and Senior Investigator at the Samuel Lunenfeld Research Institute where she has held appointments for approximately 5 years. During this time, Dr. Gingras has established a dynamic and productive laboratory and has emerged as an international leader in the field of proteomics. The Gingras laboratory is currently supported by operating grants from the CIHR and CCSRI where Dr. Gingras is P.I. and by awards from the NIH and ORF where Dr. Gingras is co-P.I. Within the past 5 years, Dr. Gingras has published ~25 papers including contributions to journals of the very highest calibre (Nature Biotechnology, Science, Nature Methods, Molecular Cell, etc.). Overall, the Gingras laboratory has demonstrated that it is ideally qualified to perform the proposed studies. Dr. Derry also has strong qualifications for the proposed studies. He is currently an Associate Professor in the Department of Molecular Genetics at the University of Toronto where he has held an appointment since 2003. Dr. Derry lists a total of 23 career publications including 8 papers in the past 5 years. The Derry laboratory is currently supported by 2 operating grants from the CIHR with additional funds coming from the Hospital for Sick Children and participation in a training initiative funded by the Terry Fox Foundation. In addition to their independent contributions, it is notable that Drs. Gingras and Derry are co-authors on 2 of these papers demonstrating that their laboratories have effective working relationships that will foster successful execution of the proposed studies.

BUDGET

The application requests partial support for a number of personnel (50% of lab manager in Gingras lab; 20%

Review Type/Type dévaluation: Committee Member 1/Membre de comité 1
Name of Applicant/Nom du chercheur: GINGRAS, Anne-Claude
Application No./Numéro de demande: 260322
Agency/Agence: CIHR/IRSC
Competition/Concours: 2011-09-15 Operating Grant/Subvention de fonctionnement
Committee/Comité: Cell Physiology/Physiologie cellulaire
Title/Titre: Molecular mechanisms of cerebral cavernous malformations

Assessment/Évaluation:

of programmer in Gingras lab, 100% of 2 PDFs and 1 grad student). I additional student will also be involved but supported by other sources. There is a thorough justification for the roles of each of these individuals presented. In total, the personnel and trainee costs are ~\$168,000. The request for expendables is approximately \$88,000 that again is thoroughly explained and justified on the basis of supporting genetic studies with worms in the Derry lab and mammalian cell culture and proteomics in the Gingras laboratory. Given the breadth of the proposed studies, the request does make sense.

Review Type/Type dévaluation: Committee Member 2/Membre de comité 2
Name of Applicant/Nom du chercheur: GINGRAS, Anne-Claude
Application No./Numéro de demande: 260322
Agency/Agence: CIHR/IRSC
Competition/Concours: 2011-09-15 Operating Grant/Subvention de fonctionnement
Committee/Comité: Cell Physiology/Physiologie cellulaire
Title/Titre: Molecular mechanisms of cerebral cavernous malformations

Assessment/Évaluation:**Applicants**

The nominated PI, Dr. Gingras is an Associate Professor in the Department of Medical Genetics at the University of Toronto and a Senior Investigator at the Samuel Lunenfeld Research Institute. Following predoctoral work with Dr. Nahum Sonenberg at McGill, Dr. Gingras did postdoctoral work in proteomics at the Institute for Systems Biology in Seattle and currently holds a Canada Research Chair Tier 2 in Functional Proteomics; renewed this year through to 2016. Although still at a relatively early stage in her career (first appointment as an independent investigator was in 2005) Dr. Gingras has published 68 peer-reviewed and highly cited articles and 14 book chapters/proceedings; of 25 peer-reviewed articles published 2006-2011 Dr. Gingras is senior author on only 5 of these 25, but is corresponding author on several others. Dr. Gingras' lab is currently funded, by operating grants from CIHR and CCRSI (as PI) and NIH and ORF (as a co-applicant).

The co-PI, Dr. Derry, is an Associate Professor in the Department of Medical Genetics at the University of Toronto and a Senior Investigator at The Hospital for Sick Children and obtained his first appointment as an independent investigator in 2003. Dr. Derry's main expertise is in molecular genetic analysis of *C. elegans* and he has published a career total of 23 refereed articles, including 8 (5 as first or senior author) over the period 2007-2011 in very good journals (JBC, Cell Death and Differentiation, Current Biology; impact factors ~5, 9 & 10 respectively). His work is well-cited (average of 52 citations per publication). Dr. Derry's lab is currently funded by CIHR (PI on 2 operating grants to study apoptosis in *C. elegans*) and he is co-PI on a Terry Fox Foundation Strategic Training Initiative for Excellence in Radiation Research for the 21st Century (EIRR21) at CIHR).

The applicants have recently published 2 papers together which form the basis of the current application.

In summary the applicants are both productive and well-funded investigators with complimentary expertise and a recent history of fruitful collaboration.

Brief Summary of Project:

Loss of function mutations in CCM1, CCM2 and CCM3 proteins are associated with cerebral cavernous malformations (CCMs) in the brain. This application proposes to use the combined approaches of proteomics and molecular genetics (in *C. elegans*) to identify novel interactors with CCM1, CCM2 and CCM3 proteins and to elucidate signaling pathways involving these protein.

Review Type/Type dévaluation: Committee Member 2/Membre de comité 2
Name of Applicant/Nom du chercheur: GINGRAS, Anne-Claude
Application No./Numéro de demande: 260322
Agency/Agence: CIHR/IRSC
Competition/Concours: 2011-09-15 Operating Grant/Subvention de fonctionnement
Committee/Comité: Cell Physiology/Physiologie cellulaire
Title/Titre: Molecular mechanisms of cerebral cavernous malformations

Assessment/Évaluation:

CCM1 and CCM2 associate with each other in a tight complex to control common downstream signaling events that modulate cytoskeletal function but evidence from the applicants' and other labs suggests CCM3 exhibits functions that are largely distinct from CCM1 and CCM2.

Most CCM3 protein resides in different molecular complexes in various cell types, including the newly described STRIPAK (STRiatin Interacting Phosphatase And Kinase) complex, in which CCM3 is responsible for bridging germinal center kinase III family members (GCKIII) to the striatin molecule. Overexpression of GCKIII kinase can rescue abnormal phenotypes caused by CCM3 mutation or knockdown, suggesting the key function of CCM3 is linked to the GCKIII kinase activity.

To follow up on these findings the applicants have 3 specific aims:

- 1: Establish physical interaction maps for CCM proteins in mammals and *C. elegans*.
- 2: Define the global genetic interaction map for CCM1 and CCM3.
- 3: Identify substrates for GCKIII kinases.

Five main sub-aims are described for aim 1:

- a) The first, to refine and expand the interactome maps for CCM proteins in HEK293 cells, is essentially an extension of ongoing work using protocols standard in the applicants' labs.

Comment

The approach of mutagenesis of CCM genes to eliminate isolated protein domain-mediated interactions has proven useful in unmasking novel interactors in the past in the applicants' hands and feasibility of these experiments is high.

- b) The second is a simple extension of procedures completed in HEK cells to endothelial cells in case cell-specific interactors may have been missed by using HEK cells and is also highly feasible.
- c) The third presents a couple of strategies (AP-MS and RNAi knockdown of candidate proteins followed by determination of synthetic lethality with CCM3) for determining whether a CCM2 orthologue exists in worms.

Comment

Review Type/Type dévaluation: Committee Member 2/Membre de comité 2
Name of Applicant/Nom du chercheur: GINGRAS, Anne-Claude
Application No./Numéro de demande: 260322
Agency/Agence: CIHR/IRSC
Competition/Concours: 2011-09-15 Operating Grant/Subvention de fonctionnement
Committee/Comité: Cell Physiology/Physiologie cellulaire
Title/Titre: Molecular mechanisms of cerebral cavernous malformations

Assessment/Évaluation:

This seems a worthwhile and necessary issue to resolve, given that worms will be used to validate and extend much of the data obtained from HEK/endothelial cells.

d) The fourth, given the reported role of the GCKIII kinases and CCM3 in stress pathways, is to determine whether various forms of stress (oxidative, osmotic, chemical) alter interactions of the CCM proteins. The effect of stimulation of endothelial cells with vascular endothelial growth factor, or of neurons with nerve growth factor, will also be investigated.

Comment

Obviously it is anyone's guess whether this will yield novel data, since no effect in interactions may be seen following any of these interventions. This could be a useful first step however in determining the possible role of CCM protein interactions in these selected processes (stress, angiogenesis, neurogenesis).

e) The fifth is to extend, to any newly identified physical and genetic interaction partners of CCM proteins, the type of analysis already used (truncation analysis followed by AP-MS, RNAi knockdown of selected proteins) to identify domains of the CCM proteins critical for binding to other proteins.

Comment

These approaches have been used very effectively to date by the applicants and are a major strength of the application.

Aim 2 consists of three sub-aims (phenotypic assessment for physical interaction partners and potential substrates; genetic modifier screen in *C. elegans* to uncover novel CCM3 signaling proteins; expression patterns and tissue-specific requirements for CCM3 signaling proteins) all of which will make very effective use of genetic analysis in *C. elegans*, combined with the identification of robust phenotypes associated with loss of CCM function, to uncover novel information regarding the CCM proteins and their signaling pathways.

Comments

This is perhaps the strongest part of an overall very strong application and the aim in which the potential for synergy resulting from the PI's and co-PI's expertise is most striking.

Review Type/Type dévaluation: Committee Member 2/Membre de comité 2
Name of Applicant/Nom du chercheur: GINGRAS, Anne-Claude
Application No./Numéro de demande: 260322
Agency/Agence: CIHR/IRSC
Competition/Concours: 2011-09-15 Operating Grant/Subvention de fonctionnement
Committee/Comité: Cell Physiology/Physiologie cellulaire
Title/Titre: Molecular mechanisms of cerebral cavernous malformations

Assessment/Évaluation:

Aim 3, the identification of substrates for GCKIII kinases is a logical goal considering that over-expression of members of this family can rescue abnormal phenotypes caused by CCM3 mutation or knockdown and both approaches described are reasonable.

Comment

This aim is the only one of the three where one wonders to any extent about the likelihood of success, as each of the two main approaches outlined has certain limitations (e.g. dependent on ability to express the recombinant candidate protein in question; effective use of FSBA to inactivate all endogenous kinases will be critically dependent on total ablation of activity of endogenous kinases, with no side effects). The alternate forward genetic screen proposed may well provide the least ambiguous approach.

Assessment

Overall an excellent and quite compelling proposal based on high quality preliminary data and the applicant's own published work. The potential for novel and significant findings coming from this work is very high. The combined and synergistic expertise of the applicants is a major strength of this proposal.

Review Type/Type dévaluation: SO Notes /Notes de l'agent scientifique
Name of Applicant/Nom du chercheur: GINGRAS, Anne-Claude
Application No./Numéro de demande: 260322
Agency/Agence: CIHR/IRSC
Competition/Concours: 2011-09-15 Operating Grant/Subvention de fonctionnement
Committee/Comité: Cell Physiology/Physiologie cellulaire
Title/Titre: Molecular mechanisms of cerebral cavernous malformations

Assessment/Évaluation:

Name of Applicant: GINGRAS, Anne-Claude

Application No 260322

Agency

Committee/ Cell Physiology

Title: Molecular mechanisms of cerebral cavernous malformations

Assessment

The proposal has two applicants, Dr. Gingras is on faculty at University of Toronto. She has an established laboratory as a leader in the field of proteomics. In the past 5 years she has published 25 papers, and the papers are of high quality. The laboratory has excellent capability for these studies. The other applicant is also very strong and contributes in the use of *C. elegans* and cell biology approaches. The synergy between the laboratories is very strong. The expertise of the individuals is also very high, and they have an excellent location and facilities for this proteomic analysis. However, prioritization of the results was not clear. It was not sure how and which of the results of the screen will be chosen for further study. It was also not clear how the results will be related back to impact the disease.

Budget

The budget is large but for two laboratories is appropriate.

**Application for Funding – Budget****Funding Opportunity**

Operating Grant 2012-03-01

Nominated Principal Applicant/CandidateLast Name
GINGRASFirst Name
Anne-ClaudeInstitution
Samuel Lunenfeld Research Institute (Toronto)**Financial Assistance Required****Year 1**

Research Staff (excluding trainees)	No.	Salary	Benefits	CIHR	Other Funding Sources		Total
					Cash*	In-Kind*	
Research Assistants	1.0	\$47,909	\$13,127	\$30,518	\$0	\$30,518	\$61,036
Technicians	0.0	\$0	\$0	\$0	\$0	\$0	\$0
Other personnel (as specified in Employment History)	1.0	\$84,000	\$23,016	\$21,403	\$0	\$85,613	\$107,016
Research Trainees	No.	Stipend	Benefits	CIHR	Other Funding Sources		Total
					Cash*	In-Kind*	
Postdoctoral Fellows (post PHD, MD, etc.)	2.0	\$80,000	\$11,600	\$91,600	\$0	\$0	\$91,600
Graduate Students	2.0	\$59,500	\$0	\$24,500	\$0	\$35,000	\$59,500
Summer Students	0.0	\$0	\$0	\$0	\$0	\$0	\$0
Materials, Supplies and Services				CIHR	Other Funding Sources		Total
					Cash*	In-Kind*	
Animals				\$0	\$0	\$0	\$0
Expendables				\$87,575	\$0	\$0	\$87,575
Services				\$1,600	\$0	\$0	\$1,600
Other (as specified in the Details of Financial Assistance Requested)				\$0	\$0	\$0	\$0
				CIHR	Other Funding Sources		Total
					Cash*	In-Kind*	
Travel				\$3,600	\$0	\$0	\$3,600
Total Operating				\$260,796	\$0	\$151,131	\$411,927
Total Equipment				\$0	\$0	\$0	\$0
Total Request				\$260,796	\$0	\$151,131	\$411,927

**Application for Funding – Budget****Funding Opportunity**

Operating Grant 2012-03-01

Nominated Principal Applicant/CandidateLast Name
GINGRASFirst Name
Anne-ClaudeInstitution
Samuel Lunenfeld Research Institute (Toronto)**Financial Assistance Required****Year 2**

Research Staff (excluding trainees)	No.	Salary	Benefits	CIHR	Other Funding Sources		Total
					Cash*	In-Kind*	
Research Assistants	1.0	\$47,909	\$13,127	\$30,518	\$0	\$30,518	\$61,036
Technicians	0.0	\$0	\$0	\$0	\$0	\$0	\$0
Other personnel (as specified in Employment History)	1.0	\$84,000	\$23,016	\$21,403	\$0	\$85,613	\$107,016
Research Trainees	No.	Stipend	Benefits	CIHR	Other Funding Sources		Total
					Cash*	In-Kind*	
Postdoctoral Fellows (post PHD, MD, etc.)	2.0	\$80,000	\$11,600	\$91,600	\$0	\$0	\$91,600
Graduate Students	2.0	\$59,500	\$0	\$24,500	\$0	\$35,000	\$59,500
Summer Students	0.0	\$0	\$0	\$0	\$0	\$0	\$0
Materials, Supplies and Services				CIHR	Other Funding Sources		Total
					Cash*	In-Kind*	
Animals				\$0	\$0	\$0	\$0
Expendables				\$87,575	\$0	\$0	\$87,575
Services				\$1,600	\$0	\$0	\$1,600
Other (as specified in the Details of Financial Assistance Requested)				\$0	\$0	\$0	\$0
				CIHR	Other Funding Sources		Total
					Cash*	In-Kind*	
Travel				\$3,600	\$0	\$0	\$3,600
Total Operating				\$260,796	\$0	\$151,131	\$411,927
Total Equipment				\$0	\$0	\$0	\$0
Total Request				\$260,796	\$0	\$151,131	\$411,927

**Application for Funding – Budget****Funding Opportunity**

Operating Grant 2012-03-01

Nominated Principal Applicant/CandidateLast Name
GINGRASFirst Name
Anne-ClaudeInstitution
Samuel Lunenfeld Research Institute (Toronto)**Financial Assistance Required****Year 3**

Research Staff (excluding trainees)	No.	Salary	Benefits	CIHR	Other Funding Sources		Total
					Cash*	In-Kind*	
Research Assistants	1.0	\$47,909	\$13,127	\$30,518	\$0	\$30,518	\$61,036
Technicians	0.0	\$0	\$0	\$0	\$0	\$0	\$0
Other personnel (as specified in Employment History)	1.0	\$84,000	\$23,016	\$21,403	\$0	\$85,613	\$107,016
Research Trainees	No.	Stipend	Benefits	CIHR	Other Funding Sources		Total
					Cash*	In-Kind*	
Postdoctoral Fellows (post PHD, MD, etc.)	2.0	\$80,000	\$11,600	\$91,600	\$0	\$0	\$91,600
Graduate Students	2.0	\$59,500	\$0	\$24,500	\$0	\$35,000	\$59,500
Summer Students	0.0	\$0	\$0	\$0	\$0	\$0	\$0
Materials, Supplies and Services				CIHR	Other Funding Sources		Total
					Cash*	In-Kind*	
Animals				\$0	\$0	\$0	\$0
Expendables				\$87,575	\$0	\$0	\$87,575
Services				\$1,600	\$0	\$0	\$1,600
Other (as specified in the Details of Financial Assistance Requested)				\$0	\$0	\$0	\$0
				CIHR	Other Funding Sources		Total
					Cash*	In-Kind*	
Travel				\$3,600	\$0	\$0	\$3,600
Total Operating				\$260,796	\$0	\$151,131	\$411,927
Total Equipment				\$0	\$0	\$0	\$0
Total Request				\$260,796	\$0	\$151,131	\$411,927

**Application for Funding – Budget****Funding Opportunity**

Operating Grant 2012-03-01

Nominated Principal Applicant/CandidateLast Name
GINGRASFirst Name
Anne-ClaudeInstitution
Samuel Lunenfeld Research Institute (Toronto)**Financial Assistance Required****Year 4**

Research Staff (excluding trainees)	No.	Salary	Benefits	CIHR	Other Funding Sources		Total
					Cash*	In-Kind*	
Research Assistants	1.0	\$47,909	\$13,127	\$30,518	\$0	\$30,518	\$61,036
Technicians	0.0	\$0	\$0	\$0	\$0	\$0	\$0
Other personnel (as specified in Employment History)	1.0	\$84,000	\$23,016	\$21,403	\$0	\$85,613	\$107,016
Research Trainees	No.	Stipend	Benefits	CIHR	Other Funding Sources		Total
					Cash*	In-Kind*	
Postdoctoral Fellows (post PHD, MD, etc.)	2.0	\$80,000	\$11,600	\$91,600	\$0	\$0	\$91,600
Graduate Students	2.0	\$59,500	\$0	\$24,500	\$0	\$35,000	\$59,500
Summer Students	0.0	\$0	\$0	\$0	\$0	\$0	\$0
Materials, Supplies and Services				CIHR	Other Funding Sources		Total
					Cash*	In-Kind*	
Animals				\$0	\$0	\$0	\$0
Expendables				\$77,575	\$0	\$0	\$77,575
Services				\$1,600	\$0	\$0	\$1,600
Other (as specified in the Details of Financial Assistance Requested)				\$0	\$0	\$0	\$0
				CIHR	Other Funding Sources		Total
					Cash*	In-Kind*	
Travel				\$3,600	\$0	\$0	\$3,600
Total Operating				\$250,796	\$0	\$151,131	\$401,927
Total Equipment				\$0	\$0	\$0	\$0
Total Request				\$250,796	\$0	\$151,131	\$401,927

**Application for Funding – Budget****Funding Opportunity**

Operating Grant 2012-03-01

Nominated Principal Applicant/CandidateLast Name
GINGRASFirst Name
Anne-ClaudeInstitution
Samuel Lunenfeld Research Institute (Toronto)**Financial Assistance Required****Year 5**

Research Staff (excluding trainees)	No.	Salary	Benefits	CIHR	Other Funding Sources		Total
					Cash*	In-Kind*	
Research Assistants	1.0	\$47,909	\$13,127	\$30,518	\$0	\$30,518	\$61,036
Technicians	0.0	\$0	\$0	\$0	\$0	\$0	\$0
Other personnel (as specified in Employment History)	1.0	\$84,000	\$23,016	\$21,403	\$0	\$85,613	\$107,016
Research Trainees	No.	Stipend	Benefits	CIHR	Other Funding Sources		Total
					Cash*	In-Kind*	
Postdoctoral Fellows (post PHD, MD, etc.)	2.0	\$80,000	\$11,600	\$91,600	\$0	\$0	\$91,600
Graduate Students	2.0	\$59,500	\$0	\$24,500	\$0	\$35,000	\$59,500
Summer Students	0.0	\$0	\$0	\$0	\$0	\$0	\$0
Materials, Supplies and Services				CIHR	Other Funding Sources		Total
					Cash*	In-Kind*	
Animals				\$0	\$0	\$0	\$0
Expendables				\$77,575	\$0	\$0	\$77,575
Services				\$1,600	\$0	\$0	\$1,600
Other (as specified in the Details of Financial Assistance Requested)				\$0	\$0	\$0	\$0
				CIHR	Other Funding Sources		Total
					Cash*	In-Kind*	
Travel				\$3,600	\$0	\$0	\$3,600
Total Operating				\$250,796	\$0	\$151,131	\$401,927
Total Equipment				\$0	\$0	\$0	\$0
Total Request				\$250,796	\$0	\$151,131	\$401,927



Human Resources

**Employment History**

Name Kean, Michelle	Position PhD student	Current Salary Rate 35000	Current Source of Funding CIHR Banting award
Name Haeri, Mehran	Position Postdoctoral fellow	Current Salary Rate 45600	Current Source of Funding N/A
Name Knight, James	Position Postdoctoral fellow	Current Salary Rate 46000	Current Source of Funding SLRI internal funding
Name Hall, Mat	Position Graduate student	Current Salary Rate 24500	Current Source of Funding N/A - just recruited
Name Liu, Frank	Position Other personnel - Program 107016	Current Salary Rate	Current Source of Funding CIHR - Pawson et al.
Name Goudreault, Marilyn	Position Research assistant	Current Salary Rate 61036	Current Source of Funding split on Gingras
Name	Position	Current Salary Rate	Current Source of Funding
Name	Position	Current Salary Rate	Current Source of Funding
Name	Position	Current Salary Rate	Current Source of Funding
Name	Position	Current Salary Rate	Current Source of Funding
Name	Position	Current Salary Rate	Current Source of Funding
Name	Position	Current Salary Rate	Current Source of Funding
Name	Position	Current Salary Rate	Current Source of Funding
Name	Position	Current Salary Rate	Current Source of Funding
Name	Position	Current Salary Rate	Current Source of Funding
Name	Position	Current Salary Rate	Current Source of Funding
Name	Position	Current Salary Rate	Current Source of Funding
Name	Position	Current Salary Rate	Current Source of Funding

Detailed Budget Justification

The majority of financial assistance requested will be used for salaries and laboratory expendables and services (no equipment). Therefore, to achieve the goals proposed we are requesting support for the following personnel:

1. RESEARCH STAFF AND TRAINEESMarilyn Goudreault, lab manager and research assistant level III, 50% effort

Marilyn is the Gingras laboratory manager, and in charge of ordering and organizing the lab (her organization and communication skills are exceptional). In addition, she is performing a project directly related to the Cerebral Cavernous Malformation studies proposed here: She is the first author of the publication highlighting the discovery of the STRIPAK complex in which CCM3 primarily resides (Goudreault et al., *Mol Cell Proteomics*, 2009). For that paper, she did the bulk of the cloning, and performed affinity purification coupled to mass spectrometry or to immunoblotting. She has since been working with graduate student Michelle Kean on further characterization of the molecular organization of the STRIPAK complex (she is an author on Kean et al., *J Biol Chem*, 2011), and has performed the cell biology work for the recent CCM3 paper by Ceccarelli et al. (*J Biol Chem* 2011) for which she is also an author. Within Aim 1, she will be in charge of creating high quality interactome maps from different cell types. Marilyn is an excellent molecular biologist, and she will also be helping other lab members in the Gingras and Derry labs with the generation of the cDNA reagents and cell lines for the completion of all aims in this grant.

\$ 47,909 p.a + 27.4% benefits (SLRI): \$ 61,036.07.

Amount requested from CIHR = 50% = \$ 30,518.03

The other 50% of Marilyn's salary is covered by other grants. Marilyn is interested in being more involved with the CCM project, and a portion of her administrative duties is being re-allocated to different laboratory members.

Guomin (Frank) Liu, programmer; 20% effort (no support for consumables requested)

Frank is the main programmer behind the LIMS system for interaction proteomics, ProHits, and first author on the submitted manuscript (Liu et al., *Nature Biotech*). Frank is also a co-author on the yeast kinase and phosphatase interaction network (Breitkreutz et al., *Science 2010*), and will be included on the upcoming submission by the Gingras and Nesvizhskii groups to *Nature Protocols*. Frank is essential to the continued development of ProHits, including the implementation of the statistical and quantification tools described in Aim1. Importantly, Frank will build in new modules within our LIMS pipeline for the implementation of the phosphorylation analysis described in Aim 3. Frank has been in charge of the support of the entire mass spectrometric group at the Samuel Lunenfeld Research Institute since 2002. Frank's salary has been contributed by a CIHR Resource grant to AJ Pawson and colleagues in the Centre for Systems Biology at the SLRI. This grant ends in July 2011. Salary support will be needed to continue the development of bioinformatics tools for MS analysis.

For this grant, Frank will continue to offer data management support, but will importantly also build in additional tools that are necessary to this proposal. For Aim 1, he will incorporate the statistical tools created in collaboration with A Nesvizhskii and also link ProHits to quantitation software. For Aim 3, he will contribute to the implementation of a peptide-level viewer for the visualization and analysis of post-translational modifications.

\$ 84,000 p.a + 27.4% benefits (SLRI): \$ 107,016.

Amount requested from CIHR = 20% = \$ 21,403.2

We are only asking for the portion of Frank's salary that I believe will be directly related to this proposal.

Mehran Haeri, Postdoctoral Fellow, 100% effort:

We seek salary support for Dr. Mehran Haeri, a postdoctoral fellow recently recruited by Dr. Derry to study the role of CCM1 in apoptosis and excretory cell development in *C. elegans*. Dr. Haeri earned his Ph.D. with Dr. Yaakov Ben-David at Sunnybrook Research Institute where he studied the role of the tissue microenvironment on leukemogenesis in a mouse erythroleukemia model. During his Ph.D. studies he published first author papers in the journals Blood and Immunogenetics, as well as 3 other co-author papers in very solid journals (Blood, Cancer Research). For this project, Dr. Haeri will be responsible for completing the genome-wide synthetic lethal screens in *kri-1* loss-of-function mutants in order to identify components of the CCM3 pathway (Aim 2). Dr. Haeri's expertise in molecular biology and mouse genetics will also allow us to pursue future translational studies in vertebrates as we identify conserved genes that exhibit strong synthetic lethality in *C. elegans kri-1/CCM1* mutants.

\$ 40,000 p.a + 14% benefits (SickKids): \$5,600 = \$45,600

James Knight, postdoctoral fellow, 100% effort

James has joined the Gingras laboratory as a postdoctoral fellow in September 2011. James has received excellent training in the structural and functional aspects of serine/threonine kinases. James is first author of two publications which analyze in details the catalytic sites of kinases. Very importantly within the context of this application, James also developed the whole cell lysate assay that we will be using in Aim 3 to attempt identifying additional substrates of the GCKIII kinases (the manuscript with James as a first author has been submitted for publication). Due to his combinations of technical skills (on kinase assays, phosphoenrichment and substrate identification) as well as proficiency in bioinformatics, James is the ideal person to lead Aim 3.

\$ 40,000 p.a + 15% benefits (SLRI): \$ 46,000

Mat Hall, Graduate student –100% effort:

The minimal stipend for graduate students in the Department of Molecular Genetics at the University of Toronto is \$24,500. We request funding for Mat Hall, a graduate student recently recruited to Dr. Derry's lab, to study the role of worm *ccm3* in excretory cell development. Mat obtained his B.Sc. Specialization in Genetics and Biochemistry from the University of Western Ontario in June 2011. Mat carried out his 4th year research thesis project in Dr. Tony Percival-Smith's lab at Western studying the role of epidermal growth factor receptor (EGFR) signaling in maxillary palp development in *Drosophila melanogaster*, where he learned a lot of genetics techniques that are transferable to *C. elegans*. Mat is a highly motivated graduate student who is already gaining momentum in the lab. For his Ph.D. project he will characterize the mechanism by which *ccm3* and the STRIPAK genes regulate excretory cell development and how they function in osmoregulation in *C. elegans*. He will also work closely with Dr. Haeri to help characterize genes from the RNAi screen that are found to regulate excretory cell development.

\$24,500 (no benefits) (U of Toronto guidelines)

Michelle Kean, graduate student, 100% effort, but no salary requested

Michelle obtained her Masters degree at Guelph with cell biology expertise (she was first author on a J Cell Science publication from her Masters), and started her PhD in my laboratory in 2008. Since joining my laboratory, she developed the endogenous AP-MS approach used in our MCP paper (Michelle is third author on this paper). She is co-supervised by an expert structural biologist and co-applicant, Frank Sicheri, and is the first author on the recent J Biol Chem publication detailing the molecular organization of the kinase•CCM3•striatin•PP2AA•PP2Acat component of STRIPAK. Michelle has also been implicated in the structural studies published by Ceccarelli et al. (J Biol Chem 2011) and is the point person for our collaboration with the Fainzilber group on CCM2. Within the context of this grant,

she will contribute to Aim 1 and 2A. In particular, as she has developing the tools to study the function of the GCKIII kinases in cell biology, she will continue to be involved in all the cell biology aspects of the project.

I am not requesting any salary for Michelle, as she has obtained a competitive Banting and Best CIHR doctoral award.

TOTAL FOR RESEARCH STAFF AND TRAINEES: **\$ 168,021.23**

2A. EXPENDABLES - DERRY

a. Plastics: A considerable amount of expendable plastic will be used in the production of worm plates for maintaining strains, crosses, and carrying out genome-wide RNAi screens. One of the major general expenses for a *C. elegans* lab is the plastic Petri dishes used for cultivation of strains, genetic crosses, phenotypic analysis and screens. Given the current catalogue prices of these expendables and the extent of screening involved in this project I estimate that the cost per year will be \$12,000. The majority of screening should be completed in the first three years. Thus, the cost for plastics will drop by 50% in years 4 and 5.

Years 1-3: \$12,000

Years 4-5: \$6,000

b. *C. elegans* and Bacterial Media: Growth media, which also must support the growth of bacteria for RNAi screens and cultivation of *C. elegans*, which they eat as a source of food, consists of salts, agar, amino acid supplements and cholesterol. It is estimated that we will go through about 6000 plates a year for screens and general cultivation of the animals, which is equivalent to about 150 liters per year (approximately \$8,000). Because genome-wide screens should be completed within the first 3 years the expenses for media will also drop by 50% in years 4 and 5.

Years 1-3: \$8,000

Years 4-5: \$4,000

c. General Molecular Biology Products: Restriction enzymes, PCR reagents, DNA polymerase, reverse transcriptase, other enzymes, plasmids.

\$4,000

d. Chemicals and Supplies: Buffers, salts, detergents, organic solvents, wet and dry chemicals, standard reagents required for electrophoresis, western blots, tips, tubes, racks, boxes, etc.

\$4,400

e. Publication expenses: Preparation of figures for publication/poster and all publication costs including page charges for one-two papers each year.

\$2,500

3A. EXPENDABLES, GINGRAS

a. Reagents for mass spectrometry. The cost of materials for the proteomics experiments we are proposing is relatively high. We require phospho-enrichment reagents, at an estimated cost of \$2,500/year. We also require synthetic isotopically labeled peptides for accurate quantification (25 year/ \$87 each from JPT = \$2,175). Although we have significantly decreased the costs associated with SILAC labelling by purchasing isotopically labelled amino acids in bulk and making our own medium from powder, the isotopes and dialyzed FBS remain expensive, and the average cost per liter of medium is ~\$500 (when both heavy Lys and Arg are used); we request 5 liters/year (\$2,500). All our experiments require sequencing-grade enzymes such as trypsin (~\$500). Lastly, we require capillary

tubing material, C18 reverse phase supports, HPLC plasticware, acetonitrile, HPLC-grade water and acids (formic acid, acetic acid, TFA) and bases (ammonium hydroxide), at an estimated cost of \$5,000. **\$12,675**

b. Mammalian tissue culture. Last year, the cost of serum, selection medium and plates for the mammalian tissue culture experiments specifically for this project were ~\$ 4,500. For example, we have used ~12 cases of 150mm plates, 25g of G418, 25 ml hygromycin, 8 bottles of serum and 80 bottles of DMEM. Tissue culture will continue to be a major item in our budget as we expand the project, and specialized growth medium for endothelial cells (using expensive growth factors) will be required.

\$6,500

c. Affinity purification reagents. Commercial antibodies and affinity reagents (e.g. FLAG M2 agarose, GFP Trap) and custom antibodies are required for the FLAG purification and other immunoprecipitation, immunoblotting and immunofluorescence experiments. This is a significant cost in our lab, and we spend nearly \$8,000 yearly on affinity reagents related to this project. We are also planning to raise phosphospecific antibodies to selected identified targets (\$1,500 per antibody; one per year).

\$9,500

d. Molecular biology and standard reagents. $\gamma^{32}\text{P}$ -ATP is required for *in vitro* phosphorylation (\$1,000). Inhibitors (e.g. okadaic acid and calyculin A, protease inhibitor cocktail, various kinase inhibitors) are estimated at \$2,500. Oligonucleotides and cloning enzymes (including Gateway clonase and PCR enzymes) are required for cloning and mutagenesis (note that the project involves a large molecular biology component; \$5,000). Standard chemicals, molecular weight ladders and plasticware are also required for the project (\$15,000). Cost-recovery access to the Lunenfeld cDNA collection (\$10 per clone), and sequencing services are estimated at \$2,000.

\$25,500

e. Publication expenses: Preparation of figures for publication/poster and all publication costs including page charges for one-two papers each year.

\$2,500

TOTAL FOR EXPENDABLES – YEAR 1: \$87,575

3A. SERVICES, DERRY (SICKKIDS)

Institutional surcharges: Mandatory institutional levy of \$800/year per person (\$500 glassware supplies and \$300 autoclaving and glass washing services): Two people on this grant - a total of \$1,600 per year.

\$1,600

4. TRAVEL (TOTAL PROJECT)

We request \$1,200 per year for each trainee paid on this grant to cover the cost of travel to scientific meetings to present their research findings on this project.

\$3,600

TOTAL SERVICES AND TRAVEL: \$5,200

TOTAL (YEARS 1-3) = \$260,796.23

TOTAL (YEARS 4-5) = \$252,393.23

157721

CV Module

This page is for CIHR use only. It will not be included in the evaluation of your application for funding.

Family Name Gingras		Given Name Anne-Claude	Middle Initial(s)
Have you previously applied to CIHR for funding? Previous family name used Previous given name used		Yes <input checked="" type="checkbox"/> No <input type="checkbox"/> Title: Dr. <input checked="" type="checkbox"/> Mr. <input type="checkbox"/> Mrs. <input type="checkbox"/> Ms. <input type="checkbox"/> Prof. <input type="checkbox"/>	
Courier Address (If different from mailing address) Samuel Lunenfeld Research Institute Mt. Sinai Hospital Joseph and Wolf Lebovic Health Complex Samuel Lunenfeld Research Institute 600 University Avenue, Room 992A Toronto, Ontario CANADA (M5G 1X5)		Temporary Address Start Date _____ End Date _____	Primary Affiliation Name Samuel Lunenfeld Research Institute of Mount Sinai Hospital Start Date 07/2011 Primary Affiliation Address Samuel Lunenfeld Research Institute Mt. Sinai Hospital Joseph and Wolf Lebovic Health Complex Samuel Lunenfeld Research Institute 600 University Avenue, Room 992A Toronto, Ontario CANADA (M5G 1X5)
Contact numbers Phone Primary (416) 586-5027 Office Secondary (416) 586-4800 #8272 Laboratory Temporary Start Date _____ End Date _____		Fax Primary (416) 586-8869 Temporary Start Date _____ End Date _____	Electronic Addresses E-Mail gingras@lunenfeld.ca Web page address
Citizenship Canadian <input checked="" type="checkbox"/> Other <input type="checkbox"/> Other Country of Citizenship		Permanent Residence in Canada Permanent Resident <input type="checkbox"/> Date of permanent residency status DD/MM/YYYY Have you applied for permanent residency? Yes <input type="checkbox"/> No <input type="checkbox"/>	
Correspondence Language English <input checked="" type="checkbox"/> French <input type="checkbox"/>		Language English (Yes or No) French (Yes or No)	Read Write Speak Understand YES YES YES YES YES YES YES YES
Gender Male <input type="checkbox"/> Female <input checked="" type="checkbox"/>	Date of Birth (DD/MM/YYYY) 10/04/1972	Other Languages:	

Expertise

List up to ten (10) key words that best describe your expertise in research, instruments and technique.

Proteomics	Mass spectrometry
CCMs	Phosphorylation
Phosphatases	Affinity purification
Signal Transduction	GCKIII kinases
Protein interactions	angioma

Indicate and rank the disciplines that best correspond to your research interests. No additional pages may be added.

Discipline			Sub Discipline	
Rank	Code	Description	Code	Description
1.	11	MOLECULAR AND CELLULAR BIOLOGY		
2.	9	BIOCHEMISTRY		
3.	13	CANCER/ONCOLOGY		
4.				
5.				
6.				
7.				
8.				
9.				
10.				
11.				
12.				
13.				
14.				
15.				

Academic Background - One additional page may be added

Indicate all university degrees obtained and those in progress (where applicable) starting with the most recent. If you hold a co-degree from more than one institution (e.g. under the Soutien aux cotutelles de these de doctorat agreement between Quebec and France) enter each institution separately. Do not enter honorary degrees here, they should be listed in the Distinctions section.

Also indicate research training, such as postdoctoral or fellowship training. Trainees only: also list undergraduate and graduate research training experience.

Degree Type	Degree Name and Specialty	Institution/Organization and Country	Supervisor name	Start date (MM/YYYY)	Date received or expected (MM/YYYY)
Doctorate (PhD)	PhD Biochemistry	McGill University CANADA	Dr. Nahum Sonenberg	09/1994	09/2001
Bachelor's	Baccalaureat, Sciences Biochimie	Laval University CANADA	Dr. Andre Darveau	09/1991	05/1994

Work Experience

Starting with the most recent, indicate your current position, where applicable, and other academic and non-academic position(s) since the beginning of your university studies. For your current positions leave the end date blank. Additional pages will be accepted.

Position	Institution/Organization and Country	Department/Division and Faculty/School	Start Date (MM/YYYY)	End Date (MM/YYYY)
Associate Professor	University of Toronto CANADA	Department of Molecular Genetics	07/2011	
Senior Investigator	Samuel Lunenfeld Research Institute of Mount Sinai Hospital CANADA	Research N/A	07/2011	
Assistant Professor	University of Toronto CANADA	Department of Molecular Genetics	04/2006	07/2011
Investigator	Samuel Lunenfeld Research Institute of Mount Sinai Hospital CANADA	Research N/A	12/2005	07/2011
Postdoctoral fellow	Institute for Systems Biology, Seattle UNITED STATES	Proteomics N/A	01/2002	11/2005
PhD Student	McGill University CANADA	Biochemistry Faculty of Medicine, McGill U	05/1994	01/2001
Trainee/ research assistant	Centre de Recherche de la Croix-Rouge, Ste-Foy CANADA	Recherche Affiliated w/ Sciences et Genie, U Laval	09/1992	04/1994

Distinctions / Awards / Credentials

Starting with the most recent, indicate any recognitions received, including awards, fellowships, scholarships, licenses, qualifications, professional designation or credentials. Do not include Academic Appointments here, as they are detailed under Work Experience. Maximum 20 entries.

Name/Title and Type	Institution/Organization and Country	Effective Date (MM/YYYY)	End Date (MM/YYYY)	Specialty	Total Amount
2011 Canada's most powerful women: Top 100 Distinction	Women's Executive Network CANADA	12/2011			
Chair in Functional Proteomics (Renewed) Research award	Canada Research Chair Tier 2	07/2011	06/2016	Functional Proteomics	\$500,000
Chair in Cancer Proteomics Research award	Lea Reichmann CANADA	09/2008			
Early Researcher Award Research award	Ontario Ministry of Research and Innovation CANADA	2007			\$100,000
Chair in Functional Proteomics Research award	Canada Research Chair Tier 2	07/2006	06/2011	Functional Proteomics	\$500,000
Prix d'excellence (doctorat) Distinction	ADESAQ/FRSQ CANADA	2002			
Gordon A MacLachlan Doctoral Award Distinction	McGill University CANADA	05/2002			
Thomas Haliburton Henry Award Distinction	McGill University CANADA	05/2002			
Governor's General Gold Medal Distinction	McGill University	05/2002			
Prix d'Excellence (Sciences) Distinction	Academie des Grands Montrealais CANADA	04/2002			

Distinctions / Awards / Credentials

Starting with the most recent, indicate any recognitions received, including awards, fellowships, scholarships, licenses, qualifications, professional designation or credentials. Do not include Academic Appointments here, as they are detailed under Work Experience. Maximum 20 entries.

Name/Title and Type	Institution/Organization and Country	Effective Date (MM/YYYY)	End Date (MM/YYYY)	Specialty	Total Amount
Harold Weintraub Graduate Student Award Distinction	Fred Hutchinson Cancer Research Center UNITED STATES	02/2002			
Postdoctoral Fellowship Research award	CIHR CANADA	01/2002	12/2004		
Doctoral Award Research award	MRC CANADA	09/1998	09/2001		
Travel Grant Research award	National Cancer Institute of Canada CANADA	10/1997	11/1997		
Centennial (1967) Award Research award	NSERC CANADA	09/1994	08/1998		
Training Fellowship Research award	Fonds de la recherche en sante du Quebec CANADA	09/1993	05/1994		

Patents and Intellectual Property Rights

Record the total numbers of patents / copyrights in the following table.

OBTAINED			APPLICATIONS UNDER PROCESS			TOTAL PATENTS AND INTELLECTUAL PROPERTY RIGHTS
Total individual	Total collective	Sub-total	Total individual	Total collective	Sub-total	
0	0	0	0	0	0	0

PUBLICATIONS AND PRESENTATIONS

Give the number of publications and presentations in the course of your career. Detailed information should be attached as specified in the "Contributions - details" section.

Publications	Refereed Articles	Books and Monographs	Proceedings / Book Chapters / Contributions to a collective work	Abstracts / Notes	TOTALS
Already Published	70	0	17	0	87
Accepted or in the Press	2	0	3	0	5
					92

Invited presentations	65
-----------------------	----

LITERARY AND ARTISTIC WORKS

Provide the number of literary and artistic works created in the course of your career. Detailed information should be attached as specified in the "Contributions - details" section.

IN CIRCULATION			IN PROGRESS			TOTAL LITERARY AND ARTISTIC WORKS
Total individual	Total collective	Sub-total	Total individual	Total collective	Sub-total	
0	0	0	0	0	0	0

Supervisory Experience: To be completed by applicants requesting research trainees as part of their budget, salary support candidates and proposed supervisors of trainees.

Indicate the number of graduate students and postdoctoral fellows that you currently supervise or co-supervise. CIHR defines supervisory experience as the formal supervision or co-supervision of trainees. Enter zero (0) if not applicable.

Master 1Doctoral 1Post-Doctoral 5

Complete this form by listing the trainees that you have supervised/co-supervised (and are currently supervising/co-supervising) within the last five (5) years. Additional pages may be added if necessary.

* Flag those where you were/are the Primary Supervisor.

*	Name of Student	Program Type	Dates		Degree received or expected	Year Degree Rec'd (YYYY)	Research Project (Short title)	Current position and Institution
			Support Period From (MM/YY)	To (MM/YYYY)				
*	McBroom-Cerajewski, Linda	Postdoctoral Fellow, PhD	02/2012				Elements of specificity within the PP2A interaction network	
*	Knight, James	Postdoctoral Fellow, PhD	09/2011				Identification of substrates for GCKIII kinases	
*	Couzens, Amber	Postdoctoral Fellow, PhD	05/2011				Interplay between PP6 and Hippo signaling	
*	St-Denis, Nicole	Postdoctoral Fellow, PhD	12/2010				Cell-cycle interactome dynamics for Ser/Thr phosphatases	
*	Lambert, Jean-Phillipe	Postdoctoral Fellow, PhD	10/2010				Systematic proteomic characterization of human bromodomain specificity	
*	Dunham, Wade	Graduate Student	09/2009		Master's		Phosphorylation networks and modeling	U of Toronto
*	Kean, Michelle	Graduate Student	01/2008		Doctorate (PhD)		kinases and phosphatases in angioma	U. of Toronto
*	Chen, Ginny	Graduate Student	04/2006	12/2010	Doctorate (PhD)		PP4 Phosphatase interaction networks	New England Biolabs

Supervisory Experience: To be completed by applicants requesting research trainees as part of their budget, salary support candidates and proposed supervisors of trainees.

Indicate the number of graduate students and postdoctoral fellows that you currently supervise or co-supervise. CIHR defines supervisory experience as the formal supervision or co-supervision of trainees. Enter zero (0) if not applicable.

Master 1Doctoral 1Post-Doctoral 5

Complete this form by listing the trainees that you have supervised/co-supervised (and are currently supervising/co-supervising) within the last five (5) years. Additional pages may be added if necessary.

* Flag those where you were/are the Primary Supervisor.

*	Name of Student	Program Type	Dates		Degree received or expected	Year Degree Rec'd (YYYY)	Research Project (Short title)	Current position and Institution
			Support Period From (MM/YY)	To (MM/YYYY)				
*	D'Ambrosio, Lisa	Graduate Student	09/2007	12/2009	Master's	2009	dynein interactions with STRIPAK	Graduate student, U. of Toronto
*	Mullin, Michael	Postdoctoral Fellow, PhD	09/2007	12/2009	Postdoctorate		cell division and PP2A	Senior Scientist, Glaxo
*	Tisayakorn, Sally	Graduate Student	01/2006	12/2008	Master's	2009	Regulation of PP2A phosphatase assemblies	Quality Assurance, Allergan Inc.

Funds REQUESTED

List all sources of support applied for (including CIHR) as an applicant or as a co-applicant. Include the principal applicant's name, title of the proposal, funding source, program name, total amount requested (in Canadian dollars) and the period of the support. Indicate your role in the funding (principal applicant/project leader or co-applicant).

Title of Proposal Molecular mechanisms of cerebral cavernous malformations		
Funding Source Canadian Institutes of Health Research (CIHR)		Program Name Operating grant; with Derry
Principal Applicant / Project Leader		Your Role Principal Applicant
Total Amount (CAN\$) \$1,303,981	Support Period From (MM/YYYY) 10/2012	To (MM/YYYY) 09/2017
Title of Proposal A systems approach towards the therapeutic modulation of the acetylome		
Funding Source Canadian Institutes of Health Research (CIHR)		Program Name Operating grant; with Pawson, Filippakopoulos
Principal Applicant / Project Leader		Your Role Principal Applicant
Total Amount (CAN\$) \$1,068,979	Support Period From (MM/YYYY) 10/2012	To (MM/YYYY) 09/2015
Title of Proposal Interplay between the PP6 phosphatase and Hippo signaling		
Funding Source Cancer Research Society (The)		Program Name
Principal Applicant / Project Leader		Your Role Principal Applicant
Total Amount (CAN\$) \$120,000	Support Period From (MM/YYYY) 07/2012	To (MM/YYYY) 06/2014
Title of Proposal		
Funding Source		Program Name
Principal Applicant / Project Leader		Your Role
Total Amount (CAN\$)	Support Period From (MM/YYYY)	To (MM/YYYY)

Funds CURRENTLY HELD

List all sources of support currently held (including CIHR) as an applicant or as a co-applicant. Include the principal applicant's name, title of the proposal, funding source, program name, total amount awarded (in Canadian dollars) and the period of the support. Indicate your role in the funding (principal applicant/project leader or co-applicant).

Title of Proposal Computational tools for mass spectrometry-based Interactome		
Funding Source National Institutes of Health (NIH) (USA)		Program Name RO1
Principal Applicant / Project Leader Nesvizhskii, A		Your Role Co-Applicant
Total Amount (CAN\$) \$60,000	Support Period From (MM/YYYY) 10/2010	To (MM/YYYY) 09/2015
Title of Proposal Global approaches to unravel PP2A function		
Funding Source Canadian Institutes of Health Research (CIHR)		Program Name Operating Grant
Principal Applicant / Project Leader Gingras, Anne-Claude		Your Role Principal Applicant
Total Amount (CAN\$) \$960,385	Support Period From (MM/YYYY) 09/2010	To (MM/YYYY) 08/2015
Title of Proposal Understanding the assembly and function of dynamic signalling networks in complex diseases		
Funding Source Ontario Research Fund (ORF)		Program Name Global Leadership Round in Genomics
Principal Applicant / Project Leader Pawson, AJ		Your Role Co-Applicant
Total Amount (CAN\$) \$898,170	Support Period From (MM/YYYY) 07/2010	To (MM/YYYY) 06/2015
Title of Proposal Structure, function and regulation of PP4cs		
Funding Source Canadian Cancer Society Research Institute (CCSRI)		Program Name Operating Grant
Principal Applicant / Project Leader Gingras, Anne-Claude		Your Role Principal Applicant
Total Amount (CAN\$) \$688,605	Support Period From (MM/YYYY) 07/2009	To (MM/YYYY) 06/2014

Funds CURRENTLY HELD

List all sources of support currently held (including CIHR) as an applicant or as a co-applicant. Include the principal applicant's name, title of the proposal, funding source, program name, total amount awarded (in Canadian dollars) and the period of the support. Indicate your role in the funding (principal applicant/project leader or co-applicant).

Title of Proposal Molecular Mechanisms of Cerebral Cavernous Malformations		
Funding Source Canadian Institutes of Health Research (CIHR)		Program Name CIHR Institute of Genetics – Bridge Funding; with Derry
Principal Applicant / Project Leader		Your Role Principal Applicant
Total Amount (CAN\$) \$100,000	Support Period From (MM/YYYY) 04/2012	To (MM/YYYY) 03/2013
Title of Proposal Core Proteomics Laboratory		
Funding Source Canadian Institutes of Health Research (CIHR)		Program Name CIHR Research Resource Grant - no direct funds to ACG
Principal Applicant / Project Leader Pawson, Anthony J.		Your Role Co-Applicant
Total Amount (CAN\$) \$497,150	Support Period From (MM/YYYY) 04/2008	To (MM/YYYY) 03/2012
Title of Proposal		
Funding Source		Program Name
Principal Applicant / Project Leader		Your Role
Total Amount (CAN\$)	Support Period From (MM/YYYY)	To (MM/YYYY)
Title of Proposal		
Funding Source		Program Name
Principal Applicant / Project Leader		Your Role
Total Amount (CAN\$)	Support Period From (MM/YYYY)	To (MM/YYYY)

Funds HELD IN THE LAST FIVE YEARS

List all sources of support held in the last five years (including CIHR) as an applicant or as a co-applicant. Include the principal applicant's name, title of the proposal, funding source, program name, total amount awarded (in Canadian dollars) and the period of the support. Indicate your role in the funding (principal applicant/project leader or co-applicant).

Title of Proposal Infrastructure for Functional Proteomics		
Funding Source Canada Foundation for Innovation (CFI)		Program Name Leaders Opportunity Fund (associated with CRC)
Principal Applicant / Project Leader Gingras, Anne-Claude		Your Role Principal Applicant
Total Amount (CAN\$) \$159,622	Support Period From (MM/YYYY) 06/2006	To (MM/YYYY) 07/2011
Title of Proposal SET and PP2A interactomes in leukaemia		
Funding Source Leukemia & Lymphoma Society of Canada (The) (LLSC)		Program Name Research Grant
Principal Applicant / Project Leader Gingras, Anne-Claude		Your Role Principal Applicant
Total Amount (CAN\$) \$116,000	Support Period From (MM/YYYY) 07/2009	To (MM/YYYY) 06/2011
Title of Proposal Ontario Proteomic Methods Centre (OMPC)		
Funding Source Ontario Research Fund (ORF)		Program Name Research Excellence Funding - 20K to ACG
Principal Applicant / Project Leader Pawson, Anthony		Your Role Co-Applicant
Total Amount (CAN\$) \$905,397	Support Period From (MM/YYYY) 10/2006	To (MM/YYYY) 03/2011
Title of Proposal Functional Proteomics of Serine/Threonine Phosphatases in the mTOR pathway		
Funding Source Canadian Institutes of Health Research (CIHR)		Program Name Operating Grant
Principal Applicant / Project Leader Gingras, Anne-Claude		Your Role Principal Applicant
Total Amount (CAN\$) \$410,922	Support Period From (MM/YYYY) 08/2008	To (MM/YYYY) 07/2010

Funds HELD IN THE LAST FIVE YEARS

List all sources of support held in the last five years (including CIHR) as an applicant or as a co-applicant. Include the principal applicant's name, title of the proposal, funding source, program name, total amount awarded (in Canadian dollars) and the period of the support. Indicate your role in the funding (principal applicant/project leader or co-applicant).

Title of Proposal Structure, function and regulation of PP4cs		
Funding Source National Cancer Institute of Canada (NCIC)		Program Name Terry Fox Foundation Research Grant for New Investigators
Principal Applicant / Project Leader Gingras, Anne-Claude		Your Role Principal Applicant
Total Amount (CAN\$) \$439,410	Support Period From (MM/YYYY) 07/2006	To (MM/YYYY) 06/2009
Title of Proposal		
Funding Source		Program Name
Principal Applicant / Project Leader		Your Role
Total Amount (CAN\$)	Support Period From (MM/YYYY)	To (MM/YYYY)
Title of Proposal		
Funding Source		Program Name
Principal Applicant / Project Leader		Your Role
Total Amount (CAN\$)	Support Period From (MM/YYYY)	To (MM/YYYY)
Title of Proposal		
Funding Source		Program Name
Principal Applicant / Project Leader		Your Role
Total Amount (CAN\$)	Support Period From (MM/YYYY)	To (MM/YYYY)

Attachment Instructions

How to prepare and format all attachments:

Most Significant Contributions, Activities/Contributions, Interruptions/Delays, Patents/Copyrights (Part 2), and Publications (Part 2) details shall be contained in a CV attachment. Note: If you are using ResearchNet, you will need to provide each section identified as a separate PDF file.

The following format should be adhered to for this attachment.

- 8.5" X 11" (21.5 X 28.0 cm) white single-sided paper.
- Margins of $\frac{3}{4}$ " (2 cm).
- Minimum font size 12 point or 10 characters per inch.
- Six lines per inch, single-spaced, with no condensed type or spacing.
- Number pages consecutively after CV (If, for example, the print-out of the CV ends on page 8, the attachment would begin with page 9.).
- Each page header must contain the name and the sub-section header, e. g., Most Significant Contributions.

Most Significant Contributions

This section applies only to researchers, not to students. Identify a **maximum of five (5) contributions, with a maximum length of one page**, that best highlight your contribution or activities to research, defining the impact and relevance of each. (A contribution is understood to be a publication, literary or artistic work, conference, patent or copyright, contract or creative activity, commission, etc.) Your complete description may include the organization; position or activity type and description; from and to dates; and the basis on which this contribution is significant (i.e. relevance, target community and impact).

Activities / Contributions

The activities and contributions defined in this section should include both academic and non-academic achievements, and their impacts. **Limit the list to one page.**

Interruption(s) / Delays

Identify any administrative responsibilities, family or health reasons, or any other factors that might have delayed or interrupted any of the following: academia, career, scientific research, other research, dissemination of results, training, etc. Common examples of an interruption/delay might be a bereavement period following the death of a loved one, maternity/parental leave, or relocation of your research environment. **Limit the list to one page.**

Descriptions might include the start and end dates, the impact areas, and the reason(s) or a brief explanation of the absence.

Patents and Intellectual Property Rights

This section should include detail for patents and intellectual property rights for technology transfer, products, and services. Do not include Publications in this section. **Limit the list to one page.**

Descriptions for patents/intellectual property rights might include the title, patent/intellectual property rights number and date, country(ies) of issue, as well as the relevance or impact of this item and any inventor name(s) which pertain to it.

Publications List

List your most important publications and other research contributions over the past five years, according to the categories below. This is not necessarily a complete list, and is only intended to provide guidance. Categories can be added as needed. Use only items pertinent to the application. **There is no limit to the number of pages you can use.**

For Training or Salary Support Awards Candidates

- Candidates for training awards or New Investigator awards should list all publications, not just those of the last five years.
- All candidates for training or salary support awards must, for each multi-authored publication, define their role in the publication and indicate their percent contribution to the team effort.
- Candidates for training awards, with or without publications, are invited to comment on environmental factors that affected their capacity to publish.
- Candidates for salary support awards should, for multi-authored publications, underline the names of trainees whose work they supervised.

For Proposed Supervisors of Training Award Applicants

- Attach a maximum of two pages listing the titles and contributions over the past 5 years that will serve the application best.

MOST SIGNIFICANT RECENT PUBLICATIONS RELEVANT TO THIS APPLICATION

- **A PP2A phosphatase high-density interaction network identifies a novel striatin-interacting phosphatase and kinase complex linked to the cerebral cavernous malformation 3 (CCM3) protein.** *Mol Cell Proteomics*, 2009, **8**:157-71. In this paper, affinity purification coupled to mass spectrometry was used to identify a new signaling complex called STRIPAK that possesses both kinase and phosphatase activities. Importantly, one of the molecules linking the kinase and the phosphatase is mutated in familial cases of cerebral cavernous malformations, which is a type of angioma that may lead to strokes. Importantly, we show that the majority of CCM3 resides within this STRIPAK complex, which raises interesting hypotheses regarding the respective roles in the biology of cerebral cavernous malformations of the CCM1•CCM2•CCM3 complex and the CCM3•STRIPAK complex.
- **CCM3/PDCD10 heterodimerizes with Germinal Center Kinase III (GCKIII) proteins using a mechanism homologous to CCM3 homodimerization.** *J Biol Chem*, 2011, **286**: 25056-64. While a recent crystal structure has been determined for a CCM3 homodimer, here we show in a collaboration with Frank Sicheri (Gingras is co-corresponding author) that an heterodimer CCM3-kinase is in fact preferred, both biochemically and inside the cell, to a CCM3 or kinase homodimer. This finding has strong implications for the understanding of cerebral cavernous malformations.
- **Structure-function analysis of core STRIPAK: a signaling complex implicated in Golgi polarization.** *J Biol Chem*, 2011, **286**:25065-75. Following on our initial characterization of the STRIPAK complex, here we report that CCM3 and striatin act as bridges to bring together the kinase and phosphatase components of the complex. We further report that CCM3 and striatin depletion have opposite effects on the Golgi localization of the MST4 kinase and in cell polarity. Since patients with CCM3 mutations are more severely affected than patients with CCM1 or CCM2 mutation, we suggest that the role of the STRIPAK complex in the disease should be further explored.
- **A global protein kinase and phosphatase network.** *Science*, 2010, **328**:1043-6. This paper (a collaboration between the Gingras, Nesvizhskii and Tyers lab; Gingras is co-corresponding author) details a comprehensive survey of interaction partners for all yeast kinases and phosphatases. Importantly, this study revealed the unexpected finding that kinases physically associate with each other, which is likely to modulate the response to different signals, as well as the output of signaling. This study was profiled in *Science*, *Science Signalling* and in the *Nature Signalling Gateway*. In addition, this work enabled the generation of tools and protocols for interaction proteomics in *S. cerevisiae*, which have benefitted University of Toronto colleagues (e.g. Costanzo et al., *Science*, 2010; Baryshnikova, *Nature Methods*, 2010; Sydorskyy et al., *Mol Cell Biol*)
- **SAINT: probabilistic scoring of affinity purification - mass spectrometry data.** *Nature Methods*, 2011, **8**:70-3. This manuscript – a collaboration between the Gingras and Nesvizhskii labs (Gingras is co-corresponding author) – describes the development of a new statistical tool for the analysis of interaction proteomics data. SAINT utilizes quantitative mass spectrometry information for given hits across the entire dataset (including, ideally, negative control runs) to calculate the probability of a bona fide protein-protein interaction. SAINT has been rapidly adopted by other research groups in Toronto and elsewhere (e.g. the Aebersold group at the ETH in Zurich) to remove contaminants from protein lists. SAINT even works on difficult cases, including a true positive interaction between the PP5 phosphatase and the chaperonin Hsp90, as we recently demonstrated (Skarra et al., *Proteomics*, 2011). This software and other tools (such as ProHits, developed by Gingras and Tyers, *Nature Biotech*, 2010) enable our group, but also other researchers worldwide, to produce higher quality protein interaction maps.

PROFESSIONAL AFFILIATIONS AND ACTIVITIES

- 2011 Invitee committee member, Canadian Institutes of Health Research (CIHR), Genomics panel
- 2011 Co-editor (with Alexey Nesvizhskii) of a special issue of *Proteomics* on protein-protein interactions
- 2011 Consultant (category new investigators/ early career) for the International review of the Canadian Institutes of Health Research (CIHR)
- 2010-2011 Full member of the CCSRI (Canadian Cancer Society Research Institute) Panel F (Signaling)
- 2010- Director of the Research Training Center; Samuel Lunenfeld Research Institute
- 2010- Co-organizer (with Laurence Pelletier) of the Annual Samuel Lunenfeld Research Institute retreat
- 2010- Member of the Canadian Research Society Panel A
- 2010- Member of the Graduate student Recruitment committee, Department of Molecular Genetics, University of Toronto
- 2010- Director of the Bioinformatics core platform for the National Technology Platform (CFI; PI = Benoit Coulombe)
- 2009- Editorial Board, Molecular and Cellular Proteomics
- 2009-2010 Scientific Officer on the CCSRI (Canadian Cancer Society Research Institute) Panel F (Signaling)
- 2009 Co-organizer of the International Interactome Initiative (I3) Toronto Workshop (with Benoit Coulombe, IRCM and Tony Pawson, SLRI); co-leader of bioinformatics breakout session (with Pascal Braun, Dana Farber, Harvard Medical School).
- 2008-2011 Member of the Research highlight advisory panel for Nature Reviews Molecular Cell Biology
- 2008- Scientific Advisory Committee for the University of California in San Francisco (UCSF) mass spectrometry facility
- 2008- Member of the Canadian Institutes of Health Research (CIHR) Institute of Genetics New Principal Investigator Meeting Organizing Committee
- 2008- Member of the University of Toronto Molecular Genetics Scholarship Committee (Chair = Brigitte Lavoie 2008-2010; Lori Frappier 2011-)
- 2007-2008 Scientific Officer on the Virology and Structural Biology panel of National Cancer Institute of Canada (NCIC)
- 2007- Ad hoc reviewer: National Science and Engineering Research Council of Canada Discovery Grants; Swiss National Science Foundation; Austrian Science Fund; National Science Foundation.

INTERRUPTIONS/DELAYS

Gingras, Anne-Claude

NONE TO REPORT

PATENTS

Gingras, Anne-Claude

NONE TO REPORT

LIST OF PUBLICATIONS (2007-2012)**h-index = 45; cited 10088 times**

* indicates co-first authorship; ** indicates corresponding author; Gingras lab members underlined

CA = collaborator**PA = principal author****SRA = senior author****Peer reviewed primary articles (from a total of 72):**

1. Major, M.B., Camp, N.D., Berndt, J.D., Yi, XH, Goldenberg, S.J., Hubbert, C., Biechele, T.L., **Gingras, A.-C.**, Zheng, N., MacCoss, M.J., Angers, S. and Moon, R.T. (2007) Wilms Tumor Suppressor WTX negatively regulates WNT/b-catenin signaling. *Science* **316**:1043-1046. (**CA**)
2. Nakada, S., Chen, G.I., **Gingras, A.-C.**** and Durocher, D.** (2008) PP4 is a gH2AX phosphatase required for the recovery from the DNA damage checkpoint. *EMBO Reports*, **9**:1019-26. (**co-SRA**)
3. Rong, L., Livingstone, M., Sukarieh, R., Petroulakis, E., **Gingras, A.-C.**, Crosby, K., Smith, B., Polakiewicz, R.D., Pelletier, J., Ferraiuolo, M.A., and Sonenberg, N. (2008) Control of eIF4E cellular localization by eIF4E-binding proteins, 4E-BPs. *RNA* **14**:1318-27. (**CA**)
4. Chen, G.I., Tisayakorn, S., Jorgensen, C., D'Ambrosio, L.M., Goudreault, M. and **Gingras, A.-C.**** (2008) PP4R4/KIAA1622 forms a novel stable cytosolic complex with phosphoprotein phosphatase 4. *J Biol Chem*, **283**:29273-84. (**SRA**)
5. Goudreault, M., D'Ambrosio, L.M., Kean, M.J., Mullin, M., Larsen, B.G., Sanchez, A., Chaudhry, S., Chen, G.I., Sicheri, F., Nesvizhskii, A.I., Aebersold, R., Raught, B., and **Gingras, A.-C.**** (2009) A PP2A phosphatase high-density interaction network identifies a novel striatin-interacting phosphatase and kinase complex linked to the cerebral cavernous malformation 3 (CCM3) protein. *Mol Cell Proteomics*, **8**:157-71. (**SRA**)
6. Lawo, S., Bashkurov, M., Mullin, M., Gomez Ferreria, M., Kittler, R., Habermann, B., Tagliaferro, A., Poser, I., Hutchins, J., Buchholz, F., Peters, J-M., Hyman, A.A., **Gingras, A.-C.**, and Pelletier, L. (2009) The Augmin complex regulates centrosome and spindle integrity in mammalian cells. *Curr Biol*, **19**:816-26. (**CA**)
7. Costanzo M, Baryshnikova A, Bellay J, Kim Y, Spear ED, Sevier CS, Ding H, Koh JL, Toufighi K, Mostafavi S, Prinz J, St Onge RP, VanderSluis B, Makhnevych T, Vizeacoumar FJ, Alizadeh S, Bahr S, Brost RL, Chen Y, Cokol M, Deshpande R, Li Z, Lin ZY, Liang W, Marback M, Paw J, San Luis BJ, Shuteriqi E, Tong AH, van Dyk N, Wallace IM, Whitney JA, Weirauch MT, Zhong G, Zhu H, Houry WA, Brudno M, Ragibizadeh S, Papp B, Pál C, Roth FP, Giaever G, Nislow C, Troyanskaya OG, Bussey H, Bader GD, **Gingras A.-C.**, Morris QD, Kim PM, Kaiser CA, Myers CL, Andrews BJ, Boone C. (2010) The genetic landscape of a cell. *Science*, **327**:425-21. (**CA**)
8. Bidinosti M., Ran I., Sanchez-Carbente M.R., Martineau Y., **Gingras A.-C.**, Gkogkas C., Raught B., Bramham C.R., Sossin W.S., Costa-Mattioli M., DesGroiseillers L., Lacaille J.C., Sonenberg N. (2010) Postnatal deamidation of 4E-BP2 in brain enhances association with raptor and alters kinetics of excitatory synaptic transmission. *Mol Cell*, **37**:797-808. (**CA**)
9. Breitkreutz A., Choi H., Sharon J., Boucher L., Neduvu V., Larsen B.G., Lin Z.-Y., Breitkreutz B.-J., Stark C., Liu G., Ahn, J., Dewar-Darch, D., Tang X., Almeida, V., Qin, Z.S., Pawson, T., **Gingras, A.-C.****, Nesvizhskii, A.**, Tyers, M.** (2010) A global protein kinase and phosphatase network. *Science*, **328**:1043-6. (**co-SRA**)
10. Mak, A.B., Ni, Z., Hewel, J., Chen, G.I., Zhong, G., Karamboulas, K., Blakely, K., Smiley, S., Marcon, E., Roudeva, D., Li, J., Olsen, J., Punna, T., Isserlin, R., Chetyrkin, S., **Gingras, A.-C.**, Emili, A., Greenblatt, J. and Moffat, J. (2010) A lentiviral-based functional proteomics approach identifies chromatin remodeling complexes important for the induction of pluripotency. *Mol Cell Proteomics*, **9**:811-23. (**CA**)

11. Choi, H., Kim, S., **Gingras, A.-C.**, Nesvizhskii, A.I. (2010). Analysis of protein complexes through model-based biclustering of label-free quantitative AP-MS data. *Mol Syst Biol*, **6**:385. (CA)
12. Sydorskyy, Y., Srikanth, T., Jeram, S.M., Wheaton, S., Vizeacoumar, F.J., Makhnevych, T., Chong, Y.T., **Gingras, A.-C.** and Raught, B. (2010). A novel mechanism for SUMO system control: regulated Ulp1 nucleolar sequestration. *Mol Cell Biol*, **30**:4452. (CA)
13. Nakada, S., Tai, I., Panier, S., Iemura, S.-I., Kumakubo, A., Munro, M., **Gingras, A.-C.**, Natsume, T., Suda, T. and Durocher, D. (2010) Non-canonical inhibition of DNA damage-dependent ubiquitylation by OTUB1. *Nature* 2010 **466**:941-6. (CA)
14. Liu, G., Zhang, J.P., Larsen, B., Stark, C., Breitkreutz, A., Lin, Z.-Y., Breitkreutz, B.-J., Ding, Y., Colwill, K., Pasculescu, A., Pawson, T., Wrana, J., Nesvizhskii, A.I., Raught, B., Tyers, M.**, and **Gingras, A.-C.**** (2010) ProHits: an integrated software platform for mass spectrometry-based interaction proteomics. *Nat Biotech*, **28**:1015-7. (co-SRA)
15. Baryshnikova A, Costanzo M, Kim Y, Ding H, Koh J, Toufighi K, Youn JY, Ou J, San Luis BJ, Bandyopadhyay S, Hibbs M, Hess D, **Gingras A.-C.**, Bader GD, Troyanskaya OG, Brown GW, Andrews B, Boone C, Myers CL. (2010) Quantitative analysis of fitness and geneic interactions on a genome scale. *Nat Methods*, **7**:1017-24 (CA)
16. O'Donnell L, Panier S, Wildenhain J, Tkach JM, Al-Hakim A, Landry MC, Escribano-Diaz C, Szilard RK, Young JT, Munro M, Canny MD, Kolas NK, Zhang W, Harding SM, Ylanko J, Mendez M, Mullin M, Sun T, Habermann B, Datti A, Bristow RG, **Gingras A.-C.**, Tyers M, Brown G and Durocher D. (2010) The MMS22L-TONSL complex mediates recovery from replication stress and homologous recombination. *Mol Cell*, **40**:619-31. (CA)
17. Choi, H., Larsen, B., Lin, Z.-Y., Breitkreutz, A., Mellacheruvu, D., Fermin, D., Qin, Z.S., Tyers, M., **Gingras, A.-C.**** and Nesvizhskii, A.I.** (2011) SAINT: probabilistic scoring of affinity purification - mass spectrometry data. *Nature Methods*, **8**:70-3. (co-SRA)
18. Templeton, G., Nimixk, M., Morrice, N.A., Campbell, D.G., Goudreault, M., **Gingras, A.-C.**, Takemiya, A., Shimazaki, K.I., Moorhead, G.B. (2011) Identification and characterization of Atl-2, an Arabidopsis homolog of an ancient protein phosphatase (PP1) regulatory subunit. *Biochem J*, **435**:73-83. (CA)
19. Skarra, D.V., Goudreault, M., Choi, H., Mullin, M., Nesvizhskii, A., **Gingras, A.-C.****, and Honkanen, R.** (2011) Label-free quantitative proteomics and SAINT analysis enable interactome mapping for the human Ser/Thr protein phosphatase 5. *Proteomics*, **11**:1508-16. (co-SRA)
20. Li, Z., Vizeacoumar, F., Bahr, S., Li, J., Warringer, J., Vizeacoumar, F., VanderSluis, B., Bellay, J., DeVit, M., Fleming, J., Stephens, A., Haase, J., Lin, Z.-Y., Baryshnikova, A., Min, R., Lu, H., Yan, Z., Jin, K., Barker, S., Datti, A., Giaever, G., Nislow, C., Bulawa, C., Costanzo, M., Myers, C., **Gingras, A.-C.**, Zhang, Z., Blomberg, A., Bloom, K., Andrews, B. and Boone, C. (2011) Systematic exploration of essential gene function with temperature-sensitive mutants. *Nature Biotech*, **29**:361-7. (CA)
21. Dunham, W., Larsen, B., Tate, S., Gonzalez Badillo, B., Tehami, Y., Kislinger, T., Goudreault M and **Gingras, A.-C.**** (2011) A cost-benefit analysis of multidimensional fractionation of affinity purification – mass spectrometry samples. *Proteomics*, **11**:2603-12. (SRA)
22. Kean, M.J., Ceccarelli, D., Goudreault, M., Tate, S., Larsen, B., Sanches, M., Gibson, L.C., Derry, W.B., Scott, I.C., Pelletier, L., Baillie, G.S., Sicheri, F., and **Gingras, A.-C.**** (2011) Structure-function analysis of core STRIPAK proteins: a signaling complex implicated in Golgi polarization. *J Biol Chem*, **15**:25065-75. (SRA)
23. Ceccarelli, D.F., Laister, R.C., Mulligan V.K., Kean, M.J., Goudreault, M., Scott, I.C., Derry, W.B., Chakrabartly A., **Gingras, A.-C.**** and Sicheri, F.** (2011) CCM3/PDCD10 Heterodimerizes with germinal center kinase III (GCKIII) proteins using a mechanism analogous to CCM3 homodimerization. *J Biol Chem*, **15**:25056-64. (co-SRA)

24. Olhovsky, M., Williton, K., Dai, A.Y., Pascalescu, A., Lee, J.P., Goudreault, M., Wells, C.D., Park, J.G., **Gingras, A.-C.**, Linding, R., Pawson, T., and Colwill, K. (2011) OpenFreezer: A reagent information management software system. *Nature Methods*, **28**:612-3. (**CA**)
25. Filippakopoulos, P., Picaud, S., Mangos, M., Keates, T., Lambert, J.-P., Barsyte-Lovejoy, D., Felletar, I., Volkmer, R., Müller, S., Pawson, T., **Gingras, A-C.**, Arrowsmith, CH., and Knapp, S. (2012) Histone recognition and large structural analysis of the human bromodomain family. *In press, Cell*, CELL-S-11-01462 (**CA**)
26. Al-hakim, A.K., Bashkurov, M., **Gingras, A.-C.**, Durocher, D and Pelletier, L. (2012) Interaction proteomics identify NEURL4 and the HECT E3 ligase HERC2 as novel modulators of centrosome architecture. *Mol Cell Proteomics, Epub PMID:22261722* (**CA**)
27. Knight, J.R., Tian, R., Lee, R.E.C., Wang, F., Beauvais, A., Zou, H., Megeney, L.A., Gingras, A.-C., Pawson, T., Figeys, D. and Kothary, R. (2012) A novel whole-cell lysate kinase assay identifies substrates of the p38 MAPK in differentiating myoblasts. *In press, Skeletal Muscle*, MS4098815215883429. (**CA**)
28. Jovic, M., Kean, M.J., Szentpetery, Z., Polevoy, G., **Gingras, A.-C.**, Brill, J.A. and Balla, T. (2011) Two PI 4-kinases control lysosomal delivery of the Gaucher disease enzyme, β -glucocerebrosidase. *In press, Mol Biol Cell*, E11-06-0553. (**CA**)

Review articles and book chapters (from a total of 20):

1. Raught, B. and **Gingras, A.-C.**** (2007) Signaling to translation initiation. In *Translational control in biology and medicine*. M.B. Mathews, N. Sonenberg and J.W.B. Hershey, eds. Cold Spring Harbor Laboratory Press, Plainview, N.Y. 369-400. (**SRA**)
2. Chen, G.I. and **Gingras, A.-C.**** (2007) Affinity-purification mass spectrometry (AP-MS) of serine/threonine phosphatases. *Methods*, **42**:298-305. (**SRA**)
3. **Gingras, A.-C.****, Gstaiger, M., Raught, B and Aebersold, R. (2007) Analysis of protein complexes using mass spectrometry. *Nature Reviews Mol Cell Biol*, **8**:645-654. (**PA**)
4. **Gingras, A.-C.**** (2009) Journal Club: 35 later, mRNA caps still matter. *Nature Reviews Mol Cell Biol*, **10**:734. (**SRA**)
5. St-Denis, N. and **Gingras, A.-C.**** (2011) Mass spectrometric tools for systematic analysis of protein phosphorylation. Progress in molecular biology and translational sciences: Protein Phosphorylation in Health and Disease, Elsevier, edited by S. Shenolikar, *in press* (**SRA**).
6. **Gingras, A.-C.**** (2011) Protein Phosphatases, from Molecules to Networks. *EMBO Reports*, **12**:1211-13 (**PA, SRA**).
7. Lambert, J.-P., Pawson, T. and **Gingras, A.-C.**** (2011) Mapping physical interactions within chromatin by proteomic approaches. *In press, Proteomics, pmic.201100547* (**SRA**).
8. Dunham, W., Mullin, M and **Gingras, A.-C.**** (2011) Affinity-Purification coupled to Mass Spectrometry: Basic Principles and Strategies. *In press, Proteomics, pmic.201100523* (**SRA**).
9. Braun, P. and **Gingras, A.-C.** (2012) Protein interactions in the 20th century: from egg white to complex networks. *In press, Proteomics* (**CA**)

CV Module

This page is for CIHR use only. It will not be included in the evaluation of your application for funding.

Family Name Derry		Given Name William	Middle Initial(s) B												
Have you previously applied to CIHR for funding? Previous family name used Previous given name used		Yes <input checked="" type="checkbox"/> No <input type="checkbox"/> Title: Dr. <input checked="" type="checkbox"/> Mr. <input type="checkbox"/> Mrs. <input type="checkbox"/> Ms. <input type="checkbox"/> Prof. <input type="checkbox"/>													
Courier Address (If different from mailing address) Developmental & Stem Cell Biology The Hospital for Sick Children Toronto Medical Discovery Tower 101 College Street West Room 12-311 Toronto, Ontario CANADA (M5G 1L7)		Temporary Address Start Date _____ End Date _____	Primary Affiliation Name The Hospital for Sick Children Start Date 10/2010 Primary Affiliation Address Developmental & Stem Cell Biology The Hospital for Sick Children Toronto Medical Discovery Tower 101 College Street West Room 12-311 Toronto, Ontario CANADA (M5G 1L7)												
Contact numbers Phone Primary (416) 813-7654 #1829 Office Secondary (416) 813-7654 #1853 Laboratory Temporary Start Date _____ End Date _____		Fax Primary (416) 813-2212 Temporary Start Date _____ End Date _____	Electronic Addresses E-Mail brent.derry@sickkids.ca Web page address http://www.sickkids.ca/AboutSickKids/Directory/People/D/Brent-Derry.html												
Citizenship Canadian <input checked="" type="checkbox"/> Other <input type="checkbox"/> Other Country of Citizenship		Permanent Residence in Canada Permanent Resident <input type="checkbox"/> Date of permanent residency status DD/MM/YYYY Have you applied for permanent residency? Yes <input type="checkbox"/> No <input type="checkbox"/>													
Correspondence Language English <input checked="" type="checkbox"/> French <input type="checkbox"/>		Language Read Write Speak Understand <table border="1" style="margin-left: auto; margin-right: auto;"> <tr> <td colspan="2">English (Yes or No)</td> <td>YES</td> <td>YES</td> <td>YES</td> <td>YES</td> </tr> <tr> <td colspan="2">French (Yes or No)</td> <td>NO</td> <td>NO</td> <td>NO</td> <td>NO</td> </tr> </table> Other Languages: _____		English (Yes or No)		YES	YES	YES	YES	French (Yes or No)		NO	NO	NO	NO
English (Yes or No)		YES	YES	YES	YES										
French (Yes or No)		NO	NO	NO	NO										
Gender Male <input checked="" type="checkbox"/> Female <input type="checkbox"/>	Date of Birth (DD/MM/YYYY) 28/07/1966														

Expertise

List up to ten (10) key words that best describe your expertise in research, instruments and technique.

Genetics	Microscopy
Functional Genomics	Signal transduction
Cancer	
Biochemistry	
Molecular Biology	

Indicate and rank the disciplines that best correspond to your research interests. No additional pages may be added.

Discipline			Sub Discipline	
Rank	Code	Description	Code	Description
1.	37	GENETICS	466	Developmental Genetics
2.	11	MOLECULAR AND CELLULAR BIOLOGY	1088	DNA Replication Damage and Repair
3.	13	CANCER/ONCOLOGY	149	Carcinogenesis, Mechanisms
4.	9	BIOCHEMISTRY	111	Protein/Amino Acid Biochemistry
5.	77	RADIOLOGY/RADIATION BIOLOGY/NUCLEAR MEDICINE	1060	Radiation Biology
6.				
7.				
8.				
9.				
10.				
11.				
12.				
13.				
14.				
15.				

Academic Background - One additional page may be added

Indicate all university degrees obtained and those in progress (where applicable) starting with the most recent. If you hold a co-degree from more than one institution (e.g. under the Soutien aux cotutelles de these de doctorat agreement between Quebec and France) enter each institution separately. Do not enter honorary degrees here, they should be listed in the Distinctions section.

Also indicate research training, such as postdoctoral or fellowship training. Trainees only: also list undergraduate and graduate research training experience.

Degree Type	Degree Name and Specialty	Institution/Organization and Country	Supervisor name	Start date (MM/YYYY)	Date received or expected (MM/YYYY)
Doctorate (PhD)	PhD Biochemistry & Molecular Biology	University of California, Santa Barbara UNITED STATES	Dr. Leslie Wilson	09/1992	06/1997
Master's	M.Sc. Biochemistry	McMaster University CANADA	Dr. Radhey S. Gupta	09/1989	06/1991
Bachelor's, Honours	B.Sc. (Honours) Biochemistry	Carleton University CANADA	Biochemistry, Carleton University	09/1985	06/1989

Work Experience

Starting with the most recent, indicate your current position, where applicable, and other academic and non-academic position(s) since the beginning of your university studies. For your current positions leave the end date blank. Additional pages will be accepted.

Position	Institution/Organization and Country	Department/Division and Faculty/School	Start Date (MM/YYYY)	End Date (MM/YYYY)
Associate Professor	University of Toronto CANADA	Molecular Genetics Medicine	07/2011	
Member	Ontario Stem Cell Initiative CANADA		04/2011	
Senior Scientist	The Hospital for Sick Children CANADA	Developmental and Stem Cell Biology	10/2010	
Member	University of Toronto CANADA	Collaborative Program in Developmental Biology Medicine	09/2010	
Assistant Professor	University of Toronto CANADA	Molecular Genetics Medicine	09/2003	07/2011
Scientist	The Hospital for Sick Children CANADA	Developmental and Stem Cell Biology Medicine	09/2003	10/2010
Research Associate	University of California, Santa Barbara UNITED STATES	Molecular, Cellular & Development Biology	09/1997	06/2003
Teaching Assistant	University of California, Santa Barbara UNITED STATES	Molecular, Cellular & Developmental Biology	09/1992	06/1997
Teaching Assistant	McMaster University CANADA	Biochemistry	09/1989	06/1991

Distinctions / Awards / Credentials

Starting with the most recent, indicate any recognitions received, including awards, fellowships, scholarships, licenses, qualifications, professional designation or credentials. Do not include Academic Appointments here, as they are detailed under Work Experience. Maximum 20 entries.

Name/Title and Type	Institution/Organization and Country	Effective Date (MM/YYYY)	End Date (MM/YYYY)	Specialty	Total Amount
New Opportunities Fund Award Research award	Canada Foundation for Innovation CANADA	06/2004	06/2008		\$254,941
Postdoctoral Fellowship Research award	Tri-Counties Blood Bank UNITED STATES	11/2000	05/2003	Cancer and Blood Research	\$105,000
Clinical Research Scholar Research award	American Association for Cancer Research/Glaxo Wellcome Oncology UNITED STATES	01/1997	06/1997		
Postdoctoral Fellowship Research award	Cancer Foundation of Santa Barbara UNITED STATES	10/1996	06/1998	Cancer Research	\$70,000
Neuroscience Research Institute Fellowship Research award	University of California, Santa Barbara UNITED STATES	01/1996	10/1997	Neuroscience Research	\$4,000
Predoctoral Student Travel Award Research award	American Society for Cell Biology UNITED STATES	07/1993	08/1993		

Patents and Intellectual Property Rights

Record the total numbers of patents / copyrights in the following table.

OBTAINED			APPLICATIONS UNDER PROCESS			TOTAL PATENTS AND INTELLECTUAL PROPERTY RIGHTS
Total individual	Total collective	Sub-total	Total individual	Total collective	Sub-total	
1	0	1	0	0	0	1

PUBLICATIONS AND PRESENTATIONS

Give the number of publications and presentations in the course of your career. Detailed information should be attached as specified in the "Contributions - details" section.

Publications	Refereed Articles	Books and Monographs	Proceedings / Book Chapters / Contributions to a collective work	Abstracts / Notes	TOTALS
Already Published	23	0	0	41	64
Accepted or in the Press	0	0	0	0	0
					64

Invited presentations	29
-----------------------	----

LITERARY AND ARTISTIC WORKS

Provide the number of literary and artistic works created in the course of your career. Detailed information should be attached as specified in the "Contributions - details" section.

IN CIRCULATION			IN PROGRESS			TOTAL LITERARY AND ARTISTIC WORKS
Total individual	Total collective	Sub-total	Total individual	Total collective	Sub-total	
0	0	0	0	0	0	0

Supervisory Experience: To be completed by applicants requesting research trainees as part of their budget, salary support candidates and proposed supervisors of trainees.

Indicate the number of graduate students and postdoctoral fellows that you currently supervise or co-supervise. CIHR defines supervisory experience as the formal supervision or co-supervision of trainees. Enter zero (0) if not applicable.

Master 2Doctoral 0Post-Doctoral 3

Complete this form by listing the trainees that you have supervised/co-supervised (and are currently supervising/co-supervising) within the last five (5) years. Additional pages may be added if necessary.

* Flag those where you were/are the Primary Supervisor.

*	Name of Student	Program Type	Dates		Degree received or expected	Year Degree Rec'd (YYYY)	Research Project (Short title)	Current position and Institution
			Support Period From (MM/YY)	To (MM/YYYY)				
*	Mateo, Abigail	Graduate Student	12/2011		Master's		Role of cep-1/p63 in Fanconi anemia	Graduate student, U of T
*	Hall, Mathew	Graduate Student	12/2011		Master's		Regulation of excretory cell development by CCM genes	Graduate student, U of T
*	Benjamin Lant	Postdoctoral Fellow, PhD	09/2011		Postdoctorate		Non-autonomous control of germline apoptosis	Postdoctoral Fellow, SickKids
*	Mehran Haeri	Postdoctoral Fellow, PhD	02/2011				Nonautonomous control of germ line apoptosis and excretory cell development by CCM genes	Postdoctoral Fellow, SickKids
*	Kristine Jolliffe	Postdoctoral Fellow, PhD	05/2011	11/2011	Postdoctorate		Role of CEP-1 in recombinational repair during meiosis	Postdoctoral Fellow, SickKids
*	Kristine Jolliffe	Graduate Student	09/2003	07/2011	Doctorate (PhD)	2011	Regulation of chromosome instability by CEP-1/p53	Postdoctoral Fellow, SickKids
*	Andrew Perrin	Graduate Student	04/2006	01/2011	Doctorate (PhD)	2011	Regulation of cep-1-dependent germline apoptosis by akt-1	MD student, U of T
*	Shu Ito	Graduate Student	09/2005	11/2010	Doctorate (PhD)	2010	Control of germline apoptosis by the CCM1 orthologue kri-1 in C. elegans	Graduate Student, U of T

William B DERRY

Supervisory Experience: To be completed by applicants requesting research trainees as part of their budget, salary support candidates and proposed supervisors of trainees.

Indicate the number of graduate students and postdoctoral fellows that you currently supervise or co-supervise. CIHR defines supervisory experience as the formal supervision or co-supervision of trainees. Enter zero (0) if not applicable.

Master 2

Doctoral 0

Post-Doctoral 3

Complete this form by listing the trainees that you have supervised/co-supervised (and are currently supervising/co-supervising) within the last five (5) years. Additional pages may be added if necessary.

* Flag those where you were/are the Primary Supervisor.

*	Name of Student	Program Type	Dates		Degree received or expected	Year Degree Rec'd (YYYY)	Research Project (Short title)	Current position and Institution
			Support Period From (MM/YY)	To (MM/YYYY)				
*	Xiangrong Gao	Postdoctoral Fellow, PhD	05/2004	04/2010		2004	Control of CEP-1-dependent apoptosis by the E3 ubiquitin ligase SCF-FSN-1	Medical technologist, CML Health Care
*	Ashley Ross	Graduate Student	01/2008	10/2009	Master's	2009	Regulation of CEP-1-dependent germline apoptosis by the E3 ubiquitin ligase EEL-1	Research associate, U of T
*	Michelle Li	Graduate Student	04/2006	07/2008	Master's	2008	Control of DNA damage-induced apoptosis by E3 ubiquitin ligases	Consultant, Millennium Research
*	Adrienne Rollie	Graduate Student	01/2005	06/2008	Master's	2008	Mechanism by which the SATB2-like protein DVE-1 controls CEP-1 activity in the germline and soma	Technician, USC
*	Jelena Kisin-Rajlic	Graduate Student	06/2004	06/2008	Master's		Regulation of chromosome stability in C. elegans	Sales representative, VWR Canada
	Celia Quevedo	Postdoctoral Fellow, PhD	10/2004	04/2007			Cross-talk between Akt and p53 in the regulation of apoptosis	Project manager, Biobide, Spain

Funds REQUESTED

List all sources of support applied for (including CIHR) as an applicant or as a co-applicant. Include the principal applicant's name, title of the proposal, funding source, program name, total amount requested (in Canadian dollars) and the period of the support. Indicate your role in the funding (principal applicant/project leader or co-applicant).

Title of Proposal Molecular Mechanisms of Cerebral Cavernous Malformations		
Funding Source Canadian Institutes of Health Research (CIHR)		Program Name Operating Grant
Principal Applicant / Project Leader Gingras, Anne-Claude		Your Role Co-Applicant
Total Amount (CAN\$) \$505,195	Support Period From (MM/YYYY) 10/2012	To (MM/YYYY) 09/2017
Title of Proposal Regulation of DNA repair by the p53 and Fanconi anemia pathways		
Funding Source Cancer Research Society (The)		Program Name Operating Grant
Principal Applicant / Project Leader		Your Role Principal Applicant
Total Amount (CAN\$) \$120,000	Support Period From (MM/YYYY) 07/2012	To (MM/YYYY) 06/2014
Title of Proposal		
Funding Source		Program Name
Principal Applicant / Project Leader		Your Role
Total Amount (CAN\$)	Support Period From (MM/YYYY)	To (MM/YYYY)
Title of Proposal		
Funding Source		Program Name
Principal Applicant / Project Leader		Your Role
Total Amount (CAN\$)	Support Period From (MM/YYYY)	To (MM/YYYY)

Funds CURRENTLY HELD

List all sources of support currently held (including CIHR) as an applicant or as a co-applicant. Include the principal applicant's name, title of the proposal, funding source, program name, total amount awarded (in Canadian dollars) and the period of the support. Indicate your role in the funding (principal applicant/project leader or co-applicant).

Title of Proposal Regulation of apoptosis by insulin signaling in C. elegans		
Funding Source Canadian Institutes of Health Research (CIHR)		Program Name Operating Grant
Principal Applicant / Project Leader Liu, Fei-Fei		Your Role Principal Applicant
Total Amount (CAN\$) \$558,470	Support Period From (MM/YYYY) 03/2010	To (MM/YYYY) 03/2015
Title of Proposal The Terry Fox Foundation Strategic Training Initiative for Excellence in Radiation Research for the 21st Century (EIRR21) at CIHR		
Funding Source Canadian Institutes of Health Research (CIHR)		Program Name Terry Fox Foundation Training Grant in Cancer Research at CI
Principal Applicant / Project Leader Liu, Fei-Fei		Your Role Co-Applicant
Total Amount (CAN\$) \$952,500	Support Period From (MM/YYYY) 04/2009	To (MM/YYYY) 03/2015
Title of Proposal Molecular control of apoptosis in C. elegans		
Funding Source Canadian Institutes of Health Research (CIHR)		Program Name Operating Grant
Principal Applicant / Project Leader Gingras, Anne-Claude		Your Role Principal Applicant
Total Amount (CAN\$) \$594,615	Support Period From (MM/YYYY) 04/2009	To (MM/YYYY) 03/2014
Title of Proposal Molecular mechanisms of cerebral cavernous malformations		
Funding Source Canadian Institutes of Health Research (CIHR)		Program Name Operating Grant: Institute of Genetics Bridge Funding
Principal Applicant / Project Leader Gingras, Anne-Claude		Your Role Co-Applicant
Total Amount (CAN\$) \$100,000	Support Period From (MM/YYYY) 04/2012	To (MM/YYYY) 03/2013

Funds CURRENTLY HELD

List all sources of support currently held (including CIHR) as an applicant or as a co-applicant. Include the principal applicant's name, title of the proposal, funding source, program name, total amount awarded (in Canadian dollars) and the period of the support. Indicate your role in the funding (principal applicant/project leader or co-applicant).

Title of Proposal Molecular mechanisms of cerebral cavernous malformations		
Funding Source Canadian Institutes of Health Research (CIHR)		Program Name CIHR Institute of Genetics - Bridge Funding
Principal Applicant / Project Leader Gingras, Anne-Claude		Your Role Co-Applicant
Total Amount (CAN\$) \$40,000	Support Period From (MM/YYYY) 04/2012	To (MM/YYYY) 03/2013
Title of Proposal Synthetic lethal interactions in the p53 signaling network		
Funding Source Hospital for Sick Children		Program Name Garron Family Cancer Centre Small Grant
Principal Applicant / Project Leader		Your Role Principal Applicant
Total Amount (CAN\$) \$50,000	Support Period From (MM/YYYY) 07/2011	To (MM/YYYY) 06/2012
Title of Proposal		
Funding Source		Program Name
Principal Applicant / Project Leader		Your Role
Total Amount (CAN\$)	Support Period From (MM/YYYY)	To (MM/YYYY)
Title of Proposal		
Funding Source		Program Name
Principal Applicant / Project Leader		Your Role
Total Amount (CAN\$)	Support Period From (MM/YYYY)	To (MM/YYYY)

Funds HELD IN THE LAST FIVE YEARS

List all sources of support held in the last five years (including CIHR) as an applicant or as a co-applicant. Include the principal applicant's name, title of the proposal, funding source, program name, total amount awarded (in Canadian dollars) and the period of the support. Indicate your role in the funding (principal applicant/project leader or co-applicant).

Title of Proposal Regulation of p53-dependent apoptosis by Akt/PKB in C. elegans		
Funding Source Canadian Institutes of Health Research (CIHR)		Program Name Operating Grant Priority Announcement: Cancer
Principal Applicant / Project Leader		Your Role Principal Applicant
Total Amount (CAN\$) \$100,000	Support Period From (MM/YYYY) 04/2009	To (MM/YYYY) 03/2010
Title of Proposal Cancer and Cell Death		
Funding Source Canadian Institutes of Health Research (CIHR)		Program Name Meetings, Planning and Dissemination Grant: Knowledge Transl
Principal Applicant / Project Leader		Your Role Principal Applicant
Total Amount (CAN\$) \$17,500	Support Period From (MM/YYYY) 01/2009	To (MM/YYYY) 03/2009
Title of Proposal Molecular control of apoptosis and cell size in C. elegans		
Funding Source Canadian Institutes of Health Research (CIHR)		Program Name Operating Grant
Principal Applicant / Project Leader		Your Role Principal Applicant
Total Amount (CAN\$) \$362,340	Support Period From (MM/YYYY) 03/2006	To (MM/YYYY) 03/2009
Title of Proposal Establishing a functional genomics laboratory to study the p53 network using C. elegans as a model system		
Funding Source Canada Foundation for Innovation (CFI)		Program Name New Opportunities Award
Principal Applicant / Project Leader		Your Role Principal Applicant
Total Amount (CAN\$) \$331,424	Support Period From (MM/YYYY) 05/2004	To (MM/YYYY) 05/2008

Funds HELD IN THE LAST FIVE YEARS

List all sources of support held in the last five years (including CIHR) as an applicant or as a co-applicant. Include the principal applicant's name, title of the proposal, funding source, program name, total amount awarded (in Canadian dollars) and the period of the support. Indicate your role in the funding (principal applicant/project leader or co-applicant).

Title of Proposal Establishing a functional genomics laboratory to study the p53 network using C. elegans as a model system		
Funding Source Ontario Research Fund (ORF)		Program Name Matching Funds
Principal Applicant / Project Leader		Your Role Principal Applicant
Total Amount (CAN\$) \$254,941	Support Period From (MM/YYYY) 05/2004	To (MM/YYYY) 05/2008
Title of Proposal		
Funding Source		Program Name
Principal Applicant / Project Leader		Your Role
Total Amount (CAN\$)	Support Period From (MM/YYYY)	To (MM/YYYY)
Title of Proposal		
Funding Source		Program Name
Principal Applicant / Project Leader		Your Role
Total Amount (CAN\$)	Support Period From (MM/YYYY)	To (MM/YYYY)
Title of Proposal		
Funding Source		Program Name
Principal Applicant / Project Leader		Your Role
Total Amount (CAN\$)	Support Period From (MM/YYYY)	To (MM/YYYY)

Attachment Instructions

How to prepare and format all attachments:

Most Significant Contributions, Activities/Contributions, Interruptions/Delays, Patents/Copyrights (Part 2), and Publications (Part 2) details shall be contained in a CV attachment. Note: If you are using ResearchNet, you will need to provide each section identified as a separate PDF file.

The following format should be adhered to for this attachment.

- 8.5" X 11" (21.5 X 28.0 cm) white single-sided paper.
- Margins of $\frac{3}{4}$ " (2 cm).
- Minimum font size 12 point or 10 characters per inch.
- Six lines per inch, single-spaced, with no condensed type or spacing.
- Number pages consecutively after CV (If, for example, the print-out of the CV ends on page 8, the attachment would begin with page 9.).
- Each page header must contain the name and the sub-section header, e. g., Most Significant Contributions.

Most Significant Contributions

This section applies only to researchers, not to students. Identify a **maximum of five (5) contributions, with a maximum length of one page**, that best highlight your contribution or activities to research, defining the impact and relevance of each. (A contribution is understood to be a publication, literary or artistic work, conference, patent or copyright, contract or creative activity, commission, etc.) Your complete description may include the organization; position or activity type and description; from and to dates; and the basis on which this contribution is significant (i.e. relevance, target community and impact).

Activities / Contributions

The activities and contributions defined in this section should include both academic and non-academic achievements, and their impacts. **Limit the list to one page.**

Interruption(s) / Delays

Identify any administrative responsibilities, family or health reasons, or any other factors that might have delayed or interrupted any of the following: academia, career, scientific research, other research, dissemination of results, training, etc. Common examples of an interruption/delay might be a bereavement period following the death of a loved one, maternity/parental leave, or relocation of your research environment. **Limit the list to one page.**

Descriptions might include the start and end dates, the impact areas, and the reason(s) or a brief explanation of the absence.

Patents and Intellectual Property Rights

This section should include detail for patents and intellectual property rights for technology transfer, products, and services. Do not include Publications in this section. **Limit the list to one page.**

Descriptions for patents/intellectual property rights might include the title, patent/intellectual property rights number and date, country(ies) of issue, as well as the relevance or impact of this item and any inventor name(s) which pertain to it.

Publications List

List your most important publications and other research contributions over the past five years, according to the categories below. This is not necessarily a complete list, and is only intended to provide guidance. Categories can be added as needed. Use only items pertinent to the application. **There is no limit to the number of pages you can use.**

For Training or Salary Support Awards Candidates

- Candidates for training awards or New Investigator awards should list all publications, not just those of the last five years.
- All candidates for training or salary support awards must, for each multi-authored publication, define their role in the publication and indicate their percent contribution to the team effort.
- Candidates for training awards, with or without publications, are invited to comment on environmental factors that affected their capacity to publish.
- Candidates for salary support awards should, for multi-authored publications, underline the names of trainees whose work they supervised.

For Proposed Supervisors of Training Award Applicants

- Attach a maximum of two pages listing the titles and contributions over the past 5 years that will serve the application best.

Unraveling the p53 network in *C. elegans*. My interests in the regulation of apoptosis inspired a career change into the genetic model organism *Caenorhabditis elegans*. As a postdoctoral fellow I discovered the elusive worm p53 family member, *cep-1*, that had evaded identification for many years (Derry *et al.*, 2001). Based on the discovery of *cep-1* and reagents I filed a US patent with my former postdoctoral supervisor Dr. Joel Rothman that was issued in 2007. Elucidating the *cep-1* regulatory network by expression profiling and RNAi screening laid the foundations for my independent lab at the Hospital for Sick Children. My lab elucidated the network of genes transcriptionally regulated by CEP-1 and discovered a novel role for *cep-1* and its target gene *phg-1* (the orthologue of human growth arrest-specific 1 or Gas1) in developmental rate and germ cell proliferation (Derry *et al.*, 2007). This provided the first evidence that *cep-1* plays an important role in cell proliferation and development.

- 1) **Derry, W.B.**, Putzke, A.P. & Rothman, J.H. (2001). *Caenorhabditis elegans* p53: Role in Apoptosis, Meiosis, and Stress Resistance. *Science*, 294: 591-594. Published online September 13, 2001; 10.1126/science.1065486 (Science Express Reports). (207 citations)
- 2) **Derry, W.B.**, Bierings, R., van Iersel, M., Satkunendran, T., Reinke, V. & Rothman, J.H. (2007). Regulation of developmental timing and germ cell proliferation in *C. elegans* by the p53 gene network. *Cell Death and Differentiation*, 14: 662-670. (21 citations)

Since establishing my lab at the Hospital for Sick Children in 2003, I have taken a multifaceted approach using genetics, functional genomics, biochemistry, and cell biology to identify and characterize genes that collaborate with *cep-1* to regulate its apoptotic functions. In a recently renewed CIHR-funded project we discovered several E3 ubiquitin ligases that regulate DNA damage-induced apoptosis, including the Skp-Cullin-F-box (SCF) E3 ubiquitin ligase SCF^{FSN-1} (Gao *et al.*, 2008) and the HECT domain E3 ligase EEL-1, a homologue of mammalian Mule/ARF-BP1 (Ross *et al.*, 2011). Interestingly, the human equivalent of SCF^{FSN-1} (SCF^{FBXO45}) was subsequently shown by Gerry Melino's lab to have a conserved role in the regulation of p73-dependent apoptosis demonstrating the power of *C. elegans* for understanding how the p53 family of proteins are regulated across phyla. My lab also discovered that protein kinase B/Akt paralogues *akt-1* and *akt-2* negatively regulate germline apoptosis by *cep-1*-dependent and *cep-1*-independent mechanisms, respectively (Quevedo *et al.*, 2007). This work has stimulated a new area of research in the lab focused on the role of insulin signaling in apoptosis, which is now supported by a 5 year CIHR grant that was awarded to me in the Fall of 2009. The most recent paper describing non-canonical control of germline apoptosis by the insulin/PI3K signaling pathway via AKT-2 is currently under review (Perrin *et al.*, 2012).

Modeling cerebral cavernous malformations. In a related project my lab discovered that the activation of germline apoptosis by DNA damaging agents requires *kri-1*, the worm orthologue of Ccm1/Krit1 and the most frequently mutated gene in the neurovascular disease cerebral cavernous malformations (CCM). We made the surprising discovery that *kri-1* is required in non-germline tissue to activate apoptosis of damaged germ cells downstream of *cep-1/p53* (Ito *et al.*, 2010). This finding completely changes our view on how multicellular organisms regulate cell survival in response to genotoxic stress. The work on *kri-1/CCM1* stimulated a deeper interest in CCM disease. We have recently developed a vascular model of CCM using the *C. elegans* excretory canals and shown that the CCM genes have conserved functions in tubulogenesis, the topic of this CIHR application. We are collaborating closely with Dr. Anne-Claude Gingras and Dr. Frank Sicheri at the Lunenfeld Institute in Toronto to study the biological functions of protein complexes that associate with CCM proteins. We have already published two collaborative papers on this work (Ceccarelli *et al.*, 2011; Kean *et al.*, 2011) and we are writing up a third paper describing the *C. elegans* CCM model that will be submitted soon.

- 3) **Quevedo, C.**, Kaplan, D.R. & **Derry, W.B.** (2007). AKT-1 regulates DNA damage-induced apoptosis in *C. elegans* by CEP-1/p53 dependent and independent mechanisms. *Current Biology*, 17: 286-292. (24 citations)
- 4) **Gao, X.**, Liao, E., Yu, B., Zhen, M. & **Derry, W.B.** (2008). The SCF^{FSN-1} ubiquitin ligase controls CEP-1/p53-dependent apoptosis in *C. elegans*. *Cell Death and Differentiation*, 15: 1054-1062. (14 citations)
- 5) **Ito, S.**, Greiss, S., Gartner, A. & **Derry, W.B.** (2010). Cell non-autonomous regulation of *C. elegans* germ cell death by *kri-1*. *Current Biology*, 20: 333-338. (3 citations)

Activities and Contributions

25728

Derry, William Brent

a) Conference and workshop organization

2009. 4th International p73/p63 Workshop, Toronto, Canada. Aug. 30 – Sept 1, 2009.

2009. Cancer and Cell Death, Toronto, Canada. June 11 – 12, 2009.

b) Committee memberships

Co-chair, Green-LEED Working group, Hospital for Sick Children (2011-)

Invited member, CIHR peer review committee: MCC panel (2009-), Full member (2011-)

Biostatics Design & Analysis Management Committee, Hospital for Sick Children (2008-2011)

Chair, Restracom Committee, Hospital for Sick Children (2008-2011)

Research & Education Building Steering Committee, Hospital for Sick Children (2008-)

Advisory Committee, Garron Family Cancer Centre, Hospital for Sick Children (2008-)

Member, Cancer Research Society, Panel A: Signaling (2007-2008)

Master Plan Committee, Hospital for Sick Children (2007-)

c) Undergraduate and graduate teaching activities – University of Toronto

MGY350 – Genetics: Model Organisms to Disease (Undergraduate, course coordinator)

MMG1015Y/MMG1017H – Molecular and Medical Genetics Student Seminars (Graduate)

MMG1012H/MMG1016H – “Cell Death and Cancer” (Graduate)

Mentor, CIHR Strategic Training in Health Research, Excellence in Radiation Research for the 21st Century (EIRR21).

d) Thesis examination committees – University of Toronto

Since 2004 served on 9 Ph.D. and 17 M.Sc. examinations and chaired 5 Ph.D. exams.

e) Invited Conferences and Workshops (since 2006)

2012. American Association for Cancer Research Annual Meeting, Chicago. March 30 – April 4.

2011. Ottawa Carleton Institute of Biology 8th annual symposium (Keynote speaker), Ottawa, ON. Apr. 28 – 29.

2010. 6th Annual Pathobiology of CCM Scientific Workshop, Washington, DC, Nov. 1 – 2.

2010. 5th Canadian Developmental Biology Conference, Mount-Tremblant, P.Q. Apr. 8 – 11.

2009. 5th Annual Pathobiology of CCM Scientific Workshop, Santa Fe, NM, Nov. 12 – 13.

2009. 4th International p73/p63 Workshop, Toronto, Aug. 30 – Sept 1.

2009. Keystone Meeting on Cell Death Pathways, Whistler, B.C, Mar. 22 – 27.

2009. EMBO Workshop: Model Organisms in Cell Death Research, Austria. Jan. 31 - Feb. 4.

2008. 4th Annual Pathobiology of CCM Scientific Workshop, Washington, DC, Nov. 20 – 21.

2008. NINDS Vascular Malformations of the Brain Scientific Workshop, Washington, DC, March 13 – 14.

2007. 3rd Annual Pathobiology of CCM Scientific Workshop, Washington, DC. Nov. 9.

2007. Italian Meeting on Apoptosis and Cancer, Palermo, Italy. June 21 – 24.

2007. 3rd International p73/p63 Workshop, Rome, Italy. Mar. 18 – 21.

2006. 7th Conference on Signalling in Normal and Cancer Cells, Banff, Alberta. Mar. 3 – 7.

2006. 2nd Annual Pathobiology of CCM Scientific Workshop, Washington, DC. Nov. 17.

f) Peer review activities

Journal reviews: PNAS, Science, Current Biology, Biochemistry, Cell Death and Differentiation, Journal of Gerontology, Molecular Genetics and Genomics, Developmental Cell, Oncogene, PLoS Genetics. Agence Nationale de la Recherche, France – International Grant reviewer (2012-), Natural Sciences and Engineering Research Council of Canada – Grant reviewer (2010-), Israeli-German Cooperation Program in Cancer Research – International grant reviewer (2010-), Alberta Heritage Foundation for Medical Research (2009-), Wellcome Trust – External grant reviewer (2009-), Cancer Research UK – External grant reviewer (2008-), The United States – Israel Binational Agricultural Research and Development Fund – External grant reviewer (2007-), Association for International Cancer Research – External grant reviewer (2005-)

g) Professional memberships

American Association for the Advancement of Science, Genetics Society of America,

Faculty of 1000

h) Supervisory experience

From 2003 to present I have supervised 5 postdoctoral fellows, 9 graduate students, 4 research assistants, and 14 undergraduate and summer students (currently serving on 8 thesis supervisory committees, U of T).

Interruptions and Delays

None

25728

Derry, William Brent

Rothman, J.H. & **Derry, W.B.** Methods for identifying novel therapeutics and diagnostics in the p53 pathway (UC Case No. 2000-028-1). Issued in the U.S.A., March 27, 2007.

- a) **Refereed manuscripts from past 5 years** (trainees underlined)
1. Ceccarelli, D.F., Laister, R.C., Mulligan, V.K., Kean, M.J., Goudreault, M., Scott, I.C., **Derry, W.B.**, Chakrabarty, A., Gingras, A.C. & Sicheri, F. (2011). CCM3/PDCD10 heterodimerizes with germinal center kinase III (GCKIII) proteins using a mechanism analogous to CCM3 homodimerization. *Journal of Biological Chemistry*, 286: 25056-25064. (Col)
 2. Kean, M.J., Ceccarelli, D., Goudreault, M., Sanches, M., Tate, S., Larsen, B., Gibson, L.C., **Derry, W.B.**, Scott, I.C., Pelletier, L., Baillie, G., Sicheri, F. & Gingras, A.C. (2011). Structure-function analysis of core STRIPAK: a signalling complex implicated in golgi polarization, *Journal of Biological Chemistry*, 286: 25065-25075. (Col)
 3. Ross, A.J., Li, M., Yu, B., Gao, M.X. & **Derry, W.B.** (2011). The EEL-1 ubiquitin ligase promotes DNA damage-induced germ cell apoptosis in *C. elegans*. *Cell Death and Differentiation*, 18: 1140-1149. (SRA)
 4. Ito, S. Greiss, S., Gartner, A. & **Derry, W.B.** (2010). Cell non-autonomous regulation of *C. elegans* germ cell death by *kri-1*. *Current Biology*, 20: 333-338. (SRA)
 5. Gao, M.X. Liao, E., Yu, B., Wang, Y., Zhen, M. & **Derry, W.B.** (2008). The SCF^{FSN-1} ubiquitin ligase controls CEP-1/p53-dependent apoptosis in *Caenorhabditis elegans*. *Cell Death and Differentiation*, 15: 1054-1062. (SRA)
 6. Taylor, R.C., Brumatti, G., Ito, S., Hengartner, M.O., **Derry, W.B.** & Martin SJ. (2007). Establishing a blueprint for CED-3-dependent killing through identification of multiple substrates for this protease. *Journal of Biological Chemistry*, 282: 15011-15021. (Col)
 7. **Derry, W.B.**, Bierings, R., van Iersel, M., Satkunendran, T., Reinke, V. & Rothman, J.H. (2007). Regulation of developmental timing and germ cell proliferation in *C. elegans* by the p53 gene network. *Cell Death and Differentiation*, 14: 662-670. (SRA)
 8. Quevedo, C., Kaplan, D.R. & **Derry, W.B.** (2007). AKT-1 regulates DNA-damage induced germline apoptosis in *C. elegans*. *Current Biology*, 17: 286-292. (SRA)

Summary of Publications

Author role	Number of contributions	Number of citations
Principle author	10	642
Co-author	12	603
Total	22	1245

h-index = 12 (55.4 citations per item)

b) **Manuscripts under revision**

Perrin, A.J., Gunda, M., Yu, B., Yen, K., Ito, S., Forster, S., Tissenbaum, H.A. & **Derry, W.B.** (2011). Noncanonical control of *C. elegans* apoptosis by the insulin/IGF-1 signaling pathway, *under review*. (SRA)

c) **Abstracts (past 5 years)**

2007. Derry, W.B. "CEP-1: Mother of invention or mother of prevention?" 3rd International p73/p63 Workshop, Rome, Italy. March 18 – 21.

2007. Li, M. & Derry, W.B. "Role of Ubiquitination in Radiation-Induced Apoptosis". 16th Biennial International *C. elegans* conference, University of California, Los Angeles, California, USA. June 27 – July 1.

2007. Gao, M.X., Yu, B. & Derry, W.B. "The SCF ubiquitin ligase regulates CEP-1/p53-dependent germline apoptosis". 16th Biennial International *C. elegans* conference, University of California, Los Angeles, California, USA. June 27 – July 1.

2007. Gao, M.X., Liao, E., Yu, B., Zhen, M. & Derry, W.B. "The SCF^{FSN-1} ubiquitin ligase controls apoptosis and synaptogenesis through CEP-1/p53 in *C. elegans*". Cold Spring Harbor Symposium on Programmed Cell Death, Cold Spring Harbor, New York, USA. Sept. 26 – 30.

2008. Derry, W.B. "Regulation of germline apoptosis by CCM genes *kri-1/KRIT1* and *C14A4.11/PDCD10* in *C. elegans*". 5th European Workshop on Cell Death, Hauenstein, Germany. June 1 – 6.

- 2008.** **Derry, W.B.** "Unraveling the CCM signaling network by functional genomics in *C. elegans*." 4th Annual Pathobiology of CCM Scientific Workshop, Washington, DC, USA. Nov. 20 – 21.
- 2009.** Ito, S., Greiss, S., Gartner, A. & **Derry, W.B.** "Novel role for the CCM1 orthologue *kri-1* in *C. elegans* germline apoptosis", EMBO Workshop on Model Organisms in Cell Death Research, Obergurgl, Austria. Jan. 31 – Feb. 4.
- 2009.** **Derry, W.B.** "Genetic regulation of cell death during germ line development in *C. elegans*." Keystone Meeting on Cell Death Pathways, Whistler, British Columbia, Canada. March 22 – 27.
- 2009.** Perrin, A.J. & **Derry, W.B.** "Multiple bifurcations in the insulin-like signaling pathway regulate DNA damage-dependent apoptosis in *Caenorhabditis elegans*." Keystone Meeting on Cell Death Pathways, Whistler, British Columbia, Canada. March 22 – 27.
- 2009.** Ross, A., Li, M. & **Derry, W.B.** "The E3 ubiquitin ligase, *eel-1*, acts as a pro-apoptotic gene in the regulation of germ cell apoptosis in *C. elegans*." 17th International *C. elegans* Meeting, University of California, Los Angeles, California, USA. June 24 – 28.
- 2009.** **Derry, W.B.** & Perrin A.J. "Bifurcations in the insulin-like signaling pathway control *cep-1*-dependent and *cep-1*-independent germline apoptosis in *C. elegans*." 4th International p73/p63 Workshop, Toronto, Canada. Aug. 30 - Sept 1.
- 2009.** **Derry, W.B.** & Perrin A.J. "Regulation of germ cell apoptosis by the insulin signaling pathway in *C. elegans*." Cold Spring Harbor Symposium on Programmed Cell Death, Cold Spring Harbor, New York, USA. Oct. 6 – 10.
- 2009.** Perrin, A.J. & **Derry, W.B.** "A novel, DNA damage-dependent regulatory pathway for Akt *in vivo*." CSCI/CITAC Annual Conference, Ottawa, Canada. September 21 – 23.
- 2009.** **Derry, W.B.** "Genetic analysis of the CCM regulatory network in *C. elegans*." 5th Annual Pathobiology of CCM Scientific Workshop, Santa Fe, NM, USA. Nov. 12 – 13.
- 2010.** Perrin, A.J. & **Derry, W.B.** "DNA damage-dependent function of Akt is maintained independently of PI3K signaling elements in *C. elegans*." Cold Spring Harbor Symposium on PTEN Pathways and Targets, Cold Spring Harbor, New York, USA. Mar. 16 – 20.
- 2010.** Ito, S., Greiss, S., Gartner, A. & **Derry, W.B.** "Non-autonomous control of germ cell apoptosis in *C. elegans*." 5th Canadian Developmental Biology Conference, Mount-Tremblant, P.Q. Apr. 8 – 11.
- 2010.** **Derry, W.B.**, Jolliffe, K.J. & Ross, A. "Synthetic lethal interactions in the p53 network". 7th European Workshop on Cell Death, Tisvildeleje, Denmark. June 27 – July 2.
- 2011.** Perrin, A.J., Yu, B., Yen, K., Ito, S., Tissenbaum, H. & **Derry, W.B.** "Noncanonical control of germline apoptosis by the insulin/IGF-1 signaling pathway." 18th International *C. elegans* Meeting, Los Angeles, California. June 22 – 26.
- 2011.** Perrin, A.J., Yu, B., Yen, K., Gunda, M., Forster, S., Ito, S., Tissenbaum, H. & **Derry, W.B.** "Noncanonical control of germline apoptosis by the insulin/IGF-1 signaling pathway." Cold Spring Harbor Meeting on Cell Death, Cold Spring Harbor, New York. Oct. 11 – 15.
- 2012.** **Derry, W.B.** "Building tubes and killing cells - Modeling CCM disease in *C. elegans*", 6th Canadian Developmental Biology Conference, Banff, AB. March 8 – 11.
- 2012.** **Derry, W.B.** "Functional genomic analysis of pediatric tumor models in *C. elegans*", American Association for Cancer Research Annual Meeting, Chicago. March 31 – April 4.

d) Oral Presentations (past 5 years)

34. Department of Molecular Genetics and Microbiology, Duke University, Chapel Hill, NC, "Functional genomic analysis of the p53 network in *C. elegans*." February 20, 2007. **Invited.**
35. 3rd International p73/p63 Workshop. "CEP-1: Mother of invention or mother of prevention?" Rome, Italy. March 18 – 21, 2007. **Invited.**
36. Italian Meeting on Apoptosis and Cancer, "Regulation of p53-dependent apoptosis by a novel SCF ubiquitin ligase in *C. elegans*", Palermo, Italy. June 21 – 24, 2007. **Invited.**
37. Cold Spring Harbor Symposium on Programmed Cell Death, "The SCF^{FSN-1} ubiquitin ligase controls apoptosis and synaptogenesis through CEP-1/p53 in *C. elegans*". Cold Spring Harbor, New York, September 26 – 30, 2007. **Invited.**

Publication List

25728

Derry, William Brent

38. 3rd Annual Pathobiology of CCM Scientific Workshop, "CCM3 and *C. elegans* – new developments". Washington, DC, USA. Nov. 9. **Invited**.
39. The Hospital for Sick Children Research Institute, Haematology-Oncology Divisional Rounds. "Understanding the molecular basis of cerebral cavernous malformation using *C. elegans* as a model system." March 6, 2008. **Invited**.
40. NINDS Vascular Malformations of the Brian Scientific Meeting, Washington, DC, USA. March 13 – 14, 2008. **Invited**.
41. 4th Annual Pathobiology of CCM Scientific Workshop, "Unraveling the CCM signaling network by functional genomics in *C. elegans*." Washington, DC, USA. Nov. 20 – 21, 2008. **Invited**.
42. EMBO Workshop on Model Organisms in Cell Death Research, "Novel role for the CCM1 orthologue *kri-1* in *C. elegans* germline apoptosis." Obergurgl, Austria. Jan. 31 – Feb. 4. **Invited**.
43. Keystone Meeting on Cell Death Pathways, Whistler, British Columbia, Canada. "Genetic regulation of cell death during germ line development in *C. elegans*." March 22 – 27, 2009. **Invited**.
44. Department of Biology, Carleton University, Ottawa, Canada. "Life and death decisions: Molecular control of apoptosis in *C. elegans*." April 3, 2009. **Invited**.
45. 4th International p73/p63 Workshop, Toronto, Canada. "Bifurcations in the insulin-like signaling pathway control *cep-1*-dependnet and *cep-1*-independent germline apoptosis in *C. elegans*." Aug. 30 - Sept 1, 2009. **Invited**.
46. 5th Annual Pathobiology of CCM Scientific Workshop, "Genetic analysis of the CCM regulatory network in *C. elegans*." Santa Fe, NM, USA. Nov. 12 – 13, 2009. **Invited**.
47. 5th Canadian Developmental Biology Conference, "Non-autonomous control of germ cell apoptosis in *C. elegans*." Mount-Tremblant, P.Q. Apr. 8 – 11, 2010. **Invited**.
48. 7th European Workshop on Cell Death, "Synthetic lethal interactions in the p53 network". Tisvildeleje, Denmark. June 27 – July 2, 2010.
49. Rosalind and Morris Goodman Cancer Centre, McGill University, "Non-autonomous control of apoptosis in *C. elegans*: a murder/suicide story." Montreal, P.Q. January 26, 2011. **Invited**.
50. Ottawa Carleton Institute of Biology 8th Annual Conference, "Modeling human disease in the nematode *C. elegans*", Keynote lecture. Carleton University, ON. April 28 – 29, 2011. **Invited Keynote speaker**.
51. 18th International *C. elegans* Meeting, Parallel session - Development and Evolution II: Evolution and Germline/Sex Determination, "Noncanonical control of germline apoptosis by the insulin/IGF-1 signaling pathway." Los Angeles, California. June 24.
52. Department of Molecular, Cellular & Developmental Biology, University of California, Santa Barbara. "Modeling cancer and vascular disease in *C. elegans*: murder, suicide and building tubes". July 5, 2011. **Invited**.
53. Cold Spring Harbor Symposium on Programmed Cell Death. "Noncanonical control of germline apoptosis by the insulin/IGF-1 signaling pathway". Cold Spring Harbor, New York. October 11 – 15, 2011. **Invited**.
54. Department of Laboratory Medicine and Pathobiology, University of Toronto, Toronto. "Control of vascular tube formation in *C. elegans* by the cerebral cavernous malformation (CCM) genes". January 9, 2012. **Invited**.
55. Department of Chemistry and Biology and the Molecular Science Graduate Program, Ryerson University, Toronto. "Regulation of cell death and vascular tube formation in *C. elegans* by the CCM genes". February 9, 2012. **Invited**.
56. American Association for Cancer Research Annual Meeting, Chicago. "Functional genomic analysis of pediatric tumor models in *C. elegans*". March 31 – April 4, 2012. **Invited**.